Università degli Studi di Trieste

PhD program in MOLECULAR BIOMEDICINE

PhD Thesis

Micrometer-Scale Systems for Regenerative Medicine Applications

Mila Toppazzini

XXII ciclo – Anno Accademico 2008-2009

UNIVERSITÀ DEGLI STUDI DI TRIESTE

Sede Amministrativa del Dottorato di Ricerca

DIPARTIMENTO DI SCIENZE DELLA VITA

XXII CICLO DEL
DOTTORATO DI RICERCA IN

BIOMEDICINA MOLECOLARE

MICROMETER-SCALE SYSTEMS FOR REGENERATIVE MEDICINE APPLICATIONS

Settore scientifico-disciplinare BIO/10

DOTTORANDO
MILA TOPPAZZINI

RESPONSABILE DOTTORATO DI RICERCA
Chiar.mo Prof. GIANNINO DEL SAL

RELATORE
Chiar. mo Prof. SERGIO PAOLETTI
Università degli Studi di Trieste

SUPERVISORE
Chiar.mo Prof. GUDMUND SKJÅK-BRÆK
University of Trondheim (NORWAY)

CORRELATORE
Dott. ANNA COSLOVI
Università degli Studi di Trieste

ANNO ACCADEMICO 2008/2009

Relatore - Prof. Sergio Paoletti, Scienze della Vita v. Giorgieri 1, C11, 34127 Trieste

Correlatore - PhD. Anna Coslovi Scienze della Vita v. Giorgieri 1, C11, 34127 Trieste

Supervisore - Prof. Gudmund Skjåk-Bræk Norwegian University of Science and Technology (NTNU) Dept. Of Biotechnology N- 7491 Trondheim Norway

Commissari

Presidente effettivo - Prof. Tonin Enrico Trieste Scienze della Vita v. Flemimg, 22 34127 Trieste

Componente effettivo - Prof. Mangoni Maria Luisa Roma "La Sapienza" Scienze Biochimiche v. degli Apuli 9, 00185 Roma

Componente effettivo - Prof. Pini Alessandro Siena Biologia Molecolare v. Fiorentina 1, 53100 Siena

Componente aggregato - Prof. Gudmund Skjåk-Bræk Norwegian University of Science and Technology (NTNU) Dept. Of Biotechnology N- 7491 Trondheim Norway

Componente aggregato - Prof. Paradossi Gaio Roma Tor Vergata Scienze e Tecnologie Chimiche v. della Ricerca Scientifica snc, 00133 Roma

Presidente supplente - Prof. Lanzetta Rosa Napoli "Federico II" Chimica Organica e Biochimica via Cintia 4, 80126 Napoli

Componente supplente - Prof. Coviello Tommasina Roma "La Sapienza" Chimica e Tecnologia del Farmaco p.le Aldo Moro 5, 00185 Roma

Componente supplente - Prof. Savoia Anna Trieste Dip. Univ. Clin. Sc. della Riprod. e dello Sviluppo e di Sc. Della Medicina Pubblica v. dell'Istria 65/1, 34137 Trieste

Coordinatore del corso di dottorato - Prof. Del Sal Giannino Trieste Scienze della Vita v. Giorgieri 1, C11, 34127 Trieste

Direttore del Dipartimento di riferimento - Prof. Gennaro Renato Trieste Scienze della Vita v. Giorgieri 1, C11, 34127 Trieste

To my “Happy Family”

Table of contents

CHAPTER 1. GENERAL INTRODUCTION 19

1.1 Regenerative medicine and tissue engineering 19

1.1.1 Regenerative medicine for bone 20

1.1.2 Human bone: structure and histology 21

1.1.3 Bone remodelling 23

Cells on bone remodelling 24

Bone morphogenesis 27

1.1.4 Injury-induced regeneration of bone 29

1.2 Biomaterials 31

1.3 Bone graft substitutes 34

1.4 Developing bioactive composite for bone graft substitutes 39

1.4.1 Bioactive bioceramics 39

1.4.2 Biomedical polymers 40

Collagens and fibrin 42

Hyaluronic acid 42

Alginate 44

Chitosan 48

ChitLac 50

CHAPTER 2. AIMS OF THE STUDY 53

CHAPTER 3. MATERIALS AND METHODS 55

3.1 Materials 55

3.2 Methods 55

3.2.1 GRGDS and CGRGDS synthesis 55

3.2.2 Synthesis of BMP fragments 56

3.2.3 Synthesis of LL-37 57

3.2.4 ChitLac synthesis 57

3.2.5 Synthesis of succinyl-ChitLac 57

3.2.6 Synthesis of thiolated ChitLac 58

3.2.7 Synthesis of ChitLac-(CONH)-RGD 58

3.2.8 Synthesis of ChitLac-(NCO)-RGD 59

3.2.9 Synthesis of ChitLac-FITC 59

3.2.10 Synthesis of the linker for BMP conjugation 59

3.2.11 Synthesis of ChitLac-“azido” 60

3.2.12 Conjugation of BMP to the polymer (ChitLac-(click)-BMP) 60

3.2.13 Ellman’s test 60

3.2.14 µBCA assay 61

3.2.15 Quantification of peptides by hydrolysis and capillary electrophoresis 62
3.2.16 CMC determination by capillary electrophoresis 63
3.2.17 Degradation by esterase 63
3.2.18 Beads preparation 64
Beads of intermediate diameter 64
CLSM µbeads 65
Microbeads used in biological tests 65
Large beads functionalized with RGD 66
3.2.19 Measure of swelling 67
3.2.20 BMP fragment release from beads 68
3.2.21 LL-37 release from beads 68
3.2.22 Circular Dichroism 69
3.2.23 MTT Assay 69
3.2.24 Antibacterial activity of LL-37/alginate mixtures in solution 70
3.2.25 Antibacterial activity of scaffolds loaded with LL-37 70
3.2.26 Alamar Blue™ Assay for cell proliferation on beads 71
3.2.27 Alamar Blue™ Assay for Cell Proliferation on LL-37 loaded scaffolds 72
3.2.28 Alamar Blue™ Assay for cell accessibility on composites 72
3.2.29 Lactate Dehidrogenase Assay 72
3.2.30 NMR 74
3.2.31 Microbeads for the injectable composite 74
3.2.32 Rheology studies 74

CHAPTER 4. RESULTS AND DISCUSSION 77

4.1 Foreword: the assembly of a strategy 77
4.1.1 The detailed research strategy 79

4.2 PRO-ADHESIVE AGENTS IN FILLER: RGD-CONTAINING PEPTIDES 86
4.2.1 Introduction 86
The dynamics of cell-ECM interactions. 87
Integrins: multifunctional receptors 89
Biomaterials in the host 92
Bio-Adhesive surfaces: biomaterials mimicking ECM 95
4.2.2 Design of an injectable bone filler with adhesive properties 103
Beads preparation 117
4.2.3 Partial conclusions 130

4.3 OSTEOINDUCTIVE AGENTS IN FILLER: BMP FRAGMENTS 132
4.3.1 Introduction 132
Discovery of BMPs 133
The use of BMP-2 in regenerative medicine 140

Functional fragments derivatives BMPs 143
BMPs delivery 144
4.3.2 Design of a BMP-2 fragment delivery system 154
Initial fast release from alginate/HAp beads 154
Beads for controlled release 159
4.3.3 Partial conclusions 171
4.4 ANTIBACTERIAL AGENTS IN FILLER: THE LL-37 PEPTIDE 173
4.4.1 Introduction 173
The need of new antimicrobial agents 173
Bone infections and post-surgical complications 175
Antimicrobial Peptides 177
4.4.2 Design of an antimicrobial composite 196
Circular Dichroism studies 197
Cytotoxicity of LL-37/polysaccharide mixtures 201
Antimicrobial activity of alginate/LL-37 mixtures 202
Application of LL-37 to solid supports: Release from alginate/hydroxyapatite beads 204
Application of LL-37 to solid supports: Adsorption on alginate/hydroxyapatite scaffolds 207
4.4.3 Partial conclusions 210
4.5 INJECTABLE FILLER 211
4.5.1 Introduction 211
Developing a bioactive composite 211
Study of composites 225
4.5.2 Design of a composite for orthopaedic applications 227
Rheological properties of hyaluronic acid 227
Measure of cell accessibility 230
Particle distribution 231
Filler construction 232
Rheological tests on the final composite 233
4.5.3 Partial conclusions 241
CHAPTER 5. CONCLUSIONS 243
CHAPTER 6. ACKNOWLEDGEMENTS 249
CHAPTER 7. REFERENCES 251

Abstract

Bone regenerative medicine is considered a potential therapeutic option for the healing of damaged bone tissue. A variety of synthetic bone graft substitutes have been investigated as alternative to current tissue based bone graft materials.

In this study efforts have been made to achieve an injectable material to fill bone defects. We have designed composite injectable filler by using polysaccharides as biodegradable materials, and by functionalizing them with bioactive elements such as adhesion mediators, osteoinductive growth factors and anti-microbial peptides.

The final construct is represented by a two-phase composite, whose parts have been initially built separately. The structure was thought as composed by bioactive alginate/HAp dried microbeads functionalized with peptides, suspended in a concentrate hyaluronic acid solution as the matrix vehicle.

With the aim to obtain bioactive alginate/HAp beads, different techniques of peptides-polysaccharides conjugation were considered and different peptide delivery systems were explored. In detail the peptides considered were three, the RGD active sequence with bioadhesive properties, a fragment of BMP-2 (bone morphogenetic protein-2) that promotes the differentiation of MSCs into osteoblasts, and LL-37 a human antimicrobial peptide.

In order to obtain a construct with bioadhesive properties, efforts have been made to improve the tissue-alginate/HAp beads interface by immobilizing RGD peptide sequence in a manner that assure the right motif orientation and high yields. After having tested various chemical strategies, the immobilization by disulfide bridge formation between a ChitLac previously modified with a thiol group and a peptide containing a cysteine residue was evaluated to be the best in terms of yield; at the same time μbeads functionalized in that way exhibit a very high osteoblast adhesion and growth promotion in *in vitro* experiments.

Another important topic regarded the incorporation of BMP-2 epitope fragment into the construct, to enhance differentiation and proliferation. Time-tuned physiological functionality suggested the development of a system being the sum of two delivery strategies: the first characterized by simple entrapment in alginate beads for a fast burst release and the second one giving a slow and constant release, obtained by the action of bone esterases on an enzymatically cleavable linker. This second strategy exploited a high selective chemistry such as that of click reactions. Starting by a γ-valerolactone the synthesis of the enzymatically cleavable spacer was performed. The linker was designed to contain a final functional group

for click chemistry. It was bound to ChitLac and then to a modified BMP fragment by a click reaction. Enzymatic cleavage was verified and an exhaustively characterization by means of NMR and capillary electrophoresis was performed.

The incorporation of antimicrobial peptides was also taken into account. Starting from the information gained by circular dichroism data on the influence on LL-37 conformation given by several polysaccharides, an optimal modulation activity of the cytotoxic effect of LL-37 was found using the peptide/alginate mixture. The demonstrated maintenance of antimicrobial activity on Gram negative strains drove to an application on solid constructs for orthopaedic applications. An effect caused by the simple contact between cells or bacteria and alginate surface loaded with the peptide, was excluded by *in vitro* experiments. The only possible release mechanism that an LL-37/alginate construct was able to show was related to the degradation of this one.

Finally, the whole construct was assembled by incorporating the dried microbeads in a concentrate hyaluronic acid solution, obtaining a paste-like construct that can facilitate the injectability of the particulate. Rheological measurements indicated an increment of the viscoelastic component by adding particulate into hyaluronate solution; this, generally, is associated to a good capacity to regain the elasticity after the injection, as expected for a biomaterial for bone filler applications.

The results collected demonstrate the applicability of the obtained composite as bone graft substitute with bioactive properties (osteoinduction, osteoconduction, bioadhesivity and antibiotic effect on Gram negative strains).

Sommario

La medicina rigenerativa applicata al campo ortopedico è considerata una possibile opzione terapeutica per la riparazione del tessuto osseo danneggiato. Si stanno studiano e sviluppando una gran varietà di sostituti ossei sintetici come valida alternativa agli innesti di tipo tissutale.

Lo scopo di questo lavoro di tesi è la progettazione e lo sviluppo di un materiale iniettabile per il riempimento dei difetti ossei. In particolare abbiamo sviluppato un riempitivo composito iniettabile usando materiali biodegradabili di tipo polisaccaridico funzionalizzati con elementi bioattivi come mediatori dell'adesione cellulare, fattori di crescita osteoinduttivi e peptidi di tipo antimicrobico.

Il costrutto finale è un composito a due fasi, le cui parti, inizialmente, sono state sviluppate separatamente. La struttura è stata progettata come composta da una parte bioattiva, costituita da microsfere disidratate di alginato e idrossiapatite recanti peptidi, immersa in una matrice veicolante rappresentata da una soluzione concentrata di acido ialuronico. Con lo scopo di ottenere le microsfere bioattive, sono state esplorate diverse tecniche per la coniugazione peptide-polisaccaride e sono stati presi in considerazione svariati sistemi di rilascio di sequenze peptidiche. In particolare sono stati considerati tre peptidi noti per la loro bioattività: peptidi di tipo RGD, sequenza favorente l'adesione cellulare, un frammento della proteina BMP-2 (*bone morphogenetic protein-2*) in grado di promuovere il differenziamento di cellule mesenchimali ad osteoblasti e LL-37 peptide antimicrobico umano.

Per ottenere un costrutto con proprietà bioadesive, gli sforzi sono stati volti ad un miglioramento dell'interfaccia fra le sfere di alginato/idrossiapatite e il tessuto osseo. Questo è stato possibile immobilizzando sulla superficie delle sfere dei peptidi contenti la sequenza RGD e assicurandone il gusto orientamento ed un'alta resa di immobilizzazione. Dopo aver testato diverse strategie chimiche, l'immobilizzazione effettuata sfruttando la formazione di un ponte disolfuro fra ChitLac preventivamente modificato con gruppi tiolici e un peptide contenente un residuo di cisteina, è stata valutata come la miglior strategia in termini di resa di reazione; allo stesso tempo le microsfere funzionalizzate in questo modo hanno dimostrato un'alta capacità di promuovere l'adesione e la crescita di osteoblasti in esperimenti effettuati *in vitro*.

Un altro importante tema ha riguardato l'incorporazione di un frammento della proteina BMP-2 nel costrutto al fine di promuovere il differenziamento e quindi la proliferazione

cellulare. La sequenza temporale degli eventi fisiologici, ha suggerito lo sviluppo di un sistema che risulta essere la somma di due diverse strategie di rilascio: la prima caratterizzata dal semplice intrappolamento del peptide in un sistema di sfere di alginato capace di un rilascio veloce, ed il secondo caratterizzato da un rilascio lento e costante ottenuto grazie all'azione idrolitica di esterasi. Questo è stato possibile inserendo un legame enzimaticamente idrolizzabile nella struttura contenente il frammento di BMP. Questa seconda strategia ha sfruttato una chimica altamente selettiva quale la "*click chemistry*". La sintesi della molecola spaziatrice recante un legame enzimaticamente idrolizzabile è stata effettuata partendo da un γ-valerolattone. Questo spaziatore è stato inoltre progettato per recare un gruppo terminale funzionale adeguato per le reazioni di *click chemistry* ed è stato legato al ChitLac. La reazione di cicloaddizone è stata poi effettuata fra il ChitLac funzionalizzato con lo spaziatore e il frammento di BMP anch'esso opportunamente funzionalizzato. L'idrolisi enzimatica è stata verificata, inoltre è stata eseguita un'esaustiva caratterizzazione tramite NMR ed elettroforesi capillare.

E' stata poi presa in considerazione l'incorporazione di peptidi antimicrobici nel costrutto. Partendo da dati di dicroismo circolare riguardanti l'influenza che alcuni polisaccaridi hanno sulla conformazione del peptide LL-37 in soluzione, è stata riconosciuta alla miscela LL-37/alginato la capacità di modulare la citotossicità del peptide. La miscela ha inoltre dimostrato la capacità di mantenere l'attività antimicrobica su batteri Gram negativi e questo ci ha spinto a considerarne l'applicazione su costrutti solidi con finalità ortopediche. In quest'ambito è stato escluso, da esperimenti *in vitro,* un effetto causato dal semplice contatto fra cellule o batteri e una superficie di alginato caricato col peptide. L'unico possibile meccanismo di rilascio riscontrato in un costrutto di alginato/LL-37 è stato tramite la degradazione di questo.

Infine, il costrutto è stato assemblato incorporando le microsfere disidratate in una soluzione concentrata di acido ialuronico, ottenendo un costrutto dall'aspetto simile ad una pasta che è in grado di facilitare il processo di iniezione del riempitivo.

Misure di tipo reologico hanno indicato in incremento della componente viscoelastica aggiungendo il particolato nella soluzione di acido ialuronico, questo generalmente è associato ad una buona capacità di recuperare l'elasticità dopo l'iniezione il che è un requisito richiesto ai biomateriali usati come riempitivi ossei.

I risultati ottenuti hanno dimostrato l’applicabilità del composito come sostituto osseo dotato di proprietà bioattivite (osteoconduzione, osteoinduzione, bioadesività ed effetto antimicrobico su ceppi di tipo Gram negativo).

List of papers included in the Thesis

A. Travan, I. Donati, E. Marsich, F. Bellomo, S. Achanta, M. Toppazzini, S. Semeraro, T. Scarpa, V. Spreafico, S. Paoletti, Surface modification and polysaccharide deposition on BisGMA/TEGMA Thermoset, Biomacromolecules, 2010, 11, 583-592.

List of papers not directly relevant to the Thesis

F. Abballe, M. Toppazzini , C. Campa, F. Uggeri, S. Paoletti, Study of molar response of dextrans in electrochemical detection, J. Chromatogr. A., 2007, 1149(1), 38-45.

M. Toppazzini, A. Coslovi, S. Paoletti, Capillary electrophoresis applied to polysaccharide characterization, *Capillary Electrophoresis of Carbohydrates. From monosaccharides to complex polysaccharides.* Ed. Humana Press. *In press*

List of abbreviations

AMPs AntiMicrobial Peptides

ASCs Adult stem cells

BMP-2 Bone morphogenetic protein-2

BMPs Bone morphogenetic proteins

BSP-II Bone sialoprotein II

c.m.c. Critical micellar concentration

CDMPs Cartilage-derived morphogenic proteins

CE Capillary electrophoresis

CPC Calcium orthophosphate cement

ECM Extracellular matrix

EnSCs Endothelial stem cells

ESCs Embryonic stem cells

FGFs Fibroblast growth factors

FITC Fluorescein 5(6)-isothiocyanate

GAGs Glycosaminoglycans

HAp Hydroxyapatite

HSCs Hematopoietic stem cells

IBS Injectable bone substitutes

IGF Insulin-like growth factors

IL-1 Interleukin-1

LPS Lipopolysaccharides

M-CSF Macrophage colony-stimulating factor

MSCs Mesenchymal stem cells

OP-1 Osteogenetic Protein-1

OPG Osteoprotegerin

PCL Poly(ε-caprolactone)

PDGF Platelet-derived growth factors

PE Polyethylene

PI Phosphate solution ionic strenght

PLA Poly lactic acid

PLGA poly(D,L-lactide-co-glycolide)

PLL poly(L-lysine)

PLLA Poly-L-lactic acid

PMMA Polymethyl methacrylate

PS Polysaccharide

RGD Arg-Gly-Asp peptide (adhesive motif)

rhBMP-2 Recombinant human bone morphogenetic protein 2

TGF-β Transforming growth factors-β

VEGF Vascular Endothelial Growth Factor

β-TCP β-tricalcium phosphate

CHAPTER 1. **GENERAL INTRODUCTION**

Aging demographics, product advances, increasing number of sport injures and the change of patient care strategies, drive the rapidly rising of orthopaedic biomaterials market.

To have an idea of the importance that this field will have in the future, it is sufficient to think that it has been predicted that the percentage of persons over 50 years of age affected by bone diseases will double by 2020 (Bone and Joint Decade's Musculoskeletal Portal 2007, http://www.boneandjointdecade.org). It is therefore not surprising that biomedical industries are dedicating a big effort towards the development of new and more performing orthopaedic devices to improve the quality of life of people affected by bone damages (Navarro et al., 2008).

Current orthopaedic products in the research field include stem cells, bone growth factors, gene therapy, synthetic bone fillers, bioactive implants coatings, biocomposites and resorbable biopolymers.

When thinking to a new biomaterial for bone healing, the attention has to be focussed on the interactions occurring between the implant and the host. It is at the level of these interactions in fact, that the majority of clinical complications occur, but at the same time these interactions localized at the surface of the implant, are an opportunity for biomaterial scientist to develop devices able not only to replace a damaged tissue but also to dynamically communicate with the surrounding environment.

The meaning of fracture healing is therefore very different today from some decades ago.

1.1 Regenerative medicine and tissue engineering

Regeneration is a repair process that maintains the original tissue architecture and it is opposed to fibrosis or "wound healing" which repairs tissues with scar tissue. Regeneration can be defined as "the induced regrowth of an organ at the anatomical site of an adult where the function of the original organ has been lost, either following accidental trauma or selective surgery or, conceivably, after an organ has become dysfunctional due to a chronic insult." The starting point of this technology can be considered the development, in the mid-1970, of the so-called "artificial skin", a protein scaffold able to induce partial skin regeneration. Advances in biology knowledge about regeneration allowed later to develop the regenerative

medicine, a new area of research about the treatment of damaged tissues (Daar and Greenwood, 2007).

Three main strategies are being followed in the development of regenerative therapies:

- **Cell transplantation.** This approach involves a source of cells usually supported by a substrate, which will finally fill the defect. Transplanted cells can be autogenic, allogenic or xenogenic and differentiated or stem cells (these latter from adult ASCs or embryonic ESCs) (Anon., 2007).The use of cell transplants is widespread, but has still some important drawbacks, such as the necessity of a correct identification of cell sources and the need to avoid and contrast immunorejection phenomena.
- **Bioartificial tissues constructs**. This definition comprises implantable matrices that could derive from biological or synthetic materials, and are able to promote the regeneration of tissues in the region of the defect by mimicking the extracellular matrix (ECM) or in some cases by supporting transplanted cells. These implants maximise cells migration offering not only suitable geometry and physical/chemical properties, but also releasing biological signals that are essentials for cellular proliferation and differentiation.
- **Induction of regeneration at the site of injury.** The reconstruction of new tissue could be promoted by signal factors such as growth factors, able to take effect on regeneration-competent cells. The strategy consists in the application of these factors topically by injection or by means of templates that support them.

These three strategies are not always simultaneously used. For instance, it is sufficient for some bone tissue engineering to use only growth factors such as bone morphogenetic proteins (BMPs), while dermal tissue can be regenerated simply by placing a porous collagen sheet on a full-thickness skin wound without cell seeding and growth factors delivery (Ikada, 2006). The type of therapy used depends on which is more appropriate for the nature of the tissue and the extent of the damage to be repaired: in general, cell transplantation and regenerative pharmaceutical induction have been employed to correct smaller tissue deficiencies, whereas bioartificial tissue constructs have been used in the treatment of larger tissue deficiencies (Stocum, 2006).

1.1.1 Regenerative medicine for bone

Mammalian endochondral or membranous bones are unable to regenerate across gaps that exceed a certain size, called the “critical size gap”. The critical size gap is different for each

type of bone and in different species. In humans the standard treatment for such defects is an autogenic bone graft, which runs the risk of morbidity at both donor and host sites. Allogenic bone grafts can also be used, but these are subject to immunorejection and to a low risk of infectious disease. Alternative to bone grafting to regenerate bone across non healing defects include the electrical stimulation, cell transplants, the use of osteogenic growth factors and acellular scaffolds, and implantation of bioartificial bone.

Regardless of the used approach, bone regeneration involves the same three requirements as bone development: osteoinductive signals; a matrix that traps the signal and provides an adhesive surface; and osteogenic cells that can adhere to the matrix and differentiate into osteoblasts in response to osteoinductive signals (Ripamonti, 2002), (Stocum, 2006). So, with the aim to develop bone regeneration constructs, the attention must be focussed on biology and biochemical mechanisms involved in bone morphogenesis.

1.1.2 Human bone: structure and histology

Bone is known to be a complex, vital and necessary composite tissue in the body, containing many individual constituents and the analysis of bone structure has provided the basis for trying to mimic each piece and the whole (Kay, 2007).

Bone is a specialized form of connective tissue and is the main constituent of the skeletal. It is composed of cells (osteocytes) embedded in a peculiar extracellular matrix that becomes calcified unlike other connective tissues. This mineralization confers multiple mechanical and metabolic functions to the skeleton.

There are two categories of bone tissue: cortical or compact bone, and trabecular or spongy bone. The dissimilar structure found in these two types of bone, is related to the different proportions of the organic and inorganic part, degree of porosity and organization of the same basic materials that constitute them. Besides also the osteocytes are equivalent, but the arrangement of how the blood supply reaches the bone cells is different. Compact bone is dense and strong, whereas trabecular bone has many open spaces containing bone marrow. All bone types (long, short, flat and irregular bones), regardless of their anatomical form, are composed of both spongy and compact bone.

In the long bone the external part is composed of cortical bone, which becomes progressively thinner in the metaphysis and epiphysis (Figure 1). The osteocytes of this bone are localized in small *lacunae*, where they form concentrically layers around blood vessels into units called Haversian canals, or osteons. Trabecular bone is localized inside the compact

bone. The medullary cavity is lined with endosteal connective tissue and is filled with bone marrow. The endosteum consists of fibroblasts, mesenchymal stem cells (MSCs), pre-osteoblasts and osteoblasts, while the bone marrow consists of a mixture of MSCs, fibroblasts, adipocytes, macrophages and endothelial cells of sinusoids. These cells constitute the stroma of the bone marrow. Hematopoietic stem cells (HSCs) and endothelial stem cells (EnSCs) are embedded in the stroma and depend on it for their survival. The external surface of the bone is covered with another connective tissue sheath: the periosteum. The periosteum and the lining of the Haversian canals also contain MSCs, pre-osteoblasts and osteoblasts.

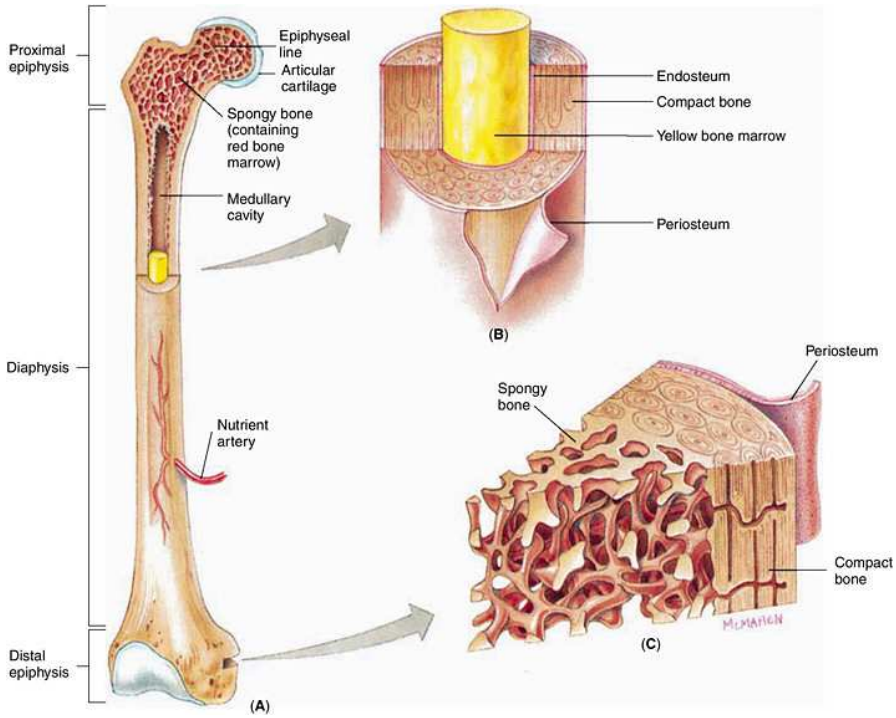

Figure 1. The structure of a typical long bone. (A) Diaphysis, epiphysis and medullary cavity. (B) Compact bone surrounding yellow bone marrow in the medullary cavity. (C) Spongy bone and compact bone in the epiphysis (Rizzo, 2006).

The cells, actually, constitute only a very small percentage of the bone tissue, whereas the bulk of the tissue is occupied by the intercellular, calcified, bone matrix.

Microscopically bone is a natural composite material, which contains about 45-60% of mineral, 20-30% of matrix and 10-20% of water. Ninety percent of the organic material in the bone is collagen I, with a remaining 10% consisting of sulphated glycosaminoglycans

(chondroitin-4-sulfate, chondroitin-6-sulfate, keratan sulphate) and various bone proteins (such as bone sialoprotein and osteocalcin). Interspersed in the organic matrix are crystals of a calcium phosphate known as hydroxyapatite (HAp).

While the organic matrix provides flexibility to bone, inorganic material is predominantly responsible for its stiffness and mechanical properties. This complex structure allows the achievement of different functions: bone tissue not only supports and protects soft tissues and serves as a lever for muscle action but also helps blood cell regeneration and acts as a storehouse that can sequester and release calcium to maintain physiological blood levels of this one.

Bone tissue possesses the ability to repair and adapt itself, in mass and in morphology, in front of functional demands, or different loading which is submitted. In fact, the combination of cortical and trabecular bone differs according to the skeleton regions, which is dependent on the applied mechanical loading (Burr et al., 2002).

1.1.3 Bone remodelling

The understanding of the processes at the basis of bone-healing is essential for the development of new orthopaedic repair materials. The bone regeneration and repair process is not completely understood, but precious secrets have been unlocked and with this ever-increasing knowledge, more effective materials have been engineered (Kay, 2007).

As mentioned, bone is a highly dynamic tissue that is involved in many functions. All these roles require bone to be continuously degraded by osteoclasts and regenerated by osteoblasts. In adult vertebrates, ten per cent of the skeletal mass is replaced every year: this physiological process, often referred as “bone remodelling”, occurs continually and simultaneously at multiple locations in the skeleton. Bone remodelling is driven by mechanical usage, systemic factors (such as parathyroid hormone, leptin and sex steroids), calcium blood level, local factors (for instance BMPs) and pharmacological stimulators or inhibitors (Figure 2) (Ducy et al., 2000; Harada and Rodan, 2003).

Biomechanical stress is an osteogenic stimulus that leads to increased bone formation (Burr et al., 2002).

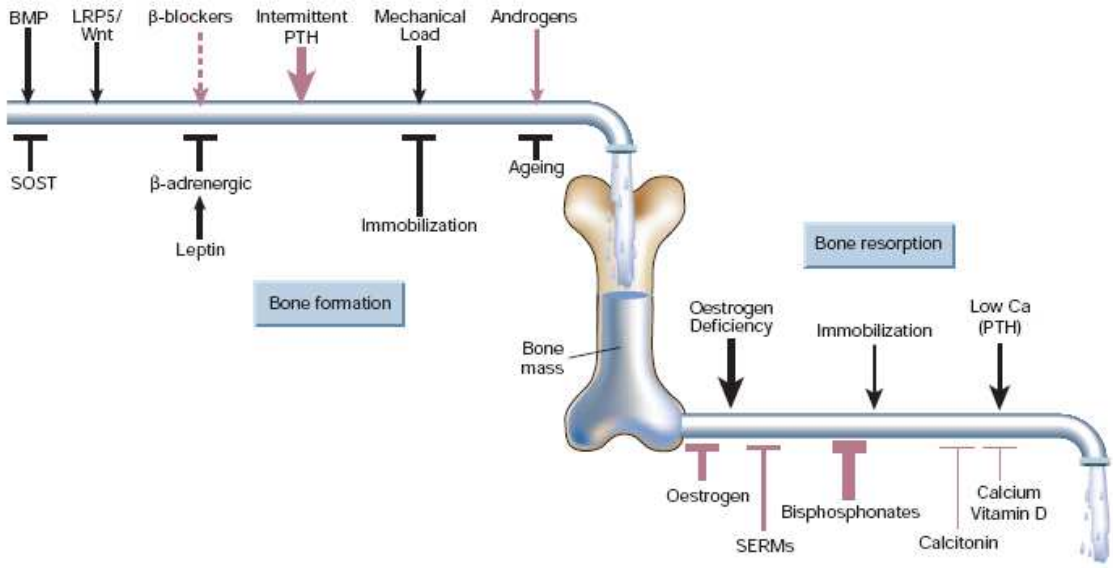

Figure 2. Determinants of skeletal homeostasis and bone mass. Schematic representation of the system that maintains bone mass at steady-state levels. Physiological (black) and pharmacological (purple) stimulators and inhibitors of bone formation and resorption are listed. The relative impact, where known, is represented by the thickness of the arrows. Solid lines are current therapies and dotted lines putative ones. Abbreviations: BMPs, bone morphogenetic protein(s); SOST, sclerostin; LRP5, low-density lipoprotein (LDL)-receptor-related protein 5; PTH, parathyroid hormone; SERM, selective oestrogen-receptor modulator (Harada and Rodan, 2003)

Imbalances in the bone remodelling provoke skeletal abnormalities such as osteoporosis when the rate of removal exceeds the rate of replacement, or osteopetrosis in the opposed situation. Besides, there are many genetic disorders that involve bone remodelling (Rodan and Martin, 2000; Zelzer and Olsen, 2003).

Cells on bone remodelling

Osteoclasts are giant cells with 4-20 nuclei, derived by the fusion of macrophages and differentiated for the specialized function of bone removal. They form on the connective tissue surfaces that line the bone: periosteum and endosteum. When stimulated by agents such as PTH, the osteoblasts in these tissues produce factors that are able to induce the differentiation of macrophages into osteoclasts.

The process of differentiation of macrophages into osteoclasts requires the presence of stromal cells, or their osteoblasts progeny. These cells express two essentials factors in the osteoclastogenesis promotion: macrophage colony-stimulating factor (M-CSF) and the ligand

of receptor for activation of nuclear factor kappa B (RANKL) which are up-regulated by osteoclastogenic molecules such as PTH. RANKL and M-CSF, interact with their receptors on macrophage cells, RANK and c-fms respectively, thus inducing, differentiation onto osteoclasts. This process is inhibited by osteoprotegerin (OPG) which is also secreted by osteoblasts and stromal cells under the PTH regulation and competes with RANK for RANKL. Osteoclasts differentiation is thus regulated by a balance between the concentrations of M-CSF and RANKL versus OPG. Osteoclast differentiation is also regulated by a negative feedback mechanism activated within the osteoclasts themselves. (Teitelbaum, 2000; Boyle et al., 2003)

The osteoclasts reabsorb the matrix by first demineralizating it and then degrading its organic components. The capacity of osteoclasts to polarize the bone permits their attachment on the bone matrix. Through ion transport, HCl is secreted by osteoclasts: while the internal pH is maintained by an Cl^-/HCO_3^- exchange, the secretion of HCl into the microenvironment promotes a pH of about 4.5 sufficient to dissolve the HAp of the matrix. Subsequently the organic components are solubilised by a lysosomal protease, the cathepsin K. The products of bone degradation are endocytosed by osteoclasts and released at the cell's antiresorptive surface. (Teitelbaum, 2000) The "resorption lacuna", created by osteoclasts, is after occupied by osteoblasts that synthesize new bone matrix (Stocum, 2006).

Osteoblasts are cells derived from MSCs of the endosteum, periosteum and bone marrow. Genetically and morphologically osteoblasts are very similar to fibroblasts. Two transcription factors that play key roles in the differentiation of MSCs into osteoblasts are Runx2 (specific for the chondrocytes/osteoblasts lineage), and Osterix (Osx) (specific for pre-osteoblasts) (Figure 3). Both Runx2 and Osx are expressed in the periosteum and together regulate osteoblasts differentiation with Osx appearing to act down-stream of Runx2. Runx2 also appear to control the rate of bone matrix formation by differentiated osteoblasts. One of the down-stream targets of Runx2 is the osteocalcin gene which is activated only in differentiated cells.

Within the mature bone, **osteocytes** are the most numerous cells that display longevity matching the host. Due to the remote location of the cell in the mineralized matrix, isolation of the cells and preservation of their phenotype is difficult. Osteocytes are derived from osteoprogenitors, a fraction of which differentiate into active osteoblasts and subsequently are encased in osteoid. Osteoblasts synthesize osteoid (unmineralized bone matrix made of collagen and other organic components). A fraction of the active osteoblasts become

incorporated within the newly laid down matrix. New osteocytes maintain direct contact with the overlying bone lining cells and osteoblasts, as well as with previous generations of osteocytes through cell processes that are created before and during matrix synthesis. The extended osteocytic network, comprised of cells interconnected by multiple biochemical processes and joined at “gap junctions”, forms a functional syncytium.

Osteocytes are actively involved in maintaining the bony matrix, and osteocyte death is eventually followed by matrix resorption. In addition, osteocytes are thought to be mechanosensors. Translation of mechanical signals at the cellular level may further involve triggering of integrin force receptors and/or changes in the conformation of membrane bound proteins that affect membrane fluidity and trafficking. Furthermore, chemical signals, modulated through diffusive, convective and active transport mechanisms, are transported intracellularly as well as through the extracellular fluid in which the cells are immersed.

Mesenchymal stem cells represent an adherent, fibroblast-like population localized not only in the bone marrow, but in a number of tissues, including blood, adipose tissue, muscle, and derma. Their extensive proliferation and transdifferentation potential makes them best suited for tissue engineering applications. Identification of growth factors and signaling pathways involved in self-renewal and differentiation is important in designing strategies to overcome replicative senescence and attaining directed differentiation. Differentiation of MSCs into bone forming osteoblasts is a multi-step process regulated by various molecular pathways. Bone cells can possess two types of progenitors:

- ESCs: Embryonic mesoderm-derived mesenchymal cells that are progenitors for bone, cartilage, tendons, ligaments, and muscle.
- ASCs: Stem cells in adult bone marrow, muscle, and fascia that can form bone and cartilage. Indentified in 1988 as bone marrow stromal stem cells to distinguish them from the hematopoietic stem cell lineage, stromal stem cells are also called mesenchymal stem cells. They possess a potential to form bone, cartilage, adipocytes, and myoblasts in response to cues from the environment and/or intrinsic factors (Figure 3). The bone marrow stromal stem cells consist of inducible and determined osteoprogenitors committed to osteogenesis.
    - Determined osteogenic precursor cells have the propensity to form bone cells, without any external cues or signals.
    - On the other hand, inducible osteogenic precursors require an inductive signal, such as BMPs or demineralized bone matrix (Reddi, 2007).

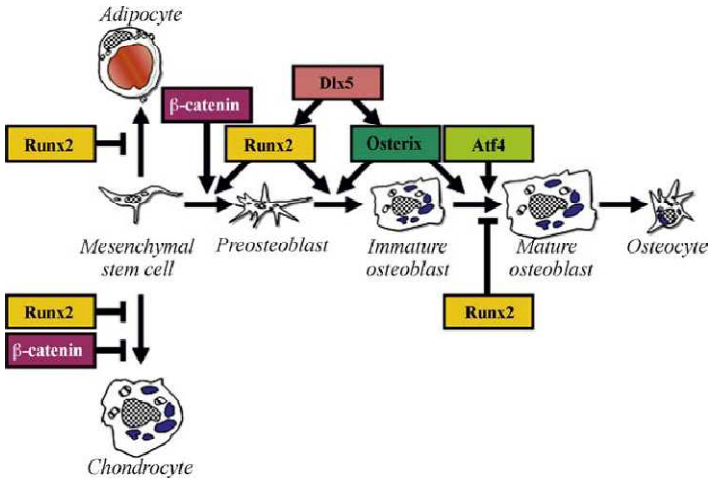

Figure 3. Differentation of mesenchymal stem cells under the influence of transcription factors (Senta et al., 2009).

Bone morphogenesis

The processes and molecular involvements in bone healing are the same occurring in normal bone and cartilage tissue development: the sequential bone morphogenesis as response to demineralised bone matrix mimics the early stages morphogenesis in the limb in embryos and the fracture-healing in adults. Bone development can occur by two mechanisms:

- **intramembranous bone formation** where mesenchymal cells differentiate along a preosteoblast to osteoblast line.
- **endochondral bone formation** characterized by the initial synthesis of cartilage followed by the endochondral sequence of bone formation.

Flat bones, such as the bones of the skull, develop during embryogenesis by the process of intramembranous bone formation. Fractures of intramembranous bone are repaired in the same way, by differentiation of MSCs into osteoblasts. Long bones exhibit endochondral development so a calcified cartilage template of the bone is formed first and is then replaced by bone, while fractured long bones exhibit characteristics of both intramembranous and endochondral bone formation (Stocum, 2006).

Bone morphogenesis cascade is a sequential process with three key phases: chemotaxis, mitosis and differentiation of mesenchymal cells into cartilage (with a subsequent replacement of cartilage by bone) or into osteoblast precursor cells (osteoprogenitor, pre-osteoblast) followed by maturation of osteoblasts, formation of matrix, and finally

mineralization. The sequential cascade (represented in Figure 4) begins with the binding of plasma fibronectin to the implanted demineralised matrix: this facilitates mesenchymal cells chemotaxis and adhesion that occur at the first day and which have its maximal proliferation on day 3. Chondroblast differentiation is evident on day 5. Maximal chondrogenesis is observed on days 7-8. On day 9, cartilage hypertrophy is observed, with concomitant mineralization of the cartilage matrix. Angiogenesis and vascular invasion is a prerequisite for osteoblast differentiation and is maximal on days 10-11.

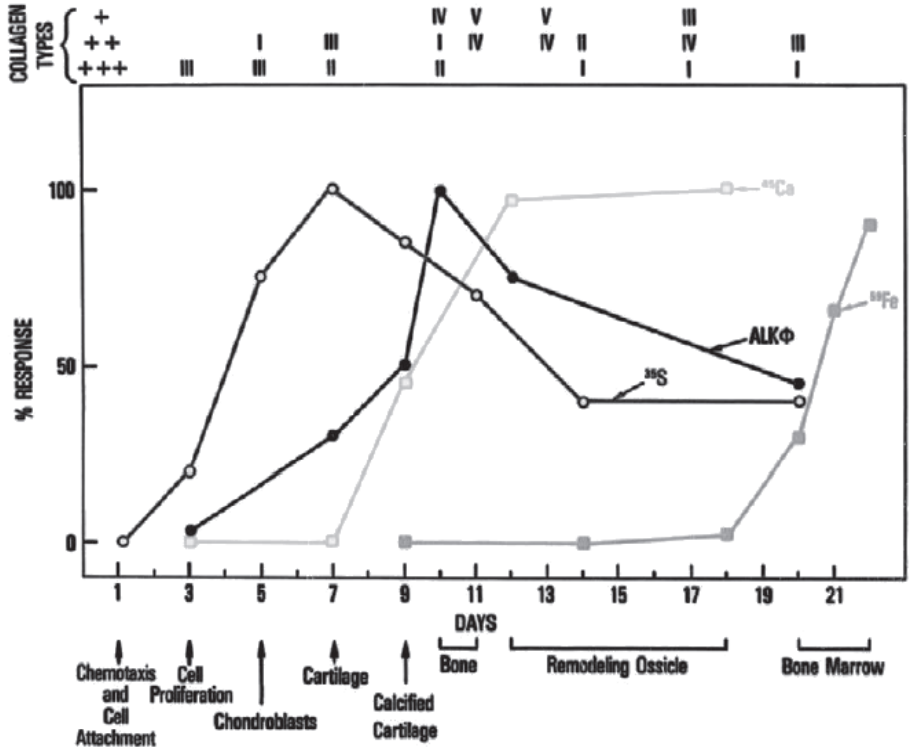

Figure 4. Developmental sequence of extracellular matrix–induced cartilage, bone, and marrow formation. Changes in $^{35}SO_4$ incorporation into proteoglycans and ^{45}Ca incorporation into the mineral phase indicate peaks of cartilage and bone formation, respectively. The ^{59}Fe incorporation into heme is an index of erythropoiesis. The values for alkaline phosphatase (ALK) indicate early stages of bone formation. The transitions in collagen types I to IV, summarized on top of the figure, are based on immunoflorescent localization polymorphonuclear leukocytes (Reddi, 2007).

The initial event is **chemotaxis**, the directed migration of cells as response to chemical signals released from the insoluble demineralized bone matrix. This one is predominantly composed of type I insoluble collagen and is the support for the attachment and the

proliferation of MSCs. Resorbing bone has been shown to produce chemotactic factors for cells with osteoblast characteristics *in vitro*. One mediator that may be responsible for this effect is TGF-β, (transforming growth factors-β) because active TGF-β is released by resorbing bone cultures and it is chemotactic for bone cells. Structural proteins such as collagen could also be involved, since type I collagen and its fragments cause the same effect.

The second event involved in the formation phase of the coupling phenomenon is the **proliferation** of osteoblast precursors. This is likely to be mediated by osteoblast derived growth factors and those growth factors released from bone during the resorption process. There are several leading candidates which represent autocrine and paracrine factors. These include members of the TGF-β superfamily and several other growth factors that are sequestered in bone matrix and stimulate osteoblast proliferation, including insulin-like growth factors (IGF) I and II, fibroblast growth factors (FGFs) and platelet-derived growth factors (PDGF).

The third event of the formation phase is the **differentiation** of the osteoblast precursor into mature cell. Several of the bone-derived growth factors can cause the appearance of markers of the differentiated osteoblast phenotype (as reported in Figure 4), including expression of alkaline phosphatise activity, type I collagen, and osteocalcin. The most important of these are IGI-I and bone morphogenetic protein-2 (BMP-2), which is a member of the TGF-β superfamily. The resorption lacunae are usually repaired completely, although it is not known how this is achieved (Hill, 1998).

1.1.4 Injury-induced regeneration of bone

Injury initiates a cascade of healing events that recapitulate some of the steps of embryonic bone formation and are described in three biological stages: inflammation, repair and remodeling.

Bone fracture healing occurs in a sequential progression of overlapping biomolecular sequences and requires the coordinated contributions of a variety of cellular activities (Mistry and Mikos, 2005). The initial acute inflammatory response entails the formation of a hematoma. This phase is followed by the repair phase, which involves osteoblasts in the formation of woven bone named “bony callus”. Gradually, the third phase of healing, the remodelling, reshapes and reorganizes collagen fibres forming mechanically strong lamellar bone. In a long bone, the regeneration, during the repair process, is accomplished primarily by

MSCs in the periosteum (Figure 5). Following fracture, blood vessels are torn, resulting in the formation of a fibrin clot, the hematoma, in and around the break. Hypoxia results in osteocyte death for a limited distance on either side of the fracture. Platelets in the clot release PDGF and TGF-β, and they initiate an inflammatory phase in which the hematoma, mainly consisting of fibrin and fibronectin, is invaded by neutrophils and macrophages. Some of the macrophages in the bone marrow become osteoclasts degrading the matrix of the dead bone. The hematoma is essential to wound healing as it provides a matrix into which cells then migrate. Within a few days after fracture, periosteal MSCs differentiate on both sides of the fracture to osteoblasts (hard callus) in a process of direct, or intramembranous, ossification. The osteoblasts secrete a bone matrix rich in Type I collagen, and containing osteocalcin, glycoproteins, osteonectin, osteopontin, bone sialoprotein II (BSP-II), and numerous proteoglycans.

The phases of repair appear to recapitulate the events of embryonic endochondral bone development through a cartilage template. MSCs in the periosteum, endosteum, and bone marrow proliferate to form a “soft callus.” These MSCs condense and differentiate into chondrocytes that secrete cartilage-specific matrix composed of Type II and XI collagens, aggrecan, hyaluronic acid, and fibronectin.

The chondrocytes undergo hypertrophy that is characterized by a switch to the production of Type X collagen with a down-regulation of the other collagen types. Subsequently, the cartilage matrix becomes calcified and the chondrocytes apoptosis occurs. Osteoclasts excavate the matrix of this calcified matrix template, and periosteal capillaries, induced by angiogenic factors produced by the hypertrophic chondrocytes, invade the matrix. The invading blood vessels are accompanied by MSCs that differentiate into osteoblasts, which replace the cartilage matrix with bone matrix. Presumably, the balance between bone matrix resorption and synthesis during fracture repair is maintained through the same systemic and local signals as in the maintenance regeneration of bone (Stocum, 2006).

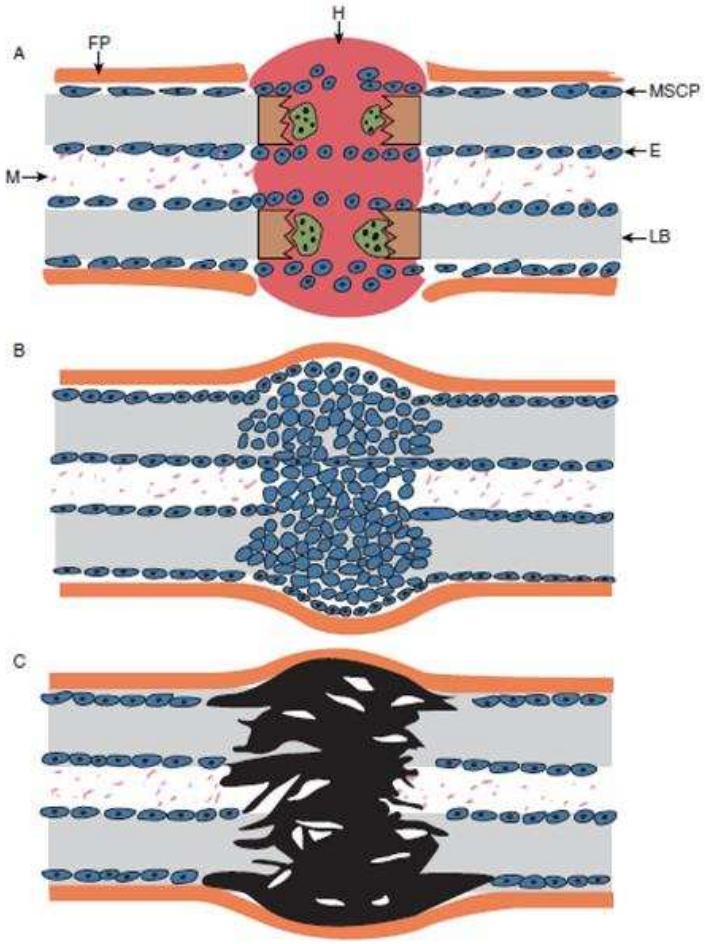

Figure 5. Diagram of fracture repair. (A) Fracture tears muscle, periosteum and blood vessels, leading to the formation of a fibrin clot (hematoma, H) within and around the fracture space. Bone dies (brown) for a short distance adjacent to the fracture space and is degraded by osteoclasts (green cells). Living bone (LB) is indicated in purple. Mesenchymal stem cells (blue) are activated in the mesenchymal stem cell layer of the periosteum (MSCP) and endosteum (E) and migrate and proliferate into the hematoma. FP = fibrous layers of the periosteum. M = marrow (pink dots). (B) Mesenchymal stem cells proliferate to form a soft callus that replaces the fibrin clot. These cells differentiate into chondrocytes (not shown) that form the template for ossification. (C) Blood vessels (not shown) invade the hypertrophied cartilage and osteoblasts derived from perivascular mesenchymal stem cells secrete new bone matrix. The new bone that overlaps the living bone externally on either side of the fracture gap is formed directly from periosteal MSCs without going through a cartilaginous phase (Stocum, 2006).

In terms of the actions that initiate the mechanism of repair leading to successful healing, the first stage that of inflammation, is the most important, because both a favourable biological environment and the mechanical stability need to be established to maximize the opportunity for a successful clinical outcome. Advances in the elements of tissue engineering are designed to aid the normal bone-healing sequence.

1.2 Biomaterials

Application of non-living biomaterials can be conceptualized as the use of materials to replace lost structures, augment existing structures or promote new tissue formation.

The range of applications in orthopaedic field is vast and includes different kinds of material: metals, ceramics, polymeric materials and composite of different components. So,

orthopaedic implants range from non-resorbable materials like titanium alloys that are commonly used for prosthetic devices, to resorbable substitute materials like bone autograft substitutes used as void filler.

In the history of orthopaedic biomaterials it is possible to distinguish three generations of materials used in the implants. Every one of these was characterised by a specific quality that the material had to possess. Initially, elementary requirements such as biocompatibility and sterility led to the idea of creating materials that would possess functional requirements without cause a negative biological response. This was the focal point of the "**first generation**" biomaterials. At that time orthopaedic biomaterials were taken by materials developed for other applications and were projected to be bioinert. They had the physical properties necessary to substitute the damaged tissue, but lacked of interactions with the host organism. Maybe the clearest example of this class of devices are the titanium prostheses used as artificial hips. These materials are still extremely useful, but in the last few decades, advances in the knowledge of the cell-material relationship led to develop the "**second generation**" biomaterials, that were projected to be bioactive or able of eliciting a desired response from the host tissue.

These materials have appeared for the first time between 1980 and 2000. They have the capability to interact with the biological environment surrounding the implant enhancing the biological response and the tissue/surface bonding. In this period the first bioabsorbable materials appeared, able to undergo a progressive degradation while new tissue regenerates and heals. The first modification of materials for bone repair had the intent to promote mineralization and binding between the bone tissue and the implant, by the in vivo deposition of a layer of hydroxyapatite at the material surface. An important innovation of these phases of research was the introduction of bioglasses and ceramics, resorbable materials, that when destroyed, release compounds useful for the bone natural reconstruction. By the mid-1980s, these bioactive materials had reached clinical use in a variety of orthopaedic and dental applications, including several bioactive glasses (BGs), ceramics, glass-ceramics and composites. Nowadays more sophisticated surface modifications have been introduced, consisting principally in adsorbed proteins and tethered polymers and biomolecules that promote certain cell responses depending on the final application.

Recently, progress has allowed the development of the "**third generation**" biomaterials, which exploits engineered surfaces to control the interactions biomaterial-host tissue at the molecular level, and regenerate functional tissue. For these biomaterials, the bioactivity and

biodegradability concepts are combined, and bioabsorbable materials become bioactive and vice versa. These materials properties should merge with their ability to signal and stimulate specific cellular activity and behaviour. Molecular modifications of resorbable polymer systems elicit specific interactions with cell integrins and thereby direct cell proliferation, differentiation, and extracellular matrix production and organization.

This generation introduce the concept of biofunctional materials: hybrid materials for orthopaedic implants capable of directing cellular behaviour. The control of cellular behaviour is possible by using bioactive factors that are normally implicated in physiological processes.

A similar know-how has growth only in the recent years as biologists have developed new tools to better understand the numerous cell signalling pathways involved in healing processes. Biological research and development of the "third generation" materials progress in the same direction: when new families of receptors, proteins, ligands and signalling mechanism are discovered, this knowledge is incorporate in systems for tissue engineering and regenerative medicine. Temporary three-dimensional porous structures that stimulate cells invasion, attachment and proliferation, as well as functionalized surfaces with peptide sequences that mimic the ECM components so as to trigger specific cell responses are being developed (Agrawal and Ray, 2001). Tissue engineering and regenerative medicine are recent research areas exploring how to repair and regenerate organs and tissues using the natural signalling pathways and components such as stem cells, growth factors and peptide sequences among others, in combination with synthetic components (Hardouin et al., 2000).

In addition to the combination of the basic tissue engineering triad (cells, signalling and scaffold), there are some processes such as angiogenesis and nutrients delivery that are crucial to stimulate tissue regeneration and must take place right after implantation. Deliveries of biochemical factors and medical drugs, as well as control of cell behaviour through mechano-transduction are some fields of interest. Polypeptide growth factors are powerful regulators of a variety of cellular behaviours, including cell proliferation, migration, differentiation, and protein expression, and these molecules are being developed as important therapeutics in tissue regeneration (e.g. in closing bone defects and in healing chronic ulcers in the skin).

Two alternative routes of repair are now available with the use of these tailored biomaterials:

- *Tissue engineering.* Progenitor cells are seeded onto modified resorbable scaffolds. The cells grow outside the body and become differentiated and mimic naturally

occurring tissues. These tissue-engineered constructs are then implanted into the patients to replace diseased or damaged tissues. With time the scaffolds are resorbed and replaced by host tissues. Clinical applications include repair of articular cartilage, skin, and the vascular system, although stability of the repaired tissues needs improvement.

- *In situ tissue regeneration.* This approach involves the use of biomaterials in the form of powders, solutions, or loaded microparticles to stimulate local tissue repair. Bioactive materials release chemicals in the form of ionic dissolution products, or growth factors such as BMPs, at controlled rates, by diffusion or network breakdown that activate the cells in contact with the stimuli. The cells produce additional growth factors that in turn stimulate multiple generations of growing cells to self-assemble into the required tissues in situ along the biochemical and biomechanical gradients that are present. For example, when a particulate of bioactive glass is used to fill a bone defect there is a rapid regeneration of bone that matches the architecture and mechanical properties of bone at the site of repair. Both osteoconduction and osteoproduction occur as a consequence of rapid reactions on a bioactive glass surface (Hench and Polak, 2002).

The delivery of growth factors and the adoption of bioactive materials with adhesive surfaces are good examples of the latest developments in the field of new bone graft substitutes.

1.3 Bone graft substitutes

In many cases, the loss of bone due to surgery, accidents or normal aging requires the substitution of bone in order to facilitate the rehabilitation of the patient. Nowadays, the need for bone substitutes includes autograftings procedures, allografting procedures or synthetic bone substitutes.

Autografting, which represents about 58% of the current bone substitutes, involves harvesting a bone from one location in the body patient (as for instance from the pelvic region) and transplanting it into another part of the same patient. Advantages of this technique are obvious, the principal being the elimination of immunogenicity problems but there are also some drawbacks as the additional surgical costs, for the harvesting procedure, infection, pain at the site of harvesting site.

The **allografting** procedure consists in harvesting and processing bone from a live or deceased donor and then transplantating it into the patient. These implants are acellular and are less successful than autografts implants for reasons attributed to immugenicity and the absence of viable cells. Besides the risk of transmitting diseases is another important disadvantage.

Due to complications related to these procedures, bone graft substitutes made with synthetics materials or partially synthetic bone replacement materials (**alloplastic implantation**) are becoming very important in bone substitutions procedures.

The main indications for bone substitutes will be in spinal fusion, hand surgery, bone defects, osteoporotic fractures, revision surgery, and vertebroplasty (Rodriguez et al., 2004).

The utilization of biomaterial should be fulfilling an entire series of requirements. Biomaterial attempt to obtain bone healing through the amount and the quality of new bone formation, the acceleration in which new bone formation and healing is positively influenced, and finally, to produce an autogenic bone transplant which is prone to mechanical stress.

Table 1. Classification of bone graft substitutes based on properties (Rodriguez et al., 2004).

	Description	*Classes*
Osteoconduction	Provides a passive porous scaffold to support direct bone formation	Calcium sulphate, ceramics, calcium phosphate, cements, collagen, bioactive glass, synthetic polymers
Osteoinduction	Induces a differentiation of stem cells into osteogenic cells	Demineralized bone matrix, BMPs, growth factors, gene therapy
Osteogenesis	Provides stem cells with osteogenic potential, which directly lays down new bone	Bone marrow aspirate
Combined	Provides more than one of the above	Composites

The ideal bone graft substitute should be osteogenic, biocompatible, bioabsorbable, able to provide structural support, sterile and easy to use at sterile conditions in operating room and cost-effective. The bone grafts can be divided according to their properties of osteoonduction, osteoinduction and osteogenesis as indicated in Table 1.

Other requirements are linked to the final application. Ideally, a paste-like consistency as well as low viscosity makes it injectable with a large luminous cannula with a processing time of 10–20 minutes. From the physical point of view, it is necessary that the bone replacement materials be prone to mechanical stress and be as elastic as healthy bone. Finally, chemical inertia and neutral pH substances are the preferences.

Another classification is provided on the basis of the material:

- **Class I**. Biological-organic material: This class deals with bone matrix extract, i.e. fraction extracted or obtained out of the organic phase of the bone tissue. They are categorized into the following subgroups:
    - Bone matrix (mineralized and demineralised)
    - Bone matrix extract from demineralised bone matrix fraction obtained after gelatinating bone collagen
    - Extracted recombinant bone growth factor, like BMPs or after protein sequence analysis and DNA-Mapping gene-technologically manufactured bone growth factor, such as rh-BMP-2 (recombinant human BMP-2)
    - Chemotactic, proliferative-inductive, auto- and paracrin-like acting non-specific bone factors.

- **Class II**. Synthetic-inorganic materials: This class will essentially summarize the calcium-phosphate ceramics. These can be divided into five subgroups:
    - Monophasic-synthetic connection (e.g. Ceros®)
    - Corals or alga; analoga hydrothermally manufactured into Hydroxyapatite ceramics (e.g. Biokorall®, Interpore®)
    - Hydroxyapatite obtained from bovine cancellous bone after thermal sintering (e.g. Endobon®, Pyros®, Bio-Oss®)
    - Polyphasic calcium-phosphate ceramic or glass ceramic
    - Composition of calcium-phosphate bone cement (e.g. Norian®, SRS®)

- **Class III.** Synthetic-organic-connective materials: this class summarizes the organic polymers and their combinations. The subgroups are differentiated as:
    - Polyesters
    - Polyaminoacids
    - Polyanhydrides
    - Polyorthoesters
    - Polyphosphates
- **Class IV.** Composites: this latter class deals with a mixture or combinations of materials from the above mentioned Classes.

Many commercial preparations exist with peculiar shapes and components. One example for the first class is the product named Targobone® (Biomet Merck) that is a natural excerpt from collagen bovine bone matrix, the product is supported by an antibiotic component (Teicoplanin) and is consequently suitable for application in infected and infect-threatened areas. Its corresponding non antibiotic loaded is the product Colloss® (Biomet Merck). Another product belonging to the first class is Tutoplast® (Tutogen Medical GmbH) that is available in different construct shapes cylinder, block, or granulate and is derived from bovine or human.

An example of a product of the second class is the Biobon® (Biomet Merck) that is a manufactured absorbent, completely synthetic, microcrystalline calcium-phosphate cement. Morphologically it presents a paste-like consistency formed after mixing the calcium-phosphate powder with the saline solution. The paste will harden at body temperature. A β-tricalcium phosphate (β-TCP) synthetic spongiosa replacement material is represented by ChronOs® (Synthes). This product can be processed as a liquid as well as a product with a paste-like consistency, but it can also be found as a granulate or in a solid block form. Similar to this one is the Cerasorb® (Curasan) that is a β -TCP ceramic in granulating form. It pertains to a synthetic pure-phase product which is completely reabsorbable (an example of application is reported in Figure 6) (von Friesen and Schäfer, 2006).

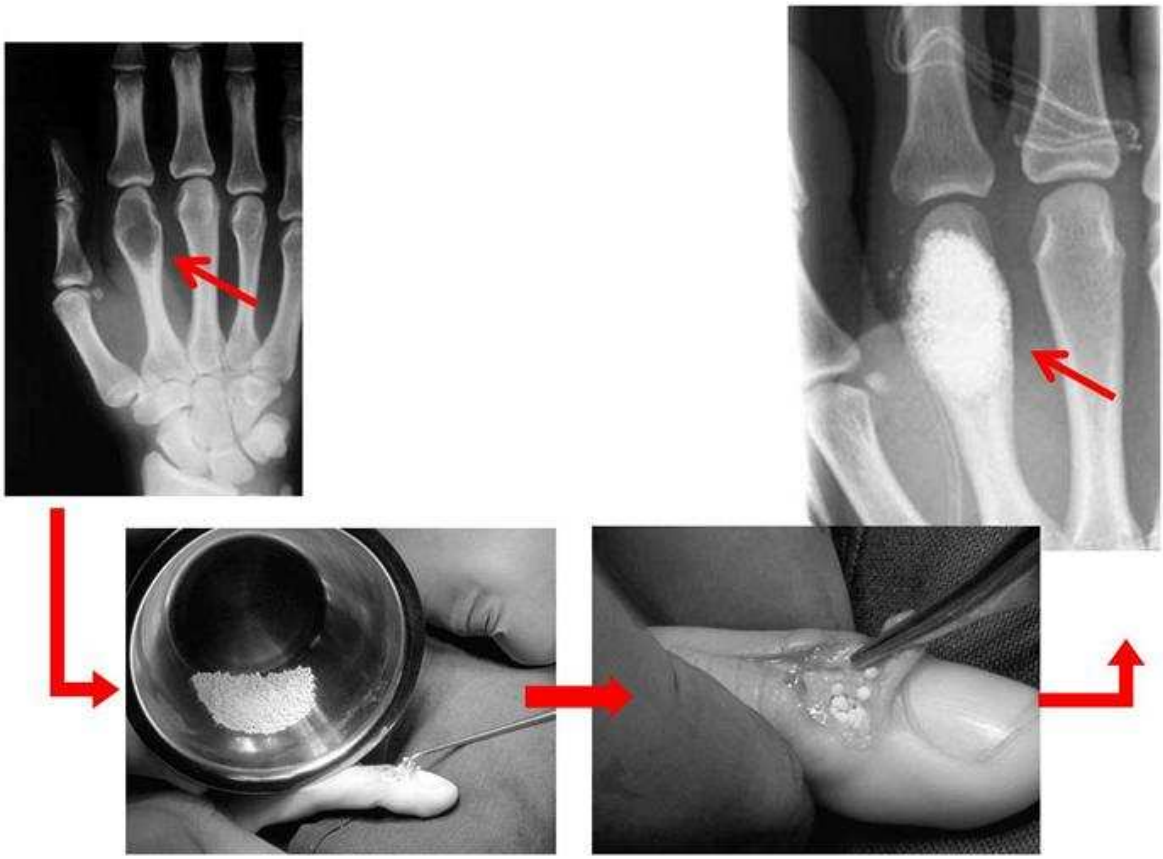

Figure 6. Example of Cerasorb® granulate application in hand surgery: the product was used as bone substitute after enchondroma removal (von Friesen and Schäfer, 2006).

The choice of the opportune bone replacement material is based on the conditions and the quality of bone to be operated, and could be hard block or cylinder of bovine bone, a good molded and applicable bone cement, a cotton swab-like lyophilized collagen possibly with an antibiotic additive, or a granulate. The improvements in the project of new bone replacement materials is directed to absorbable materials that will be replaced and regenerated by new bone during the absorbency process (von Friesen and Schäfer, 2006). The research is moreover involved in the use of additional components such as new antimicrobial components, osteogenic factors (OP-1 (Osteogenetic Protein-1) or BMPs) and components mimicking extracellular matrix.

1.4 Developing bioactive composite for bone graft substitutes

Bone tissue may be considered as a template in the construction of new materials for hard tissue replacement. Ideally an artificial implant temporarily replaces the function of the damaged bone and subsequently induces a regeneration of the natural tissue. This behaviour can be achieved by designing the artificial bone using biocompatible materials which degrade slowly after implantation as the body heals, and which contain biologically active phases and/or molecules that stimulate the regenerative tissue growth. As already stressed, bone is a natural composite material constituted by collagen and hydroxyapatite. To engineer bone composite properly it should split the materials, developing them independently, creating the best analogues to each constituent and then recombining them in a manner that provides function in an orthopaedic procedure. This will, no doubt, change with the future offering replacement bones and bone segments "grown" (Kay, 2007).

1.4.1 Bioactive bioceramics

Bone hydroxyapatite is one of the biological apatites that constitute the mineral phase of calcified tissues in the body. Using a synthetic compound that is similar to this one is perceived to be advantageous for replacing the hard tissue over other synthetic materials (Wang, 2003).

These synthetic substrates, capable of supporting the natural process of bone remodelling, were used mainly in bone tissue engineering applications. These include the *ex vivo* generation of cell-scaffold complexes, in vivo resorbable bone cements, coatings that enhance the bonding of natural bone to the implant, various forms of prostheses and bone-repair agents. Among the materials used for bone tissue engineering, ceramics are most frequently exploited in bone-replacement strategies. These are:

- Hydroxyhapatite: $[Ca_{10}(PO_4)_6(OH)_2]$
- β-tricalcium phosphate (β-TCP): $[Ca_3(PO_4)_2]$
- HAp/ β-TCP bi-phase ceramics
- Bioglass® and A-W glass–ceramic

Calcium phosphate materials have various degrees of stoichiometry. HAp is the most frequently used among calcium phosphate compounds being one of the main natural components of the bone. Other calcium phosphate materials recommended in bone tissue engineering include octacalcium phosphate, whitlockite or magnesium-substituted tricalcium

phosphates, zinc-substituted tricalcium phosphate, carbonate-substituted apatites and fluoride-substituted apatites. Substitution of single elements in the calcium phosphate or apatite structure, affects the crystal and dissociation properties of calcium phosphate. Carbonate substitution, for example, causes not only the formation of smaller and more soluble apatite particles, but also better pH stability. On the other hand fluoride incorporation has the opposite effects upon material degradation, having no effect on the pH stability. Magnesium or zinc substitution in different calcium materials also affects the properties, for instance magnesium incorporation in apatite is limited but causes a reduction in cristallinity (smaller crystal size) and increases the extent of dissolution. Moreover, the properties of ceramic materials can be influenced by the fabrication process. Parameters like porosity, crystal size, composition, and dissolution largely affect the destiny of the material *in vivo* and *in vitro* (Dorozhkin, 2009). Due to their ionic, hydrophilic composition, ceramic materials have a particular affinity to bind proteins. They may therefore be suitable carriers for bioactive peptides or bone growth factors. However, it is important to note that although calcium phosphates biomaterials are osteoconductive, they do not have osteoinductive properties, meaning that they are unable to support *de novo* bone tissue generation at non-bony sites (Rodriguez et al., 2004).

Bioglass® is a family of bioactive glasses that contain SiO_2, Na_2O, CaO and P_2O_5 in specific proportions. A particular advantage is its ability to bond to both hard and soft tissues. The primary limitation of Bioglass® is its mechanical weakness and low fracture toughness due to an amorphous two-dimensional glass network. The bioactivity of A-W glass-ceramic, a product structurally similar to Bioglass®, is much higher than that of sintered HAp. A-W glass-ceramic possesses excellent mechanical properties and therefore has been used clinically for iliac and vertebrae prostheses and as intervertebral spacers.

Bioceramics such as HAp, β-TCP, Bioglass® and A-W glass may be used in the form of particulates as reinforcing phase in bioactive bone tissue substitutes (Wang, 2003).

1.4.2 Biomedical polymers

Polymers are incredibly versatile structures. Synthetic polymers are obtained by copolymerization of conventional monomers to achieve nearly monodisperse molecular weights distributions. It is possible to produce polymers containing specific hydrophilic or

hydrophobic entities, biodegradable repeating units, or multifunctional structures that can become points for three-dimensional expansion of networks.

Among biocompatible and **bio-stable polymers**, there are a few polymers as potential matrices of bone analogues. Although PE (Polyethylene) is the leading candidate due to its proven record as biomaterial and its ductile characteristics, polymers such as PEEK (Polyether Ether Ketone) and PSU (Polyether sulphone) can also be considered as matrix polymers in bone-substituting composites.

If a **biodegradable** tissue substitute is required, composites based on polymers such as PLA (Poly lactic acid), PCL (Poly(ε-caprolactone) and PHB (Poly(2-hydroxybutyrate) may be produced (Seal et al., 2001). On the other side, **natural polymers** (biopolymers) are extremely interesting for industrial and biomedical applications: there is a large availability of the raw materials, they are biocompatible, biodegradable and their use has a minor ecological impact with respect to synthetic approaches. Based on their chemical structure and their physical properties, hydrogels are able to perform many functions for tissue engineering. Firstly, hydrogel can function as cell carriers, supporting the three-dimensional growth of cells. In this case hydrogels must be biocompatible in order to prevent interference with the proliferation and growth of adhering cells. Moreover the hydrophilic material has to provide a sufficient number of adhesion sites to allow close contact between the cells and the material. In addition, most hydrogels must be chemically modified through the introduction of cell adhesion ligands which can be for instance small peptides that associate with cell surface receptors.

Another possible function of hydrogels in tissue engineering includes their application as a carrier for drugs, a technique which is frequently used in conventional drug-delivery systems.

As a final application, hydrogels can also be usesd as “space fillers” for various tissues that are not capable of being restored or replaced in a short time. Here the hydrogels offer the ability to act as a template to guide the growth of repair cells and, with the support of incorporated drug substances, they are able to control their differentiation and overall behaviour.

Based on their final application, many different polymers can be chosen to provide suitable hydrogels for tissue engineering. Natural polymers comprise a large range of materials, from mammalian ECM to polymers derived from plants like algae. All these polymers have weak intrinsic gelling capacity, but chemical modifications or physical filling increase their stability (Teßmar et al., 2009).

Naturally derived materials have frequently been exploited in tissue engineering applications because they are either components of the natural extracellular matrix (ECM) or have similar macromolecular properties. For example, collagens, fibrin, hyaluronan or some proteoglycans are the main components of hard-tissue ECM of vertebrates. Non-mammalian molecules like alginate and chitosan are candidates for bone biomaterials.

Collagens and fibrin

Collagens are attractive materials for bone and cartilage tissue engineering, as this group of secreted proteins is present in skeletal tissues, where they constitute the main substrate of the ECM. Whereas type I collagen is the predominantly expressed collagen found in bone tissue, type II collagen is present in the ECM of cartilage. The basic structures of collagen is composed of three polypeptide chains, building up a three-stranded rope structure. The various types of collagen are naturally degraded by secreted collagenases. Collagen-based biomaterials do not usually provoke a foreign-tissue response. In order to obtain particular mechanical properties, as in the case of scaffolds, it is possible to modify collagen by incubation with chemical cross-linkers (i.e. glutaraldehyde, formaldehyde, carbodiimide), by physical treatments (i.e. ultraviolet irradiation, heating, freeze-drying) or by copolymerisation with other polymers (e.g. polyhydroxyacids).

Fibrin associated with fibronectin, has been shown to support keratinocyte and fibroblast growth both *in vitro* and *in vivo*, and appears to enhance cellular mobility in the wound. Fibrin glue works as an adhesive by emulating the exudative phase of wound healing. Early products were made with human fibrin and thrombin. When the two substances are mixed, the thrombin, in the presence of calcium, converts fibrinogen to fibrin. The resulting fibrin polymer presents a stable structure that facilitates the growth of collagen-producing fibroblasts. Further development has led to the addiction of factor XIII, a fibrin-stabilizing factor present in blood, or aprotinin, which is an antiplasmin that protects the fibrin polymer clot from premature fibrinolysis. Fibrin deposition depends on the relative rates of formation, degradation and dissolution. Fibrin glue has also been shown to be a suitable delivery vehicle for exogenous growth factors that may in the future be used to accelerate wound healing.

Hyaluronic acid

Hyaluronic acid is the simplest glycosaminoglycan, found especially in cartilage tissue. It is an unbranched unsulfated glycosaminoglycane composed of repeating disaccharide units of

D-glucuronic acid and N-acetylglucosamine linked α-(1→4) and β-(1→3) respectively (Figure 7).

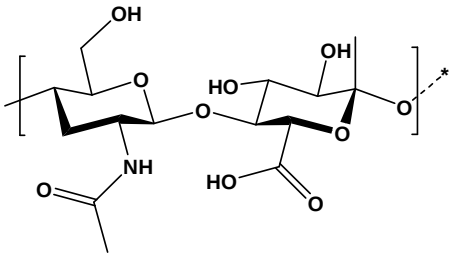

Figure 7.Chemical structure of hyaluronic acid

While hyaluronic acid is produced from *Streptococci* for industrial purposes, it is also present in human connective tissues, where it plays an important role in many biological mechanisms. Hyaluronic acid is mainly found in the cartilage and in the vitreous, where it primarily lubricates body tissue and blocks the spread of invading microorganisms.

The remarkable viscoelastic properties of hyaluronic acid and its complete lack of immunogenicity make it an attractive biomaterial.

Hyaluronic acid possesses several pharmacological properties, as it inhibits platelet adhesion and aggregation, and stimulates angiogenesis, making it suitable for vascular applications (Coviello et al., 2007). Similarly to collagens, hyaluronan is naturally degraded by secreted proteases, termed hyaluronidases, allowing tissue turnover by cells in the skeletal defect site.

Clinically, this polymer is used as a viscoelastic material in ophthalmologic surgery and as an injectable solution for the treatment of joint diseases in orthopaedics as viscosupplementation product (Coviello et al., 2007). More than 20 commercial viscosupplement formulations are available worldwide from different manufacturers. Viscosupplementation is the symptomatic treatment of osteoarthritis by intra-articular injection of exogenous hyaluronic acid or its derivatives. This therapy aims to restore the physiological homeostasis of the pathologically altered joint and induce a restoration of normal hyaluronic acid metabolism.

Hyaluronic acid possesses chondro-protective effects and it is reported to inhibit the loss of proteoglycans from the extracellular matrix of joint cartilage. Hyaluronic acid is also reported to protect the cartilage against proteoglycan loss, chondrocyte cell death caused by free

oxygen radicals or interleukin-1 (IL-1), and against other alterations. In fact, injection of exogenous hyaluronic acid induces a decrease of inflammatory and proliferative processes within the synovium.

In tissue engineering the main application of hyaluronic acid hydrogels has been the regeneration of cartilage and bone. Porous hyaluronic acid scaffolds transplated into osteochondral defects led to bony filling of the defects and growth of hyaline cartilage on the surface (Liu et al., 1999). Supplementing hydrogels with transforming growth factors-β and BMP-2 may enhance bone formation (Bulpitt and Aeschlimann, 1999).

Typical cross-linked hydrogels have improved mechanical properties and degradation rates. For this reason, in order to control physical properties, hyaluronan is presents also as chemically modified, or combined with both collagen and alginate to form composite hydrogels.

Alginate

Alginate is a polysaccharide extracted from marine brown algae that has been used in a variety of tissue engineering applications, because it can be processed as a gel and possess a low toxicity. Alginate as a polymer is composed of polymerized α-L-guluronic acid (G units) and β-D-mannuronic acid (M units) monomers (Figure 8).

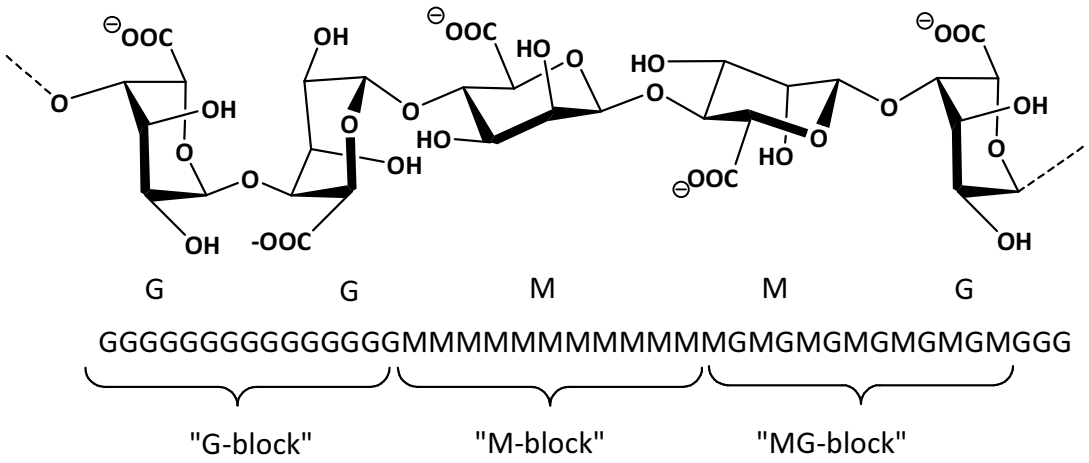

Figure 8. Molecular structure of alginate molecules. G: α-L-guluronic acid; M: β-D-mannuronic acid.

Applications are related to its ability to form ionotropic gel in aqueous solutions. Gels are formed when divalent cations (such as Ca^{2+}, Ba^{2+} and Sr^{2+}) interact with blocks of G units, involving their carboxylic acid groups (Figure below), to form ionic bridges between different

polymer chains. This gel network formation follows the so named “egg-box” model (Donati and Paoletti, 2009).

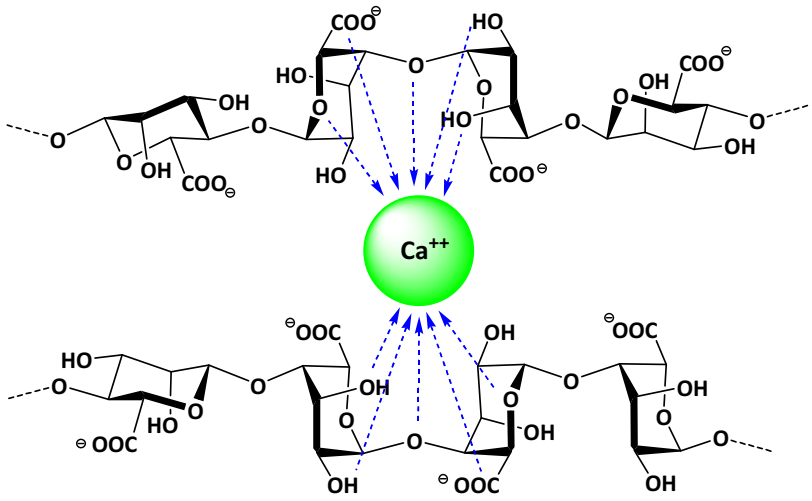

Figure 9. Probable interaction between calcium ion and G residues.

Properties of alginate have been found to be highly affected by the M/G ratio as well as by the structure of the alternating zones. An enzymatic pathway was recently used to obtain sequences with a known M/G ratio and this procedure is potentially very helpful in rationalizing the conformational, and therefore the gelling properties, of the alginate samples (Donati et al., 2005), (Hartmann et al., 2006). The kinetic of the gel formation is usually very fast and the resulting gels are strong enough to be suitable for many industrial and biomedical uses. Many applications of alginate are linked to its capacity to form capsules able to entrap various biomolecules, cells, and inorganic compounds. The entrapment is carried out by mixing an aqueous solution of sodium alginate with the compound, and dripping the mixture into a solution containing divalent cations such as Ca^{2+}, Sr^{2+} or Ba^{2+}. The divalent ions will diffuse into the sodium alginate droplets, instantaneously forming hydrogel spheres entrapping the substance within a three-dimensional network of ionically cross-linked polymer. The size of the resulting capsules is determined by the size of the droplets but the use of different techniques allows the production of capsules with various dimensions.

Encapsulation techniques include (Prüsse et al., 2008):

- **Electrostatic beads generator.** This technique generates µbeads with diameters below 1 mm and down to < 200 µm by establishing an electrostatic potential between the needle feeding the alginate solution and the gelling bath. The electrostatic potential pulls the droplets from the needle tip into a gelling bath. In addition to needle size, adjusting the voltage magnitude easily controls the droplet size.
- **Extrusion through a needle**: Alginate solution is dripped from a syringe with a needle of appropriate diameter directly into a gelling bath. While this method does not require any instrumentation, the size and size distribution of the produced beads are difficult to control.
- **Coaxial air or liquid flow**: The coaxial air jet system is a simple way of generating small beads (down to around 500 µm), although the size distribution will normally be larger as compared to an electrostatic system. A coaxial air stream is used to pull droplets from a needle tip into the gelling bath.
- **Vibrating jet breakage:** A vibrating nozzle generates drops from a pressurized vessel.
- **Rotating jet breakage:** Bead generation is achieved by cutting a solid jet of fluid coming out of a nozzle by means of a rotating cutting device. The fluid is cut into cylindrical segments that then form beads due to surface tension while falling into a gelling bath.
- **Emulsification methods:** An emulsion of alginate in oil can be added to a $CaCl_2$ solution, leading to bead formation. However, the particle size cannot be easily controlled and the capsules tend to coagulate into large masses before hardening properly.

Due to the intrinsic properties of calcium alginate gels biocompatibility, mucoadhesion, porosity, and ease of manipulation, much attention has recently been focused on the delivery of proteins, cell encapsulation, and tissue regeneration. The majority of small and large molecules are currently delivered into patients systemically (e.g. by means of an oral or intravenous delivery), without the use of a specific carrier. Consequently, large doses are usually required for a desired site specific effect because of enzymatic degradation of the drug and non specific uptake by other tissues. This is not only costly, but can result in serious side effects. Thus, an appropriate carrier allowing a local and specific delivery to the desired tissue

site is highly desirable. Calcium alginate gel is reported to be useful for this purpose. To optimize the modulation of drug release from such systems, most studies have focused on improving the mechanical stability and the resistance to erosion in different organic fluids. With this aim, alginate gel matrix surface can be modified by means of macromolecules, which are able to establish ionic interactions with the alginate carboxylate ions. In this way a shell is formed around the alginate gel systems that become more resistant and suitable for numerous applications. For instance, chitosan, chitosan derivatives, and poly-L-lysine were used as typical surface modifying agents.

Another topic, closely related to drug delivery, is the possible use of alginate calcium hydrogels as scaffolds for tissue regeneration and as encapsulating matrices for secretory cells. Nowadays several hydrogel systems exist in which proteins are successfully incorporated into a scaffold and then released. Vascular Endothelial Growth Factor (VEGF) has been incorporated into ionically cross-linked alginate hydrogels and delivered both by diffusion and by mechanical stimulation. It has been pointed out that the bioactivity of VEGF delivered from alginate microspheres was larger than that obtained when VEGF was administered without the microspheres (Lee et al., 2000).

A further application is the *in vivo* engineering of cartilage by injection of autologous chondrocytes loaded into alginate gels.

Finally, alginate has been used to regenerate bone tissue, and alginate hydrogels have been optimized in the cellular interaction ability and degradation behaviour increasing their contribution in this application field. Grafting RGD-containing oligopeptides to alginate molecules increased the differentiation to bone-forming cells in alginate gels, and resulted in an enhanced formation of bone tissue following gel/bone precursor cell implantation (Rowley et al., 1999). Strikingly, cotransplantation of bone and cartilage-forming cells in RGD-modified alginate hydrogels led to the development of structures that structurally and functionally resembled normal growth plates (Alsberg et al., 2002). Accelerating the degradation of RGD-modified alginate-derived gels has also been reported to contribute to the formation of mineralized bone tissue (Lee et al., 2001). To stimulate the growth of bone BMPs naturally derived or synthetic have also been incorporated into alginate gels. BMP-2 derived oligopeptides have been covalently coupled to alginate to control their availability, as simply dispersing the oligopeptides would likely result in a rapid diffusion out of the gels (Suzuki et al., 2000).

Chitosan

Chitosan is another polysaccharide sometimes used as material in tissue engineering applications because of its structural similarity to naturally occurring glycosaminoglycans and its degradability by human enzymes.

Chitosan is a partially deacetylated derivative of chitin, the second most abundant natural biopolymer on earth, which is the main component of the exoskeleton of marine crustaceans and cell walls of fungi. It is a linear polysaccharide of (1-4)-linked D-glucosamine and N-acetyl-D-glucosamine residues.

The main parameters influencing the characteristics of this copolymer are its molecular weight (MW) and the degree of deacetylation (DD), representing the proportion of deacetylated units. In particular, the cristallinity of chitosan, depending on the degree of N-deacetylation, influences the kinetics of degradation. Depending on the source and preparation procedure, chitosan's average molecular weight may range from 300 to over 1000 kDa, with a degree of deacetylation from 30 to 90%. In its crystalline form, chitosan is normally insoluble in aqueous solutions above the pH 7; however, in dilute acids (pH<6), the protonated free amino groups on glucosamine facilitate solubility of the molecule (Athanasiou et al., 2001), (Madihally and Matthew, 1999).

Nowadays chitosan is receiving a great deal of interest for medical and pharmaceutical applications. The main reasons for this increasing attention are the interesting intrinsic properties of this polymer. In fact, chitosan is known for being biocompatible allowing its use in different medical fields such as topical ocular application, implantation or injection (Muzzarelli et al., 1984). Moreover, chitosan is considered as biodegradable because it is metabolized by certain human enzymes, especially lysozyme (Muzzarelli, 1997). This latter is the primary enzyme responsible for in vivo degradation of chitosan through hydrolysis of acetylated residues; other proteolytic enzymes have shown low level of degradation activity on the molecule. Highly deacetylated forms may thus last several months in vivo; eventual degradation of the polymeric chain produces chitosan oligosaccharides of variable length. Moreover, a direct correlation between degree of deacetylation of the chitosan and cell adhesion has been reported (Mao et al., 2004).

It has been demonstrated that chitosan acts as a penetration enhancer by opening epithelial tight-junctions (Kotze et al., 1999). Due to its positive charges at physiological pH, chitosan is also bioadhesive, a property that determines an increase in retention at the site of application.

Finally, chitosan is very abundant, and its production is of low cost and ecologically interesting.

Its positively charged chemical groups are responsible for electrostatic interactions with anionic glycosaminoglycans (GAGs), proteoglycans and other negatively charged molecules. This property is of paramount interest because a large number of bioactive molecules, such as cytokines/growth factors are linked to GAG (mostly with heparin and heparan sulphate), and therefore a chitosan-GAG complex may retain and concentrate growth factors secreted by colonizing cells (Madihally and Matthew, 1999). Moreover, the presence of the N-acetylglucosamine moiety on chitosan also suggests related bioactivities. In fact, chitosan oligosaccharides have a stimulatory effect on macrophages, and both chitosan and chitin are chemo-attractants for neutrophils both in vitro and in vivo.

Host tissue response to chitosan-based implants has been characterized widely: in general, these materials stimulate a minimal foreign body reaction, with little or no fibrous encapsulation (Vandevord et al., 2002). This immunomodulatory effect has been suggested to stimulate the integration of the implanted material by the host (Suh and Matthew, 2000).

Chitosan also promotes wound-healing and has bacteriostatic effects. Studies have shown that chitosan can reduce the infection rate of experimentally induced osteomyelitis by *Staphylococcus aureus* in rabbits. Its cationic amino group associates with anions on the bacterial cell wall, suppressing biosynthesis; moreover, chitosan disrupts the transport across the cell wall accelerating the death of bacteria. Chitosan is used as carrier for drug delivery, thus combining its intrinsic antibacterial activity with that of a bonded antibiotic (Aimin et al., 1999).

When added to HAp and plaster of Paris (calcium sulphate) to obtain a composite for sustained vancomycin or fosfomycin release, the composite material was able to inhibit methicillin-resistant *S. aureus* in vitro for as long as 3 months, a period compatible with the treatment of most orthopedic infections (Buranapanitkit et al., 2004).

Chitosan has been reported to direct the differentiation of osteoprogenitors cells and support the adhesion of human osteoblasts and expression of type I collagen by cells. These findings suggest that chitosan may be a desirable material for bone regeneration.

To enhance the osteoconductivity of chitosan and mechanically reinforce the gels, chitosan has been blended with bioactive inorganic particles, such as HAp, or calcium phosphates, which induce the formation of apatites. These composites were usually processed to provide an in situ forming injectable gel or porous scaffold. Porous chitosan-ceramic composites

exhibited an enhanced compressive modulus and an increased strength, potentially allowing the use of these composites under load-bearing conditions.

Chitosan has been used as a scaffolding material in articular cartilage engineering, due to its structural similarity with various GAGs found in articular cartilage (Suh and Matthew, 2000). Chitosan-based scaffolds can deliver growth factors to promote the growth and biosynthetic potential of chondrocytes. Lee et al. reported on porous collagen/CS/GAG scaffolds loaded with TGF-β1. This scaffold exhibited controlled release of TGF-β1 and promoted cartilage regeneration (Lee et al., 2004).

In addition, cells within composites demonstrated high expression of bone-specific genes and deposition of mineralized phases, *in vitro*. Alternatively, specific growth factors (e.g. BMP-7 and PDGF) have been immobilized in chitosan gels to enhance the osteoconductivity of the chitosan. Release of the growth factors was mainly controlled by the degradation of the gels and regeneration of bone tissues in defect sites was demonstrated.

Chitosan has been combined with a variety of delivery materials such as alginate, hydroxyapatite, hyaluronic acid, calcium phosphate, PMMA (Polymethyl methacrylate), Poly-L-lactic acid (PLLA), and growth factors for potential application in orthopaedics. In conclusion, chitosan offers many possibilities for cell-based tissue engineering: matrix preparations for cell cultures include gels sponges, fibres, or porous compositions of chitosan with ceramic or other polymeric materials such as collagen or gelatine to adjust cell seeding properties and mechanical behaviour of cell transplanted for the intended clinical application (Zhang and Zhang, 2004), (Chenite et al., 2000).

ChitLac

One of the most interesting feature of chitosan as biomaterial is connected with the presence of amino groups located on the glucosamine units. Chemical derivatization based on the reactivity of the glucosamine residues leads to strong modification of the physico-chemical and biological properties of the polycation. Derivatization examples include acylation (Soriler et al., 2001), alkylation (Yang et al., 2005) and carboxymethylation (Muzzarelli et al., 1984).

In this scenario, our group has modified highly deacetylated chitosan by grafting lactose moieties on the free amino groups of the polymer to obtain, the corresponding lactitol derivative by reductive amination.

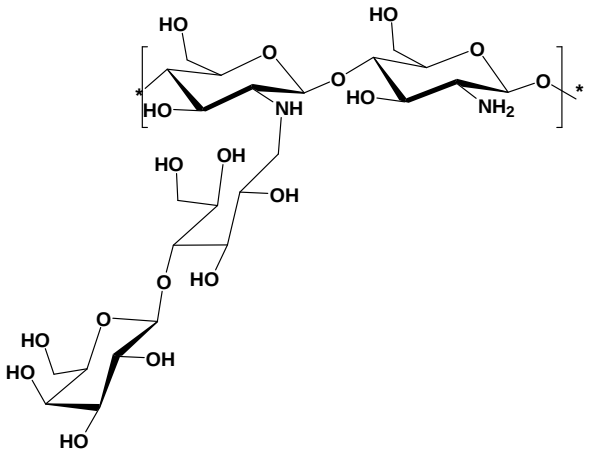

Figure 10. Structure of ChitLac.

A low charged, highly hydrophilic chitosan derivative was obtained, namely ChitLac. This synthetic glycopolymer exhibited the ability to induce chondrocyte aggregation leading to the formation of nodules of high dimensions (up to 0.5–1 mm) within 12–24 hours. It also showed the ability to stimulate the biosynthesis of markers typical of articular cartilage, such as type II collagen and glycosaminoglycans (Donati et al., 2005).

These findings seem promising in the view of a possible application of ChitLac in protocols of tissue engineering applied to the regeneration of articular cartilage. The localization of Chitlac at the plasma membrane of isolated chondrocytes and its permanence at the same site also after nodule formation indicate that the process is mediated by a specific binding of Chitlac to cells, most likely through its β-galactose residues (Donati et al., 2005). Further experiments demonstrated the role of Galectin-1 as a molecular bridge between Chitlac and chondrocyte cell surfaces (Marcon et al., 2005). Galectin-1 is a member of the S-type galactoside-binding animal lectins. The discovery that Galectin-1 binds with high affinity to polylactosamine-containing ligands (such as laminin) and the co-localization of Galectin-1 with laminin in extracellular matrix suggested that its major function could be to promote cell adhesion to glycoconjugates (Ramkumar and Podder, 2000).

Finally, ChitLac was modified with RGD peptide and tested as coating for orthopaedic constructs demonstrating its ability to promote adhesion on osteoblasts (Travan et al., 2010).

CHAPTER 2. **AIMS OF THE STUDY**

It is estimated that more than 500,000 bone-grafting procedures are performed annually in the United States. This reality has stimulated a proliferation of corporate interest in supplying what is seen as a growing market in bone replacement materials. The comparison between efficacy of cellular autografts and synthetic allografts, suggests the implementation of bioactivity of new bone grafts.

The aim of this thesis is therefore the design of a composite injectable filler for bone defects enriched with bioactive properties. The strategy used to develop the final product consists in the preparation of a polysaccharide based gel phase where alginate beads are dispersed. The goal is to prepare materials able to be resorbed by the host without the need to be replaced after implantation. At the same time, their bioactive properties should be improved by the functionalization of the dispersed beads with elements such as adhesion mediators, osteoinductive growth factors and anti-microbial peptides. With this aim, polysaccharidic hydrogels like alginate, lactose modified ChitLac, and hyaluronic acid, have been the first choice as material support, while peptides like RGD motif, BMP-2 fragment and LL-37 were selected to give adhesivity, ostoinduction and antimicrobial properties to the construct.

Every bioactive molecule presents peculiar requests associated with its action mechanisms. The functionalization of materials with the cell recognition motifs RGD promotes cell adhesion: these peptides require a stable linking to a surface to explicate their action, then the importance of an appropriate immobilization strategy is fundamental. On the other hand to make the construct osteoinductive, the use of growth factors or their active fragments, like the BMP-2 epitope fragment, necessitates the development of a delivery system that is able to prolonged release during the time of bone healing, preceded by a fast burst release at the firsts days. Finally, the function of protection against microbial infections can be obtained through the incorporation of a human antimicrobial peptide, like LL-37.

All these aims require specific polysaccharide-peptide conjugation strategies, which encompass both chemical linkage and electrostatic interactions, which have to be optimized and modulated depending on the biological role of the immobilized peptide. At the same time the rheological properties of the gel phase and of the final constructs have to be adequate to the application as injectable filler.

This work was supported by the European project “NEWBONE”, finalized to obtain innovative materials for orthopaedic biomaterials of the last generation.

CHAPTER 3. MATERIALS AND METHODS

3.1 Materials

ChitLac (CAS registry number 85941-43-1) was synthesized starting from commercial chitosan from Aldrich, USA (degree of acetylation 11%, [η]=6.43 dL/g, viscosity-average relative molar mass approximately $6.9 \cdot 10^5$) (Donati et al., 2005). The used degree of substitution was 70%, which leaves 19% of free amines. The estimated relative molar mass of ChitLac was $1.5 \cdot 10^6$. Alginate (sodium salt) from *Laminaria hyperborea* LF 10/60 (F_G=0.69; F_{GG}=0.56; [η]=5.46 dL/g, viscosity-average relative molar mass approximately $1.3 \cdot 10^5$) (Donati et al., 2004) was from Protanal (Norway). Hyaluronic acid ([η]=15 dL/g, viscosity-average relative molar mass approximately $7.75 \cdot 10^5$) was from FMC Biopolymer AS/NovaMatrix (Japan). Dialysis membranes with cut-off of 12.000 were purchased from Sigma-Aldrich Co. (St. Louis, MO). HAp powder was from Fluka (U.S.A.) with an average dimension of the particles of 150 nm as characterized by Turco and co-workers (Turco et al., 2009). Succinic anhydride (Sigma), NHS N-hydroxysuccinimide (Sigma), EDC ethyl-3(3-dimethylaminopropyl)carbodiimide (Sigma), MES 2-(N-Morpholino)ethanesulfonic acid hydrate (Sigma), HEPES 4-(2-hydroxyethyl)piperazine-1-ethanesulfonic acid (Sigma), 2-imminethiolane (Sigma), FITC (fluorescein 5(6)-isothiocyanate (Sigma). 4-pentynoic acid (Sigma). Propiolic acid (Sigma).

Resins and aminoacids form Novabiochem, PyBOP Benzotriazol-1-yloxy)tripyrrolidinophosphonium hexafluorophosphate (Sigma), DIPEA N,N-Diisoopropylethylamine (Sigma)

QuantiPro BCA Assay Kit (Sigma). Alamar Blue™ assay (Biosurce), LDH assay TOX-7 (Sigma). Kaiser test kit (Sigma).

3.2 Methods

3.2.1 GRGDS and CGRGDS synthesis

Solid phase peptide syntheses were performed by using Fmoc-chemistry on Liberty Microwave Peptide Synthesizer (CEM Corporation, Matthews, NC, USA) with a computer-assisted operation system at a 0.24 mmol scale (1 g of PEG-PS resin for each peptide, 0.24 meq/g). Couplings were carried out with PyBOP and DIPEA as activators. Resin with loaded peptide was divided in two parts, to obtain GRGDS and CGRGDS. To obtain GRGDS the

peptide was cleaved from the resin and deprotected using a mixture consisting of trifluoroacetic acid, water, TIPS (triisopropylsilane), thioanisole and DODT (3,6-dioxa-1,8-octane-dithiol) (85:2:2:3:8, by volume).

To obtain the coupling of a Cys, the second part of resin was functionalized in reaction syringe with a preactivated cysteine (Fmoc-Cys(Trt)-OPfp) (MW 751,8) without the use of activators, and a second coupling was performed with (Fmoc-Cys(Trt)-OH) (MW 585,7) and PyBOP and DIPEA as activators. Before the cleavage from the resin, Kaiser's test (using the appropriate kit) was performed on a small fraction of resin.

The crude peptide was precipitated by the addition of *tert*-butylmethyl ether, washed several times with the same ether and its mass was confirmed by ESI-MS spectrometer Bruker Esquire 4000 (Bruker Daltonics, Billerica, MA, USA). The obtained peptide resulted in very good yields and quality and thus no further purifications were necessary.

3.2.2 Synthesis of BMP fragments

Solid phase peptide syntheses were performed by using Fmoc-chemistry on Liberty Microwave Peptide Synthesizer (CEM Corporation, Matthews, NC, USA) with a computer-assisted operation system at a 0.25 mmol scale (1,563 g of resin loaded with Leucine, 0.16 meq/g). The coupling was performed with PyBOP and DIPEA in NMP. Double coupling was carried out for each Leucine, Lysine and Isoleucine, and for Tyrosine, Valine, Proline and Alanine. Fmoc deprotection was performed with a mixture of Pyp and HoBT in DMF. Before the final cleavage, resin with loaded peptide was fractionated in three parts, one of these was functionalized in reaction syringe with 5 eq of 4-pentynoic acid with PyBOP and DIPEA as activators, the coupling was performed one time for two hours. A second part was used to coupling propiolic acid following the same conditions. Finally, peptides were cleaved from the resin and deprotected using a mixture consisting of trifluoroacetic acid, water, TIPS, thioanisole and DODT (85:2:2:3:8, by volume). The crude peptides were precipitated and washed several times with chilled *tert*-butylmethyl ether and their masses were confirmed by ESI-TOF-MS (microTOF Bruker Daltonics). In the case of BMP conjugated with propiolic acid, reaction did not occur. For the other two products, no further purifications were necessary.

3.2.3 Synthesis of LL-37

Solid phase peptide synthesis was performed using the Fmoc-chemistry on a Liberty Microwave Peptide Synthesizer (CEM Corporation, Matthews, NC, USA). The synthesis was carried out at a 0.05 mmol scale (208 mg of PEG-PS resin with a substitution of 0.24 meq/g). Double coupling with O-(6-Chloro-1-hydrocibenzotriazol-1-yl)-1,1,3,3-tetramethyluronium hexafluorophosphate (HCTU) as an acylating agent was carried out at all positions. The peptide was cleaved from the resin and deprotected using a mixture consisting of trifluoroacetic acid, water, and triisopropylsilane (95:2.5:2.5, by volume). The crude peptide was obtained in high yield and was precipitated and washed several times with chilled *tert*-butylmethyl ether. Its mass was confirmed by ESI-MS using a Bruker Esquire 4000 instrument (Bruker Daltonics, Billerica, MA, USA). No further purification was necessary since homogeneity of the peptide was >95% in analytical RP-HPLC.

3.2.4 ChitLac synthesis

The synthesis of lactose-modified chitosan (ChitLac) was performed according to the procedure reported by Yalpani and co-worker (Yalpani and Hall, 1984).

Briefly, chitosan (200 mg) was dissolved in 14 ml of a mixture 1:1 of methanol and acetic acid 1% (pH 4.5); 8 ml of the same methanol:acetic acid solution containing lactose (840 mg) and sodium cyanoborohydride (350 mg) were slowly added. The obtained solution was then incubated under stirring at room temperature for 24 hours. At the end of the reaction 60 ml of water were added and the reaction mixture was dialyzed exhaustively against deionized water, filtered through 0.45 μm Millipore filters and the polymer recovered by freeze-drying.

3.2.5 Synthesis of succinyl-ChitLac

150 mg ChitLac (0.40 mmol) was dissolved in 30 mL of a bicarbonate buffer 50 mM at pH 9 and a solution of 10 equivalents (corresponding to 90 mg) of succinic anhydride (MW 100.08 g/mol) dissolved in 0.5 mL of DMF solvent with 1.5 equivalents of NHS, corresponding to 156.30 mg (MW 115.9) was added.

The obtained solution was then incubated under stirring at room temperature overnight and then dialyzed against deionized water and lyophilized.

The substitution degree was determined by NMR spectroscopy.

3.2.6 Synthesis of thiolated ChitLac

200 mg of ChitLac (0.54 mmol) were solubilized in 30 mL of an aqueous solution of 1% acetic acid (pH 6) under nitrogen. The solution was stirred at RT for 1h.

10.7 mg (0.08 mmol) of 2-imminethiolane (MW 137.5) or 35.7 mg (0.26 mmol) were added calculating respectively 0.6 and 2 equivalents of 2-imminethiolane with respect to the free amines. The solution was further stirred under nitrogen at RT overnight. At the end of the reaction, the solution was dialyzed as follows:

1. against HCl 5 mM
2. against HCl 5 mM + 1% NaCl
3. against HCl 5 mM + 1% NaCl
4. against HCl 5 mM

and freeze-dried.

The total substitution degree was determined by ^{1}HNMR spectroscopy. The free thiol groups were determined by Ellman's test.

3.2.7 Synthesis of ChitLac-(CONH)-RGD

76.2 mg (0.18 mmol) of succinyl-ChitLac (410.56 g/mol PUR) were dissolved in 15 mL 0.2 M MES buffer at pH 6.5).

Separately a second solution was prepared containing NHS and EDC activators. Amounts of activators were calculated using the ratios: [EDC/COOH = 2.5] (where COOH reactive groups corresponds to the 24% of mol of repeating unit) and [NHS/EDC = 0.2]. 2.3 mg (0.02 mmol) of NHS (MW 115.9 g/mol) and 20.6 mg (0.11 mmol) of EDC (MW 191.7 g/mol), were dissolved in 1 mL of MES buffer and then added to the succinyl-ChitLac solution. The reaction mixture was then incubated under stirring at room temperature for 15 minutes.

Finally, a solution containing 1.8 equivalents of peptide GRGDS (MW 490.47 g/mol) (corresponding to 37.3 mg, or 0.076 mmol) was added drop by drop. The obtained solution was then incubated under stirring at room temperature overnight and then dialyzed against deionized water and lyophilized.

The functionalization was calculated by recovering the amount of arginine in the hydrolysed by capillary electrophoresis.

3.2.8 Synthesis of ChitLac-(NCO)-RGD

96.0 mg of ChitLac (0.26 mmol) were dissolved in 20 mL of 25 mM MES buffer (pH 6.5).

68.7 mg (0.14 mmol) of the peptide GRGDS (2 equivalents with respect to the free amine groups) (MW 490.47) were dissolved in 1 mL of buffer and activated with 66.8 mg (0.35 mmol) of EDC (MW 191.7 g/mol) and 8.1 mg (0.07 mmol) of NHS (MW 115.9 g/mol). The ChitLac containing solution was then added and the mixture was stirred overnight at room temperature. At the end of the reaction, the solution was dialyzed and freeze-dried.

The functionalization was calculated by recovering the amount of arginine in the hydrolysed by capillary electrophoresis.

3.2.9 Synthesis of ChitLac-FITC

100 mg of ChitLac (0.27 mmol) were dissolved in 33 mL of 0.5 M sodium bicarbonate buffer. After the total dissolution an aqueous solution of FITC 5 mg/mL was added. Reaction was stirred for 24 hours at RT and then dialysed first against 0.1 M sodium bicarbonate and then against water. The purified solution was freeze-dried.

3.2.10 Synthesis of the linker for BMP conjugation

2 mL of δ-valerolactone were solubilized in 11 mL of a 3N NaOH solution to hydrolyze the lactone. After 24h 2 mL of the obtained δ-hydroxypentinoic acid were acidified at pH 6 with HCl and added to 25 mL of a 0.5 M MES buffer, pH 6. A solution containing EDC (1.5 mg) and NHS (190 mg) dissolved in 1 mL of the same buffer was added and after 10 minutes 250 μL (1.25 mmol) of O-(2-azidoethyl)-O'-[2-(diglycolyl-amino)-ethyl]heptaethylene glycol (Fluka) were added to the solution, which was stirred overnight.

Solvent was evaporated and the mixture was re-dissolved in methanol and filtered on paper. The liquid phase was eluted on a flash column (eluent: chloroform/methanol from 95/5 to 90/10). Yield: 45%

77 mg (0.25 mmol) of the product were dissolved in 2 mL of pyridine and 1.11 g (11.1mmol) of succinic anhydride (MW 100.08 g/mol). The mixture was stirred overnight. Pyridine was than co-evaporated with toluene. The precipitate was re-dissolved in water, filtered and purified on size-exclusion columns eluted with water. Yield: 30%.

3.2.11 Synthesis of ChitLac-“azido”

75 mg of ChitLac (0.20 mmol) were dissolved in 22 mL of 0.2 M MES buffer, pH 6.2. The linker was solubilised in 2 mL of the same buffer and in a third solution 34 mg of EDC and 3.9 mg of NHS were dissolved in 1 mL of buffer. After a few minutes, solution 3 was added to solution 2, and the resulting mixture was stirred for 10 minutes and added to solution 1. This was stirred overnight, dialyzed against bidistilled water and freeze-dried.

3.2.12 Conjugation of BMP to the polymer (ChitLac-(click)-BMP)

50 mg (0.13 mmol of r.u., 1% substituted with azido group) of the polymer conjugated to the ester were dissolved in 10 mL of bidistilled water. The copper solution was prepared, by solubilising 7.98 mg of $CuSO_4$ and 44 mg of ascorbic acid in 10 mL of water. When the polymer was completely dissolved, 100 µL of the copper solution were added, together with 28 mg (10 equivalents) of the modified BMP peptide. The resulting solution was stirred overnight, dialyzed first against a 10 mM EDTA solution and then against bidistilled water and finally freeze-dried.

3.2.13 Ellman’s test

The quantitative determination of the thiol groups amount was performed spectrophotometrically with Ellman’s reagent (5,5’-Dithio-bis(2-nitrobenzoic acid)) or DTNB (Hornof et al., 2003). With Ellman test it is possible to quantify free -SH groups and disulfide bridges on the polymer.

4 mg of ChitLac-SH were dissolved in 1 mL of water. When the dissolution was complete, the solution was divided in two equal parts and two different treatments were performed on these ones, the first to quantify free thiol groups, and the second one to determine the amount of total thiol group present in the polymer.

Ellman’s test to quantify free thiol groups:

At 500 µL of ChitLac aqueous solution were added 500 µL of 0.5 M sodium phosphate buffer at pH 8 and 1 mL of a solution of DTNB 0.3 mg/mL in buffer.

The reaction solution was stirred for 2 hours at RT and filtered

Ellman’s test to quantify total thiol groups:

At 500 µL of ChitLac aqueous solution were added 500 µL of an aqueous solution of $NaBH_4$ (40 mg/mL).

The reaction solution was stirred for 1 hour at 30°C.

At the end 100 uL of HCl 5M were added drop by drop to deactivate the $NaBH_4$

500 µL of of 0.5 M sodium phosphate buffer at pH 8, and 50 uL of a solution containing DTNB 4 mg/mL in buffer were then added

The reaction solution was stirred for 2 hours at RT and filtered

The DTNB reacts with free thiol groups releasing 2-nitro-5-benzoate (TNB) a yellow compound quantifiable at 450 nm (as indicated in Scheme 1).

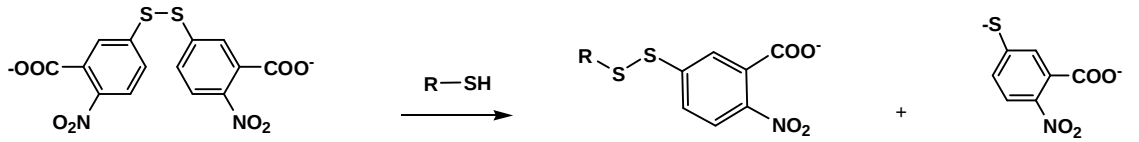

5,5'-dithiobis(2-nitrobenzoate)
DTNB
λ 324 nm

2-nitro-5-benzoate
TNB
λ 450 nm

Scheme 1. Ellman's test.

Sulphydryl groups in samples were estimated by comparison with a standard curve, built using known concentrations of a thiolated compound. In this case, the calibration curve, performed using cysteine dissolved in phosphate buffer, ranges from 6.25 µM to 200 µM. Absorbance was measured in an Agilent 8453 UV-Visible spectrophotometer at 450 nm.

3.2.14 µBCA assay

The commercial kit for µBCA assay (QuantiPro BCA Assay Kit (Sigma)) is a formulation for the detection and the quantification of total protein content. Thos is an adaptation of the BCA assay that permits the identification of diluted proteins concentrations (0.5-20 µg/mL). The method uses the bicinchoninic acid (BCA) as the detection reagent for Cu^+ which is formed when Cu^{2+} is reduced by protein in an alkaline environment. In fact, it has been shown that some amino acids, cysteine, tryptophan, tyrosine and the peptide bond are able to reduce copper ions. A purple-coloured reaction product is formed by chelation of the two molecules of BCA with one copper ion (Cu^+). This water soluble complex exhibits a strong absorbance

at 562 nm that is linear with increasing protein concentration. Some substances are known to interfere with the microBCA Assay including those with reducing potential, chelating agents and strong acids or bases.

Kit provides three components: QA reagent, a mixture of sodium buffers (tartrate, carbonate and bicarbonate) in NaOH 0.2 M at pH 11.25; QB reagent that is a solution of 4% w/v bicinchoninic acid at pH 8.5 and a solution of 4% w/v Copper(II) sulfate pentahydrate.

To quantify the LL-37 peptide content in the supernatant of loaded scaffolds, 150 µL of supernatant were collected each time (at 1, 2, 5 and 24 hours) and the same volume of a solution composed by the three kit components (QA, QB and copper) was added. Samples and standards were incubated at 60°C for one hour. At the end the absorbance was measured at 544 nm. The peptide concentration was calculated by comparison with a standards solution of LL-37 dissolved in the same buffer of supernatants. Calibration curve was achieved in the range 5-120 µg/mL obtaining a good linearity R^2=0.9968.

3.2.15 Quantification of peptides by hydrolysis and capillary electrophoresis

This method permits the quantification of peptides bonded on polymers, on beads surface or entrapped in a substrate.

Analyses were performed on lyophilized RGD functionalized polymers, on dried beads functionalized with RGD peptide and on scaffolds and beads containing LL-37.

In order to verify and quantify the amount of peptide, the product (respectively 2 mg of functionalized polymer, or 5 mg of dried µbeads, or 1 scaffold or 15 wet large beads) were dissolved in 2 mL (or 4 mL in the case of scaffold and large beads) of 6M HCl and stirred at 110°C for 20 h under reflux (Li et al., 2006). After evaporation of the hydrochloric acid, the residue was re-dissolved in 200 µL of capillary electrophoresis running buffer (100 mM borate buffer pH 8.95). The obtained solution was then filtered and the degree of substitution was evaluated by the quantification of Arginine derived from the peptide degradation.

Quantitative analysis was performed by capillary electrophoresis (CE-UV conditions: buffer borate 100mM pH 8.95; potential 15 kV; fused silica capillary total length 64 cm, effective length 56 cm, i.d. 50 µm; wavelength 195 nm). At these conditions, arginine presents a migration time of 3.7 min.

3.2.16 CMC determination by capillary electrophoresis

The analysis was performed in a fused-silica capillary coated (length 56 cm, inner diameter 50 um), with a 20 mM phosphate buffer at pH 7.0 applying a separation voltage of 20 kV in normal polarity and monitored with a UV detector at 350 nm and 195 nm. The procedure consists in the analysis of the sample (the neutral compound Sudan III) dissolved in methanol at increasing concentrations of the surfactant, added to the anode buffer. The migration time of the peak corresponding to Sudan III is a linear function of the surfactant concentration until the c.m.c.: after that it becomes a linear function of micelles concentration. By plotting the migration time of the SUDAN III against surfactant concentration, it is possible to obtain a graph where the intersection of two segments indicates the CMC of the surfactant.

3.2.17 Degradation by esterase

10.2 mg of modified ChitLac were dissolved in 1 mL of 20 mM bicarbonate buffer, pH 8.2. 0.14 mg of esterase from Hog liver (Sigma) were dissolved in 140 µL of the same buffer. 70 µL of this solution were added to the first one and the resulting solution is incubated at 25°C. At regular intervals 15 µL aliquots were sampled.

The action of esterase was tested on the modified polymer and the kinetics of the ester hydrolysis was followed by CE-UV (MECK) and ESI-MS. Capillary electrophoresis analyses were performed at 25°C with a coated capillary (length 54 cm, inner diameter 50 um) and an applied voltage of 20 kV. Preconditioning: 3 min with NaOH, 3 min with H_2O, and 3 min with running buffer.

The running buffer was prepared by mixing a 25 mM borax solution with a 50 mM dihydrogenophosphate solution and adjusting the pH to 7 with phosphoric acid. 1 mmol of SDS was added and the resulting solution was filtered and let stand overnight prior to use.

UV detection was performed following the signal at 270 and 195 nm (quantifications occurred at 195 nm). For quantification of the released molecule, a calibration curve was built in the concentration range of 10-100 mg/L. Hydrolyzed polymer aliquots were analyzed after 1:2 dilution.

3.2.18 Beads preparation

All beads were prepared with hydroxyapatite 3% w/v and alginate 2% w/v *via* gelation in 50 mM $CaCl_2$ solution under stirring. In order to obtain beads with different dimensions to perform various experiments, diverse production techniques were adopted:

- µbeads (about 600-700 µm at the wet state)
- beads of intermediate diameter (about 1 mm at the wet state)
- large beads (about 2 mm at the wet state)

Beads of intermediate diameter

This kind of beads was produced by means of an air coaxial flow and they were used to determine the swelling properties of beads presenting various compositions. The procedure was standardized for all samples fixing the following parameters: distance between the needle and the gelling bath was adjusted to 10 cm, the air-flow was controlled at 12 psi, each time 100 µL of solution containing alginate/HAp or alginate/HAp/ChitLac or alginate/HAp/ChitLac-SH was dripped in 150 mL of $CaCl_2$ 50 mM; beads were magnetically stirred in gelling solution for 7 minutes and after dripping and then they were washed three times in milliQ water; besides the treatment with saline solution was achieved the day after.

By this methodology were produced different kind of beads:

- Beads composed by a mixture of alginate 2% w/v, hydroxyapatite 3% w/v and unmodified ChitLac 0.5% w/v
- Beads composed by a mixture of alginate 2% w/v, hydroxyapatite 3% w/v and ChitLac-SH 0.5% w/v
    - Samples treated with H_2O_2
    - Samples not treated with oxidant
- Beads composed by a mixture of alginate 2% w/v, hydroxyapatite 3% w/v coated with two different percentages of unmodified ChitLac (0.1 and 0.5 % w/v)
- Beads composed by a mixture of alginate 2% w/v, hydroxyapatite 3% coated with ChitLac-SH 0.1% w/v
    - Samples treated with H_2O_2
    - Samples not treated with oxidant
- Beads composed by a mixture alginate 3% and hydroxyapatite 3% with a higher concentration of alginate as control.

The coating of alginate/HAp beads with a polycation was performed by immersing these ones in aqueous solutions at the concentration indicated. For beads obtained by blends of different polysaccharides, the procedure was dissolved the polymer separately in a buffer containing 10 mM HEPES and 150 mM NaCl at pH 7.4. Beads were washed with water three times at the end of each phase and between different steps. The treatment with H_2O_2 was performed by stirring beads in a solution 0.3% v/v H_2O_2.

CLSM µbeads

Fluorescein-labelled beads were obtained by coupling FITC with ChitLac as mentioned.

Microbeads were obtained using an electrostatic beads generator (with a 0.7 µm needle, a voltage of 7 kV and an injector syringe pump with controlled speed) developed at the mechanical workshop at the Departement of Physics at the Norwegian University of Science and Technology (NTNU) in Trondheim (Strand et al., 2002). Layered µbeads were obtained by immersion of 2% w/v alginate beads in an aqueous solution of 0.5% w/v ChitLac-FITC. Mixed beads were achieved by blending of a solution of 4% w/v alginate in 10 mM HEPES and 150 mM NaCl at pH 7.4 and 1% w/v ChitLac-FITC dissolved in the same buffer. Beads were washed with water three times at the end of each phase.

Individual beads were place on a coverslip and mounted on the stage of an inverted microscope LEICA TCS SP2 associated with confocal argon-ion laser scanning microscope with a 63×/1.4 objective. Laser excitation light was provided at a wavelength of 488 nm and fluorescent emissions were collected at wavelengths between 510 and 580 nm. . To obtain an image of the beads core centre, all beads were examined by scanning through an equatorial slice of the capsules.

Microbeads used in biological tests

Microbeads, were obtained using a high-voltage electrostatic bead generator setting 7 kV, with a steel needle with 0.7 mm outer diameter and an injector syringe pump with controlled speed.

2 mL of a mixture of alginate 2% and HAp 3% dissolved in water were dripped in 400 mL of 50 mM $CaCl_2$ and stirred for 30 minutes. At the end, beads were washed three times with water. At this point three different procedures were followed to obtain different kind of µbeads:

- **unfunctionalized µbeads**: in this case no successive treatment were performed and µspheres were directly dried with air flow.
- **µbeads layered with ChtiLac-(NHCO)-RGD**: wet alginate/HAp beads were immersed in a 0.1% w/v aqueous solution of ChtiLac-(NHCO)-RGD for 30 minutes. At the end µbeads were washed three times with water and dried with air flow.
- **µbeads layered with ChtiLac-(SS)-CRGD**: µspheres were immersed in a 0.1% w/v aqueous solution of ChitLac-SH. During the stirring in the presence of the polycation, a layer of this one is deposited on the bead surface, where it remains electrostatically bound. At the end of the process, beads were transferred to a CGRGDS peptide containing solution to which, after 5 minutes, the same volume of 0.6% v/v of H_2O_2 (obtaining a final concentration of 0.3% v/v) was added and the solution was stirred for further 30 minutes. At the end µbeads were washed three times with water and dried with air flow.

Large beads functionalized with RGD

Beads with an average diameter of 1mm were obtained by dropping manually with a syringe the mixture containing alginate into the 50 mM $CaCl_2$ solution. Beads functionalized with adhesive motif and tested on cells (AH-ThL and AH-ThM) exploited the use of ChitLac-SH.

- **AH-ThL beads** were obtained by dripping 2 mL of alginate/HAp (2% and 3% w/v respectively) in 400 mL of $CaCl_2$ 50 mM. The stirring was performed for 30 minutes and then beads were washed three times with water. At this point, they were immersed in 10 mL of 0.1% w/v aqueous solution of ChitLac-SH and stirred for 30 minutes. At the end beads were washed with water for three times and stirred in 10 mL of 0.3 mM CGRGDS aqueous solution, after 5 minutes 10 mL of a solution 0.6 v/v H_2O_2 were added and the stirring proceeded for other 15 minutes. Then beads were washed and dried.
- **AH-ThM beads** were obtained by blending a solution of alginate 4% w/v and HAp 6% w/v dissolved in 10 mM HEPES buffer, and 150 mM NaCl at pH 7.4 with a 1% w/v Chitlac-SH solution dissolved in the same buffer. Then the mixture was dripped under stirring in the 50 mM $CaCl_2$ solution and after 30 minutes beads were removed and washed. As for the production of AH-ThL the functionalization

with CGRGDS of beads followed the same procedure. Procedures are represented in the figure below

.

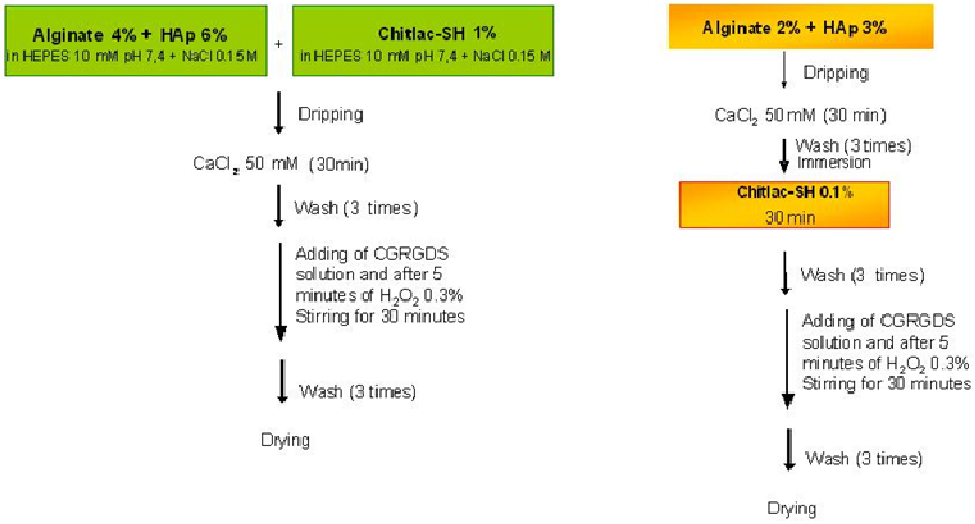

Figure 11. AH-ThM (green chart) and AH-ThL (orange chart) beads production procedures.

3.2.19 Measure of swelling

Test was performed on the intermediate diameter beads indicated in the table below:

Table 2. Beads used for swelling comparison (the percentage w/v of alginate and HAp is always 2 and 3% respectively when not differently indicated)

Chitlac/Alginate/HAp	mixed	with 0.5% ChitLac
	layered	with 0.1% ChitLac
	layered	with 0.5% ChitLac
Chitlac-SH/Alginate/HAp	mixed (with 0.5 % ChitLac-SH)	treated with H_2O_2
		not treated with H_2O_2
	layered (with 0.1% ChitLac-SH)	treated with H_2O_2
		not treated with H_2O_2
Alginate/HAp	(alginate 3%)	

The swelling was measured as the average surface variation upon treatment with 2 mL of saline solution (0.9% NaCl). Each test was performed three times on a known amount in a 70-100 number beads range.

The total area variation of beads was measured by photographing them with a common type of document scanner and in order to obtain the initial surface values, microbeads were put in a little plastic box filled with water milliQ and scanned; water was subsequently substituted with 2 mL of NaCl 0.9% and stirred for 1 hour. After this time, the box was filled with saline solution and acquisition by scanner was performed at a resolution of 1600 dpi. NaCl solution was removed after each acquisition and the box was re-filled with 2 mL of fresh saline solution. Saline solution removal and refilling was performed three times for each set of analysed beads. Surface of total beads population was measured by means of image manipulation software.

3.2.20 BMP fragment release from beads

Beads were prepared by blending the mixture of alginate and hydroxyapatite with an aqueous solution of BMP peptide and dripping manually with a syringe the mixture into the gelling solution under stirring for 15 minutes.

The preparation was performed both in water and in acid buffer, in this latter case all compounds, gelling solution and washing solution contained 10 mM HEPES buffer pH 4.5.

In detail, 1 mL of a solution containing alginate 2% w/v, HAp 3% w/v and BMP fragment 1.3 mg/mL (615 µM) (MW 2118.5 g/mol) was dripped in 100 mL of 50 mM $CaCl_2$. After 15 minutes beads were washed three times with water or buffer.

Release profiles of the beads were obtained incubating beads in 2 mL of phosphate buffer (PBS), and agitated on a rotary stirrer at (5 rpm). Each hour, 10 µL of supernatant were collected, without replacing it, and analysed by capillary electrophoresis. (Capillary electrophoretic conditions: running buffer borate 100 mM at pH 10.00, silica fused capillary length 56 cm, i.d. 50 µm, applied voltage 20 kV normal polarity, UV detection at 214 and 195 nm). The calibration curve of BMP ranges from 20 to160 µg/mL.

Amount of encapsulated peptide was estimated by subtraction of BMP lost during the process of gelation.

3.2.21 LL-37 release from beads

Beads were prepared by blending the mixture of alginate and hydroxyapatite with an aqueous solution of LL-37 peptide. 2.5 mL of this solution containing alginate 2% w/v, HAp 3% w/v and LL-37 0.5 mg/mL (110 µM) (MW 4493.3 g/mol) was dripped manually with a

syringe into 400 mL of 50 mM $CaCl_2$ under stirring for 30 minutes. At the end beads were removed and washed with water.

To achieve the release profile beads were divided in several fractions containing 15 beads each one. These fractions were incubated with 1 mL of PBS buffer and at each interval time beads were removed and hydrolysed under reflux with HCl. Arginine in hydrolysed was quantified by capillary electrophoresis and the release was calculated as the percentage of the total subtracted by this value.

In a second series of experiments, the supernatant was removed from some fractions and replaced. The quantification of the peptide released was performed in the same manner.

3.2.22 Circular Dichroism

Circular Dichroism measurements were carried out with a Jasco-700A spectro-polarimeter in the wavelength range between 205 and 370 nm, using a quartz cuvette with 1 cm optical path. Spectra were recorded in PBS buffer, pH 7.4, with a value of the ionic strength corresponding to 150 mM (Phosphate solution at Ionic Strength of 150 mM, PI-150) and in 5 mM sodium phosphate buffer, pH 7.4, with a value of ionic strength corresponding to 20 mM (PI-20). The former ionic strength was selected as it corresponds to standard physiological conditions, the latter one for comparison with the conditions used by others (Chan et al., 2005), (Chan et al., 2004).

Polysaccharides were solubilised both in PI-150 and in PI-20 at a concentration of 12.8 mM of the repeating unit. Solutions of LL-37 were also prepared in the two buffers. The PSs were stepwise added to each of the LL-37 solutions so as to have a constant peptide concentration of 10 μM and the following polysaccharide concentrations: 50.4, 100.8, 151.8, 201.6, 302.4, 403.2, and 504 μM.

3.2.23 MTT Assay

Cell viability was evaluated by the MTT (3,4,5-dimethylthiazol-2yl-2,5-diphenyltetrazolium bromide) assay. The experiments were performed by using two osteoblast-like cell lines, MG63 and Saos-2, treated with LL-37 alone and in mixture with alginate, ChitLac or hyaluronic acid.

The cells (5000 cells/well) were plated in a 96-well microtiter plate and incubated for 24 h at 37°C. After incubation, the MTT solution was added at a final concentration of 0.5 mg/mL and the plates were further incubated for 4 h at 37°C in 5% CO_2 atmosphere. The MTT-containing medium was then removed and 100 µL of DMSO per well were added to solubilise violet formazan crystals. Absorbance was measured in a microplate reader (Tecan) at 620 nm, and cell viability was expressed as percent relative to untreated control.

3.2.24 Antibacterial activity of LL-37/alginate mixtures in solution

The antibacterial activity of LL-37 and of its mixtures with polysaccharides was tested on four bacterial strains: two Gram-negative, namely *Escherichia coli* ATCC 25922 and *Pseudomonas aeruginosa* ATCC 27853, and two Gram-positive, i.e. *Staphylococcus aureus* ATCC 25923 and a clinical isolate of *Staphylococcus epidermidis*. All bacterial strains were grown in Mueller-Hinton (MH) broth at 37°C.

The inhibition of the bacterial growth was evaluated with a Tecan microplate reader (Tecan Trading AG, Switzerland). Mid-log-phase bacterial suspensions were dispensed in triplicate in microtiter plates at approximately $1 \cdot 10^6$ cells/mL in 20% MH broth in the presence or absence of LL-37 and polysaccharides (final volume of 200 µL). Microtiter plates were then incubated for 4 h at 37°C in the plate reader with 5 sec shaking every 5 min and recording of the OD_{620} every 10 minutes.

3.2.25 Antibacterial activity of scaffolds loaded with LL-37

Alginate/HAp scaffolds were prepared by mixing alginate 2% w/v and HAp 3% w/v in water under stirring. When the dissolution was complete, were added GDL (D-glucono-δ-lactone) 60 mM to release calcium ions from HAp. Aliquots of this gelling solution were then cured in 24-well tissue culture plates (h=18mm, internal diameter 16 mm), for 24 hours at room temperature to allow the complete gelation. The hydrogels in well-plate were then stepwise cooled by immersion in a liquid cryostat. Temperature was decreased stepwise from 20 to -20° C by 5°C steps with 30 minutes intervals for equilibration; samples were then freeze-dried for 24 hours to obtain porous scaffolds.

To load LL-37 on scaffolds, they were immersed in a solution containing 2 mL of LL-37 120 µg/mL buffered with 10 mM HEPES buffer at pH 7.4 and incubated under mild agitation

for 5 hours. At the end they were washed and freeze-dried and sterilized by UV lamp treatment for 30 minutes.

The antimicrobial activity of scaffolds loaded with LL-37 was determined by using the colony count method. Cultures of *S. aureus* and *E. coli* were diluted in fresh Muller-Hinton medium 20% to give a number of 10^6 colonies in the final solution. 1 mL of bacteria suspension were added to dried scaffolds and incubated in a shaking water bath at 37°C. At the indicated times (30, 180 and 300 minutes), scaffolds were removed, wring out and washed with 1 mL of PBS that was recuperated. Suspension and washing buffer were then serially diluted with PBS buffer and plated in duplicate on agar and incubated overnight to allow colony counts.

Two scaffolds for each time test were used and other two scaffolds without loaded LL-37 were treated at the same manner as control.

3.2.26 Alamar Blue™ Assay for cell proliferation on beads

Dried beads were prepared and sterilized by exposure to a UV lamp for 30 minutes. Before performing biological tests they were rehydrated in DMEM medium overnight.

MG63 cells were incubated with rehydrated beads on vials at a concentration of approximately 1.6 x 10^5/vial in 500 mL DMEM culture medium (Dulbecco's Modified Eagle's Medium added of inactivated Fetal Bovine Serum (10%), penicillin (100 units/mL), streptomycin (100 µg/mL) and L-glutamine (2mM)). The cells were incubated under rotation in an incubator at 37° to let the adhesion on beads surface. After this time, beads were removed and plated on not treated multiwell plates normally used for bacteria that doesn't allow the adhesion, besides fresh DMEM was added.

Cellular adhesion and growth were tested by means of Alamar Blue™ assay that is based on the detection of metabolic activity of cells. The assay reagent, Alamar Blue™, contains a reduction-oxidation (REDOX) indicator (resazurin); this is a nontoxic, cell permeable compound that is blue in colour and virtually no fluorescent. The metabolic activity of cells, conferring reducing properties to the medium induces a chemical reduction of the reagent, leading to the formation of resorufin, a pink fluorescent product. Decreased fluorescence levels are indicative of a decrease in the synthetic rates of cells and therefore suggestive of cells being cultured in a less favourable environment and having a lower relative viability compared to cells that show higher fluorescence levels when incubated with Alamar Blue™.

To perform this assay, beads were washed with PBS and incubated with 100 uL of 10% Alamar Blue™ in DMEM culture medium for 5 hours in darkness within the humified incubator at 37°C and 5% of CO_2. During this time, cells continuously convert resazurin to resorufin, thereby generating a quantitative measure of viability. After the time indicated the medium was removed from each well and replaced and the fluorescence was measured (λ_{em} 590 nm; λ_{ex} 530 nm). As a control, beads without cells were incubated at the same conditions and analysed. Since Alamar Blue™ is non toxic, it was possible to repeat the test the successive days on the same sample to evaluate the successive growth. The experiment was performed in quadruplicate.

3.2.27 Alamar Blue™ Assay for Cell Proliferation on LL-37 loaded scaffolds

Scaffolds were produced as indicated in the paragraph 3.2.25. Cellular viability on LL-37 loaded scaffolds was evaluated by Alamar Blue™ assay.

Before cell-seeding, scaffolds were sterilized with a cycle (15 minutes) of UV irradiation on each side of the structure, rehydrated with DMEM overnight and arranged in well plates. About $4x10^4$ of cells in a small volume of DMEM (50 µL) were plated on scaffolds, after 2 hours of incubation, 1 mL of fresh DMEM was added. After 24 hours to avoid any interference from the cells growing without being attached to the scaffolds, the structures were moved in a new multi-well plate before each Alamar Blue™. Alamar Blue™ assay was performed as described previously.

3.2.28 Alamar Blue™ Assay for cell accessibility on composites

Beads AH-Th-L (produced as described in the paragraph 0) were sterilized with UV lamp treatment for 30 minutes and the rehydrated with DMEM, or a 0.5 % w/v solution of hyaluronic acid or ChitLac dissolved in DMEM overnight. The procedure was the same used for Alamar Blue™ Assay for cell proliferation on beads.

3.2.29 Lactate Dehidrogenase Assay

Dried beads were prepared and sterilized by exposure to a UV lamp for 30 minutes. Before performing biological tests they were rehydrated in DMEM medium overnight.

The quantification of LDH permits an evaluation of the cytotoxicity of a material. LDH is a soluble cytosolic enzyme presents in most eukaryotic cells released into culture medium upon cell death due to damage of plasma membrane. The increase of the LDH activity in culture supernatant is proportional to the number of lysed cells and is an indicator of cellular death. The evaluation of LDH is performed quantifying its enzymatic NAD^+ reduction to NADH in the presence of L-lactate. The formation of NADH can be measured in a coupled reaction in which tetrazolium salt is reduced to a red formazan product. The amount of the highly coloured and aqueous soluble formazan can be measured at 492 nm spectrophotometrically. With the aim to evaluate the cytotoxicity of beads, the commercial kit TOX-7 was employed.

MG63 cells were plated on multiwall plate and incubated in the humified incubator (37° C; 5% of CO_2). The day after, DMEM medium was refreshed and beads and controls were deposed on the plates. After 24 hours of incubation, 50 uL of each DMEM were collected and centrifugated to eliminate suspended cells. A solution constituted by three components provided by the kit (Substrate, Dye solution and co-factor) was added to collected fractions, and after 30 minutes at dark, the reaction was stopped with 10% v/v of HCl 1M.

Controls are provided by DMEM medium without cells or materials, cells without any kind of material, cells in the presence of a negative control (polystyrene disk) and cells in the presence of a positive control (toxic polyurethane) which cause cellular damage. The percentage is calculated on the basis of maximum cellular death represented by cells lysed by a specific solution (Lysis Solution) added before to perform the DMEM collections on some plates without samples or controls. The enzymatic activity was measured by spectrophotometer at 490 nm with subtraction of 690 nm absorbance. The percentage of LDH released was calculated following the relation below:

$$LDH\ \% = [(Abs_A - Abs_B) / (Abs_C - Abs_B)]x\ 100$$

Where: A is the LDH recovered in the sample medium; B is the LDH recovered in DMEM medium without cells; and C is the total LDH obtained in the cell lysate solution.

The experiment was performed in quadruplicate at 24 and 72 hours.

3.2.30 NMR

NMR measurements were performed at 300 K on a Bruker Avance III Ultra Shield Plus 600 MHz spectrometer provided with a two channel BBI probe. Solutions for NMR were typically at a concentration of 10 mg/ml in D_2O. Residual water suppression was achieved by excitation sculpting.

Hydrogen and carbon assignment of ChitLac was accomplished by a series of 2D spectra, namely: 2D-NOESY, 2D-COSY, 2D-TOCSY, $^{1}H,^{13}C$-HSQC, 2D-$^{1}H,^{1}H$-TOCSY-$^{1}H,^{13}C$ HSQC, and 2D-$^{1}H,^{13}C$-HMBC. TOCSY mixing type was either 75 ms or 30 ms (for COSY-like 2D-$^{1}H,^{1}H$-TOCSY-$^{1}H,^{13}C$ HSQC) while NOESY mixing time was typically 100 ms.

^{1}H longitudinal relaxation rates were measured by conventional inversion recovery pulse sequence. 2D-DOSY with bipolar gradients was performed using a big and little deltas of 0.8 ms 4.4 ms, respectively.

3.2.31 Microbeads for the injectable composite

The µbeads droplet size was controlled by use of a high-voltage electrostatic bead generator with a steel neddle with 0.7 mm outer diameter, a voltage of 7 kV and pump with controlled speed. 2 mL of a mixture of alginate 2% and HAp 3% dissolved in water were dripped in 400 mL of 50 mM $CaCl_2$ with distance between the needle and the gelling bath adjusted to 1 cm. Gel beads were stirred for 30 minutes in gelling solution. At the end, beads were washed three times with water and dried with an air flow. Their size distribution was evaluated using a Stereomicroscope Leica DMR objective 5x/0.12 N PLAN BD, by measuring the average of the two diameters in a population of 60 µbeads at the dry state.

3.2.32 Rheology studies

Dynamic rheological tests were performed on hyaluronic acid (4% w/v in water) and on the composite prepared at the moment by mixing 200 µL of dried µbeads with 300 µL of hyaluronate solution. Measurements were performed on HAAKE controlled stress rheometer (RS150 Rheostress) with a plate-plate geometry (knurled type HPP20) with diameter 20 mm and at working temperature of 25°C. Data were achieved at shear oscillatory conditions to individuate the linear viscoelastic range (stress sweep analysis at 1 Hz), and to determine the mechanical spectra (frequency sweep). In the stress sweep tests the stress was evaluated in a

range between 2 and 20000 Pa with a plate gap of 2.0 mm and a frequency of 1 Hz. In frequency sweep measurements, the stress was constant to 2 Pa while frequencies range from 100 and 0.01 Hz. The plate gap was 2.4 mm. Moreover, analyses to determine the steady viscosity were performer in a range of acquisition between 0.1 and 100 s^{-1} with a plate gap of 2.6 mm.

CHAPTER 4. **RESULTS AND DISCUSSION**

4.1 Foreword: the assembly of a strategy

The designing of a resorbable injectable filler with bioactive properties, is a complex task that requires a precise strategy. In the present case, the injectable was planned as a two-component composite constituted by a dispersion medium - which provides flowability and injectability - and the bioactive filler – which provides bioactivity and elasticity at rest. The specific filler requirements just mentioned, both physical ("flowability" and "elasticity at rest") and biological ("bioactivity"), should provide an idea of the complexity of the approach and planning of the composite construction.

INJECTABLE: **Dispersion medium (**provides flowability**) +**
Bioactive filler (provides bioactivity and elasticity at rest**)**

1 <u>Dispersion medium</u>: hyaluronan
Hyaluronan: highly biocompatible, bioactive, viscoelastic

2 <u>Bioactive filler</u>: Microcomposite + Specific bioactive agents

A <u>Microcomposite</u> (dried microbeads): alginate + HAp
Alginate: biocompatible + hydrophilic
HAp: bioactive ("inorganic" bioactivity)

B <u>Specific bioactive agents</u> in filler:
<u>RGD</u>-containing peptides: pro-adhesive
<u>BMP</u>-fragment peptides: pro-proliferative
<u>LL37</u>-peptide: antibacterial

In these cases, the common suggested approach is to separate the individual components and develop them independently. The following step is to develop bioactivity in the filler and on the other side to select a matrix with proper viscoelastic properties; only at this point it is possible to combine them in order to obtain a product with peculiar properties. The properties

of the final construct are the result of the synergism of the two phases, unavailable from the individual constituent materials.

The choice of the raw materials for the structure of the final construct is an important feature of this project. Our attention is addressed to polysaccharide hydrogels such as those obtained from alginate, hyaluronic acid and from chitosan derivatives, to design a filler that is biocompatible and, especially so, bioresorbable, thanks to the optimal properties of polysaccharides.

The dispersion medium is the component able to render the filler injectable in small bone defects and responsible for its rheological (flow) properties. The attention is focussed on hyaluronic acid; hyaluronate, in fact, is known to be a bioactive biomaterial and presents good viscoelastic and hydrating properties in the dissolved state. Its biocompatibility is due to its capacity, in the extracellular matrix (ECM), to contribute to the build-up of a hydrated network acting as an organizing core in the ECM, connecting complex intercellular aggregates (Brown and Jones, 2005). In the literature, the use of hyaluronate added to a calcium phosphate was compared to the use of alginate or chitosan and it showed not only an enhancement of anti-washout ability but also an improvement of injectability properties, improving the performance of the product (Kai et al., 2009). Moreover, another important feature of hyaluronic acid is its capacity to protect peptides and proteins form tryptic degradation as it was verified with growth factors complexed with hyaluronate (Uebersax et al., 2009). The capacity of hyaluronic acid to form a physical (soft) gel in water is fundamental, because the matrix of the filler is the component that should permit the injectability of the manufacture product. With the purpose of obtaining a final system with a good capacity of injection in a bone defect, the suspending hydrogel must respond to parameters such as a characteristic viscosity and sedimentation time of the beads in the suspending component.

On the other hand, the planning of the bioactive filler was more complex. Fibres and particulates are normally used as reinforcements for biomedical composites in order to give elasticity. In designing injectables, elasticity at rest is highly desirable to keep the administered product in the right anatomical place. In this case we consider the use of a microcomposite whose core structure is made by dried microbeads of alginate and HAp, both bioresorbable. To allow a suitable HAp release, the best architecture of the biomaterial results to be its entrapment in alginate beads.

Besides providing bioactivity using HAp, specific bioactive agents are inserted into the microcomposite. In particular three different bioactive properties are provided by three diverse peptides: RGD containing peptides, known to be pro-adhesive sequences, BMP-fragment peptides, that provide osteoinduction, and LL-37 antimicrobial peptide.

4.1.1 The detailed research strategy

The biomolecules selected for this work are essentially charged polysaccharides and peptides, so the charge is a property that is particularly taken into account and exploited in this project. The interactions between the microcomposite and specific bioactive agents are, essentially, of electrostatic type. Electrostatic interactions occurred between the alginate polyanion and a polycation, which can be represented by a peptide, like in the case of LL-37, or ChitLac carrying covalently bound BMP-fragment peptide or RGD-containing peptides.

Interaction between Microcomposite and Specific bioactive agents:

electrostatic, between

1. **Polyanion: alginate**
   and
2. **Polycation**
   Polycation is :directly the LL-37-peptide as such

or

ChitLac carrying covalently bound

BMP-fragment

and/or

RGD-containing peptides

The immobilization strategies of bioactive agents are the focal point of this work of Thesis, because they were selected on the basis of the physiological biofunctionality of these peptides.

To make the filler able to promote cell adhesion, **RGD-containing peptides** are immobilized. The sequence GRGDS, belonging to fibronectin family, is selected for its

specific interaction with integrins localized on osteoblasts. As it will be highlighted in the Introduction to the RGD Chapter, RGD peptides need to be covalently linked to the biomaterial, in order to promote adhesion on it. The immobilization problem is tackled first, by choosing the chemical approaches to covalently bond the RGD peptide to the selected polysaccharide. With the aim of obtaining beads which a RGD functionalized surface, the strategy of superficial coating is applied. Chemical modifications cannot directed to alginate, because the most reacting functional group, *i.e.* the carboxylic groups on guluronate residues, will be then consumed, compromising the gelling properties of alginate by reducing the ability of the modified alginate to form instantaneous calcium gels. A different approach exploits electrostatic interactions of alginate with cationic polyelectrolytes. In fact, being alginate a polyanion, an alginate bead can be coated with a polycation like ChitLac decorated with RGD peptides. In this way the chemical modification is introduced on ChitLac and not on alginate, keeping intact the ability of the latter to give rise to gels and thus to form stable beads. We take into consideration several kinds of bead structures exploring the use of layered beads or beads where polycation and polyanion are mixed together. Moreover, we apply different chemical strategies (amide and disulfide bond formation) that permit the conjugation of peptides on polysaccharide chains, considering also the possibility of modifying the polycation with a functional linker. With this aim, chemical modifications are introduced on the polymer and during peptide synthesis to allow the linkage, and beads are assembled. The most promising beads are tested on cells to observe the promotion of the initial adhesion and the successive cellular growth.

A different strategy was necessary to insert **BMP-fragment** in the microcomposite. This is the recognition motif of growth factors implied in fracture repair. These peptides do not require a covalent stable immobilization but a release system. The design of a controlled release system to easily deliver BMP for bone reconstruction is still an open problem. To produce a growth factor delivery it is important to mimic the release profile, kinetics, dosage and duration found *in vivo*. In the orthopaedic field BMP-2 and BMP-7 are the bone morphogenetic proteins most used and they were also approved for clinical uses. Mechanisms and functions of these biomolecules will be explored in the corresponding section but in order to understand how the strategy has been planned, it is useful to address to their time expression in physiological conditions. BMP-2 is expressed during the entire temporal range of fracture repair, considering this one as a range of three weeks; while for BMP-7, its role in the first two weeks is not so clear, and discordant opinions are reported (Figure 12).

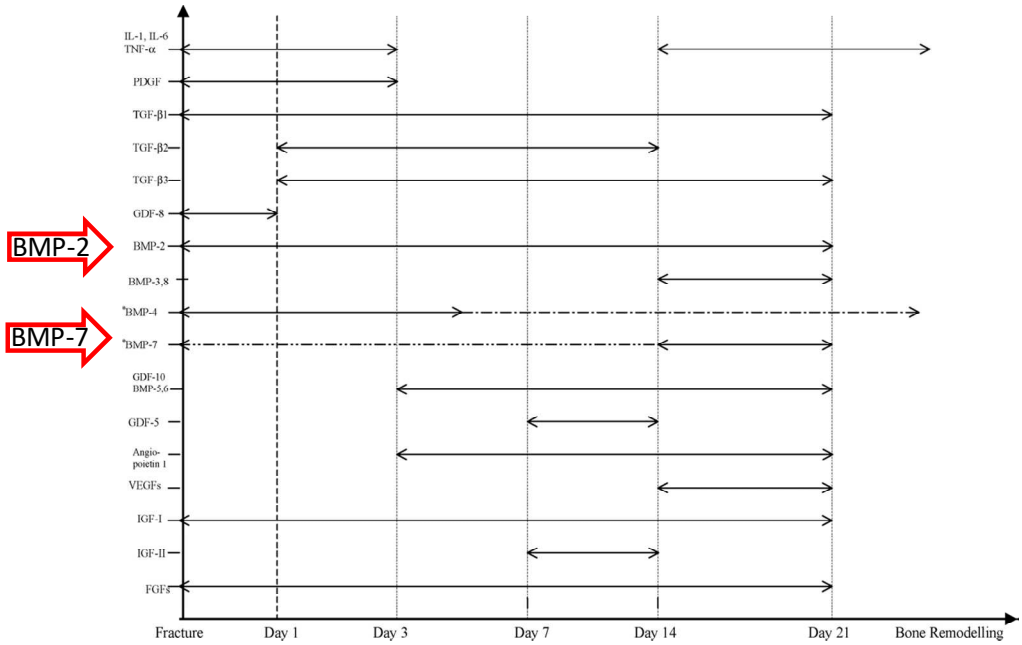

Figure 12. Schematic summary of the temporal expression patterns of the signalling molecules during fracture healing (the dashed line represents a difference of opinion amongst scientists in terms of the timing of expression) (Dimitriou et al., 2005).

In order to design a delivery system containing BMP, our attention is focalised on a system with a known and well-defined temporal expression, like as BMP-2.

Starting from the temporal activity of BMP-2 *in vivo*, the system for its delivery is planned so as able to give a fast immediate release, followed by a constant slower discharge of active biomolecule. Because of drawbacks by using entire proteins, as active components, a fragment of BMP-2 is selected, corresponding to residues 73-92 of the BMP-2 knuckle epitope. This sequence (KIPKASSVPTELSAISTLYL) represents the more promising oligopeptide into the group of epitope fragments discovered and tested until now (Suzuki et al., 2000). For the delivery, also in this case hydrogels properties are exploited, to obtain a bioresorbable system. The entrapment of the peptide in alginate/hydroxyapatite beads is performed taking advantage of the encapsulation properties of alginate. Calcium alginate gel is a well-known method to encapsulate and deliver pharmaceutics but also peptides and proteins. Many results have been reported concerning the use of alginate as drug-controlled release formulation (Coviello et al., 2007). Thanks to its gelling properties in the presence of bivalent cations, alginate is used as an immobilization matrix for cells and enzymes as well as pharmaceutical and food components. The main advantage of using alginate to encapsulate

proteins is that alginate gelation process occurs under very mild conditions without using high temperatures or chemical cross-linking agents avoiding, in this manner, the risk of denaturing biomolecules (Gu et al., 2004). However, the porosity of alginate beads results in a low efficiency of incorporation for drugs that have a low molecular weight and are water-soluble, producing a very fast release of incorporated active compounds. This is exploited for the initial phase of the release system. With this aim the suitability of alginate as an encapsulation matrix for delivering BMP fragment at a therapeutic initial level was explored. The peptide encapsulation yield is studied using different pH cationic gelling solutions to modify the charge of the peptide. Finally, the release kinetic profile will be achieved.

The simple encapsulation that can be exploited for the rapid kinetic of the treatment with BMP fragment, need to be complemented by another release system to obtain also a long-term and constant therapeutic effect. The second part of the section dedicated to BMP-fragment release, regards the development of a long-term release of this peptide. The idea is to exploit the chemical immobilization of the peptide on a polysaccharide, introducing a peculiar linkage cleavable when the construct is introduced in the site of implant. The proposed approach combines the selectivity offered by a chemical strategy like the "click-chemistry" with the release-potentiality of a cleavable linkage like an ester. The advantage over a "conventional" covalent immobilization is that the release allows for a higher number of molecules to reach receptors and in the right conformation, optimizing interaction. (Figure 13) depicts schematically this strategy. The selected polymer for this immobilization is ChitLac.

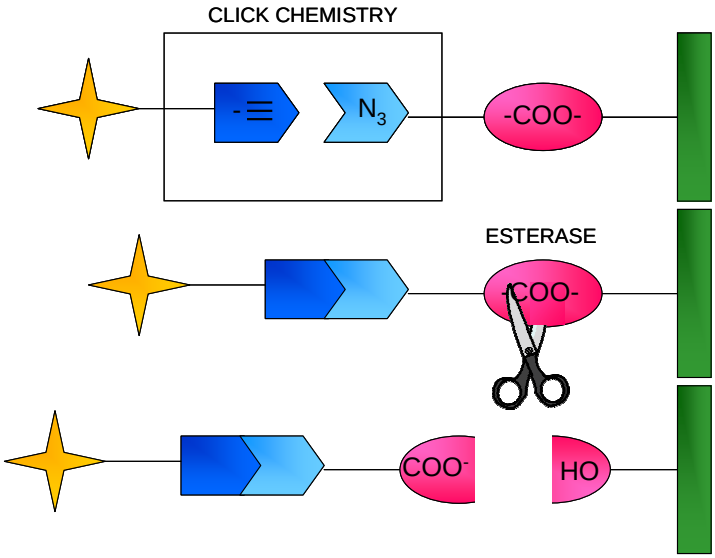

Figure 13. Immobilization strategy. The yellow star represents the BMP peptide, the green rectangule the polysaccharide.

This approach is based on the formation of a covalent bond between ChitLac and BMP fragment with a cleavable spacer. Two aspects are peculiar and deserve to be emphasized:

- The spacer
- The selective chemistry adopted.

The *spacer* is the cleavable part of this functionalised polysaccharide. It was planned as a long linear molecule which can be cleaved only in desired conditions; in fact, the goal is to obtain a manufacture product that will be able to release the active molecule only at the site of implant and not, for instance, during the storage of the latter. Exploiting specificity and catalytic efficiency of enzymes, the spacer was planned as a molecule containing a functional group which is enzymatically hydrolysable. With this aim, esterase is selected as the enzyme. Esterases is a class of hydrolytic enzymes that split esters into an acid and an alcohol. A wide range of different esterases are expressed in the different tissues and they differ for their substrate specificity, their protein structure, and their biological function. Esterase activity has been demonstrated histochemically in developing bones and in teeth in calcifying dentine, and in the periodontal ligament of rats. Esterase fractions identified in bone were presumably nonspecific organophosphate-sensitive esterases (Semb, 1970) and their presence has been demonstrated in undifferentiated cells, osteoclasts, osteoblasts, in cartilagineous callus and a their strong activity was shown also at early stages in healing fractures (Gudmundson and Semb, 1971), (Gudmundson and Semb, 1971 (b)). In this view, when the modified polysaccharide is situated in the site of injure, the activity of esterases involved in bone regeneration processes will allow the BMP fragment to be released from the polymer structure. Moreover, the local concentration of the BMP fragment could be modulated by varying the degree of substitution of the polymer.

The second point regards the selection of the *chemical strategy*. When conjugations involve peptides as reagents, the high number of functional reactive groups that are present in the lateral chains should be given adequate consideration. To this end the use of selective chemical strategies becomes fundamental. An approach that excels for its specificity towards functional reactive groups is the click chemistry. The click chemistry concept was introduced by Kolb and co-workers in 2001 (Kolb et al., 2001). Reactions were classified as click chemistry if they were modular, stereospecific, wide in scope, resulted in high yields and generate safe byproducts. Furthermore, the reaction must proceed under simple reaction conditions, with readily available starting materials, and without any solvent or in a benign solvent.

A variety of click reactions exist, but the Huisgen 1,3-dipolar cycloaddition of azides and alkyne (Scheme 2) plays an important role in organic synthesis, and has evolved into a common coupling procedure (Becer et al., 2009).

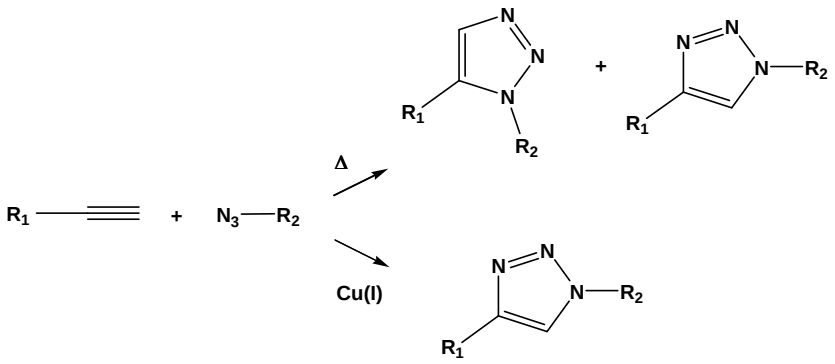

Scheme 2. 1,3-dipolar cycloaddition between azides and alkynes.

The reaction, carried out at high temperatures and for long reaction times, gives a mixture of the 1,4- and the 1,5-regioisomers; however, the introduction of the copper catalyst directs towards the formation of the 1,4 regioisomer only. The use of this kind of strategy in medicinal chemistry (Tron et al., 2008), in hydrogels (Crescenzi et al., 2007) and in peptide and protein chemistry was also successful (He et al., 2008), (Li et al., 2008).

The section dedicated to the bonding of the BMP fragment regards in particular chemical modifications both on ChitLac and on the peptide, and a control of esterase activity on this kind of polymers.

Electrostatic interactions are exploited also in another strategy that is the release from the microcomposite of **antimicrobial peptide LL-37**. The cytotoxicity of this peptide and the complex interaction between LL-37 and differently charged polysaccharides reported in literature, suggested the possibility to modulate the peptide availability, thus reducing its cytotoxicity by making interaction with eukaryotic membranes, while maintaining its antimicrobial properties. In particular, we initially focus our attention, onto three polysaccharides (PS) namely alginate, hyaluronic acid and ChitLac. The plan is to explore the behaviour of mixtures LL-37/PS in solution both as to peptide conformation and cytotoxicity and antimicrobial effect. The following phase deals with the use of the peptide/PS complexes in localized (semi)solid systems for orthopaedic applications. To this end in the second part of the corresponding research section the application of LL-37 peptide conjugated with alginate

on solid supports is investigated. The immobilization of a peptide in a delivery system may be performed following different methodologies: *via* adsorption, entrapment, ionic complexation or by covalent binding; in this section, we explore the encapsulation and the electrostatic adsorption of LL-37 onto two different solid supports, with the final aim to prepare orthopaedic fillers. A first method exploits the encapsulation properties of alginate to entrap the peptide in alginate beads, while in a second technique the adsorption of LL-37 on the surface of an alginate support is explored. In this manner we can test both the mechanism of peptide release from loaded beads and the action of LL-37 when deposed in an alginate construct. In both cases these strategies present the advantage of the simplicity but also some drawbacks that can occur such as the possible conformational changes and denaturation of the protein which cause the failure of its activity, as it is the case of some growth factors which bind irreversibly to their carrier. In those circumstances the chemical properties of the polymeric carrier are fundamental to avoid those drawbacks (Luginbuehl et al., 2004). Alginate is a carrier that can run into this kind of problems: literature reports that although the microenvironment in an alginate bead can be relatively inert to protein drugs and cells, a positively charged protein can potentially compete with Ca^{++} ions for available carboxylic acid sites on the alginate (George and Abraham, 2006). This has been observed with small drugs and has been shown to result in protein inactivation in the case of the protein transforming growth factor-beta (TGF-β_1) (Mumper et al., 1994). Nevertheless the peculiar modulating activity exhibited on LL-37 by alginate justifies an examination of these interactions when applied in the solid state.

After defining all techniques useful to incorporate peptides in the microcomposite, we pass to optimize the assembly of the **composite injectable filler**, where dried microbeads are dispersed in hyaluronic acid solution. The first part of this important Section deals with the characterization of the dried µbeads as particulate, studying size, size distribution, and cell accessibility. Finally, after a brief excursus of data reported in the literature on the rheological properties of hyaluronic acid, the investigation on the rheological properties of the injectable are given the deserved relevance as to the performance of the final product.

4.2 PRO-ADHESIVE AGENTS IN FILLER: RGD-CONTAINING PEPTIDES

4.2.1 Introduction

The future improvement of new biomaterials is aimed at minimising adverse responses and device failure, promoting rapid and controlled healing and implant integration. The long term success of a material implanted in the body depends on the controlled macro-functional and physical-chemical properties of the material at micro and nano-scale. The first point to take into consideration is that a long term success is possible when at the basis there is a complete acceptation of the biomaterial by the living tissue. Biocompatibility is correlated to the behaviour of cells in contact with the implant surface, which, because of its peculiar role in the cell-material adhesion, permits a correct future assimilation of the implant. A major cause of implant failure in skeletal tissue is in fact failure of osteointegration, often due to lack of *adhesion* of cells to the implant interface. Surface interactions play a primary role during the first phase of implant integration: the specific nature of a biomaterial surface, both from a chemical and physical point of view, is crucial, because it determines how the living tissue will interact with the implant. The integration of bone implants could therefore be improved by controlling these interfacial reactions. Nowadays, implant characteristics such as surface chemistry, charge, texture and porosity are optimized to enhance tissue response *in vivo*. Promising approaches involve in particular implant surface treatments with biologically active substances which, when exposed with the correct orientation and conformation, may permit a specific interaction with selected receptors, thus mediating cell attachment during the implant assimilation. Biocompatibility of surfaces is closely related to the response of cells in contact with the surface and in particular to adhesion phenomena (Roach et al., 2007). The design of new materials focused on bioactive surfaces, capable of eliciting specific cellular responses is a hot topic of regenerative medicine and requires knowledge about the basic processes by which cells form, maintain and repair tissues. It is based on the understanding of what happens inside the cell but also between the cells and between cells and their environment, the extracellular matrix, ECM. In this direction, understanding the regulating factors cell-matrix interaction and applying this knowledge to the biomaterial design will make it possible to develop new strategies to manipulate the adhesive cell-implant interactions, creating a biomaterial able to stimulate cell adhesion, and as a consequence obtaining an excellent integration of the implant.

The dynamics of cell-ECM interactions.

Investigations of the basic cell and molecular mechanisms of the integration between cells and extracellular matrix during developmental and developmental-like processes, such as wound healing, have contribute to advancements in preparation of “second and third generation” biomaterials.

In vivo, cells are surrounded by a biological matrix, the extracellular matrix, constituted by a tissue-specific combination of insoluble proteins (such as collagen and elastin), glycosaminoglycans and, in bone tissues, inorganic crystals. The varied composition of the ECM components not only provides the necessary physical architecture and mechanical strength to the tissue, but also contains a reservoir of cell-signalling ligands and growth factors which guide cellular anchorage and behaviour. The distribution and concentration of ECM ligands provides signalling gradients which direct cell migration and cellular production of ECM constituents, creating a bidirectional flow of information between the matrix and the cells (Jell et al., 2009).

The adhesive interactions between cells and the matrix involve many biological processes: they are central to embryonic development, wound healing, and the organization, maintenance, and repair of numerous tissues. Cell-matrix interactions provide tissue organization generating anchoring forces which mediate cell spreading and migration, neurite extension, muscle-cell contraction and cytokinesis. Cell adhesion is fundamental for the cell survival as demonstrated by genetic deletions in mice for adhesion molecules, which lead to absolute lethality at early embryonic stages. Abnormalities in adhesive interactions are often associated with pathological states, including blood-clotting and wound healing defects as well as cancer formation. Cell adhesion occurs not only in various events of physiological processes but also during pathological events, it assumes a central role in embryogenesis, maintenace of tissue structure, wound healing, immune response and metastasis.

In addition to cited pivotal roles, cell adhesion on surfaces is crucial to cellular and host-responses to implant devices, biological integration of biomaterials and tissue-engineered constructs (García, 2006). Attachment, adhesion and spreading belong to the first phase of cell-material interactions and their correct development will influence the capacity of cells to proliferate and differentiate on the implant. Morphologically, the efficacy of orthopaedic implants is ensured by the formation of a mechanically solid interface with complete fusion between the biomaterial surface and the bone tissue without fibrous tissue interface: this situation is possible only when a correct cell adhesion on the implant surface occurs. In this

view, surface characteristics of materials (their topography, chemistry or surface energy) play an essential role in the adhesion of osteoblasts on biomaterials.

Cell adhesion is defined as a sequence of four steps: cell attachment, cell spreading, organization of an actin cytoskeleton, and formation of focal adhesions (Lebaron and Athanasiou, 2000). But when we talk about "adhesion" in the biomaterial domain, we can think to it as a process constituted by two different phenomena: the attachment and the adhesion. The attachment involves short-term events such as physico-chemical linkages between cells and the biomaterial, driven by ionic and van der Walls interactions; while the adhesion phase occurs over a longer time span involving various biological molecules, like extracellular matrix proteins, and cell membrane proteins, cytoskeleton proteins which, thanks to a signal transduction, are able to regulate the gene expression (Anselme, 2000).

A modern biomaterial needs, therefore, to have the capacity to mimic the biological molecules that control the relationships between cells and their natural biomaterial interface, the ECM. These biological factors involved in the adhesion process are localized not only in the matrix but also in the cytoskeleton and on cellular membrane and they can be resumed as follows:

- Proteins of extracellular matrix
    - Structural proteins (collagen)
    - Glycosaminoglycans and proteoglycans (heparin)
    - Adhesive proteins (fibronectin, laminin, vitronectin)
- Components of cytoskeleton
- Adhesion molecules belonging to cell membrane
    - Involved in cell-cell interaction
        - Selectin family
        - CAMs (Cell Adhesion Molecule proteins denoted also as Ig-CAMs)
        - Cadherins family
    - Involved in cell-extracellular matrix interaction
        - Integrins family (which interacts with fibronectin, osteopontin, bone sialoprotein, thrombospondin, type I collagen, vitronectin)

Among these molecules, the primary family of cell membrane proteins which mediate the adhesion of cells to the substrate are the integrins. Integrin-mediated adhesion is a highly regulated, complex process involving receptor-ligand binding as well as post-ligation

interactions with multiple binding biomolecules. Most integrins are expressed on a wide variety of cell types, and most cells express several integrin receptors; however, some subclasses are only expressed in particular lineages. Because of their crucial role in the attachment, they are critically involved in host and cellular responses to biomaterials.

Integrins: multifunctional receptors

Integrins, a widely family of glycosylated transmembrane receptors, are involved in both cell-cell and cell-ECM binding, and represent constituting the primary adhesion mechanism to ECM components.

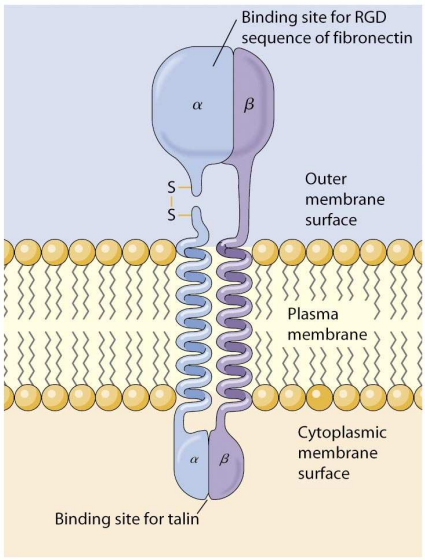

Figure 14. Schematic configuration of the subunit structure of an integrin cell-surface matrix receptor.

The integrins are dimeric proteins which consist of two transmembrane glycoprotein subunits, the α chain and the β chain, assembled non covalently into an active dimer. The two subunits interact through their extracellular parts, which give rise to a functional heterodimer (Figure 14). Thanks to their structure, integrins are able to interact with the ECM, through their extracellular domains, and with components of the cytoskeleton and signaling molecules, through their intracellular domains (Figure 15).

Upon ligand binding, integrins rapidly associate with the actin cytoskeleton and cluster together to form focal adhesions, supramolecular complexes containing structural proteins, such as vinculin, talin, and α-actinin, and signaling molecules, including FAK, Src, and paxillin. In this manner, integrins regulate many cellular functions, such as cell adhesion, motility, shape, growth and differentiation (Siebers et al., 2005).

There are many known α and β subunits with at least 24 αβ combinations and each combination has the capacity to bind one or more ligands.

In particular, for what concerns bone cells, integrins expression on osteoblastic cells has been described in various studies. Osteoblasts are capable to express a wide variety of integrins; and in particular the expression of subunits α_1, α_2, α_3, α_4, α_5, α_6, α_V, β_1, β_3 and β_5 is frequent (Bennett et al., 2001).

Generally, for β-subunits it can be said that the β_2 integrins are involved primarily in cell-cell recognition, while the β_1, β_3 and β_4 integrins are involved in cell-ECM interactions. The β_1 and β_3 integrins bind to numerous proteins localized in the ECM, such as collagen, fibronectin, vitronectin, von Willebrand factor and laminin:

- Collagen is the primary structural protein of the tissues.
- Fibronectin is a globular protein present in nearly all tissues.
- Vitronectin is a multifunctional adhesion protein found in the circulation and in many tissues.
- The von Willebrand factor is an adhesion protein which is involved primarily in the adhesion of vascular cells.
- Laminin is a complex adhesion protein generally localized in the basement membrane, immediately beneath epithelia and endothelia, as well as in many other tissues.

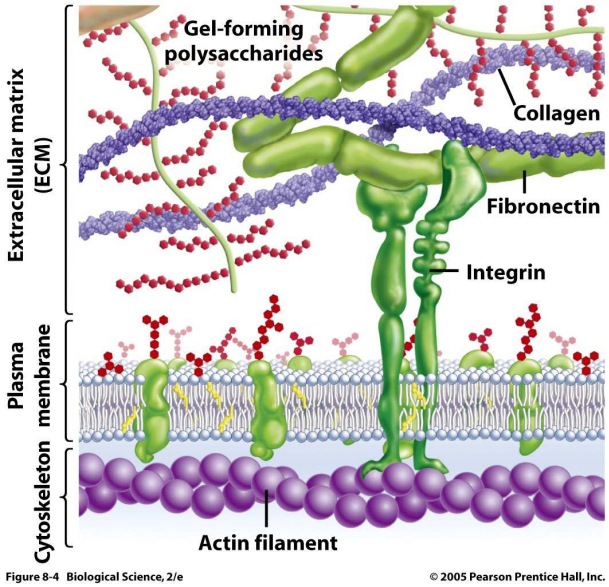

Figure 15. Interactions of extracellular and intracellular domains of integrins. Integrins act to integrate the cytoskeleton and the extracellular matrix.

All these proteins are structurally very complex and contain sites responsible for binding to collagen and to glycosaminoglycans, for cross-linking to other extracellular matrix proteins via tranglutaminase activity, for degradation by proteases and for binding to integrin and other adhesion receptors. Fibronectin was demonstred to be the primary bone ECM protein expressed during bone formation, and has also been found in demineralised bone implants and osteoblast cultures during active osteoblast progenitor proliferation and condensation. Type I collagen appears later during *in vivo* bone development in osteoblast cultures. Fibronectin binds to the integrin $\alpha_5\beta_1$, whereas, integrins $\alpha_1\beta_1$, $\alpha_2\beta_1$, $\alpha_3\beta_1$ and $\alpha_V\beta_1$, bind type I collagen in osteoblasts. (Meyer et al., 2006).

Table 3. Selective synthetic peptide sequences of extracellular matrix proteins used in tissue engineering applications (Hubbel, 2007).

Protein	*Sequence* [a]	*Role*
Fibronectin	RGDS	Adhesion of most cells, via α5β1
	LDV	Adhesion
	REDV	Adhesion
Vitronectin	RGDV	Adhesion of most cells, via αVβ3
Laminin A	LRGDN	Adhesion
	SIKVAV	Neurite extension
Laminin B	YIGSR	Adhesion of many cells, via 67-kDa laminin receptor
	PDSGR	Adhesion
Laminin B2	RNIAEIIKDI	Neurite extension
Collagen I	RGDT	Adhesion of most cells
	DGEA	Adhesion of platelets, other cells
Thrombospondin	RGD	Adhesion of most cells
	VTXG	Adhesion of platelets

[a] **Single-letter amino acid code.**

Given the multifunctionality of these proteins, the sites involved in the singular function of binding to integrins comprise only a small fraction of the protein mass. In most cases, the receptor-binding domain is localized in an oligopeptide sequence, smaller than a decapeptide, and this site can be mimicked on the biomaterial surface.

Encoded by specific amino acid sequences, these motifs target and bind to specific cell surface receptors, such as integrins, activating different intracellular signaling pathways.

Many receptor-binding sequences are known and some of them are presented in Table 3 (Hubbel, 2007). The most common binding site is the tripeptide RGD (Arg-Gly-Asp) present in most of the ECM proteins, like fibronectin and vitronectin. There is a full class of proteins where RGD represents the central sequence, but the presence of peculiar residues near to the tripeptide can drastically change the receptor specificity. For example, the sequence found in fibronectin is RGDS, while in vitronectin is RGDV. After the binding with the ligand, the integrins cluster into focal contacts, an area of close contact between cell and the ECM. These focal contacts are pivotal elements in the adhesion process, acting as structural linkers between the cytoskeleton and ECM. It is during this phase that, involving additional cytoskeleton proteins, adapter molecules and kinases, integrins are able to activate a cascade of intracellular signaling, leading to changes in gene expression and affecting most aspects of cell behaviour (Siebers et al., 2005). In such manner, integrins are able to modify adhesion, differentiation, proliferation, activation of growth factors, and the maintenance of survival signals to prevent apoptosis and in this point of view, they have a pivotal role in the cellular response to biomaterials.

Biomaterials in the host

The first interaction between cells of the host organism and the implanted material occurs only after a first series of non specific interactions. The response to the implant starts nanoseconds after it has been placed in the human organism and, after an initial contact with water molecules, the interaction with biomolecules of body fluids takes place in the early minutes of implantation. This latter process is named “protein adsorption”, and generates a layer of proteins on the material surface. The time and size scales of interaction between materials and the mineralized tissue are shown schematically in Figure 16. Subsequently cells indirectly interact with the biomaterial surface through this layer of adsorbed ECM proteins. This is a dynamic process because time-dependent changes in the composition of the adsorbed layer can occur. Variables related to both activity and availability of biomolecules at the surface contribute to determine the profile of molecules adsorbed on the implant surface.

Thus factors like affinity and kinetics (concentration and size) are able to influence this layer stability.

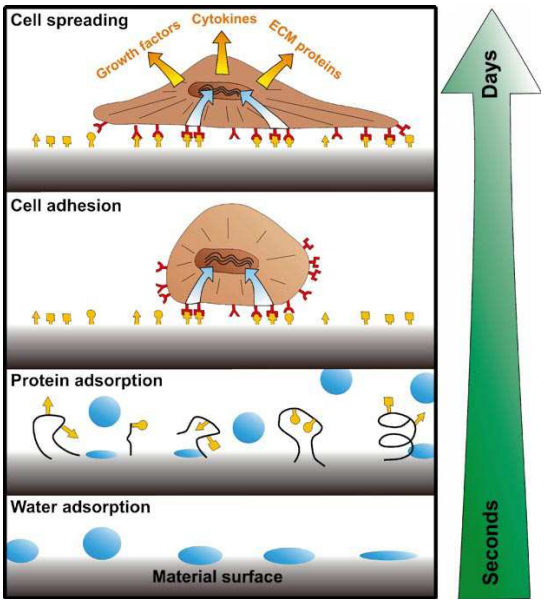

Figure 16. Implant-surface interactions: the initial response to a material surface placed in a biological environment, is for water molecules; in the second stage (from seconds to hours after implantation) the material becomes covered in an adsorbed layer of proteins initially present in the ECM; in the third stage, cells reach the surface interacting through the protein covering. Only during these phases, material surface-bound proteins provide the recognition sites which enable cell adhesion via specific cell receptors (e.g. integrins) (Jell et al., 2009).

With time, molecules having greater affinity for the surface, but with a slower rate of arrival, approach the surface and even though it can be already occupied by a monolayer of proteins, they are able to compete for the binding site. In this manner, the first molecules are released from the surface and the substrate becomes occupied by the new molecules. Exchange proceeds until the surface is populated with proteins having strong interaction with the substrate. This hierarchical series of collision, adsorption, and exchange processes has been termed ‘‘the Vroman effect’’ (Dee et al., 2002).

Cell attachment occurs only after this process, which can take hours or days to complete. Then, when a cell approaches an implant material, it will not be in directly contact with the biomaterial surface, but it will first interact with the layer of adsorbed proteins. Because cells depend on specific proteins for anchoring and transference of extracellular instructions, the composition of this layer influences their behaviour and can even attract undesired cells. A method to promote an appropriate cell adhesion could be the use of proteins bound to the surface, which are able to enhance the affinity for certain receptors localized on specific cells like integrins, thus increasing their affintiy for the biomaterial and permitting their exchange with pre-adsorbed proteins (Meyer et al., 2005), (Chen et al., 2008).

Integrins mediate cellular interactions with biomaterial surfaces by interacting with adhesive extracellular ligands which can be (Figure 17):

- adsorbed from environment solution (such as in protein adsorption from blood, plasma, or serum)

- engineered at the interface (for example, bioadhesive motifs such as RGD)
- deposited by cells (like fibronectin and deposited collagen)

As mentioned, these interactions are often highly dynamic in nature. For instance, the dominant adhesive ligand present on a surface may change because of the exchange with other proteins in solution (Anderson, 2001), (García, 2005).

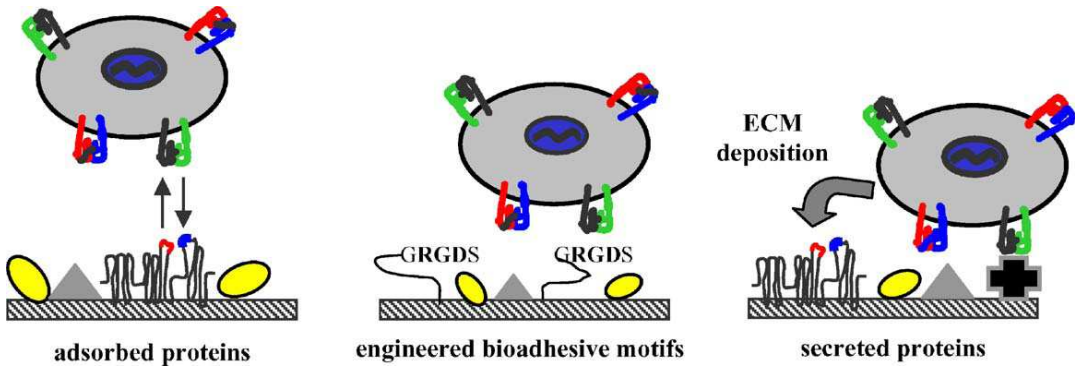

Figure 17. Mechanisms controlling cell adhesion to biomaterials (García, 2005).

Additionally, cells adhesion to synthetic surfaces can involve also proteins adsorbed from solution, but they can rapidly degrade/reorganize this layer of adsorbed proteins and deposit their own ECM with a very dynamic state.

Since adsorbed proteins are viewed as the primary and the most important players in mediating biomaterial-organism interactions, their behaviour at the surface plays a vital role in determining the ultimate biocompatibility of the implant device. The adsorbed protein layer, in fact, will influence the subsequent biological reactions including platelet adhesion, complement activation and bacterial and cell adhesion.

It is therefore clear that the understanding of the interactions occurring between proteins and material is critical, and control of protein-surface interactions is an important factor to be considered in the design of biocompatible surfaces. In order to achieve specific responses by the adjacent cells and to reduce non-specific interactions, the principles for designing biocompatible polymer materials are principally two: passivating the polymer surfaces to minimize non-specific protein interaction, or decorating polymer surfaces with biomolecules to induce specific protein adsorption and cell responses (Chen et al., 2008).

Bio-Adhesive surfaces: biomaterials mimicking ECM

Over the last decade, biomimetic approaches have been exploited to obtain synthetic materials with specific characteristics of biocompatibility and biofunctionality. The development of biomaterials for tissue engineering applications has focused the attention on the design of biomimetic materials which are able to interact with surrounding tissues by biomolecular recognition. The recognition function can be achieved by two major design strategies. One approach is to provide bioactivity by the incorporation of soluble bioactive molecules, such as growth factors and plasmid DNA into the biomaterial. In this manner it is possible to obtain the release of bioactive molecules from the material and thus to modulate new tissue formation. The second approach involves the incorporation of cell-binding peptides into the biomaterial via chemical or physical modification. The cell-binding peptides include either intact ECM proteins as well as a short peptide, whose sequence is part of the ECM protein and is able to interact with cell receptors. The biomimetic materials potentially mimic many roles of matrix in tissues (Shin et al., 2003). Implant coating or modifications are currently of particular interest, with the aim to control cell attachment and spreading by means of a tailored chemistry. In some studies, substrates have been coated with the native ECM proteins in order to understand the influence on integrin expression and on the cell adhesion. The substrates (usually, titanium, titanium alloy, glass or poly(styrene)) have been coated with fibronectin (Cowles et al., 2000), (Krause et al., 2000), demonstrating an increase in osteoblasts adhesion, proliferation an differentiation; with collagen type I, which demonstrate an effect not yet clear (Cowles et al., 2000), (Geißler et al., 2000), (Becker et al., 2002) and with vitronectin which gives a decrease in osteoblasts adhesion with respect to the not coated poly(styrene) surface (Verrier et al., 2002).

The use of native proteins for coatings, however, could present some disadvantages especially when they are employed in medicine. On a first place, the synthesis is very expensive and difficult; proteins are obtained by means of a complex isolation and purification process from cell cultures or other organisms; undesirable immune responses or infections can happen when they are placed in a human body. Moreover, enzymatic degradation of the proteins could give rise to inflammatory processes. Proteins can also undergo proteolytic degradation and are not useful for long time applications. Moreover, inflammation and infection can even accelerate protein degradation. From the point of view of the cell adhesion stimulation, these proteins are able to act only if they are located on the surface with the right conformation and orientation (Elbert and Hubbell, 2001). Actually,

when the protein is adsorbed (Hern and Hubbell, 1998), or covalently bound (Huebsch et al., 1996), on a surface it is not easy to obtain and preserve the correct orientation and conformation. Moreover, it should be reminded that the structuring ability of the surface, its hydrophobicity and the surface charge could be able to denature the protein or to expose the binding motif in a different conformation, that is not recognized by the receptor (Lhoest et al., 1998), (Altankov et al., 1996), (Fields et al., 1998), (Hlady and Buijs, 1996).

A valid alternative which permits to overcome these disadvantages is to use only the small active sequences involved in cell recognition rather than the entire protein. Peptides present a higher stability towards sterilization procedures, heat treatment and pH variation, storage and conformational modifications, an easier molecular characterization and a synthesis in large scale much cheaper compared to protein synthesis. Moreover, enzymatic degradation *in vivo* is slower than for bigger proteins (Hersel et al., 2003), (Meyer et al., 2006).

Osteoblasts adhere by means of different mechanisms involving a wide range of biochemical signals that can be exploited to promote adhesion, migration, proliferation and differentiation of cells:

1. interaction with RGD motif via cell membrane integrin receptors
2. interaction between cell membrane heparin sulfate proteoglycans and heparin-binding sites on extracellular matrix proteins

This second class of proteins contains a heparin binding domain able to interact with cell surface proteoglycans containing heparan sulfate or chondroitin sulfate glycosaminoglycans. Since glycosaminoglycans, especially heparin and heparan sulfate, have a negative net charge, the peptide sequences that bind to cell surface proteoglycans are rich in cationic residues such as arginine (R) and lysine (K); in particular the amino acid sequence containing -X-B-B-X-B-X- (where X and B represent hydrophobic and positively charged basic segments, respectively) was identified as a heparin-binding domain. In this case the interactions are much less specific than those with integrins: in fact, the same effect can be obtained simply by immobilizing R or K residues on a supporting surface. A proteoglycan-binding substrate exhibits a reduced ability to support initial cell attachment and spreading. In fact, proteoglycans, as compared with the integrins, appear to play a more marginal role in the early events of cell adhesion. When compared with the same cells on an integrin-binding substratum, the attachment of a smaller number of cells is observed, as well as a less effective spreading and organization of an actin cytoskeleton (Lebaron and Athanasiou, 2000). Therefore binding by proteoglycan interactions have always to be tested in combination with

the integrin-binding sites, rather than alone (Hubbel, 2007). Peptides containing RGD motifs are more active than heparin-binding sequences in inducing cells adhesion (Dettin et al., 2005). For this reason, even if this signal sequence mediates a mechanism of attachment which is not cell specific, the major part of the current biomimetic strategies engage RGD peptides, targets of integrin receptors, which have demonstrated to control cell adhesion and differentiation *in vitro*, and more importantly, bone formation and integration in *in vivo* tests (see following paragraphs). The employ of RGD-mimetics presents also critical factors that should be considered when adopting this strategy for bone repairing. In the first place, RGD peptides exhibit limited specificity among integrins, because of redundancy in the affinity of integrins for adhesive proteins, and, in some cases, RGD is not sufficient for an efficient binding of particular integrins receptors (García and Reyes, 2005). Moreover, linear RGD peptides may experience enzymatic degradation, though alternatively small cyclic peptides more resistant to proteolytic degradation can be employed. Finally, it has been observed, the biological activity of the short adhesive peptides is significantly lower than that of the complete protein, because of the absence of other domains, present in the native molecule, that normally cooperate synergistically with the short peptide (Pierschbacher et al., 1983). This problem can be solved by introducing a higher amount of peptides, a strategy which is impossible to employ in the case of the entire protein.

RGD-coatings

An important approach to improve surface biocompatibility involves implant surface treatment with biologically active substances such as adhesion molecules. The incorporation of ECM ligands, such as the sequence RGD, into artificial surfaces enhances functionality of cell behaviour, allowing to obtain biomaterials with new levels of biofunctionality. The immobilization of bioactive molecules on a synthetic and natural “inert” material, such as some glass products, various metals or some polymers, can convert the material into a bioadhesive support. This strategy allows obtaining a bioactive surface able to induce specific cell and tissue responses or to control the tissue-implant interface with molecules directly delivered at the interface. Peptide immobilization on a material is generally accomplished by formation of covalent bonds between a material surface and introduced components, and by other non-covalent interactions. Because of its role in the cell attachment, the strength of the immobilization of RGD sequence on the substrate is fundamental. The stable linkage of RGD peptides to a surface is essential to promote strong cell adhesion, because formation of focal

adhesion occurs only if the ligands withstand the cells contractile forces. Immobilized ligands act as agonists of the ECM, leading to cell adhesion and cell survival, while non-immobilized ligands act as antagonists, leading to cell detachment, a round cell shape and apoptosis (Lebaron and Athanasiou, 2000) (Figure 18).

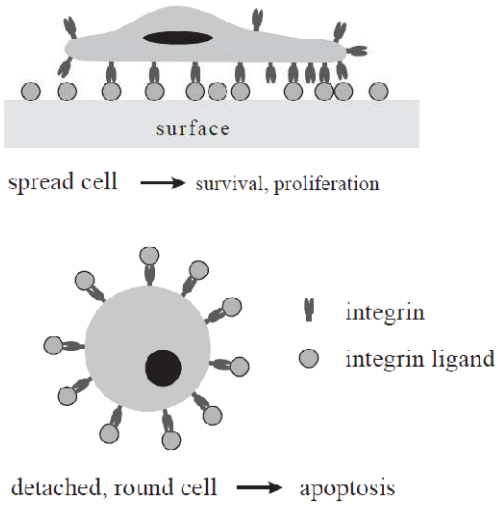

Figure 18. Opposite effect of integrin ligands. (Hersel et al., 2003)

Studies with substrates coated with this kind of sequence demonstrated *in vitro* an increase in cell diffusion, proliferation and differentiation and successful results were obtained also *in vivo*, where RGD coated implants have shown to increase bone formation. The many examples of materials coated with RGD reported in literature can be classified on the basis of their material support:

- Metallic substrates The major part of metallic substrates is represented by titanium and titanium alloys. In order to encourage bone growth directly at the titanium surface, it was decorated with adhesive peptides obtaining good results on osteoblasts. This effect was observed *in vitro* for Titanium discs covered with the peptide RGDS (Secchi et al., 2007), and gold-coated titanium surfaces enriched with a RGDC peptide (Huang et al., 2003). The activity of the RGDC titanium coating was demonstrated also *in vivo* where was able to enhance osteointegration in rat femurs (Ferris et al., 1999). Tests *in vivo* were performed also for titanium implants coated with cyclic RGD peptides, and it revealed an increase in bone formation on, and around, the implant with a significant reduction in fibrous tissue fixation (Elmengaard et al., 2005).

- Polymeric substrates: A large use of peptide coating regards also polymeric substrates, both non-degradable and degradable. For example, to improve the biocompatibility of non-degradable PMMA implants they were coated with cyclic RGD peptides and examined in a rabbit model, where they demonstrated an improved ability to promote bone regeneration (Kantlehner et al., 2000). Encouraging results were obtained also on polymeric degradable substrates both *in vitro* and *in vivo* experiments. Chitosan films modified with GRGDS peptide were used with good results as a substrate for the *in vitro* culture of osteoblasts: cell attachment, proliferation, migration, differentiation, and mineralization were remarkably greater with respect to unmodified chitosan (Li et al., 2006). The coupling of RGD to alginate is another important topic; tests on alginate gel with RGD peptide, revealed that it was able to promote the adhesion and the differentiation of preosteoblasts, suggesting their use for the construction of injectable gel particles for the promotion of bone regeneration (Evangelista et al., 2007). Moreover, the coupling with alginate was also explored in terms of nanopatterning showing that in kinase phosphorylation of focal adhesion, cell spreading, and osteogenic differentiation can be controlled in preosteoblasts by this kind of RGD structures (Comisar et al., 2007). Polymeric degradable substrates were tested with success *in vivo*. This is the case, for example, of porous poly(lactic-glycolic acid) (PLGA) disks coated with RGD peptide and implanted in cortical wounds in rat tibiae. They were able to demonstrate good osteocompatibility and osseous ingrowth (Eid et al., 2001). *In vivo* studies have regarded also the positive synergism of RGD peptides with other bioactive component, such as in the case of the combined addition of phosphoserine and RGD-peptide to hydroxyapatite/collagen composites, which demonstrate an enhancement of the bone remodelling (Schneiders et al., 2007).

In order to provide a stable linking to RGD peptides, polymeric substrates are optimal candidates because of their chemical versatility. Even if many polymers do not possess functional groups on their surface, these can be introduced by blending, co-polymerization or chemical and physical treatment:

- Functional groups for peptide immobilization on polymer surfaces can be generated by **blending** with other polymers containing the desired chemistry. Functional groups of hyaluronic acid and chitosan were used for example to coat a titanium

implant *via* formation of polyelectrolyte multilayers. The immobilized RGD peptides demonstrated to have a significant influence on osteoblast adhesion and proliferation (Chua et al., 2008), (Cai et al., 2007). Another example is the poly(lactic acid) (PLA) which has been coated with poly(L-lysine) (PLL) *via* adsorption. The free amino groups of the PLL can be used for further modification (Quirk et al., 2001), (Yang et al., 2001).

- Targeted **co-polymerization** is another possibility to introduce functional groups into permanent and biodegradable polymers. Co-polymerization with acrylic acid, as used in the case of N-isopropylacrylamide leads to carboxylic groups as side chains (Stile and Healy, 2001). A poly(lactic acid-co-lysine) was synthesized to immobilize peptides on the pendant amino groups onto the lysine side chains (Cook et al., 1997).
- Alternative ways to introduce modifiable groups on the polymer surface are **chemical and physical treatment**, such as alkaline hydrolysis, reduction, oxidation, or plasma deposition. For instance hydroxyl groups on poly(vinyl acetate) were obtained after alkaline hydrolysis. PLA and poly(caprolactone) (PCL) films have been aminofunctionalized through allylamine pulsed plasma deposition (PPD). This procedure was followed by coupling of RGD modified PEG chains. After the introduction of functional groups on the polymer, for the chemical immobilization, it is possible to use various chemical strategies for peptide coupling. The most used is the formation of a covalent amide bond between the activated carboxylic acid group of the polymer and the terminal amine of the peptide (Hersel et al., 2003).

Another important factor is the amount of immobilized peptide, in fact the number of attached cells is related to the density of RGD on the surface and a sigmoid increment can be observed when reporting the cell attachment as a function of RGD concentration (Kantlehner et al., 2000), (Jeschke et al., 2002). Moreover, there is a critical minimum density which is necessary to reach in order to obtain a cell response. Massia and Hubbell found that a minimum amount of 1 fmol RGD peptide/cm^2 was sufficient for cell spreading, while 10 fmol/cm^2 was sufficient for the formation of focal contacts on a RGD in a rigid glass surface but this parameter is strongly depending on the substrate. One should always, in fact, take into account the entropic penalty resulting from the attachment of the peptide to a flexible polymer chain as opposed to a rigid surface (Elbert and Hubbell, 2001). Finally, a comparison of the impact of RGD density on different cells adhesion can be made only when other effects

contributing to cell adhesion are absent. Even the same cell expresses integrins in different ways in different moments of its life.

A crucial factor contributing to a successful cell attachment is the design of the RGD peptide. This regards both the choice of the sequence peptide and the chemical spacer used to link the peptide onto the surface. Many researchers have tested the role of the spacer length: it seems that a distance of 35 - 46 Å between the active sequence and the surface is required to permit the binding between integrin and the active site; when the spacer is too long, a reduced cell attachment is achieved (Beer et al., 1992). Moreover, there are some examples where no spacing between the anchoring group and the RGD moiety were used and an excellent adhesion was achieved (Massia and Hubbell, 1991); these conflicting data suggest that the need for a spacer and its length have to be tested in each single type of system.

By choosing the proper sequence of the RGD peptide, it is possible to improve integrin binding selectivity. Apart from activity, the selectivity of different RGD sequences was attributed to the neighbouring amino acids in the sequence or to spatially next-neighbouring residues in the used peptides. The addition of amino acids to the sequence can change its integrin affinity, generating a different cell response. In some applications, selective adhesion of a certain cell type to a RGD functionalized surface is crucial for success; this is the case of vascular grafts for endothelialization where adhesion of endothelial cells but not platelets is required. Since each cell line has its own typical pattern of different integrins, this suggests the employment of RGD peptides not only with high receptor affinity, but also with high receptor selectivity. Moreover, it should be reminded that cells express more than one type of integrins and that the integrin expression pattern on the cell surface is not static. For what concerns the integrins used in cell adhesion studies and mainly involved in bone functions, they are the $\alpha_V\beta_3$, the $\alpha_5\beta_1$ and the $\alpha_{IIb}\beta_3$ (see Figure 19) (Petreaca and Martins-Green, 2007).

An interesting member of RGD family is the GRGDS peptide, a fibronectin motif. It has been shown to have comparable affinity for $\alpha_V\beta_3$, $\alpha_5\beta_1$ and $\alpha_{IIb}\beta_3$ at an intermediate level, and it may be useful if no particular integrin is to be addressed for cell adhesion (Hersel et al., 2003). This peptide is one of the more used in promoting osteoblast adhesion (Quirk et al., 2001), (Li et al., 2006), and has been reported to play an essential role in adhesion, remodeling, and osteointegration at the interface between a biomaterial and bone (Yang et al., 2001).

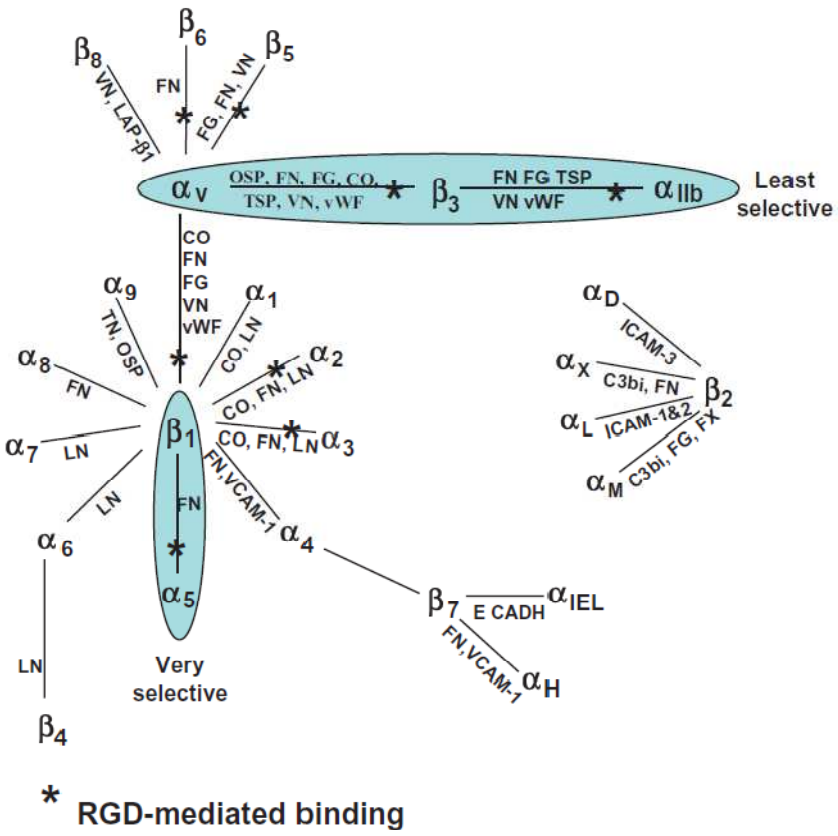

Figure 19. Members of the integrin family of ECM receptors and their respective ligands. Integrins receptors, are capable of binding a variety of ligands, including Ig superfamily cell adhesion molecules, complement and clotting factors, and ECM molecules. Cell-cell adhesion is mediated through integrins with β_2 subunits, while cell-matrix adhesion is mediated primarily via integrins containing β_1 and β_3 subunits. In general, the β_1 integrins interact whit ligands found in the connective tissue matrix, including laminin, fibronectin and collagen, whereas the β_3 integrin interact with vascular ligand, including thrombospondin, vitronectin, fibrinogen, and von Willebrand factor. *Abbreviations*: CO, collagens; 3bi, complement component; FG, fibrinogen; FN, fibronectin; FX, factor X; ICAM-1, intercellular adhesion molecule-1; ICAM-2, intercellular adhesion molecule-2; ICAM-3, intercellular adhesion molecule-3; LN, laminin; OSP, osteopontin; TN, tenascin; TSP, thrombospondin; VCAM-1, vascular adhesion molecule-1; VN, vitronectin; vWF, von Willebrand factor; ECADH, E-cadherin; LAPβ1, latent activating protein β1.

4.2.2 Design of an injectable bone filler with adhesive properties

Given the complexity of the system, bookmark will help orienting in the text

INJECTABLE: Dispersion medium (provides flowability) + Bioactive filler (provide bioactivity and elasticity at rest)

1 Dispersion medium: hyaluronan
Hyaluronan: highly biocompatible, bioactive, viscoelastic

2 Bioactive filler: Microcomposite + Specific bioactive agents

A Microcomposite (dried microbeads): alginate + HAp

Alginate: biocompatible + hydrophilic

HAp: bioactive ("inorganic" bioactivity)

B Specific bioactive agents in filler:

RGD-containing peptides: pro-adhesive

BMP-fragment peptides: pro-proliferative
LL37-peptide: antibacterial

Immobilization of RGD peptides on polysaccharides

The chemical strategies taken into consideration studied for the conjugation of the peptide with the polycation ChitLac are summarized in Figure 20. Two kinds of bond formation, the amide and the disulfidic ones, and different linkers between the polymer and the peptide were considered:

- Amide bond formation on Chitlac modified with succinic anhydride (succinyl-ChitLac): ChitLac-COOH + NH_2-GRGDS-COOH → ChitLac-(CONH)-RGD
- Amide bond formation on unmodified ChitLac:
  ChitLac-NH_2 + NH_2-GRGDS-COOH → ChitLac-(NCO)-RGD
- Disulfide bridge formation on thiolated ChitLac:
  ChitLac-SH + SH-CGRGDS-COOH → ChitLac-(SS)-CRGD

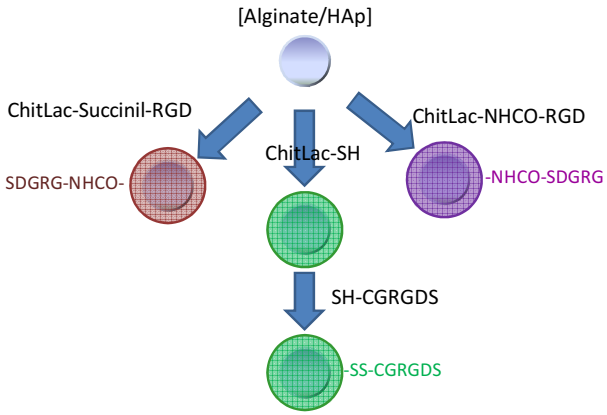

Figure 20. Approaches to immobilize RGD peptides on alginate/ hydroxyapatite beads.

Characterization of polymers: development of analytical methods.

Since the focal point of this research was the conjugation peptide-polysaccharide, a great effort was dedicated to the development of analytical methods to verify and characterize the modifications introduced on polysaccharides. The characterization of polysaccharides is not an easy matter because of their complexity of their structures and their polydispersity, which render its analysis by means of separation techniques very difficult. Carbohydrates are not volatile compounds and do not have chemical properties which permits an easy revelation with classical methods such as UV-visible or fluorescence. Moreover, the large size of polysaccharides used in biomaterials applications and at the same time, the relatively low mass of the peptides, reduces the number of useful investigative methods able to simultaneously monitor the introduction of a modification on the polysaccharide and the consumption of the peptide.

Capillary electrophoresis (CE) is the most powerful technique for the analysis of this type of compounds, thanks to its ability to investigate a wide range of molecular weights and to identify modifications also on large structures. Capillary electrophoresis permits in fact the determination and quantification of a large variety of molecules and is used in a wide range of applications. CE is used for example for the separation of inorganic and organic molecules, such as carbohydrates, peptides, proteins, DNA and all of these separations are possible in a wide variety of matrices (Schmitt-Kopplin, 2008). Capillary electrophoresis is an efficient tool also for amino acids analysis, and it is able to reveal more amino acids in a single run with lower detection limits.

We developed therefore an electrophoretic analytical method for the quantification of peptides bound on polysaccharide chains in order to determine their degree of substitution. This method involves the analysis of the hydrolyzed of a known amount of the modified polymer by capillary electrophoresis.

The analysis of the hydrolyzed is a common procedure to quantify peptide-polysaccharide conjugation (Li et al., 2006), in fact the acid treatment at high temperature (HCl 6 M, 110°C under reflux, overnight) is able to break amide bonds and the free amino acids constituting the peptide are found in the hydrolysed mixture. The amino acids containing mixture can then be analysed, generally with an amino acid analyser.

On the contrary, given the type of analysis and the complexity of the matrix sample, we preferred to exploit a separation technique, such as capillary electrophoresis.

The first method we developed involved the use of an acid buffer (silica capillary, running buffer citrate 20 mM at pH 2.5, with an applied potential of 15 kV), which permits the identification and the quantification of the entire peptides GRGDS and CGRGDS. But, since the peptide is covalently linked to the polysaccharide and is a poor chromophore, it is necessary to break the linkage before quantification. Therefore, we optimized a method to perform quantification on the basis of free amino acids released after acid hydrolysis, which breaks every amide bond in the molecule. The method was obtained after optimization of electrophoretical conditions used in literature for the identification of *N*-acetylcysteine in pharmaceutical products control (Jaworska et al., 1999). In this second approach the use of a basic running buffer permits the identification of all amino acids composing the peptides. A study was carried out, on the basis of the isoelectric point of every single amino acid, to obtain their separation.

Table 4. Influence of pH on charge of amino acids belonging to RGD peptides.

		D	G	S	R	C	GRGDS	CGRGDS
MW		**133,10**	**75,07**	**105,09**	**174,20**	**121,15**	**490,47**	**593,61**
p.I.		3,81	5,50	5,50	10,00	5,50	6,25	6,25
pH	**2.50**	0,8	0,8	0,8	1,8	0,8	1,8	1,8
	3.00	0,5	0,6	0,6	1,6	0,6	1,5	1,5
	3.50	0,2	0,3	0,3	1,3	0,3	1,2	1,2
	4.00	-0,2	0,1	0,1	1,1	0,1	0,8	0,8
	4.50	-0,5	0,0	0,0	1,0	0,0	0,5	0,5
	5.00	-0,8	0,0	0,0	1,0	0,0	0,2	0,2
	5.50	-0,9	0,0	0,0	1,0	0,0	0,1	0,1
	6.00	-1,0	0,0	0,0	1,0	0,0	0,0	0,0
	6.50	-1,0	0,0	0,0	1,0	0,0	0,0	0,0
	7.00	-1,1	-0,1	-0,1	0,9	-0,1	-0,1	-0,1
	7.50	-1,2	-0,2	-0,2	0,8	-0,3	-0,2	-0,3
	8.00	-1,5	-0,5	-0,5	0,5	-0,7	-0,5	-0,7
	8.50	-1,8	-0,8	-0,8	0,2	-1,3	-0,8	-1,3
	9.00	-1,9	-0,9	-0,9	0,1	-1,7	-0,9	-1,7
	9.50	-2,0	-1,0	-1,0	0,0	-1,9	-1,0	-1,9
	10.00	-2,0	-1,0	-1,0	0,0	-2,0	-1,0	-2,0

Working at pH 9.00 how it is indicate in Table 4, it was possible to obtain the better combination of analyte charges, which allowed the separation of all investigated amino acids and of the entire peptide (as it can see in the electropherogram below in Figure 21).

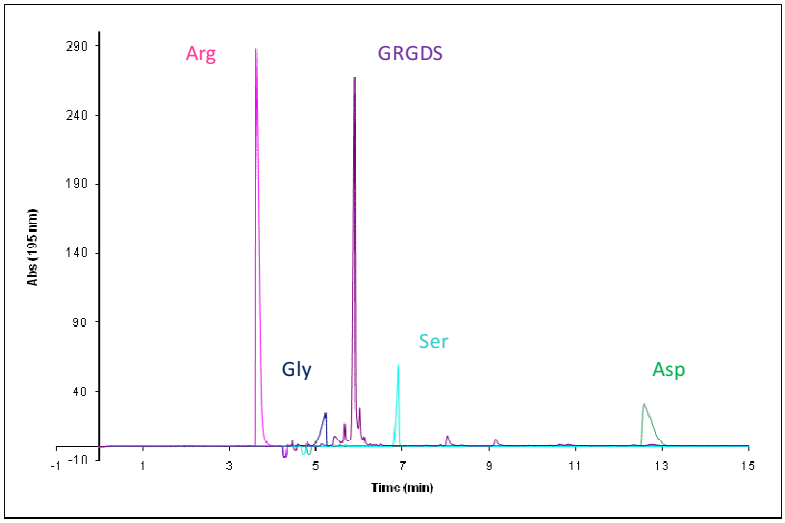

Figure 21. Electropherogram of the amino acids arginine, glycine, serine, aspartate and the GRGDS peptide. (all compounds were measured at a concentration of 1 mg/mL). Electrophoretic conditions: fused silica capillary effective length 56 cm, total length 64 cm, internal diameter 50 µm, running buffer borate 100 mM at pH 8.95, applied potential 15 kV, wavelength 195 nm).

As an example of the strategy used for amino acids separation and peptide quantification, the analysis after acid hydrolysis of a known amount of the peptide GRGDS was verified. At the end of hydrolysis, after evaporation of hydrochloric acid, the residue was re-dissolved in a known amount of running buffer. The electrophoretic analysis revealed that the amino acid more suitable for the quantification was arginine, so after having performed the calibration curve, obtaining a good linearity (in a range 2-10 mg/L), recovered arginine in the hydrolysed sample was quantified. The correspondence between the initial and the final amounts of peptide was verified and the matrix effect was investigated by co-injection of an Arginine standard; the evaluation of the recovery parameter (R%) demonstrates the efficacy of the method (R% = 107%). The same approach was exploited for the quantification of all peptides-conjugates reported in this thesis and investigated in the following chapters.

Recovery% was calculated using the formula:

$$R\% = \frac{(C_a - C_o)}{C_t} \times 100$$

Where C_t is the theoretical concentration of the spike; C_a is the concentration of the sample spiked with C_t, evaluated from the calibration curve; C_o is the concentration of the sample, evaluated from the calibration curve (Desimoni, 1996). Acceptable values range is dependant from the method analysis; generally, a value in a range between 80% and 120% is accepted.

After assessment of the characterization method, it was applied to the quantification of RGD peptide immobilized on ChitLac following the different strategies reported below.

Amide bond formation on succinyl-ChitLac

The formation of a stable, covalent amide bond to conjugate a peptide to a polymer, is the most common procedure of immobilization. This is usually done by means of the reaction of a properly pre-activated carboxylic acid group, localized on the polymer, with a nucleophilic *N*-terminus of the peptide. Carboxylic acid groups can be easily activated by means of the carbodiimide chemistry, applying some precautions. Carboxylic groups can also be introduced on polymers which normally do not expose them, by means of chemical functionalization: for instance, a general strategy for polymers containing amino groups, like chitosan (and ChitLac), is the treatment with anhydrides in order to generate carboxylic groups, which can then reacted with RGD peptides (Li et al., 2006). To this aim, ChitLac was treated with succinic anhydride to generate carboxyl groups, which can react with the peptides GRGDS to form a short four carbon atoms arm. Moreover, the presence of this minimum spacer between the RGD sequence and the anchoring moiety could improve the cell attachment mimicking the situation in native protein, where the active sequence is exposed in a loop.

Synthesis of succinyl-ChitLac

The reaction with succinic anhydride was performed exploiting ChitLac amines not involved in the bond with lactose (Scheme 3). Since, the reaction was performed in water, because of the insolubility of ChitLac in other solvents, it was necessary to use a large excess of succinic anhydride, because of its instability in this medium.

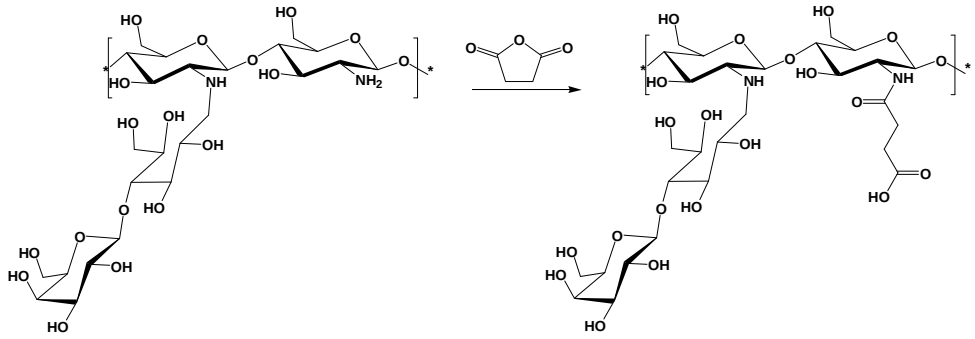

Scheme 3. Synthesis of succinyl-ChitLac by reaction of succinic anhydride with primary amine on ChitLac.

For the reaction 40, 30, 20 and 10 equivalents of succinic anhydride were used with respect to free amino groups of the polysaccharide.

After the ^{1}HNMR characterization, it was decided to use only the polymer modified with 10 equivalents, because for higher quantities the alkylation of secondary amines was observed.

Peptide conjugation on succinyl-ChitLac

For the successive formation of the amide bond with the peptide, the reactivity of the introduced carboxylic group towards the amine of amino acid *N*-terminus (Scheme 4) was exploited. The coupling of unprotected RGD peptides in water is articulated in a two-step procedure. Initially, carboxylic groups are activated as active esters using 1-ethyl-3-(3-dimethylaminopropyl)-carbodiimide (EDC) and *N*-hydroxysuccinimide (NHS): the first one is able to activate carboxylic groups, the second one is then bound forming an ester, a good leaving group, inside the molecule. In a second step, the peptide is added to the activated polymer, and the amide bond formation occurs.

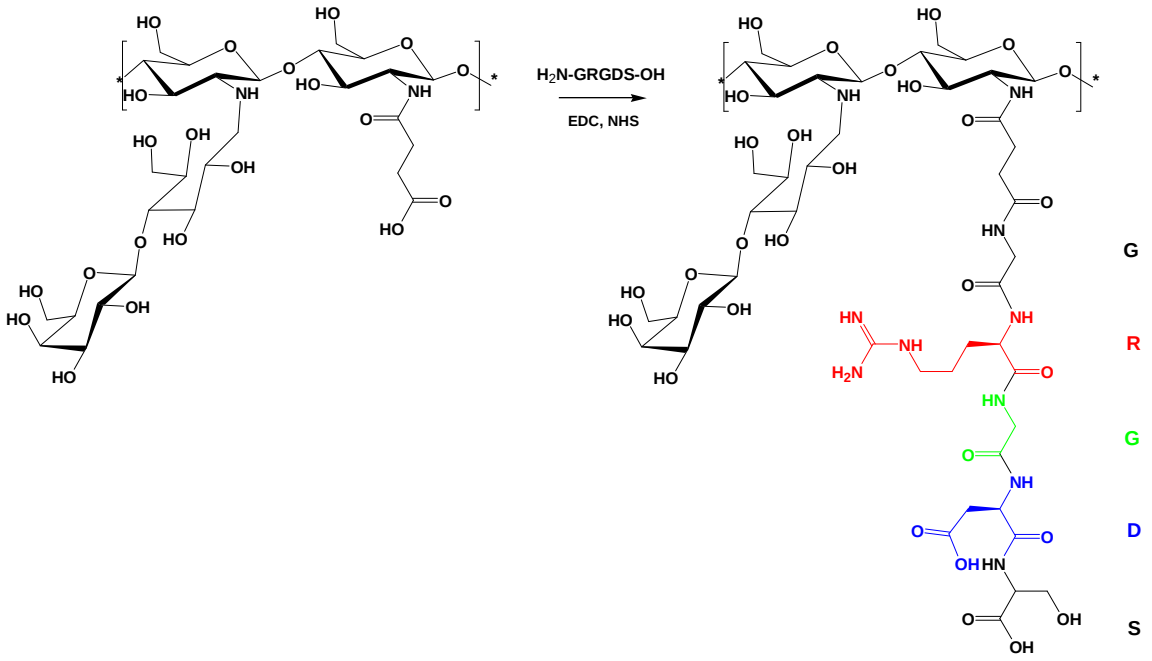

Scheme 4. Synthesis of ChitLac-(CONH)-RGD obtained by GRGDS peptide conjugation to succinylated ChitLac: the carboxylic groups of the polymer was preactivated by carbodiimide chemistry, and in a second moment the peptide was added.

With this procedure, it is not necessary to introduce protecting groups on peptide side chains: in fact, usually, the principal problem using peptides is the presence of reactive groups on lateral chains (Scheme 5), which can give rise to side-reactions.

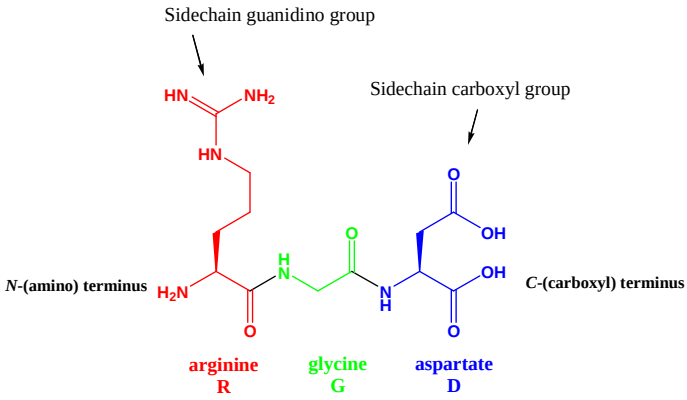

Scheme 5. The RGD sequence, its molecular formula and nomenclature, possible reactive groups are evidenced.

In this case, considering the core sequence (RGD) of the peptide, there are two amino groups: one in *N*-terminus position and the second one on the side chain of arginine. Arginine lateral chain consists of three methylene groups which are not polar and a δ-guanidinium group, highly basic, which at physiological pH conditions, is ionized. Because of resonance forms, the guanidinium group presents a planar structure and the positive charge is delocalized on the entire group. Due to its protonation in water, the nucleophilicity of the arginine side chain is nearly abolished and is significantly less reactive than the amino group of glycine. Other reactive functional groups in RGD sequence are the carboxylic groups which are present both on arginine side chain and in the *C*-terminus amino acid. A strategy to avoid side reactions caused by these carboxylic groups is to perform the synthesis on two steps, first preactivating the carboxylic groups of the polymer and only after that, to introduce the peptide (Scheme 6). In such manner, peptide carboxylic acid groups are not activated for coupling.

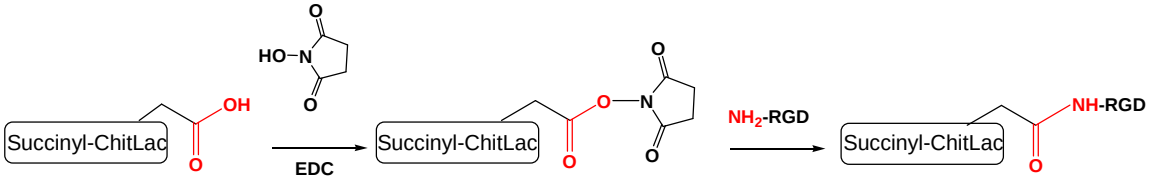

Scheme 6. RGD peptide reacts via the *N*-terminus with polymer carboxyl group preactivated with a carbodiimide (EDC) and NHS to generate an active ester.

Characterization of the polymers succinyl-ChitLac and ChitLac-(CONH)-RGD

Before conjugation with the peptide, succinyl-ChitLac was characterized by means of ^{1}HNMR spectroscopy and, as it has been already anticipated, the analysis revealed the substitution also of secondary amines for high concentrations of succinic anhydride.

To determine the degree of RGD substitution in ChitLac-(CONH)-RGD polymer, a known amount of lyophilized polymer sample was hydrolysed in acidic conditions and the final peptide amount was derived from the arginine quantification after hydrolysis and performed by capillary electrophoresis. The quantification of substitution in the final modified polymer indicates a good yield: using 1.7 equivalents of peptide with respect to succinyl groups, a peptide substitution equal to 5.4% with respect to the average repeating unit was obtained, corresponding to 23.3% of reacting groups.

Unfortunately, the final modified polysaccharide was not soluble in water, probably because of the simultaneous presence of negative and positive charge along the polymeric chain, which caused precipitation. Therefore, for the preparation of the final product, only the strategy involving the direct formation of a covalent amide bond between unmodified ChitLac and RGD peptide was considered, as reported in the following paragraph.

Amide bond formation on unmodified ChitLac (ChitLac-(NCO)-RGD)

Given the problems arisen with succinyl-ChitLac, a different strategy for the conjugation through direct amide bond was carried out. Without performing any modification on ChitLac, the reaction was realized between the activated carboxylic acid groups of the peptide with the nucleophilic amine groups of the polycation (Scheme 7).

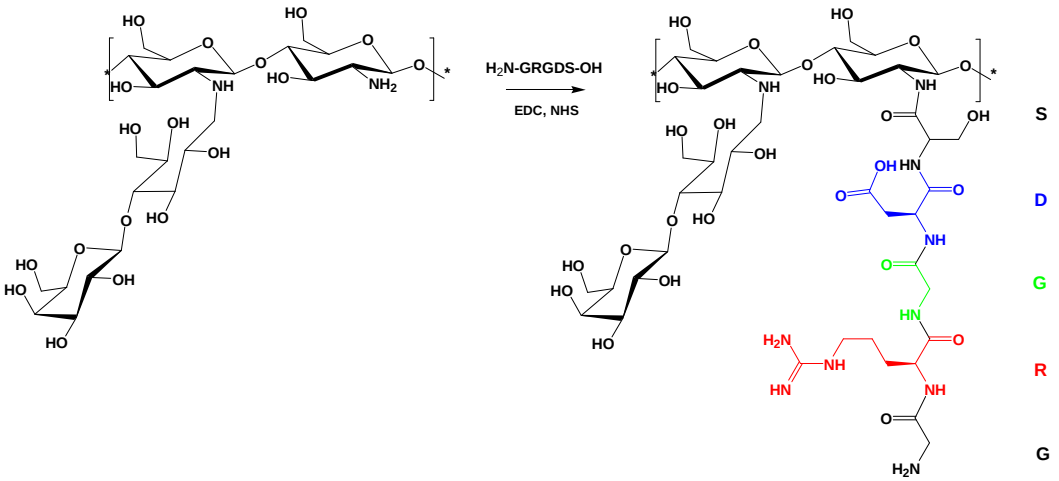

Scheme 7. Synthesis of ChitLac-(NCO)-RGD obtained by GRGDS peptide conjugation to unmodified ChitLac.

The strategy of carbodiimide chemistry was applied by activation of carboxylic group of peptide followed by grafting to ChitLac (Scheme 8). Two problems may arise by this coupling method. Firstly, there are further reactive functional groups in the RGD peptide such as the N-terminus of the peptide which could give rise to the peptide dimerization; secondly, the presence in the peptide sequence of the carboxylic group in the aspartate side chain could cause the attachment of the peptide trough amino acid, rather than with the *C*-terminus, causing a different conformation that will be presented to the receptor. Probably, because of all these possible side-reactions, the RGD peptide coupling yields are very low, when using this chemistry. Another problem of this strategy is that the obtained polymer presents the RGD peptide in a reverse sequence, if compared to polymers normally described in literature. This could compromise the biological activity of the modified polysaccharide, reducing or totally annihilating it. Therefore, special attention was devoted to the characterization of the biological properties of this compound.

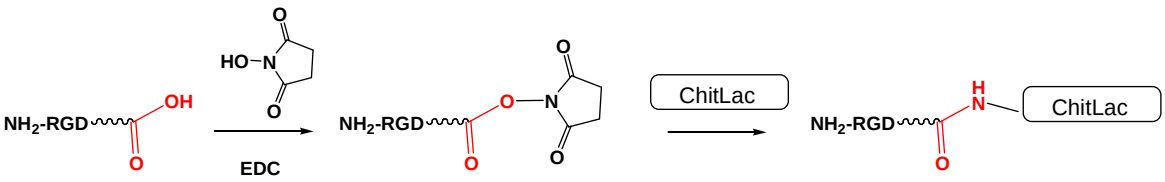

Scheme 8. RGD peptide reacts via the preactivated *C*-terminus with the primary amine of ChitLac. The preactivation of peptide is performed with the carbodiimide (EDC) and NHS to generate an active ester.

Characterization of the polymer ChitLac-(NCO)-RGD

The composition of the modified polymer was characterized with ^{1}H NMR spectroscopy (data not shown) and CE-UV. In particular this second technique was useful for the quantification of bound peptide.

CE-UV data To determine the degree of RGD substitution in ChitLac-(NCO)-RGD polymer, a known amount of lyophilized polymer was dissolved in hydrochloric acid and stirred at 110°C overnight under reflux, as described in the Materials and Methods section. The final peptide quantification is derived from the arginine quantification in the hydrolysed, performed by capillary electrophoresis. The degree of polymer functionalization resulted equal to 0.45% with respect to the average repeating unit, corresponding to 2% of primary amines.

Biological tests on ChitLac-(NCO)-RGD

Since the RGD conjugation to ChitLac by means of direct amide bond had a very low yield and the orientation of the peptide was not usual, the polymer ChitLac-(NCO)-RGD was tested on osteoblasts cultures, in order to control the dependence of adhesion promotion from the peptide orientation. In order to test *in vitro* the bioactivity of RGD peptide, the functionalized polysaccharide was deposited on solid supports. These supports are constituted by methacrilate-based reins that were surface-functionalized by acid treatment to expose carboxylic negative charges (Travan et al., 2010).

A cell proliferation assay using MG63 osteoblasts-like was performed on disks coated with ChitLac-(NCO)-RGD and their activity was compared with disks coated with unmodified ChitLac; standard titanium disks with a roughened surface were used as control. The results were normalized at the day 1 to obtain a relative cell proliferation rate which allows a direct comparison between the different coatings (Figure 22). Thanks to its slightly positive charge, the coating with the unmodified ChitLac stimulates weakly the cell proliferation, but is not sufficient to increase the cell growth rate to the values observed for the titanium disks. On the contrary, despite the low degree of substitution and the unusual bond of the peptide, the coating with ChitLac-(NCO)-RGD favours cell proliferation with respect to ChitLac-coated substrates presenting a cell growth rate comparable with the used titanium standard.

From these data, it is clear that RGD peptides maintain their activity when linked on ChitLac. The chemical-physical characteristics of the polysaccharide do not interfere with the interaction of RGD sequence with osteoblast integrins, regulating and increasing the cell proliferation.

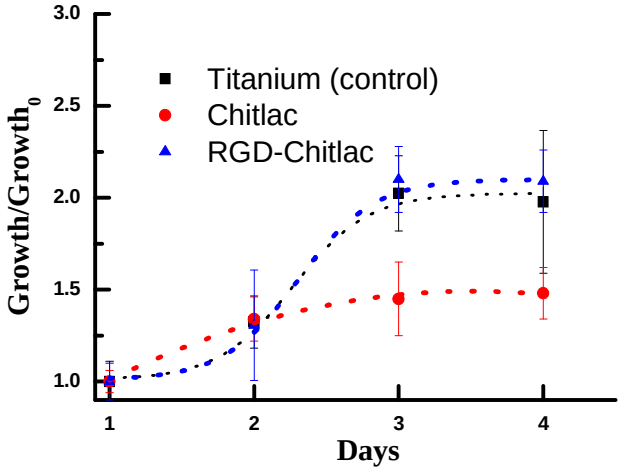

Figure 22. Adhesion of cells (osteoblasts MG63) promoted by different supports. The cell growth was normalized at the first day.

Disulfide bond formation on thiolated ChitLac

The amide-bond strategy has several advantages, the principal on being its ease, but drawbacks are a low yield, probably due to the formation of auto-condensation products, and the possibility to have peptides partially not correctly linked to the polymer *via* aspartic acid, and therefore unable to perform their biological activity. Therefore, also another and more selective immobilization approach was explored.

This consisted in the formation of a disulfide bridge between a proper ChitLac derivative and RGD peptide with an additional Cysteine (H_2N-Cys-Gly-Arg-Gly-Asp-Ser-COOH). With this aim, ChitLac was modified by a thiolation reaction, obtaining thiolated ChitLac (Chitlac-SH). Successively, the ChitLac-SH was deposited on the bead surface or mixed with alginate and hydroxyapatite before the gelation step. In this manner, bead constructs exhibits thiol groups which are able to react with the sulfhydryl group localised in the lateral chain of the peptide CGRGDS, enabling the peptide-polysaccharide conjugation via disulfide bridge formation.

The reaction is spontaneous at normal oxidants conditions (air exposition), but can be enhanced using proper oxidants, such as hydrogen peroxide and thus obtaining higher yields and shorter reaction times. This conjugation presents a major specificity compared with the amide bond formation because the only reacting groups are thiols, moreover the conjugation is performed only on the external layer, so the peptide is more available for the interaction with integrins. On the other hand the high reactivity of sulfhydryl group is also the cause of the disadvantage of this approach which is the un-handiness of the thiolated ChitLac: during oxidation of sulfhydryl groups it is easy to obtain intramolecular disulfide bridges, which are also favoured by the high local density of thiols along the polymeric chain.

Synthesis of thiolated ChitLac

The first step of the synthesis to be optimized regarded the ChitLac thiolation procedure. This functionalization was achieved by the reaction of amino groups on ChitLac with 2-imminothiolane in a one-step coupling reaction which does not needs of activation (Bernkop-Schnürch et al., 2003). 2-imminothiolane reacts with the primary amino group of ChitLac creating a covalent bond by ring opening. The chemical structure of the reagent is protected towards oxidation due to its chemical structure and thiol group is exposed only after the reaction with primary amine after ring opening. The 2-iminothiolane is well known as reagent for the immobilization of thiol groups on primary amines of proteins. In order to obtain

various degrees of polymer substitution, different equivalents of reagent were used. Because of the easy formation of disulfide bonds, the reaction was performed with particular precautions which involve working under nitrogen, in the dark, and dialyzing against hydrochloric acid. Really, despite the presence of antioxidants conditions, it was not possible to avoid completely the disulfide bond formation between ChitLac chains.

In contrast with the modification with succinic anhydride, the modification with 2-iminothiolane provides the introduction of a cationic amidine substructure. So, by modifying ChitLac with 2-iminothiolane, as illustrated in Scheme 9, the cationic character of the polymer can be maintained, with a positive effect on solubility and on layer beads deposition. After ChitLac modification with thiol groups, the polysaccharide was used to coat beads of alginate and hydroxyapatite.

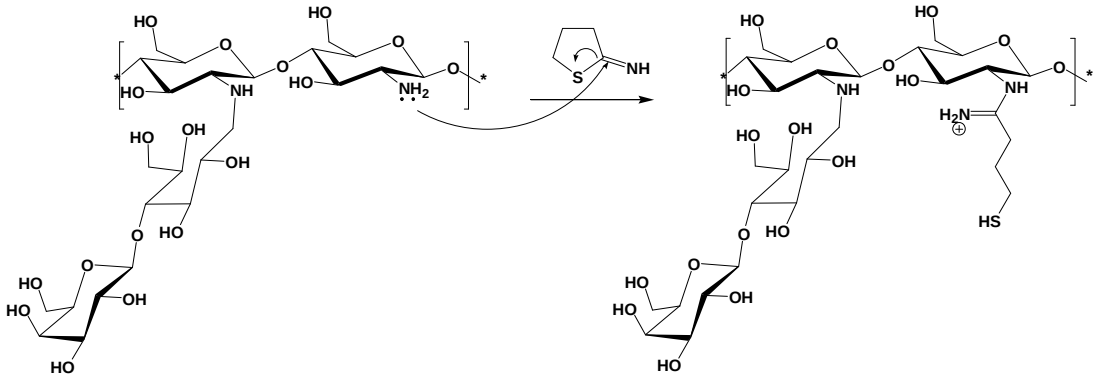

Scheme 9. Synthetic pathway of the ChitLac derivatization with 2-iminothiolane.

Peptide conjugation to structures containing ChitLac-SH

The thiol groups introduced into the ChitLac structure, demonstrated to be able to form disulfide bonds with the peptide according to Scheme 10. This ability was applied and demonstrated when the modified polymer was previously deposited on a surface, such as that one of beads. Disulfide bond is a covalent bond which is formed from the oxidation of sulfhydryl groups; this reaction is promoted by a variety of oxidants including air and hydrogen peroxide. The great advantage of the disulfide bond strategy in this kind of conjugation is the high coupling selectivity, which permits the preservation of the correct peptide orientation. Moreover, the possibility of performing the binding at the surface of the

final manufacture product, without the use of compounds needing purification, is very functional.

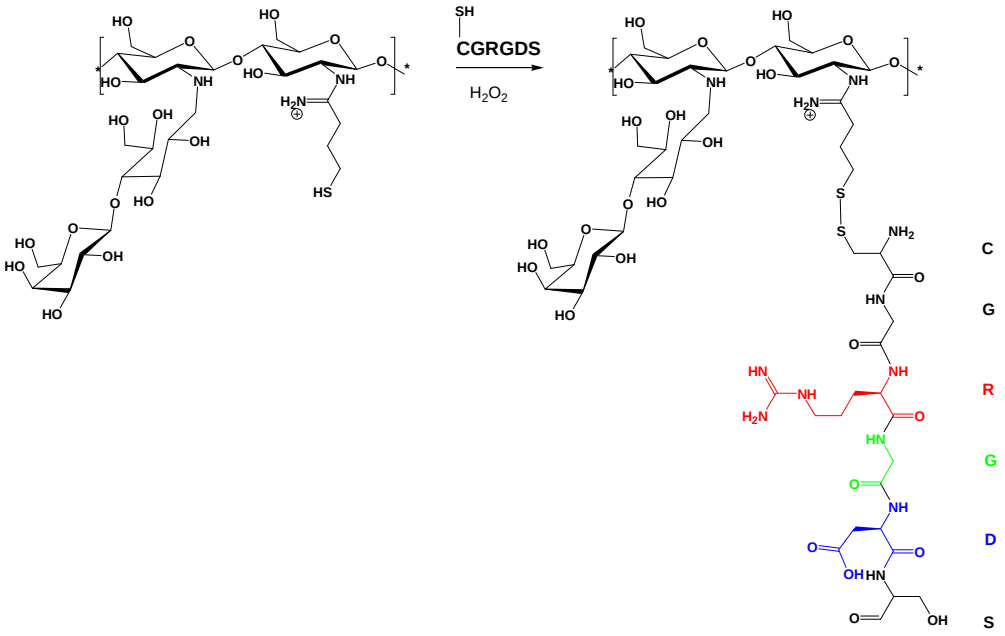

Scheme 10. ChitLac-(SS)-CRGD. Obtained by conjugation of the CGRGDS peptide to ChitLac-SH.

Scheme 11 reports two possible strategies to perform the conjugation of the peptide on thiolated beads. In the first case (panel A) the peptide is bound to an external layer of ChitLac-SH which was deposited on alginate/HAp beads surface; in the second strategy (panel B), the peptide is bound to beads obtained by an alginate/HAp/ChitLac-SH blend. In both ways the peptide is bound on preformed beads. Procedure will be discussed, in the detail, successively.

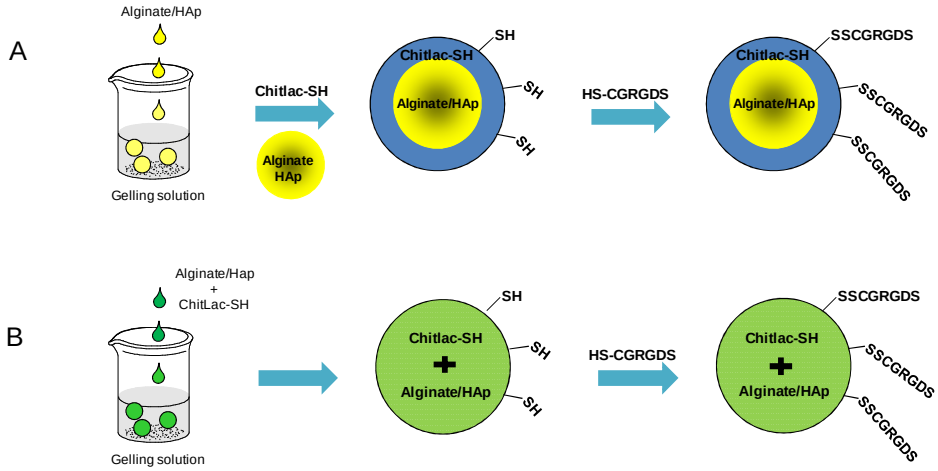

Scheme 11. Strategies for the deposition of CGRGDS peptide on beads containing Chitlac-SH. The ChitLac-SH can used to coat preformed alginate/HAp beads (panel A) or it can be mixed with alginate and HAp, before dropping them into the gelling solution (panel B).

Characterization of ChitLac-SH

Different degrees of functionalized thiolated ChitLac (1% and 3% on the total polymer) were obtained by using different equivalents of 2-imminothiolane, and they were characterized with the colorimetric "Ellman's test" and by ^{1}H NMR analyses.

In the first procedure, the quantitative determination of the thiol groups amount was performed spectrophotometrically with Ellman's reagent (5,5'-Dithio-bis(2-nitrobenzoic acid) or DTNB). The Ellman's test is a standard colorimetric analysis normally used to quantify free thiol groups present in proteins and peptides. To apply the method to modified polysaccharides, the procedure was accurately optimized for this kind of systems (Hornof et al., 2003). DTNB reacts with free thiols group releasing 2-nitro-5-benzoate (TNB) a yellow compound quantifiable at 450 nm. Sulphydryl groups may be estimated in a sample by comparison with a standard curve, built using known concentrations of a thiolated compound, like cysteine. This reaction permits to quantify free thiol groups; for the evaluation of disulfide bonds, a certain amount of sample is treated, before the reaction with Ellman's reagent, with a highly reducing agent like sodium borohydride ($NaBH_4$). In this manner, it is possible to distinguish and quantify free thiol groups and disulfide bridges on the polymer. In fact, as it has been already anticipated, despite the antioxidants conditions employed during the reaction, it was not possible to avoid completely intramolecular disulfide bridges formation, because they are very close to each other on the polymeric chain. The amount of immobilized thiol groups in reduced and oxidized form was determined with and without previous quantitative reduction of disulfide bonds with borohydride and can be resumed as follows:

- The low substitution degree ChitLac showed a total thiol content of 1.3% with respect to the average repeating unit, (corresponding to 5.8% of primary amines), and a percentage of 0.3% of free thiol groups.
- The high substitution degree ChitLac revealed a total thiol content of 3.0% with respect to the average repeating unit, (corresponding to 13.3% of primary amines), and a percentage of 1.6% of free thiol groups. This substitution degree polymer was used in the beads production.

Data were confirmed by ^{1}H NMR evaluation where the total contents of sulfhydryl groups were estimated as 1.0% and 3.1% with respect to the average repeating unit for the low and the high substitution degree respectively.

The conjugation of C-RGD peptide to beads surface was determined by means of hydrolysis of these ones and successive quantification of arginine in the hydrolysed solution by capillary electrophoresis. Data will be reported in the section of biological tests on p.124.

2	**Bioactive filler: Microcomposite + Specific bioactive agents**	
	A	**Microcomposite (dried microbeads): alginate + HAp**
		Alginate: biocompatible + hydrophilic
		HAp: bioactive ("inorganic" bioactivity)

Beads preparation

Composite beads were prepared with hydroxyapatite and alginate via gelation in calcium chloride solution under stirring. The contact with a calcium solution induces ionic cross-linking of alginate chains, giving rise to hydrogel beads. In order to obtain beads with different dimensions to perform various experiments, diverse production techniques were adopted:

- µbeads (about 600-700 µm at the wet state) were obtained using an electrostatic beads generator.
- beads of intermediate diameter (about 1 mm at the wet state) were produced by means of an air coaxial flow.
- large beads (about 2 mm at the wet state) were obtained by dropping manually with a syringe the mixture of alginate into the gelling solution.

LAYERED BEADS: For the preparation of layered beads, a bead core of alginate/hydroxyapatite was created. Alginate/hydroxyapatite beads were prepared by dropping in the gelling solution an alginate/hydroxyapatite mixture using the standard procedure developed for alginate beads (see **Materials and Methods** section). Since bead formation occurs as soon as alginate gets in contact with calcium solution, hydroxyapatite remains entrapped into alginate beads. The beads so obtained were stirred for 30 minutes, then washed with water and successively stirred in a 0.1% w/v solution of polycation (ChitLac-SH or ChitLac-(NCO)-RGD) dissolved in water. During the stirring in the presence of the polycation, a layer of this one is deposited on the bead surface, where it remains

electrostatically bound. At the end of the process, the beads coated with thiolated ChitLac were transferred to an aqueous solution containing the peptide (CGRGDS), to which, after 5 minutes, hydrogen peroxide (H_2O_2) was added and the solution was stirred for further 30 minutes. During this time, the external free thiol groups of ChitLac-SH, deposited on the beads surface, are able to react with sulphydryl groups of the peptide, and the hydrogen peroxide addition favours this process (Scheme 11, panel A). The oxidant is added five minutes after the peptide in order to avoid intramolecular disulfide bridges or dimerization of the peptide. In order to optimize the disulfide bridge formation, the hydrogen peroxide oxidant capacity involved in this chemical step was evaluated. In detail, a comparison between three mediums was performed by adding to beads previously layered with ChitLac-SH a solution of CGRGDS peptide to which either water, or basic buffer (buffer borate pH 8.95) or hydrogen peroxide (0.3% v/v) were added. At the end of the reaction time, the three kinds of beads were degraded and the content of bound peptide recovered in their amino acidic hydrolysed broth was quantified with the capillary electrophoretic method cited above. The higher oxidant power of hydrogen peroxide with respect to other mediums was evident, as expected, and it was then chosen to be the most apt to accelerate the reaction.

MIXED BEADS: Mixed beads are obtained by dripping a mixture containing alginate, hydroxyapatite and polycation dissolved in buffer 10 mM HEPES and 150 mM NaCl at pH 7.4, into the gelling solution. Also in this case for the functionalization with CGRGDS, beads were stirred in a solution containing peptide and hydrogen peroxide (Scheme 11, panel B).

Beads are then dried in dynamic conditions in the presence of an air flow to maintain them detached and spherical. Drying allows beads to remain stable and offers the possibility to sterilize them by exposure to a UV lamp in order to perform biological tests.

Bead properties

In this part of the work, the influence of the beads preparation technique on their final structure was investigated. We observed the effective deposition of the external cationic layer in alginate beads coated with a fluorescent ChitLac by means of confocal laser scanning microscopy (CLSM). Moreover, we studied how a different distribution of the polycation in the bead can influence the swelling behaviour and consequently the future mechanical stability *in vivo*.

Visualization of the beads by Confocal Laser Scanning Microscopy (CLSM)

Two types of µbeads produced with an electrostatic beads generator were considered in order to verify the distribution of ChitLac in alginate beads. ChitLac derivatized with fluorescein isothiocyanate (FITC) was used to coat preformed beads, obtaining "layered beads", or in combination with alginate before the gelation procedure, obtaining mixed beads. The distribution of ChitLac in alginate µspheres was analysed in wet conditions using confocal fluorescence microscopy. Since the thickness of the measurable volume of interest is limited to about 160 µm, the laser visible light can penetrate into the solid material not completely to dissect the bead at the hemisphere (µbeads have an average diameter of about 700 µm). In this manner, the analysis is limited to a spherical cap of the total bead: in spite of this limitation, CLSM analysis demonstrates a clear different distribution of the polycation in the different kinds of beads. The first picture reported (Figure 23) represents a µbead obtained by suspension of an alginate µbead in a Fluorescein-labeled ChitLac solution (ChitLac-FITC green); variation in FITC intensity is still more evident observing the distribution profile of labelled polysaccharide reported beside. It is clear that labelled-polymer is localized on the outer border of the capsule

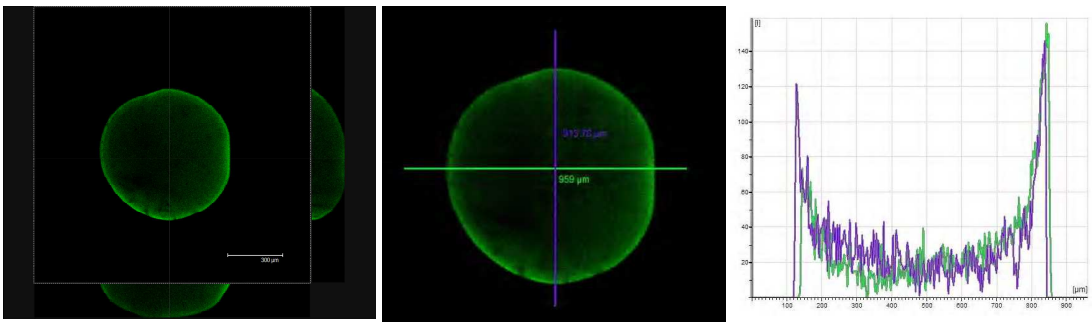

Figure 23. CLSM image of an alginate bead obtained by immersion in Fluorescein-labeled ChitLac solution.

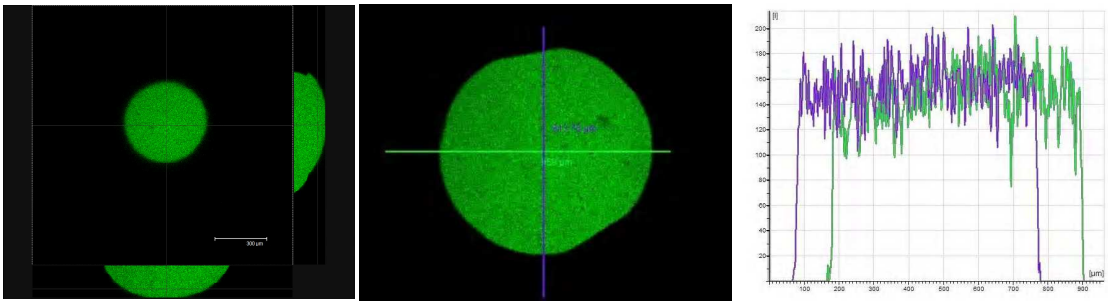

Figure 24. CLSM image of an alginate bead obtained by mixing Fluorescein-labeled ChitLac with alginate before gelation.

The second picture (Figure 24) shows a µsphere obtained by mixing alginate and ChitLac-FITC before gelation. As demonstrated by the distribution profile, this kind of µbead presents a very homogenous distribution of the labelled-polymer in the entire volume of the bead.

Stability and swelling

Alginate beads, gelified with calcium ions, tend to swell and dissolve in physiological conditions. The swelling of the beads is promoted by chelating compounds such as phosphate, citrate and lactate, but also by cations such as sodium and magnesium which are able to compromise the gel network stability, by replacing calcium ions.

Alginate gels can be intended as osmotic swelling systems, where the gel surface is similar to a semi-permeable membrane where the polysaccharide molecules are entrapped in. The force of swelling is the result of the presence of alginate fixed charges and it could be identified with the osmotic pressure across the semi-permeable membrane (Donnan equilibrium). Because of the string electrical field in the alginate network, the concentration of "mobile" cations will always be greater in the gel than outside and consequently, the osmotic pressure of the solution inside it will exceed that of the external solution. In general, the osmotic contribution to swelling of an ionic network is composed by two terms: the polymer-solvent mixing term ($\Delta\mu_{mix}$) and the chemical potential difference of water due to irregular distribution of ions between the inside and the outside of the gel, ($\Delta\mu_{ion}$).

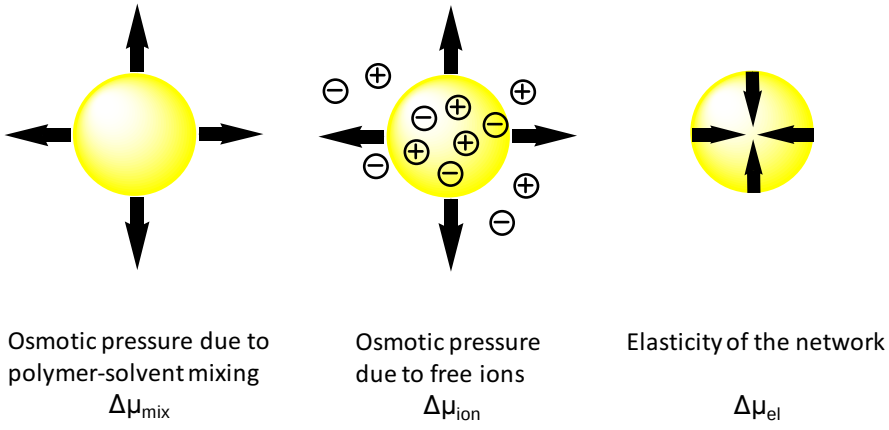

Figure 25. Factors influencing the swelling of the beads gel network.

In alginate gel the term $\Delta\mu_{ion}$ is dominating and the contribution comes from the non-cooperatively bound counter ions. The swelling is opposed by the physical cross-links,

leading an elastic network retraction force (Figure 25). This hydrogel network is able to stabilize the volume of the gel:

$$\Delta\mu_1=\Delta\mu_{mix} + \Delta\mu_{ion} + \Delta\mu_{el} = 0$$

The term $\Delta\mu_{mix}$ will mostly depend on the interactions between the polymer and the solvent and then on the hydration of the polymer (Hoffman, 2002), while the elastic term is highly dependent on the number and on the strength of the crosslinks in the polymer network. The ionic term will depend on the salt concentration outside the gel, the valence of the counter ion and the effective charge density of the polymer (Moe et al., 1993).

The swelling of Ca-alginate gels under physiological conditions depends on the alginate composition and polymer concentration. When calcium ions are exchanged with non-gelling sodium ions, the junctions in the network dissolves, reducing the elastic term. At the same time, the number of dissociable counter ions increases and each calcium ion will be replaced by two sodium ions, enhancing in this manner the ionic term. These effects contribute to the hydrogel network swelling which can be reduced by using alginate with a high content of guluronic acid blocks or by replacing calcium ions with divalent ions such as Sr^{2+} or Ba^{2+} (Thu et al., 1996) having a stronger affinity for alginate. A polyanion-polycation complex can be stabilize against swelling both by increasing the elastic forces and by partly discharging the polymer network (King et al., 2003), (Marsich et al., 2008).

Bead stability is very important for the final application of this work, useful to understand the structure and to compare different typologies of constructs. Swelling and dissolution represents a parameter largely studied in the use of alginate gel for encapsulation of cells. The swelling characteristics of beads (with an average diameter of 1mm) were determined by immersing them in the wet state into a saline solution. At specific time intervals, the measures of beads area were taken with a scanner and the swelling medium was substituted with fresh solution. Afterwards, by means of computer graphics software it was possible to obtain a value indicating the average area of each sample of beads. The stability of beads was analysed by selecting given combinations of alginate and ChitLac, considering the influence of different functional groups in modified and unmodified ChitLac.

We tested the swelling of different kinds of beads, produced by a coaxial air flow:

- Beads composed by a mixture of Alginate, hydroxyapatite and unmodified ChitLac
- Beads composed by a mixture of Alginate, hydroxyapatite and thiolated ChitLac (ChitLac-SH)
    - Samples treated with H_2O_2

- Samples not treated with oxidant

- Beads composed by a mixture of alginate and hydroxyapatite coated with two different percentages of unmodified ChitLac
- Beads composed by a mixture of alginate and hydroxyapatite coated with thiolated ChitLac (ChitLac-SH)
    - Samples treated with H_2O_2
    - Samples not treated with oxidant
- Beads composed by a mixture alginate and hydroxyapatite with a higher concentration of alginate as a control.

Beads stability was tested by measuring the average area variation upon treatment with saline solution (0.9% NaCl) using calcium alginate beads (3% of alginate) as control. In this test extreme conditions were used (high saline solution/beads ratio and a little thermal shock were applied) to compare the bead resistance. Tests were performed in triplicate considering the average swelling of about 80-90 beads for each sample.

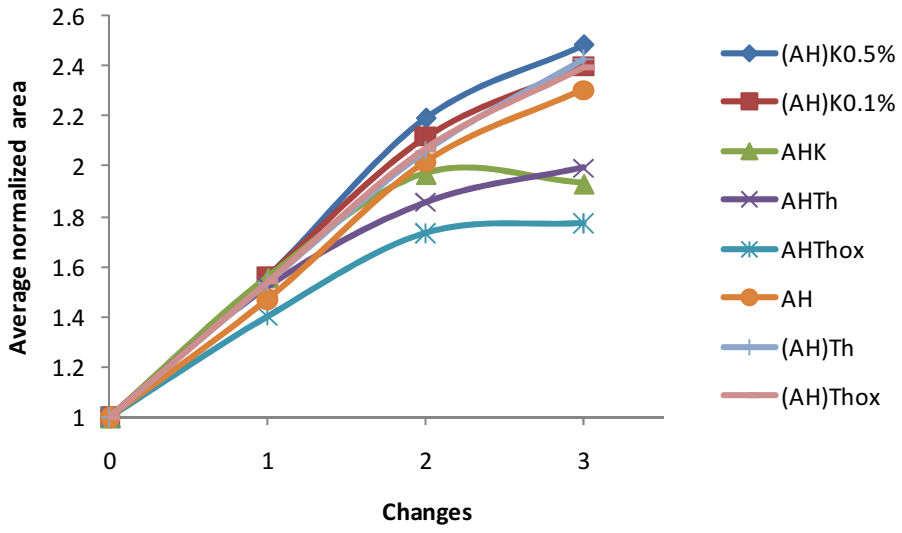

Figure 26. Swelling behaviour in function of saline changes. Values were normalised for the initial value. (AH)K0.5%, Beads composed by a mixture of alginate and hydroxyapatite coated with 0.5% unmodified ChitLac; (AH)K0.1%, Beads composed by a mixture of alginate and hydroxyapatite coated with 0.1% unmodified ChitLac; AHK, Beads composed by a mixture of alginate, hydroxyapatite and unmodified ChitLac; AHTh, Beads composed by a mixture of alginate, hydroxyapatite and ChitLac-SH; AHThox, Beads composed by a mixture of alginate, hydroxyapatite and ChitLac-SH treated with H_2O_2; AH, Beads of alginate 3%; (AH)Th Beads composed by a mixture of alginate and hydroxyapatite coated with ChitLac-SH; (AH)Thox, Beads composed by a mixture of alginate and hydroxyapatite coated with ChitLac-SH treated with H_2O_2.

Obtained values were normalized for the initial area value; subsequently the "slope" measured in the first two hours was reported in the graph underneath. A low value corresponds to a superior resistance to swelling. The comparison between the different samples allows to note a better swelling behaviour of beads containing ChitLac-SH mixed with alginate and hydroxyapatite and subsequently treated with H_2O_2 (AHThox, orange histogram). The values obtained confirm previous experiments performed with larger beads, where the measure of diameters was performed by means of a digital camera (data not reported).

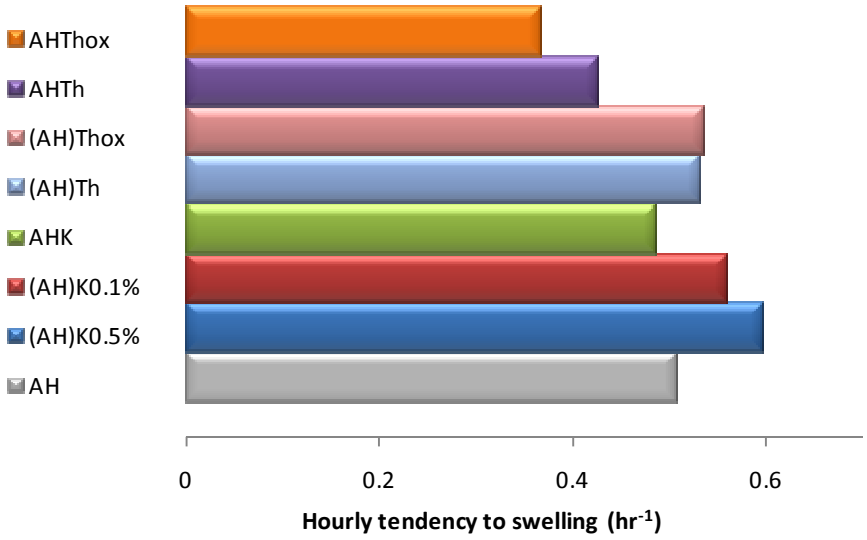

Figure 27. Tendency to swelling of intermediate diameter beads (defined as the difference between relative area at time 2 hours minus that at zero time, divided by the time interval – *i.e.* two hours). The slope achieved in the first two hours was reported to determine the tendency to swelling. (AH)K0.5%, Beads composed by a mixture of alginate and hydroxyapatite coated with 0.5% unmodified ChitLac; (AH)K0.1%, Beads composed by a mixture of alginate and hydroxyapatite coated with 0.1% unmodified ChitLac; AHK, Beads composed by a mixture of alginate, hydroxyapatite and unmodified ChitLac; AHTh, Beads composed by a mixture of alginate, hydroxyapatite and ChitLac-SH; AHThox, Beads composed by a mixture of alginate, hydroxyapatite and ChitLac-SH treated with H_2O_2; AH, Beads of alginate 3%; (AH)Th Beads composed by a mixture of alginate and hydroxyapatite coated with ChitLac-SH; (AH)Thox, Beads composed by a mixture of alginate and hydroxyapatite coated with ChitLac-SH treated with H_2O_2.

As said before, the gel beads dimensional stability is determined by an equilibrium between the positive osmotic pressure (swelling) and the negative pressure, correlated with the number of cross-links in the gel and therefore with the network elasticity. The sodium

counter ions present in the saline solution compete with calcium ions displacing them. In this manner the number and the length of the alginate Gul-junctions are reduced and an increase of the total area of the bead occurs. Therefore, performing a certain number of saline changes, an increase of the volume dimension is observed, which corresponds to a lower stability of the bead. When the system alginate/hydroxyapatite is mixed with ChitLac, the polyanion-polycation interactions enhance the total number of effective cross-links (which counterbalance the osmotic pressure), and the bead stability increases, confirming literature data (Marsich et al., 2008). Moreover, this effect is more evident using thiolated ChitLac where thiol groups which can undergo oxidation provide strong cross-links which improve the resistance to swelling. A further enhancement of the bead stability is provided by the oxidation of sulphydryl groups with hydrogen peroxide, which produces a high number of disulfide bridges.

Size

With the aim to insert µspheres in the final construct, their size characterization was necessary, since the injectability of the filler is strongly dependant on it. Microsphere size was characterized by means of an optical microscope at wet and dry state. The granulometry and the distribution of µbeads dimensions were determined. Their characterization will be treated more extensively in the last section ("4.5 Injectable filler"), where the physical chemical characterization of the final product will be discussed.

Biological tests

Two kinds of biological assays were performed on beads. The Lactate dehydrogenase (LDH) assay, which gives an evaluation of the cytotoxicity and the adhesion assay measured with Alamar Blue^{TM} reagent.

LDH assay: this test quantifies the LDH, which is a soluble cytosolic enzyme presents in most eukaryotic cells released into culture medium upon cell death due to damage of plasma membrane. The increase of the LDH activity in culture supernatant is proportional to the number of lysed cells and is an indicator of cellular death. The evaluation of LDH is performed quantifying its enzymatic NAD^+ reduction to NADH in the presence of L-lactate. The formation of NADH can be measured in a coupled reaction in which tetrazolium salt is reduced to a red formazan product. The amount of the highly coloured and soluble formazan

can be measured at 492 nm spectrophotometrically. By performing this test, it is possible to control the cytotoxicity caused by the contact with biomaterial. The test is carried out also on a positive and a negative control. The positive control is constituted by polyurethane certified to be cytotoxic, while the negative control is an inert poly(styrene) disk.

Adhesion assay: In order to perform an adhesion assay on the beads surface, it was not sufficient to seed cells on plates containing beads, but it was necessary to assess a method which permits to discriminate cells adhered on beads, to avoid any interference from cells growing without being attached to the beads. After having suspended the beads in the presence of cells in DMEM medium, they were put on a rotary stirrer and incubated at 37°C; after 4 hours beads were transferred on plates in no treated plastic normally used for bacteria, preventing the adhesion to the bottom of the well. At definite time intervals the cell proliferation was assessed with the Alamar Blue™ method. Alamar Blue™ is a cell viability indicator that uses the neutral reducing power of living cells to convert resazurin to the fluorescent molecule, resorufin. The active component of Alamar Blue™ (resazurin) is a nontoxic, a cell permeable compound which is blue coloured and virtually nonfluorescent. Upon entering cells, resazurin is reduced to resorufin which presents a characteristic red-fluorescent colour. The amount of fluorescence produced is proportional to the number of living cells. Since Alamar Blue™ is a non-toxic compound, at the end of the test it is possible to wash out substrates and follow the cellular growth in the same samples.

Biological tests on large thiolated beads

A biological comparison was performed in beads with thiol functionalization prepared in two different ways. With this aim, a first type of beads was prepared by mixing alginate, hydroxyapatite and thiolated ChitLac and dripping the blend in the gelling solution (AH-ThM), while a second kind of beads was prepared from alginate/hydroxyapatite beads which were successively coated with ChitLac-SH (AH-ThL). Both types of beads were treated with the peptide and hydrogen peroxide. Beads were then dried. Immediately before cell seeding, all beads were sterilised with exposure to a UV lamp and immersed in medium solution where they remained overnight to rehydrate. A test to exclude cytotoxicity and an adhesion assay were performed.

LDH ASSAY The cytotoxicity of large thiolated beads was evaluated on MG63 osteoblasts-like cell line by LDH assay. Lactate dehydrogenase activity was measured at 24 and 72 hours after the cells seeding. Results presented in Figure 28 show that no cellular

death is observed during the time test using both mixed (AH-ThM) and layered (AH-ThL) beads. Cells seeded on poly(styrene) disk, used as negative control (C- in the graph) showed the same trend, while in the case of the positive control, represented by toxic poly(urethane) (C+), the cellular damage is more important as demonstrate in the graph.

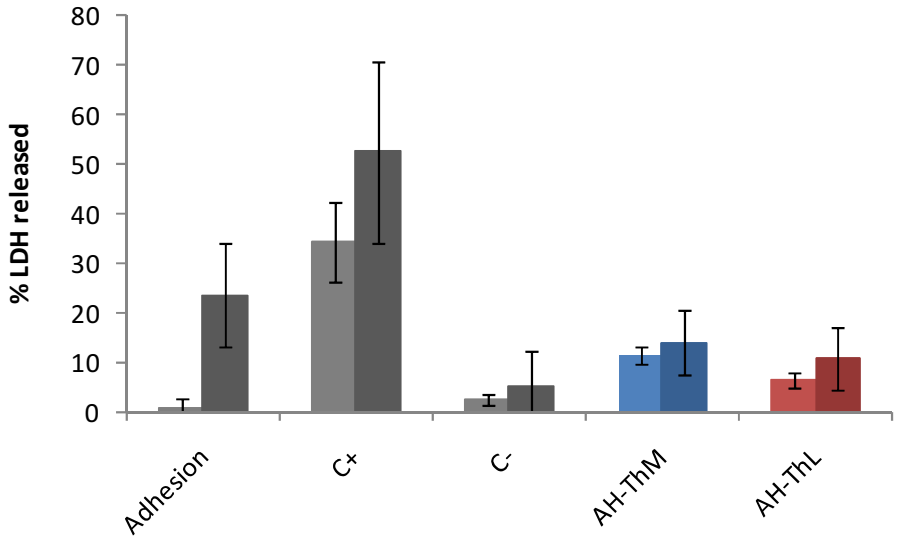

Figure 28. LDH assay performed on (MG63) osteoblasts-like cell line for the evaluation of cytotoxicity for contact with thiolated beads (AH-ThM and AH-ThL representing beads functionalized with RGD obtained by mixing alginate, hydroxyapatite and ChitLac thiolated, and beads obtained by coating of alginate/hydroxyapatite beads with thiolated ChitLac, respectively). The controls are represented by adherent cells (Adhesion), cells in contact with toxic poly(urethane) (positive control C+) and cells in contact with inert poly(styrene) (negative control C-). Test was performed at 24 and 72 hours.

ADHESION ASSAY In order to analyze possible differences in adhesion promotion resulting from the different conjugation technique, a culture of MG63 cells on beads was carried out, comparing the two types of material, mixed and layered, as adhesive substrates for the cells. In the following 3 days an increase in the cell number on the constructs was observed. Results presented in Figure 29, demonstrate a constant growth during the culture time using both thiolated mixed (AH-ThM) and thiolated layered (AH-ThL) large beads. However the mixed beads presented a lower number of adhered cells in the first day despite the equal amount of RGD conjugated at the surface. The amount of RGD peptide was

estimated through beads degradation and capillary electrophoretic analysis and was calculated to be equal to 1.75 nmol *per* each bead for both types.

The layered beads presented a better performance not only in terms of initial adhesion, but also for what concerns the number of viable cells in comparison with mixed beads at the end of the culture, with a higher growth rate. These suggest that the layered bead overcompensate the disadvantage of a two-step production with respect to the one-pot mixed beads with a superior biological performance in relation to attachment and cellular proliferation of osteoblasts.

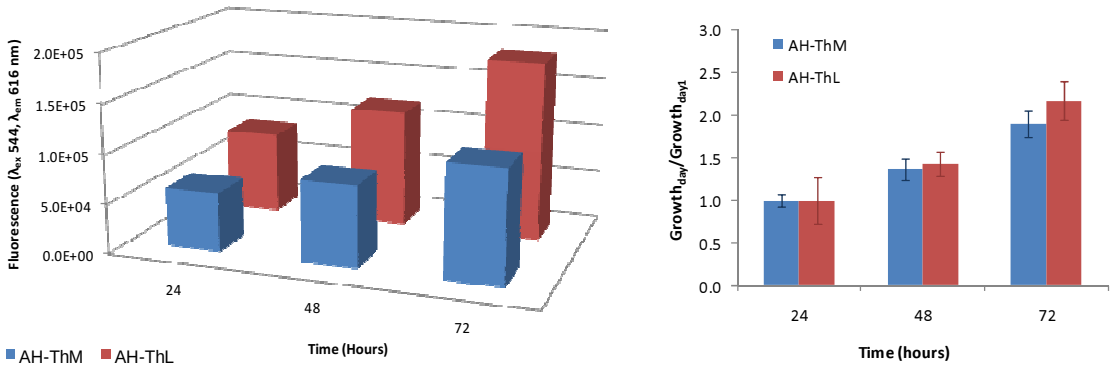

Figure 29. Adhesion assay on large beads covered with CGRGDS peptide by disulfide bond. The growth on two types of thiolated beads were analysed: thiolated mixed (AH-ThM) and thiolated layered (AH-ThL) beads. The first graph represents the obtained cell growth and the initial adhesion is well demonstrated. In the second graph the growth values were normalised for the corresponding value on the first day in order to underline the cellular growth promoted by the supports.

Biological tests on thiolated and amide µbeads

A final comparison was performed between µbeads where RGD peptide was bound *via* direct amide bond or by disulfide bridge. Given the better results obtained with layered thiolated (AH-ThL) beads with respect to mixed thiolated beads, these experiments were carried out only with beads built following the strategy of external coating.

LDH ASSAY The cytotoxicity of µbeads was evaluated on MG63 osteoblasts-like cell line by measuring the percentage of LDH released (see Figure 30). Also in this case LDH activity was measured 24 and 72 hours after the cells seeding.

The test was performed considering three types of µbeads:

- non coated µbeads ("Alginate" in the graph)
- µbeads coated with non functionalised ChitLac ("ChitLac" in the graph)
- µbeads with an external layer of ChitLac-(NCO)-RGD.

The test revealed that none of the beads causes cellular suffering, as it is highlighted by the comparison with toxic positive control ("C+" in the graph).

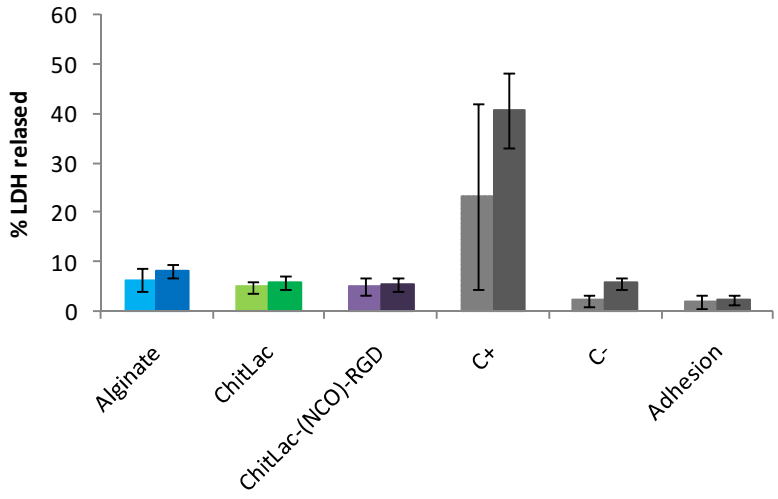

Figure 30. LDH assay performed on (MG63) osteoblasts-like cell line for the evaluation of cytotoxicity for contact with µbeads without functionalization (Alginate), coated with unfunctionalized ChitLac (ChitLac) and coated with ChitLac covalently bound to the peptide GRGDS by an amide bond (ChitLac-(NCO)-RGD). The controls are represented by adherent cells (Adhesion), cells in contact with toxic polyurethane (positive control C+) and cells in contact with inert polystyrene (negative control C-). Test was performed at 24 (first histogram in each series) and 72 hours (second histogram).

ADHESION ASSAY After having verified the biocompatibility of the layered µbeads, a comparison was performed between the used coating strategies, measuring the initial adhesion and the successive growth. Before passing to the results it is to be clearly stated that, due to un-escapable combination of experimental production procedures, it was not possible to expose on the surface of the two types of beads the same (or closely similar) number of RGD peptides. In fact, analysis of amino acid recovery gave an amount of 5 $nmol_{RGD}/mg_{dry}$ in beads where the conjugation was performed through disulfide bridge, and an amount of 0.85 $nmol_{RGD}/mg_{dry}$ in beads where the conjugation was performed by amide bond. As represented in Figure 31, the more bioactive constructs are represented by the µspheres in which peptide

is conjugated through a disulfide bridge, (ChitLac-(SS)-CRGD). In this case, in fact not only the adhesion at the earlier stages but also the cellular growth during the whole time span were improved with respect to the beads layered with ChitLac-(NCO)-RGD. However, the measured effect if evidently much larger than the bare 5.9:1 ratio of the RGD surface concentration.

Therefore, this result, besides suggesting a determinant role of the degree of substitution focuses on the on the spacer length and mobility. In the case of direct amide bond the peptide is closer to polymeric chain and altogether certainly less mobile, producing a decrease of its biological activity. Moreover, the role of the different assembly strategy should also considered. Althought both methods involve outer coating, in the case of ChitLac-SH the peptide conjugation takes place on effectively exposed -SH groups only, maximizing the exposure efficiency to integrins. At variance, in the case of the beads coated with pre-derivatized ChitLac-(NCO)-RGD some RGD peptides may be directed towards the inner side of the bead being hidden to receptors.

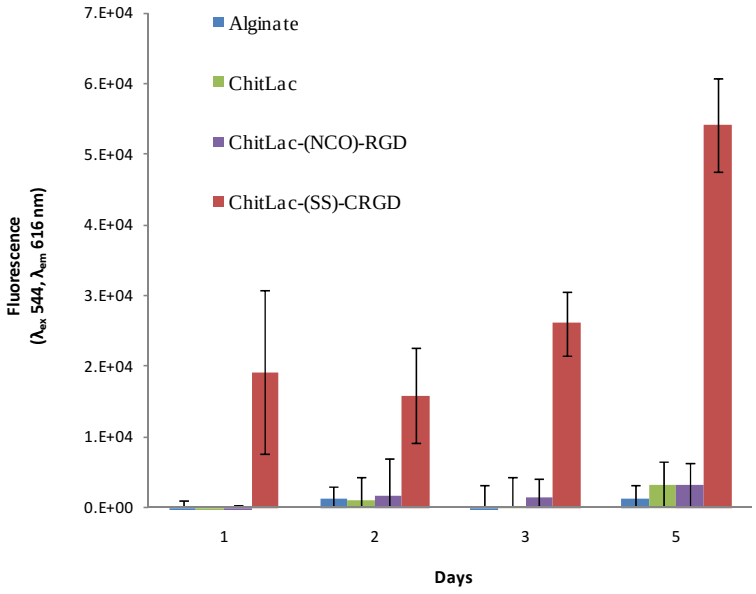

Figure 31. Adhesion test on different types of µbeads on MG63 cells.

Considering the high promotion of cell adhesion reached using this strategy, µbeads of alginate and hydroxyapatite layered with thiolated ChitLac and successive functionalised with the peptide CGRGDS, were considered as bioactive part of the final construct, the injectable filler.

4.2.3 Partial conclusions

The development of an implant with peculiar characteristics of bioadhesivity encompassed three aspects:

1. The choice of the most suitable chemical approach to functionalize the polysaccharide allowing the (covalent) peptide conjugation.
2. The application of the obtained polysaccharides in a manufactured product such as beads and their characterization.
3. The biological tests *in vitro* to assure the non-cytotoxicity of manufactured products and to evaluate their adhesive properties.

1. Three chemical strategies were designed for this kind of application. Initially the functionalization of ChitLac to succinyl-Chitlac in order to introduce carboxylic groups in the polysaccharide was performed, but the successive conjugation of RGD peptide gave rise to an insoluble product, not useful for this kind of application. Then the conjugation of peptide with unmodified ChitLac was tested obtaining a low conjugation yield, as it was expected. Nevertheless biological tests revealed a higher adhesion with respect to unmodified ChitLacThe last strategy involved the functionalization of ChitLac with *thiol* groups: the obtained product, ChitLac-SH, demonstrated a high capacity to form disulfide bonds with a RGD peptide containing a cysteine, and following this way, two kinds of beads were produced.
2. In fact, it was possible to *mix* ChitLac-SH, alginate and hydroxyapatite together to obtain beads which structure demonstrated a high resistance to swelling. Following another strategy it was possible to *coat* preformed beads of alginate and hydroxyapatite with ChitLac-SH. The bond with the peptide was verified to occur with very high yields. Moreover, in both cases the conjugation of the peptide was carried out on beads which had been already assembled: in this case the conjugation occurs only at the surface of these ones and with the correct peptide exposition.
3. The last part of this research is dedicated to biological assays to test bioactivity, no one of the considered manufactured products resulted cytotoxic. For what concerns the bioadhesivity, beads layered with ChitLac-(SS)-CRGDS presented an excellent activity.

Similar successful results are promising for the application of this product in the preparation of bioactive injectable fillers for orthopaedic surgery.

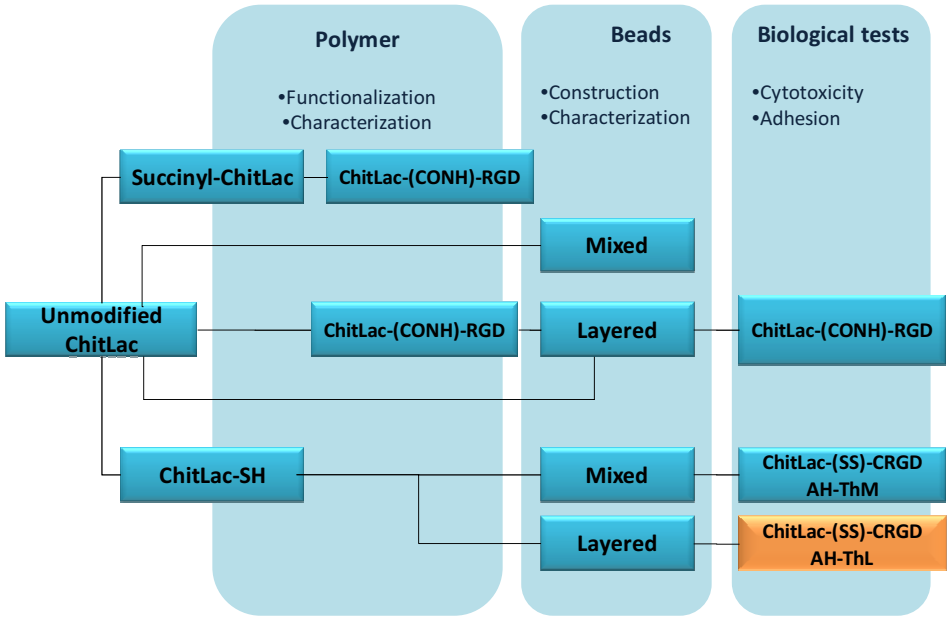

4.3 OSTEOINDUCTIVE AGENTS IN FILLER: BMP FRAGMENTS

4.3.1 Introduction

Bone repair is a physiological key phenomenon necessary to preserve skeleton stiffness and strength. It is not only important for fracture repair, but also to repair bone microdamages resulting from mechanical stresses. The high regenerative capability of bone, which allows the rapid fracture healing, is characteristic of this tissue and is principally due to the ability of specific growth factors to stimulate stem cells to develop into chondroblasts and osteoblasts.

Normal fracture-healing process involves a number of osteogenic factors that are released from bone and the surrounding soft tissues during the repair process. Osteogenic factors are involved in numerous processes related to bone formation and bone-remodeling, including chemotaxis, proliferation, and differentiation of bone-forming and bone-remodeling cells. Local release of physiologic quantities of these osteogenic factors is generally sufficient to elicit fracture repair, so, bone healing is a predictable process that presents a high rate of success. Nevertheless, for some patients, and in certain clinical settings, this process can be limited by the anatomy and physiology of bone tissue, as well as by the limitations of medical technology. This leads to significant morbidity and may also result in prolonged medical treatment, and continued pain at the site of non-union.

Given the enormous biomedical weight of skeletal injury, and the need to treat congenital, post-traumatic and post-surgical conditions in which bone regeneration is unsuccessful, the understanding of osteogenesis and biomolecular mechanisms involved in skeletal repair has important clinical implications. From a biochemical point of view, when bone is fractured cells and cell mediators, in the form of extracellular signals, collectively ensure the restoration of form and function. Fracture healing is a complex physiological phenomenon which involves the coordination of several different cell types in a process similar to the molecular cascade characterizing natal bone formation. In this signalling cascade the focal role played by growth factors has been well demonstrated. Growth factors regulate different cellular activities and their application as external bioactive agents has been demonstrated to enhance bone healing, control growth and differentiation of cells. In nature multiple growth factors are involved in the process of bone healing, among these bone morphogenetic proteins (BMPs) were shown to induce bone formation by inducing mesenchymal stem cells toward chondroblastic or osteoblastic differentiation. Now that the role of BMPs in bone formation

during development and fracture repair is well established, BMPs are becoming of particular interest for the field of orthopaedics, with the possibility to obtain delivering systems of these growth factors. This is a biomimetic approach towards bone healing able to replace the standard autogenous bone grafts.

Discovery of BMPs

Many osteogenic molecules reside in bone and have the potential to mediate and control fracture repair. Over 40 years ago, an intrinsic activity able to initiate the reparative response was found in the bone matrix and the term “bone morphogenetic proteins” (BMPs) was used to describe biomolecules with this peculiar ability. The turning point in the bone morphogenesis knowledge was the isolation of the key signals from demineralised bone matrix (Reddi, 2001). From this discovery started a significant effort to enhance bone healing process by using decalcified bone matrix as an inducer. During the 7-year period from 1964 to 1971, a systematic procedure permitted to separate the BMP from the bone matrix (Reddi, 2007). Evidence data suggested that the bone morphogenetic activity was associated with a relatively acid-resistant, trypsin-labile, water-insoluble and non-collagenous protein that had not been characterized before. These studies have been followed by an extensive work directed toward the purification of factors possessing a peculiar bone morphogenetic potential. Subsequently the possibility to generate active recombinant molecules of human origin, culminating in the production of large amounts of many recombinant human BMPs (rhBMPs) (Nimni, 1997) allowed their use for clinical applications such as spinal fusion, fracture repair and dental tissue engineering. In 2002 FDA approved two products containing rhBPM-2 and rhBMP-7 in collagen carriers for spinal fusion and long bone non-unions.

BMPs structure

BMPs are present naturally as dimeric biomolecules. Each monomer is stabilized by three intramolecular disulfide bonds, formed between six highly conserved cysteines, a structure known as “cysteine knot motif”. Dimers are covalently linked via a disulfide bond; this requires seven conserved cysteine within each monomer for the formation of three intrachain disulphide bonds and a single interchain bond. Dimeric conformation is crucial for the bioactivity in fact the reduction of a single interchain disulfide bond results in the loss of biological activity (Reddi, 2007). BMPs are expressed as large precursor polypeptide chains. The mature monomer molecule consists of about 120 amino acids. The raw molecule is characterized by an N-terminal signal peptide which directs the protein to the secretory

pathway, a prodomain that ensures proper folding, and a C-terminal that is a domain conserved in the mature peptide. The differences in hydrophobic core explain the different affinities for the various cell receptors and possibly its different physiological roles.

BMPs family

Bone morphogenetic proteins are multifunctional growth factors belonging to the transforming growth factor β (TGF-β) super family and were identified on the basis of their ability to initiate ectopic bone formation in adult animals. TGF-β members bind to serine/threonine kinase cell surface receptors initiating various intracellular signalling cascades. The presence of the "cysteine knot" is a peculiar characteristic of this group, and each member contains cysteine residues that afford significant stability to the mature protein (Axelrad and Einhorn, 2009). Other than BMPs, the members of the extended TGF-β superfamily are represented by inhibins and activins, that are implicated in follicle-stimulating hormone release from pituitary, Müllerian duct inhibitory substance (MIS), and growth differentiation factors (GDFs) (Reddi, 2007).

At the moment in humans, 17 members of the BMPs family have been isolated and characterized, from BMP-2 to BMP-18 (see Table 5). It is to note that BMP-1 is not comprised in the BMPs table, in fact it is a metalloprotease involved in TGF-β activation. The biological activities of BMP are related to bone and cartilage formation, but some of them, such as BMP-8b, BMP-10 and BMP-15, do not have known roles in bone or cartilage. Besides, since BMP-12, BMP-13 and BMP-14 induce only chondrogenesis they are named cartilage-derived morphogenic proteins (CDMPs) and only BMP-2 to BMP-11 are considered to be BMPs.

BMPs are involved in embryonic patterning (Kishigami and Mishina, 2005), in skeletal formation and in organogenesis of other tissues behind the bone (Tsumaki and Yoshikawa, 2005). This response multiplicity is caused by the peculiar property of pleiotropy characteristic of BMPs: they possess the faculties of acting on a multiplicity of cellular phenomena and targets (Reddi, 2007); to underline this peculiar property, recently Reddi, in a review, proposed naming BMPs also as "body morphogenetic proteins", due to their extensive roles in various tissues and organs beyond the bone (Reddi, 2005).

Many of them have been shown to be intimately involved in both, bone formation and fracture healing, governing the three key steps in the bone induction cascade (chemotaxis, mitosis and differentiation) (Reddi, 2001). In bone formation a clear inducing role is observed

for BMP-2, BMP-4, BMP-6 and BMP-9, demonstrating an induction of mineralization and increase in osteocalcin levels in cells (Chen et al., 2003), as well as ossification in mouse models (Kang et al., 2004).

Table 5. Bone morphogenetic proteins members in humans and their main physiological roles. (Bessa et al., 2008)

BMP	*Other names*	*Function*
Bone morphogentic proteins		
BMP-2	BMP-2a	Bone and cartilage morphogenesis/heart formation
BMP-3	Osteogenin	Negative regulator of bone morphogenesis
BMP-3b	GDF-10	Negative regulator of bone morphogenesis
BMP-4	BMP-2b	Cartilage and bone morphogenesis/kidney formation
BMP-5	-	Bone morphogenesis/limb development
BMP-6	Vrg1, Dvr6	Cartilage/bone hypertrophy, morphogenesis/oestrogen mediation
BMP-7	Osteogenic protein-1 (OP-1)	Cartilage/bone morphogenesis, kidney formation
BMP-8	Osteogenic protein-2 (OP-2)	Bone morphogenesis, spermatogenesis
BMP-9	GDF-2	Bone morphogenesis/development of cholinergic neurons/glucose metabolism
BMP-11	GDF-11	Axial skeleton patterning/eye development/ pancreas development/ kidney formation
Cartilage-derived morphogenetic proteins		
BMP-12	CDMP-3, GDF-7	Ligament and tendon development/development of sensory neurons
BMP-13	CDMP-2, GDF-6	Cartilage development and hypertophy
BMP-14	CDMP-1, GDF-5	Chondrogenesis/angiogenesis
Others		
BMP-8B	OP-3	Spermatogenesis
BMP-10	-	Heart morphogenesis
BMP-15	GDF-9b	Ovary physiology
BMP-16	Nodal	Embryonic patterning
BMP-17	Lefty	Embryonic patterning
BMP-18	Lefty	Embryonic patterning

In the detail, during fracture healing different BMPs follow specific temporal sequences: BMP-2 appears to be an early factor peaking at the day 1 after fracture, while BMP-14 peaks

at the day 7 during cartilage formation and BMP-3, BMP-4, BMP-7 and BMP-8 are expressed mainly after 2 weeks (Cho et al., 2002) (Yu et al., 2009). Analogously, different BMPs are expressed in different sites during bone formation (Zoricic et al., 2003).

BMP signalling: from cell receptor to gene activation.

When the BMPs bind to cell surface receptor on mesenchymal stem cells, a BMP signalling cascade is activated. Signals are sent via specific proteins to the cell nucleus and this results in the expression of genes that lead to the synthesis of macromolecules involved in cartilage and bone formation. At this point, the mesenchymal stem cell differentiates in a chondrocyte or in an osteoblast.

The BMP proteins, like all members of the TGF-β superfamily, bind to receptors localised on the cell surface, the serine-threonine kinase receptors, characterized by an extracellular ligand binding domain and an intracellular serine/threonine kinase domain. By means of this binding, BMPs are able to generate accurate effects on cell proliferation and differentiation, leading into specific intracellular pathways that, at the end, activate and influence the gene transcription. There are three known types of receptors for TGF-β superfamily members (I, II and III) but only the types I and II appear to play significant roles in BMP binding and signalling. In particular, six different receptors were identified to bind BMPs:

- **type I receptors** Activin receptor Ia (ActR-Ia or Alk2), BMP receptor type Ia (BRIa or Alk3) and BMP receptor type Ib (BRIb or Alk6).
- **type II receptors** BMP receptor type II (BRII), Activin receptors type IIA and IIB (ActRIIA and ActRIIB).

These receptors have highly specific functions during embryogenesis and in the adult individual. BRIb for example triggers differentiation of mesenchymal precursor cells into osteoblasts, while BRIa causes the same cell type to undergo adipogenic differentiation (Chen et al., 1998). Type I receptors, but not type II receptors, have a region rich in glycine and serine residues named “GS domain”. Each member of the TGF-β superfamily binds to a characteristic combination of type I and type II receptors, but both of them are necessary for the signalling. TGF-β first binds to the type II receptor, which occurs in the cell membrane in an oligomeric form with activated kinase. Then, the TGF-β type I receptor, which may also occur in an oligomeric form, and cannot bind to TGF-β in the absence of type II receptor, is recruited into the complex. Type II receptor, phosphorylates type I receptor in the GS domain

to activate it. The assembly of the receptor complex is provoked by ligand binding, but the complex is also stabilized by direct interaction between the cytoplasmatic parts of the receptors (Heldin et al., 1997). BMP ligands bind to type I and type II receptors with different affinities. For example BMP-2 and BMP-4 show high affinity for the type I receptors BRIa and BRIb, and a low affinity for the type II receptor BRII (Koening et al., 1994). The specificity of intracellular signals is mainly attributed to type I receptors (Miyazono et al., 2005), but are the different combinations of type I and type II receptors that provide the different and specific signals for different cell effects. In conclusion, the action of both receptor types is necessary for BMPs to activate specific signalling pathways (both Smad and non-Smad signalling pathways) (Bessa et al., 2008). Several studies demonstrate the versatility of BMP signalling: BMPs can activate distinct signalling pathways through different receptor complexes. This also suggests that the activation of distinct pathways greatly depends on the availability of specific receptors and their complexes at the cell surface and not only by the ligand-receptor affinities.

The initial steps of signal transduction, the binding of the ligand to distinct receptors, the subsequent internalization of the ligand-receptor complex, and the initiation of signalling pathways, are strongly controlled. Each BMP signalling molecule is subject to interaction with an extensive range of proteins: antagonists bind to and inactivate the ligands, decoy-receptors sequester ligands at the cell surface, co-receptors and intracellular proteins interact with the receptors to regulate downstream targets. Below an overview of principal signal regulatory biomolecules is reported:

- **Anatagonists**: BMP antagonists are secreted peptides that are able to bind to BMP ligands, blocking the receptor epitopes on the ligands, and thus inhibiting ligand-receptor oligomerization. Like the BMP ligands, the antagonists are homodimeric proteins that contain a cystine knot motif, which stabilizes their structure. The classification of antagonists is based on this cystine knot motif: the Chordin/Noggin family exhibits a ten-membered cysteine ring, Twisted Gastrulation (Tsg) has a nine-membered cysteine ring and the DAN/Cerberus family contains an eight-membered cysteine ring (Sieber et al., 2009). One of the well known BMP antagonists is Noggin, which binds BMP-2, BMP-4, BMP-7 and GDF-5 and GDF-6 with different affinities and whose expression represents a physiological negative feedback that attenuates BMP-2, BMP-4, and BMP-7 signalling in osteoblasts (Yanagita, 2005).

- **Co-receptors**. BMP signaling is regulated by co-receptors from various protein families. Co-receptors that potentiate BMP signaling include the RGMs (repulsive guidance molecules) a and c, Dragon (RGMb), the RTK (receptor tyrosine kinase) c-Kit, and the TGF-β/BMP type III receptors Endoglin and Betaglycan (Figure 32). These co-receptors typically bind BMPs and one or both receptors to enhance signalling via Smads in specific tissues. Betaglycan, also named TGF-β type III receptor, enhances binding of TGF-β to its high affinity type II receptor. Recent data indicate that Betaglycan also interacts with BMP-2, BMP-4, BMP-7, and GDF-5 and promotes the binding of BMP-2 to BRIa and BRIb. BMPs are negatively regulated by the decoy-receptor BMP and activin membrane-bound protein (BAMBI) and the RTKs Ror2 and TrkC, through diverse inhibitory effects (Sieber et al., 2009).
- **Intracellular regulatory proteins**. The complexity of the signaling cascade amplifies as it descends downstream. Besides interacting with extracellular ligands and co-receptors, BMP receptors also bind to an excess of intracellular proteins, which act as signal transducers or regulators that control BMP signalling. The mode of receptor oligomerization allows receptor-associated proteins to join the signalling complex in a sequential manner (Sieber et al., 2009). For simplicity, only intracellular regulators are indicated in Figure 32.

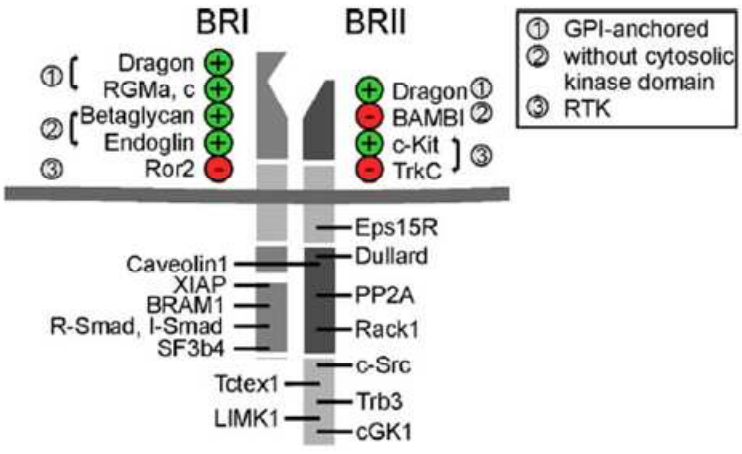

Figure 32. BMP receptor interactome. BMP receptors BRI (left) and BRII (right) are positively (+) and negatively (-) regulated by many different co-receptors. These are either GPI-anchored (1), have very short cytosolic parts (2) or they are RTK (3). On the intracellular side the receptors interact with proteins that contribute to receptor regulation and finetuning or progression of receptor signaling (Sieber et al., 2009).

Upon BMP binding, type I receptors phosphorylate receptor-regulated Smads (R-Smads); Smads represent the main signal transducers of serine-threonine receptors (Derynck and Zhang, 2003). So far, 8 mammalian Smad proteins have been isolated (Smad1-Smad8). The Smad proteins are divided into three groups according to their functions. The first group is the receptor regulated Smads (R-Smads), which include Smad1, Smad2, Smad3, Smad5 and Smad8. These Smad proteins bind to membrane bound serine/threonine receptors, and are activated by the kinase activity of the receptors. The second group includes only one member: the Smad4 that acts as a co-factor (Co-Smad) that binds to the activated R-Smads to form a heterotrimeric complex (two phosphorylated R-Smads with one Co-Smad) that translocate into the nucleus and modulates gene transcription with the cooperation of other transcription factors (Figure 33). The third group comprises the inhibitory Smads (I-Smads), which includes Smad6 and Smad7 that exert an inhibitory effect on the signaling cascade by various mechanisms (Song et al., 2009). Generally, all R-Smads are activated by BMP-2 or BMP-4, whereas BMP-6, BMP-7 and BMP-9 only efficiently induce Smad1 and Smad5 but not Smad8 (Bessa et al., 2008). BMP signalling is modulated also by ubiquitin-dependent protein degradation: this control occurs by the activation of Smad ubiquitin regulatory factors (Smurfs) which induct the ubiquitination and the degradation of Smads.

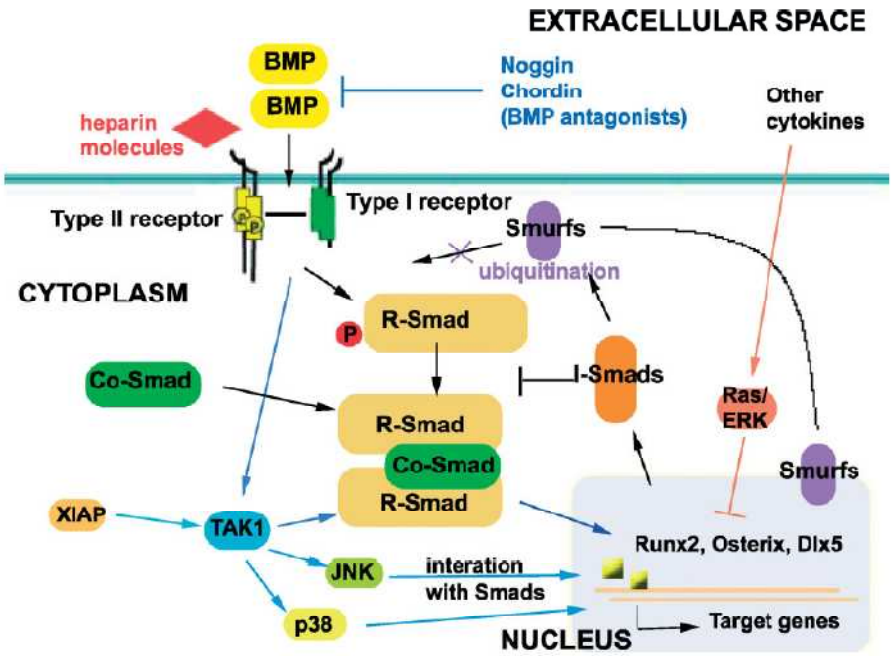

Figure 33. BMP signalling pathways: schematic representation of Smad-dependent and -independent pathways and their main mechanisms of modulation (Bessa et al., 2008).

Besides classical Smad pathways, BMPs are able to induce gene transcription independently for Smad molecules. In fact, BMPs was shown to induce the Mitogen-activated protein kinase (MAPK) that is also implicated in the signal transduction of BMPs (Derynck and Zhang, 2003). MAPK pathways are connected to a wide range of cellular responses. It exists also a cooperative interaction between different pathways such as Smads and transcription factors activated by MAPK pathways (Bessa et al., 2008).

At the end, when transolcated into the nucleus, Smads regulate gene transcription by interacting with specific DNA sequences and DNA-binding proteins (such as transcriptional factors). Smads also interact with transcriptional factors and transcriptional coactivators and corepressors. The Runt-related transcription Factor (Runx), in three isoforms (Runx1, Runx2 and Runx3), is one the most studied transcription factors for BMP signalling, regulating processes such as bone formation and haematopoiesis (Ito and Miyazono, 2003). Osterix (OSX) is another transcription factor that is mediated by BMP/Smad signals and probably by MAPK signalling and other pathways (Celil et al., 2005). Osterix, together with Runx2, are the most studied transcription factors specific for BMP signalling, involved in the differentiation of mesenchymal stem cells into bone cells.

The use of BMP-2 in regenerative medicine

BMP-2 is a necessary component of the signaling cascade that governs fracture repair. It has been demonstrated that in bones lacking BMP-2, the earliest steps of fracture repair seem to be inhibited: mice without the ability to produce BMP-2 in their limb bones had normal spontaneous fractures that do not resolved with time, indicating that mice were unable to initiate a healing response upon fracture, and that the absence of BMP-2 was not compensated by other osteogenic molecules. In the same study it was observed that those newborn mice had normal skeletons, with the conclusion that BMP-2 expression during embryogenesis is not required for events determining a normal skeletal development (Tsuji et al., 2006). The examination at the cellular level of osteoprogenitor cells from mice lacking expression of BMP-2 showed that they exhibited a severe defect in the ability to proliferate, and to differentiate functional osteoblasts able to regenerate and repair bone. These findings confirm that the lack of BMP-2 hinders the progression from osteoprogenitor to osteocyte (Bais et al., 2009), (Rosen, 2009). Besides, BMP-2 is implicated at the embryonic state with cardiac development; in fact in mice the total targeted disruption of BMP-2 caused embryonic

lethality, with an evident abnormal heart development (Zhang and Bradley, 1996). Experiments have also shown that BMP-2 does not stimulate mature osteoblasts or fibroblasts. This indicates that the osteogenic effects of BMP-2 are directed towards multipotent or pluripotent cells such as mesenchymal stem cells that can differentiate to chondrocytes and osteoblasts that will develop into cartilage and bone (Kim et al., 1997).

BMP-2 is a member of the BMP family. It is a homodimer consisting of two chains of 114 amino acid chains that are connected by disulfide bonds. The molecular weight of the BMP-2 monomer has been reported to be approximately 12,000-14,000 Da (Scheufler et al., 1999). BMP-2 interacts with cells via a complex of two types of serine/threonine kinase receptor chains. This protein has two epitopes referred as the "wrist epitope" and the "knuckle epitope". The wrist epitope is thought to bind to BRIa and the knuckle epitope to BRII. The structure of BMP-2 and the model of the BMP-2 forming a complex with receptor (BRIa), are represented in Figure 34. However, the precise receptor-binding region in BMP-2 has not yet been identified.

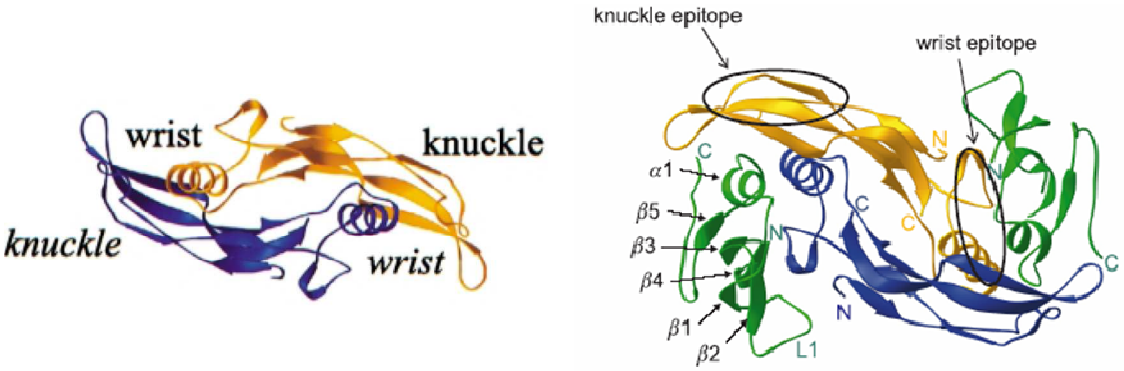

Figure 34. The first model represent a view of BMP-2 showing the location of wrist and knuckle epitopes (Kirsch et al., 2000). The second picture represents the top down view of the BMP-2/BRIa complex. The BMP monomers are in gold and blue with the receptors shown in green. The chain termini are identified with "N's" and "C's" that represent the amino-terminus and the carboxyl terminus, respectively. In BMP-2 two symmetrical pairs of juxtaposed epitopes were described: the "wrist epitope", with affinity to BMP receptor Ia (BRIa), containing residues from both monomers; and the "knuckle epitope", which includes residues from only one monomer, with low affinity for BMP receptor II (Kirsch et al., 2000).

In the forming of the signalling complex, BMP-2 can follow two different pathways: BMP-2 can either bind to its high affinity receptor BRIa, upon which BRII is recruited into the

complex, or it can bind to a preformed complex (PFC) of BRIa and BRII (Gilboa et al., 2000), (Nohe et al., 2002). The former oligomerization mode is termed BMP-induced signaling complex (BISC) and results in internalization via caveolae and activation of non-Smad pathways, such as via MAPK signalling. The preformed complex oligomerization triggers Clathrin-dependent internalization and initiates the Smad pathway (Hartung et al., 2006), (Sieber et al., 2009). Once BMP-2 binds with the receptor, the BRII receptor phosphorylates the type I receptor which then phosphorylates a Smad intracellular protein. This phosphorylation sequence triggers the activation of other Smad proteins that eventually lead to gene transcription initiating the differentiation in osteoblasts.

The osteoinductive characteristics of locally expressed BMPs have been widely studied for clinical applications. In fact when large bone defects occur, as for example in the case of bone tumour resections, trauma or joint replacement, bone fails to regenerate large portions of the tissue. In these cases BMPs local administration is a powerful alternative to autogeneic or allogeneic bone grafting, which are often accompanied by immunogenic complications.

Based on all these findings, regulation of endogenous BMP-2 production should be considered as a target for bone regeneration strategies. In this perspective the biotechnological production of rhBMP-2 is a force point: the isolation of native BMP from bone, results in very low yields so, the need for obtaining larger amounts of BMPs induced the production of these growth factors by DNA recombinant technology. Active recombinant BMPs are produced by means of mammalian cells or bacteria as expression systems. In the first case low expression rates and low yields represent the principal problems, while in the second strategy, the product undergoes denaturing treatments. A common disadvantage is that the recombinant protein is obtained in a not glycosilated form, as instead, it occurs in the human body, with a consequently lower stability or biological activity. Various observations accompanied by biochemical modifications in the original protein structure permits to obtain products with a different quality, for example by adding additional heparin binding domains, it was possible to obtain a significantly different bioactivity and bioavailability of the rhBMP, decreasing its specificity *in vitro* but increasing bone formation *in vivo* (Ruppert et al., 1996), (Bessa et al., 2008). Recombinant human bone morphogenetic protein 2 (**rhBMP-2**) is known to induce orthotopic and ectopic bone formation *in vivo*. It has been found that it is able to induce *de novo* formation of cartilage in rats (Wang et al., 1990) and it has been demonstrated

an increase in osteoblastic parameters in human bone marrow, meaning that osteoblast precursor cells were induced to differentiate into osteoblasts (Kim et al., 1997).

The efficacy of rhBMP-2 for the treatment of orthopaedic patients is now being evaluated in clinical trials (Govender et al., 2002), (Swiontkowski et al., 2006), (Reddi, 2001). Two products containing recombinant human bone morphogenetic proteins, rhBMP-7 and rhBMP-2, delivered in adsorbable collagen sponges, were approved in 2002 by the Food and Drug Administration (FDA) for specific clinical cases. The product containing rhBMP-2, is marketed as Infuse^{TM} (Medtronic Sofamor Danek) and has been extensively studied in both animals and humans. It has received premarket approval for specific indications in open tibial fractures, anterior single-level lumbar spinal fusion and certain oral maxillofacial and dental regeneration applications. Several clinical trials have been reported for the use of Infuse^{TM} on patients with open tibial shaft fractures (Mont et al., 2004), (Valentin-Opran et al., 2002) postoperatorial spinal fusion (Gupta and Khan, 2005) and in patients with pyogenic vertebral osteomyelitis. In all cases, improvements in wound healing and reduced infection rates were observed. In certain cases complications were observed, like for the use of rhBMP-2 in the cervical spine, or ossification in soft tissues (Axelrad et al., 2008). But generally, results obtained with the use of BMPs demonstrate that, for most applications, the union rates are comparable or possibly better than with the use of autografts, with clear clinical benefits (Axelrad and Einhorn, 2009). Preclinical and clinical studies have shown that the amount and the density of induced bone are positively correlated with the initial concentration of rhBMP-2 at the application site and the length of time that rhBMP-2 is present at the site.

Despite being so promising, recombinant technology is still at its early stages, since there is a need to bypass some fundamental limitations, such as optimising the stability and bioactivity of recombinant BMPs, obtaining glycosylation patterns identical to that of native BMP, and reducing the possibility of triggering immunogenic responses when used in clinical situations.

Functional fragments derivatives BMPs

The main problems that occur during the use of native or recombinant BMPs carriers include early dose release and protein degradation in biological environments. Besides there are also a series of unwanted effects connected with the use of large proteins such as organogenesis, apoptosis, and immunogenicity. Biochemically, large proteins are labile and expensive and are active only when folded in the correct tertiary structure. To overcome these

drawbacks, the activity of these large, insoluble molecules has been mimicked by short peptide sequences of a few amino acids. The short sequences are relatively more stable during the modification process, besides they can be massively synthesized in laboratories more economically as well as be used as a tool to elucidate cellular behaviour. The BMPs fragments are chemically synthesized peptides and can be easily immobilized on a matrix to maintain their activity in a localized area for a long time. Therefore, they may be a promising component in the construction of materials for bone repair.

Although the precise BMP signaling pathways have not yet been clarified, it was experimented the hypothesis that synthetic peptide containing knuckle epitope of BMP-2 which binds with BRII may promote osteoblastic differentiation (Akiyama et al., 1997). The effect of diverse synthetic peptides whose sequence corresponds to fragments of the knuckle and the wrist epitope in BMP-2 were individuated and tested on cells. In particular the more active sequence was represented by the peptide corresponding to residues 73-92 of the BMP-2 knuckle epitope in which Cys78, Cys79 and Met89 are changed to Ser, Ser and Thr respectively. This sequence was demonstrated to induce differentiation of murine pluripotent cells in osteoblasts by observing a high ALP activity. Besides the demonstration of the antagonist effect towards rhBMP-2 on receptors type Ia and type II, suggests an important role of this region on differentiation. In this peptide an essential region was identified as the hydrophobic amino acid residues located in the C-terminal region of the 73-92, which may be necessary to bind the BMP type II receptor (Saito et al., 2003). The activity of the fragment, in opportune carrier, was tested also on animal models revealing an induced calcification as fast as rhBMP-2 is loaded in a collagen carrier tested as reference (Saito et al., 2004), (Cho et al., 2008).

BMPs delivery

Because of its pleiotropic activity, the BMPs therapeutic use should be planned carefully: it is necessary to concentrate the peptides osteogenic activity only at the location where bone repair is required. Besides, in order to exploit BMPs bioactivity, it is necessary to maintain an opportune biomolecule concentration at the site of the injury. In fact, notwithstanding the increasing comprehension of the BMPs action mechanisms and the large effort made to exploit them to stimulate bone healing, their release *in situ* remains a complex problem. There are many evidences that when the BMP (protein or peptide) containing mixture is administered alone, in formulation buffer, no regenerative activity in human or large animals

is observed. BMPs without particular carriers, can lead to a faster rate of union than for autogenous bone graft in the healing of femoral defects of rats (Einhorn et al., 2003), and rabbits (Bax et al., 1999). However, the efficacy of formulation buffer as a delivery vehicle for BMPs to accelerate bone healing in large animal models, is not as clear and achieved no better results than autogenous bone graft did (den Boer et al., 2002). Reduced efficacy observed in large animal models using BMPs delivered in formulation buffer may be caused by the combination of a reduced pool of available responsive stem cells and insufficient retention of the BMPs at the repair site to stimulate an appropriate increase in the number of responsive cells: in large mammals, the BMPs may have to be present for a longer period of time (Seeherman, 2001).

In fact, when BMPs are combined with injectable or implantable carriers with longer residence time, an accelerate bone healing has been observed in numerous studies in both small and large animal models, as well as in human individuals (Sotome et al., 2004), (Brekke, 1996), (Uludag et al., 2001). In this optic, the main role of a delivery system for BMPs is to retain the growth factors at the site of injury for a prolonged time, to recruit progenitors and to stimulate tissue healing processes.

The choice of the ideal type of carrier, remains an open question. This choice may be done taking into consideration a group of carriers satisfying some criteria. Firstly, the carrier should be biocompatible, limiting the effect of inflammation responses on bone healing. Possibly, it should be bioresorbable: biodegradable carriers are generally preferred to non-degradable carriers. This is not an absolute requirement, but the complete replacement of the carrier by bone permits to eliminate any potential effect associated with prolonged exposure to the carrier material that can provoke toxicity and can also compromise the mechanical strength of the repair (Seeherman and Wozney, 2005). Another requirement is the adequate porosity to allow the chemoattraction of cells and the formation of blood vessels at the new bone. Furthermore, the carrier should protect BMP from proteolytic enzymes or conformational changes and at the same time maintain its bioactivity releasing the protein in a controlled time and circumscribed space, promoting the formation of new bone only at the treatment site. An important role of the carrier, in fact, is that of avoiding the risk of the peptide dispersion in the surrounding area of the implant.

The time of release may be carefully delicate balanced, different types of fracture or specific applications require specific pharmacokinetic profile designing, so, more than one pharmacokinetic profile is desirable.

The factors that influence the pharmacokinetic profile are the material and formulation considered and the type and amount of BMP in use. By means of a chemical modification of the carrier or the BMP, it will be possible to achieve a specific release profile. Several idealized profiles are presented in Figure 35 where the cell responses in relation with different BMP release profiles are illustrated.

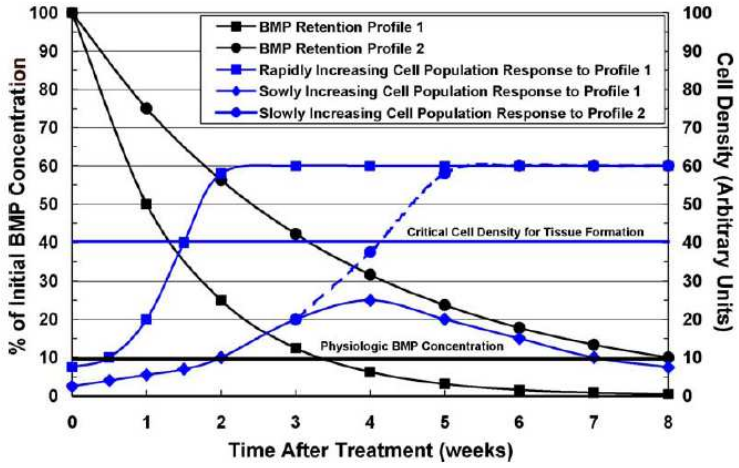

Figure 35. Three idealized cellular responses for orthopaedic repair tissues to two different BMP retention profiles at the site of the repair (retention profiles 1 and 2) as a function of time after treatment (weeks). Some assumptions are obligatory in the analysis of this graph: first of all it should assume that there is a critical density of BMP responsive cells, and in some cases vascular support cells, required for effective orthopaedic tissue formation. In addition, the scenarios assume there is a minimal concentration of exogenous BMPs required to induce these cells to generate the desired orthopaedic tissue formation response (Seeherman and Wozney, 2005).

- In the first scenario, the BMP retention profile of carrier 1 maintains the required minimum exogenous BMP concentration for sufficient time to allow the rapid cell population to surpass the required critical cell density and generate the desired tissue formation response.
- In the second scenario, the BMP retention profile of carrier 1 does not maintain the minimum exogenous BMP concentration for a period of time long enough to allow the slower cell population to exceed the critical cell density. Once the exogenous BMP concentration falls below the minimum level, the responsive cell density either begins to fall or alternatively may remain constant. As a result, the tissue

formation response is either insufficient for the desired effect or the response is aborted.

- In the third scenario, the increased BMP retention profile of carrier 2 now maintains the minimum exogenous BMP concentration for a long period of time enough to allow the slower cell population to reach the critical cell density.

These scenarios help to explain why certain BMP carriers are effective at certain BMP concentration in rodents but not in larger animals (Seeherman et al., 2002) demonstrating the potential need for higher initial concentrations of BMPs delivered in the same carrier, which seems to be required in large animal models compared to rodents. A higher starting BMP concentration in a BMP carrier will maintain the minimum exogenous BMP concentration for a longer period of time allowing to a smaller initial cell population or to a slower responding cell population to reach the critical cell density for the tissue formation (Seeherman and Wozney, 2005).

It is evident that the choice of the correct release system is the crucial point in the design of new biomaterials for osteointegration. A part the influence of the structural characteristics of the carrier, the retention time of the BMP at the site of implantation is affected also by many others parameters, such as the interaction between the biomaterial and the BMPs, the influence of pH, temperature, porosity and salt concentrations (Bessa et al., 2008). Extremes in release profiles, such as long low-amount release of BMPs or initial burst of BMPs, are known not to be beneficial to bone healing.

Biomaterials for BMP delivery

When planning a new biomaterial with immobilized BMPs, two main parameters have to be taken into account: the material and the immobilization strategy. The categories more explored as BMP delivery carriers, regards:

- **natural polymers** that can be protein based such as gelatin (Patel et al., 2008), collagen, silk (Kirker-Head et al., 2007) and fibrin, or carbohydrate based, like hyaluronan (Brekke, 1996), chitosan, alginate (Saito et al., 2004) agarose, and dextran (Chen et al., 2006). Natural polymers are bioresorbable and can be formulated into many configurations obtaining carriers with diverse residence time.
- **inorganic materials**, such as calcium orthophosphates, calcium sulfate cements and bioglass (Fu et al., 2010) (Seeherman et al., 2002). The most commonly used is

the low temperature calcium orthophosphate cement (CPC) produced by apatite precipitation in aqueous solutions of calcium phosphates. The protein introduction in these materials is performed for example by mixing the components prior to the cementing reaction or by coating preformed CPC granules or blocks with BMP.

- **synthetic materials** have been widely used for tissue engineering. The poly(α-hydroxy acid) polymers such as polylactide, polyglycolide and their copolymers (poly(D,L-lactide-co-glycolide) (PLGA) are the most commonly used synthetic polymers to deliver BMPs (Saito et al., 2001) (Schliephake et al., 2008). Since BMPs generally do not attach to the surface of most synthetic polymers, these factors are incorporated into microspheres, beads and more complex structures during formulation. Successful use requires formulation and sterilization methods that do no damage the protein and have a well-defined stability and show regular profiles. Alternatively, surface modifications can be introduce to enhance BMP binding and further structural modification can be used to trap BMPs within the polymer matrix.
- **composites** of them that have been used to optimize the benefits of each of these materials. Calcium orthophosphate granules can be added to natural polymers to improve compression resistance (Sotome et al., 2004). The controlled release properties of synthetic polymers have been combined with the biocompatibility of natural polymers (Brekke, 1996), (Higuchi et al., 1999), (Kenley et al., 1994). Natural and synthetic polymers have also been added to ceramics to improve handling characteristics, provide injectability, and add porosity (Greish et al., 2005). Metal and polymer or ceramic composites have also been evaluated (Burg et al., 2000), (Seeherman and Wozney, 2005).

Among synthetic polymers, polylactic acid and polyglycolic acid have given interesting results, but generally, a major disadvantage of the use of synthetic polymers is the risk of an inflammatory response, due to acidic by-products of degradation (Martin et al., 1996), which may also damage the incorporated BMPs.

Nowadays a great attention is dedicated to natural polymers. In fact, the materials for tissue engineering applications should ideally mimic the natural environment of tissues and, in this regard, natural polymers can send signals to guide cells at the various stages of their development and thus accelerate healing (Bessa et al., 2008). Besides, one of the greatest problems in protein release technology is the loss of the biological acitivity of the protein

from the carrier-protein formulation. This activity loss is often the result of the denaturation or the deactivation of proteins during the preparation of the formulation. From this viewpoint, hydrogels may be a preferable candidate as carrier, because of their biosafety and their high inertness towards proteins (Tabata, 2003).

There are several natural polymers that may be used as carriers for BMP delivery. These include collagen, fibrin, starch-based polymers, chitin and chitosan, hyaluronans, alginate, silk, agarose, soy- and alga-derived materials, and poly(hydroxyalkanoates) (Mano et al., 2007). All these polymers are biocompatible and bioresorbable, moreover, the possibility to obtain them from microorganisms and recombinant technologies have make them safe from an immunological point of view.

Natural polymers can be formulated into many configurations with variable residence time using enzymatic treatment and chemical cross-linking. In order to understand the effect of the carrier composition on release profile, an example where a wide range of retention profiles achieved with different BMP/carrier combinations is reported in the Figure 36.

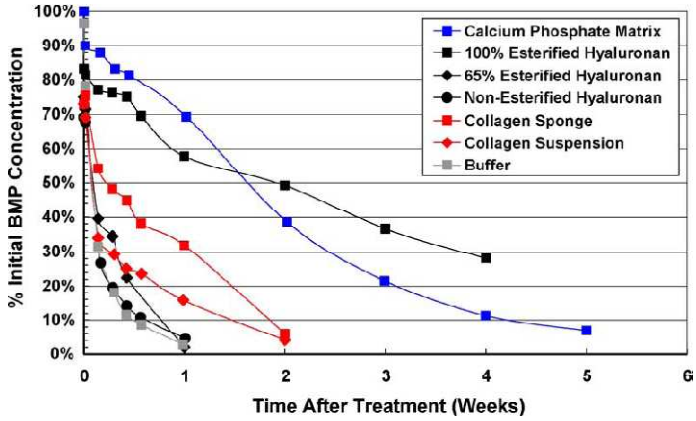

Figure 36. Retention profiles (percentage of initial BMP concentration) for several BMP/carrier combinations used to treat rabbit mid-diaphyseal ulna osteotomies as a function of time treatment (weeks) (Seeherman et al., 2003).

The addition of a carrier increases the rhBMP-2 retention compared to deliver in buffer alone (grey line). It is interesting to note the effect of structural modifications on the total release profiles: in the case of hyaluronic acid chemical modifications like esterification, are able to increase the retention time of BMP at the site of implant, besides, the effect of the different substitution degrees is also evident, in fact, by increasing the esterification levels from 0 to 65% and up to 100% it is possible to note an increase of the residence time of hyaluronan carriers with a consequent higher retention of rhBMP-2 (Seeherman and Wozney, 2005).

Among the cited natural polymers, ***chitosan*** is one of the polysaccharides which has given particularly interesting results. Several studies have reported the use of chitosan for BMPs delivering, particularly in composites with synthetic polymers or with other natural polymers (Yilgor et al., 2009), (Park et al., 2005), (Niu et al., 2009). The use of derivatives of chitosan is also reported. Chemical modification of chitosan may enhance certain bioactive properties and increase its solubility in water, thus aiding in the incorporation of rhBMPs, such as in the case of carboxymethyl chitosan.

Another factor influencing the good results of the implant is the three-dimensional structure of the matrix. In fact, the three-dimensional structure of the biomaterials explored for BMPs delivery is as vary as the used materials. It ranges from porous scaffold to sponges, nanofiber, including ceramics, such as hydroxyapatite and micro- and nanoparticles made of synthetic materials, natural polymers and hydroxyapatite-based particles. However, the type of three-dimensional structure used is function of the type of tissue to be regenerated and has to satisfy also different mechanical requirements when applied for the repair of bone, cartilage or tendon.

The unique common prerequisite is that the successful bone repair requires a BMP carrier able to allow cell infiltration. For example, carriers for bone replacement are simplified by the fact that, upon fracture, bone is immobilized, but they should allow also vascular ingrowth, due to the highly vascularised nature of bone. In cartilage, defects are subject to high compressive and shear stresses, thus making healing more challenging. In tendon, finally, the regenerative ability appears to be intermediate between those of bone and cartilage, so tendons are very difficult to immobilize, needing a carrier that is able to withstand considerable tensile forces. The geometry of the carrier also significantly affects the biophysical process of osteoinduction and capillary penetration (Jin et al., 2000). Taking all these factors into consideration, researchers have also to keep in mind that the carrier is evidently aimed to be available for common usage by surgeons and physicians (Bessa et al., 2008).

Immobilization strategies

The immobilization of BMPs in a delivery system may be performed by different methodologies: *via* adsorption, entrapment, ionic complexation or by covalent binding (Luginbuehl et al., 2004).

- **Physical entrapment** is a controlled delivery system of *reservoir* type, where osmotic pressure combined with polymer membranes regulates the rate of drug release (Figure 37 A-C). Actually, the use of these kind of delivery systems is limited because of difficulties in the control of the release of large molecules and because of problems related to dose dumping.
- The most common way to incorporate osteoinductive factors into the natural polymer-based porous carrier is **physical adsorption** (Figure 37 D). A big application of this technique is the rhBMPs impregnation in collagen sponge (Patel et al., 2006). Although this strategy has the benefit of simplicity it presents also some drawbacks such as the possible conformational changes and denaturation of the protein, that cause the failure of its activity, as well as the irreversible binding of growth factors. In this case the chemical properties of the polymeric carrier are fundamental to avoid these drawbacks. For example, exploiting the strong affinity of BMPs and some other growth factors towards heparin sulphate/heparin proteoglycans of the extracellular matrix (Blanquaert et al., 1999), it is possible to protect BMP from proteolytic inactivation, allowing at the same time a slow release of the protein in the surrounding environment. However, in the case of physical adsorption it is generally difficult to achieve a perfect control over release kinetics. Because of the high burst effect, the local concentration of BMP drops below the therapeutic level very quickly and loses its biological activity.
- A third approach for non-covalent immobilization is **ion complexation** (Figure 37 F). Depending on their isoelectric point, proteins can be bound to charged polymers, as in the cases of chitosan, alginate, hyaluronans or synthetic polyelectrolytes. As with passive adsorption, problems arise from possible irreversible interactions, like in the case of highly positive proteins (e.g. TGF-β) with alginate (Mumper et al., 1994).
- An alternative to non-covalent bond is the **protein crystallization**. Crystallized growth factors in fact demonstrate a low dissolution rate in aqueous systems suggesting their possible use as release systems (Jen et al., 2002).
- The **covalent immobilization** is another strategy developed to retain growth factors for longer periods of time at the delivery site. The key point of this strategy is to maintain the peptide biological active after coupling, because linkage can affect their binding to receptors and the subsequent dimerization of receptors in the plane

of the membrane, so an appropriate conjugation design is necessary, as in the case of the conjugation of the active BMP-2 fragment to alginate (Suzuki et al., 2000).

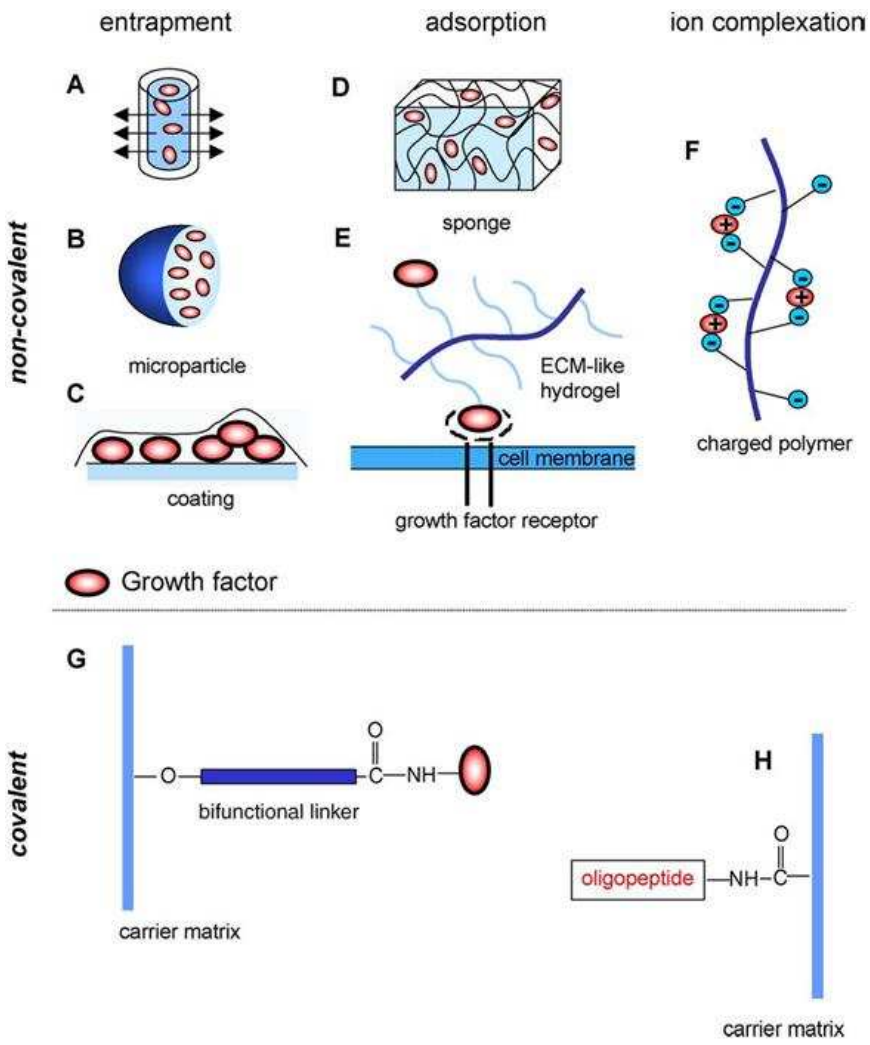

Figure 37. Growth factor delivery systems and strategies for bone repair, encompassing non-covalent (A-F) and covalent (G, H) growth factor entrapment. (A-C). Physically entrapped growth factors in a reservoir device (A), a microparticle (B), or polymeric coating implant (C), which can be released by diffusion through a polymeric matrix or membrane, with or without concomitant bioerosion of the delivery system. (D) Adsorption of growth factors through physico-chemical interactions with sponge material; release occurs upon desorption, which is highly sensitive to the environmental conditions. (E) Heparin-binding growth factors bound to heparan sulfate-substituted proteoglycans from the extracellular matrix are favourably presented to their receptors. (F) Ionic complexation of growth factors with oppositely charged macromolecules, mostly derived from natural polymers; release occurs by ion exchange mechanism, which is highly sensitive to the environmental conditions. (G, H) Covalently bound growth factors attached *via* bifunctional linker (G) or by direct coupling of growth factor derived oligopeptide (H) to the carrier matrix (Luginbuehl et al., 2004).

Several works report successful covalent immobilization of growth factors on polymeric matrixes. One of the most interesting ones is reported by He and co-workers, which exploited the ease and specificity of click chemistry to prepare a hydrogel derivatized with BMP and RGD peptides, a biomaterial which showed good biological properties (He et al., 2008).

Another interesting strategy is the immobilization not directly of the growth factor, but of statins, that represent a group of molecules able to increase the production of BMP-2 by stimulating its promotion. Their clinical use is limited by the lack of a suitable delivery system to localize and sustain their release. Benoit and co-workers describe the covalent linkage of a modified statin to a dimethacrylated poly(ethylene glycol) hydrogel. The subsequent hydrolysis of lactic acid ester bonds results in the release of the statin into the surrounding solution. The proposed mechanism of hydrolysis is either an autocatalytic hydrolysis of the ester or an enzymatic cleavage due to esterases and lipases produced by cells.

On the whole, good results have been obtained with BMPs in the treatment of bone defects, spinal fusion and other types of applications. It was exhaustively clarified that the therapeutic success of growth factors depends on their optimal localized delivery in the site of injury and that, despite the significant evidence of potential bone healing demonstrated in animal models, future clinical investigations must be performed to better define main variables such as dose, scaffolding and route of administration. The dose is in fact not yet optimal; the concentrations of BMP in use are supraphysiological: the actual amount used in assays is on the order of milligrams compared with nanogram range *in vivo*. Moreover different fractures may require different dosages. The comprehension of the BMPs regulation pathways can be useful in the design of novel strategies. In this manner, for instance, mimicking the intricate network of molecules, the suggestion of the employ of a cocktail of different BMPs, with simultaneous or sequential release would be the most desirable approach for clinical use (Yilgor et al., 2009). In any case, the development of different delivery systems able to modulate the BMP release represents an attractive point for the construction of implants for tissue repair. Finally, a new concept of carrier is that of “intelligent drug delivery systems”, meaning those delivery systems providing growth factors in response to a variety of physiological physical, chemical, or biological stimuli. This is the strategy of enzyme-sensible rhBMP-2 drug delivery engineered by Lutolf and co-workers where the biomolecule is released in presence of a particular enzyme localized in primary

human fibroblasts. The presence of integrin binding ligands permits to attract cells that can explicate their enzymatic activity (Lutolf et al., 2003). This approach needs to be demonstrated but the suggestion of exploiting enzymatic cleavable linkages is very intriguing.

4.3.2 Design of a BMP-2 fragment delivery system

INJECTABLE: Dispersion medium (provides flowability) +
Bioactive filler (provide bioactivity and elasticity at rest)

1 Dispersion medium: hyaluronan
Hyaluronan: highly biocompatible, bioactive, viscoelastic

2 Bioactive filler: Microcomposite + Specific bioactive agents

A Microcomposite (dried microbeads): alginate + HAp

Alginate: biocompatible + hydrophilic

HAp: bioactive ("inorganic" bioactivity)

B Specific bioactive agents in filler:

RGD-containing peptides: pro-adhesive

BMP-fragment peptides: pro-proliferative

LL37-peptide: antibacterial

Initial fast release from alginate/HAp beads

The initial phase of the release was considered as a burst release from beads. In order to obtain a similar effect, the diffusion properties of alginate gels were exploited. The objective of this first part of the study was to examine the suitability of alginate as an encapsulation matrix for delivering BMP fragment at a therapeutic initial level. The peptide encapsulation yield was studied using different pH cationic gelling solutions to modify the charge of the peptide. Finally, the release kinetic profile was achieved.

Preparation of BMP-containing alginate beads.

Alginate/hydroxyapatite spheres were used to entrap the oligopeptide with a simple procedure. Beads were prepared by extruding a mixture of sodium alginate, hydroxyapatite and peptide, as droplets into a divalent cross-linking solution containing calcium ions. The gel formation, which is assumed to be an almost instantaneous process, permitted the entrapment

of the peptide. Although calcium alginate beads can be prepared by simple and mild procedures, this method has a major limitation that is the drug loss during bead preparation which happens by leaching through the pores in the beads. Since this represents a common problem in alginate encapsulation procedures, many modifications of this polymer have been tested to solve this inconvenient, (for instance, the cross-linking of alginate with aldehydes) but these modifications although able to increase the capacity to retain the entrapped drugs, showed also a slower release profile of these ones (George and Abraham, 2006), and this was not the objective of this release kinetic.

Other important factors that are able to influence the entrapment efficiency are represented by peptide characteristics such as the charge and the size of this one. The charge is a delicate characteristic because if a more positive charge consents an efficient entrapment (molecules do not diffuse during the gelling process), on the other hand, although the micro-environment in the alginate bead can be considered relatively inert to biomolecules, a positively charged protein can potentially compete with calcium ions for available carboxylic acid sites on the alginate. This has been observed with small drugs and has been shown to result in protein inactivation in the case of the protein transforming growth factor-beta (TGA-β1) (Mumper et al., 1994), (George and Abraham, 2006).

Independence of entrapment efficiency of pH.

The peptide charge plays an important role in encapsulation efficiency; besides, it represents a parameter that is possible to be modified also without performing chemical modifications on the BMP sequence but simply by changing the pH environment where the peptide encapsulation takes place.

In order to obtain a high loading efficacy of the BMP-fragment in alginate beads, the influence of the pH, during the cross-linking process, was evaluated. The pI of the BMP fragment is approximately 8.69 and the pKa value for alginate is about 3.5 (Gu et al., 2004). At neutral pH BMP fragment carries a net charge near to neutrality and it cannot interact electrostatically with alginate, which is negatively charged. Reducing the pH, the charge of the peptide slightly increases (1.5) the electrostatic interaction with the alginate in these conditions was tested. To evaluate if the amount of BMP fragment entrapped in alginate beads may vary with the charge of the molecule, the encapsulation was performed in two different conditions: in water and in HEPES buffered at pH 4.5. The encapsulation efficiency, which is

the percentage of peptide contained in the gel beads in relation to the initial amount employed (Xing et al., 2003), was then calculated by the equation:

$$\boldsymbol{Encapsulation\ efficiency}\ \% = \frac{[\boldsymbol{peptide}]_{\boldsymbol{in\ beads}}}{[\boldsymbol{peptide}]_{\boldsymbol{initial\ amount}}} \times \mathbf{100} \qquad \textbf{(4.1)}$$

The amount of peptide loaded in the beads was estimated by capillary electrophoresis, by subtracting the concentration of free peptide, which was recovered in the gelling solution after the bead production. From the initial concentration, the quantification of the BMP-fragment was performed by capillary electrophoresis optimizing the method explicated at p. 104. Given the neutral charge of the peptide, a borate buffer with the same molarity but a higher pH was used to perform the analysis in order to avoid the overlap of the electroendosmotic flow (EOF) and peptide peaks (Figure 38).

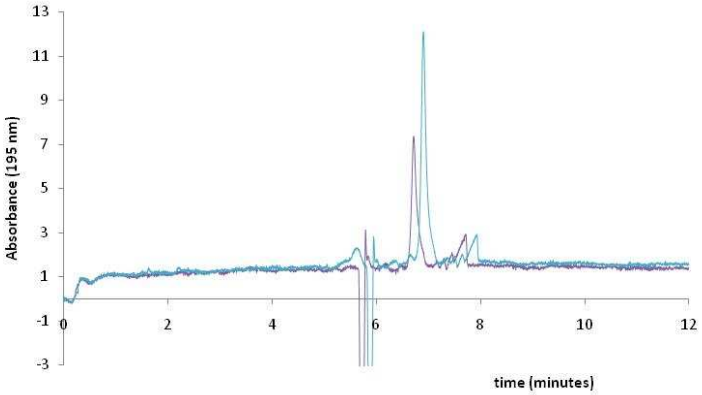

Figure 38. Capillary electrophoretic analysis of BMP fragment standards (100 and 120 µg/mL). Running buffer: borate 100 mM at pH 10.00, silica fused capillary length 56 cm, i.d. 50 µm, applied voltage 20 kV normal polarity, UV detection at 214 and 195 nm. At this pH the peptide carries a negative net charge of -1.5.

Nevertheless, the encapsulation efficiencies of the two procedures, in water and in acidic buffer, resulted to be almost the same, about 22% and 23% respectively, probably because the charge variation of BMP fragment was not so relevant to influence its entrapment in alginate beads.

Release from beads loaded with BMP-fragment.

The further quantification of the peptide released from calcium-alginate microspheres revealed a very fast release.

Proteins encapsulated in alginate matrices are released by two mechanisms: the diffusion of the protein through the pores of the polymer network, and the degradation of the polymeric network. In this case the peptide discharge occurs *via* diffusion through pores in the matrix and depends from the permeability of gel alginate beads. The pore size of alginate gel microbeads has been shown to be between 5 nm and 200 nm, and it depends from many parameters (George and Abraham, 2006). The permeability of gel alginate spheres is determined essentially by two factors that are connected and of equal importance for quantification of the capsule permeability characteristics:

- rate of **diffusion** of the molecules.
- **molecular weight cut-off** (MWCO)

The driving force in a diffusion process is the concentration gradient of molecules in a solution: solutes move from an area of high concentration to an area of low concentration. In hydrogels, the diffusion of solutes is determined by many. The first is the hindrance caused by the presence of polymer chains that increase the path length for diffusion. The second process is the hydrodynamic drag on the moving solute at the polymer-solvent interface. The third is the heterogeneity of the membrane material with fluctuation of diffusion properties across this one. Finally, residual charges, presence of counter ions, hydrogen bonds, polar and hydrophobic interactions of the membrane material will affect the diffusion of solute. For large molecules such as proteins, diffusional resistance occurs, although even large proteins with molecular weights majors to $3 \cdot 10^5$ g/mol will leak out of the gel beads with a rate depending on their molecular size, shape and pH of the solution. Instead, diffusion of small molecules, such as a BMP fragment, seems to be very little affected by the alginate gel matrix.

Hence, in addition to size, the diffusion of proteins through the alginate membrane will also depend on the total net charge of the protein. In fact, if the entrapped protein presents a net positive charge, it can interact with negatively charged alginate, and the results is the inhibition of its diffusion from the gel, whereas a protein with a net negative charge may be released more rapidly from the matrix. Therefore the charge of the entrapped protein drug is an important factor determining the efficiency of the controlled release (Smidsrød and Skjåk-Bræk, 1990), (George and Abraham, 2006).

In addition to diffusion characteristics, the **molecular weight cut off** (MWCO), pore-size and pore size distribution may be essential parameters in an immobilization system.

Over and above, alginate concentration and composition will all affect the permeability of the gel. Increasing polymer concentration decreases the permeability. For what concerns the composition of alginate, it has been observed an highest diffusion rates of proteins in beads made from high G-alginates, that indicates a most open pore structure (Martinsen et al., 1989) because of a more static network of these gels compared to the dynamic and entangled network structure of the low-G gels. Lastly, the divalent cation concentration in the gelling solution is able to influence the porosity of the alginate gel: high concentrations of cation results in lateral association of junctions, with a more space between the junction zones giving rise to a more porous gel (Alsani and Kennedy, 1996), (Gåserød et al., 1998), (Strand et al., 2000). Finally, the porosity of calcium alginate gel may significantly be reduced by partially drying the beads: these will re-swell only slightly in water and the increased alginate concentration will reduce the average pore size.

Release profile from alginate loaded BMP-fragment

To drain the release profiles of the beads obtained following the two different procedures, reported above, some beads at wet state were incubated in phosphate buffer (PBS), and shaken on a magnetic stirrer. Each hour, the supernatant was collected, without replacing it, and analysed by capillary electrophoresis. Phosphate ions in the buffer are able to swell calcium-alginate beads. With the swelling, the expansion of the polymer network is enhanced, resulting in an easier diffusion of peptide from the beads. As shown in Figure 39 both beads types exhibited similar profiles.

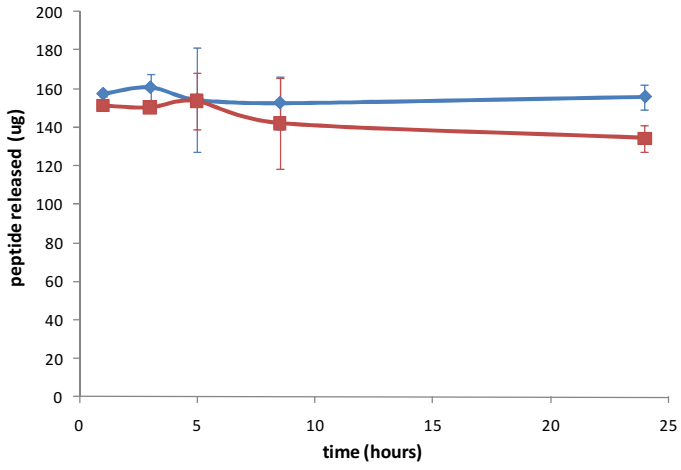

Figure 39.Amount of the BMP fragment recovered on the supernatant. Blue curve: beads produced in acid conditions; red curve: beads produced in neutral conditions.

The entire percentage of loaded peptide was released within the first hour and corresponds with the estimation of the total amount of peptide in beads obtained by subtraction of the used peptide and the peptide lost during cross-linking procedure.

Beads for controlled release

Synthesis of enzymatic cleavable ChitLac-(click)-BMP

The functionalization of ChitLac with BMP was planned in four synthetic steps that are graphically represented in Figure 40:

1. The synthesis of the linker with an ester group and a final functional group for click chemistry
2. The functionalization of the ChitLac with the spacer to obtain ChitLac-azido
3. The synthesis of the BMP fragment opportunely functionalised for the click reaction, to obtain BMP-alkyne
4. The click reaction between ChitLac-azido and BMP-alkyne to obtain the final product ChitLac-(click)-BMP

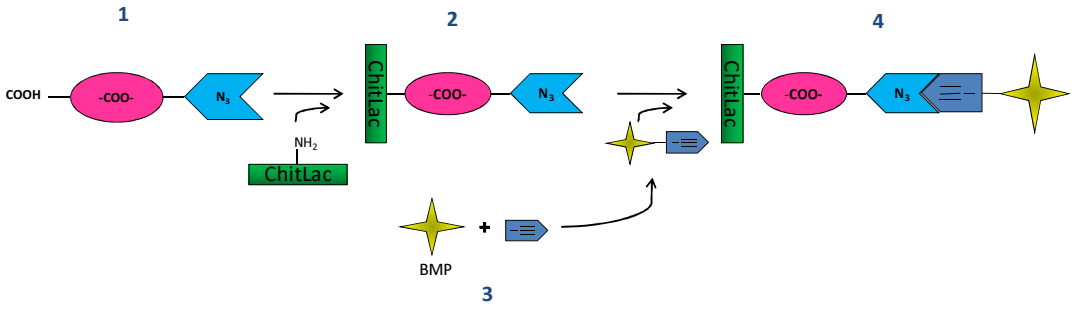

Figure 40. Chemical steps in the synthesis of ChitLac-(click)-BMP

Synthesis of the linker

In the linker molecule, it was planned the presence of three functional groups: the ester bond for the enzymatic hydrolysis in the middle and at the opposite terminals an azido group necessary for the click chemistry and a carboxylic group to functionalize ChitLac.

This spacer was synthesized (Scheme 12) starting from hydrolyzed γ-valerolactone (1) (Long and Friedman, 1950). This compound was coupled with a typical building block for 1,3-dipolar reactions, the 11-azido-3,6,9-trioxoundecan-1-amine, *via* carbodiimide activation. The use of carbodiimides (EDC and NHS) permits the activation of carboxylic groups and the

formation on the amidic bond. Subsequently, to introduce the ester group, the product of the coupling was succinylated (3), in typical conditions for reactions with anhydrides. A nucleophilic substitution of succinic anhydride with the alcoholic group of compound (2) occurs and in this manner the introduction of the ester group, was achieved. The obtained linker, a chain of more than 20 atoms, was suitable for both the linkage to amino-containing polymers, like ChitLac, and, at the opposite terminal, to click reactions.

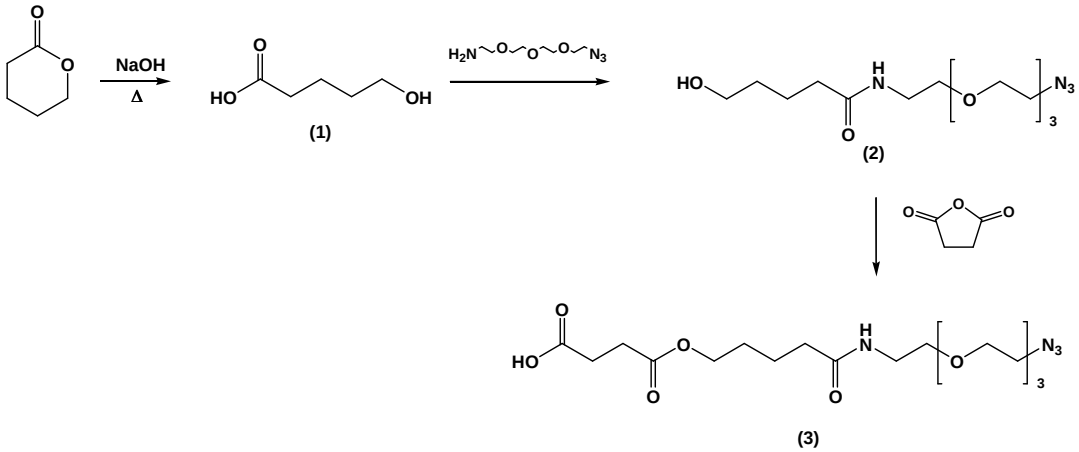

Scheme 12. Three steps synthesis of the linker.

Functionalization of ChitLac

Synthesis and characterization of ChitLac-azido

As above anticipated, the functionalization of the polysaccharide ChitLac with the linker was performed *via* carbodiimide chemistry. After activation of the carboxylic groups of the linker with opportune activators, an aqueous solution of ChitLac was added (Scheme 13).

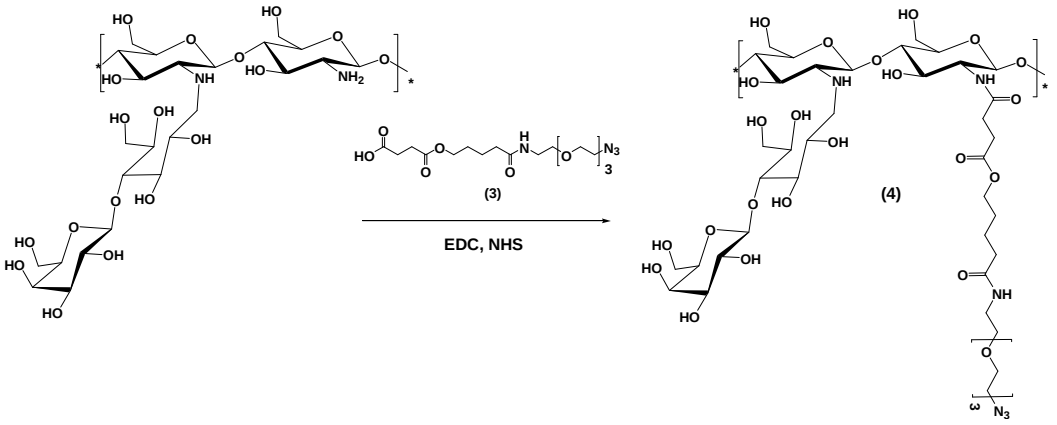

Scheme 13. Synthesis of ChitLac-azido by unmodified ChitLac and the linker (3).

The characterization of the functionalized polymer was performed by ^{1}H-NMR spectrometry. In a first series of experiments, the ^{1}H-NMR spectra of the modified polymer revealed the formation of the amidic bond with a good yield, but further bidimensional analyses showed that the linker was presented in solution but not covalently bound to the polymer. This result was quite surprising, since the reaction mixture had been extensively dialyzed. Our hypothesis was that the amphiphylic nature of the linker and its length could give rise to micelles in water. In such manner, the molecules, organized in micellar structures would be unable to react with the polymer, and at the same time, would remain inside the dialysing tube.

To verify this hypothesis, a characterization with a different technique was performed and in the detail a particular application of MEKC (micellar electrokinetic chromatography) technique was explored. Applying the electrophoretic procedure published by Nakamura and co-workers (Nakamura et al., 1998) it is possible to determine the tendency of a compound to give rise to micelles, besides, whit the same method, a value of critical micellar concentration (c.m.c.) of the analysed compound is obtainable. The method is based on the shift of migration times of a neutral compound (which is injected as a sample) in relation to increasing concentrations in the running buffer of micellar analyte. Below the c.m.c., the response appears linear, but when the concentration of the analyte is over this one, it is possible to note a more rapid increasing of this linearity: it is possible to note two different linear trends whose intersection corresponds to c.m.c..

In this procedure an important point is the selection of an opportune marker. To select it, the method was first tested on SDS to replicate the experiment performed in literature. As neutral compound SUDAN III was used and the resulting graph was similar to results reported by Nakamura (data not shown) obtaining the same value of c.m.c. (3.83 mM). In Figure 41 are reported four electropherograms where the shift of migration time of the neutral marker SUDAN III is particularly evident.

Exploiting this marker, the c.m.c. of the linker was then calculated. In Figure 42, the migration times as function of surfactant concentrations are reported. It can be observed that the linker actually forms micelles, starting from a concentration of 0.1 mg/mL.

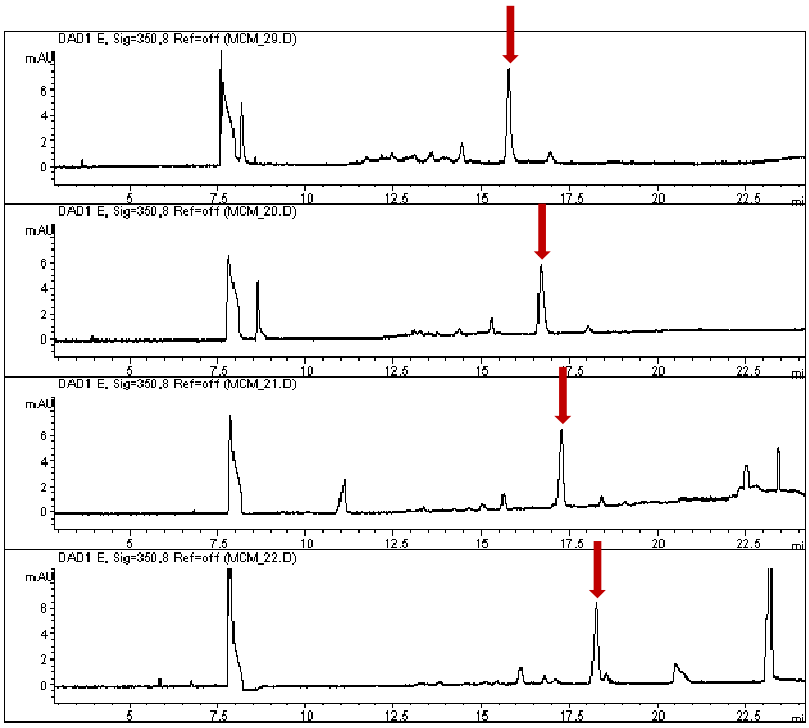

Figure 41. Time migration shifting of SUDAN III in the presence of different concentrations of micellar analyte. (SUDAN III marker dissolved in MeOH; running buffer: phosphate 20 mM at pH 7.00, silica fused capillary length 56 cm, i.d. 50 µm, applied voltage 20 kV normal polarity, UV detection at 350 and 195 nm).

The experiment was carried out also on 11-azido-3,6,9-trioxoundecan-1-amine, showing that also this shorter molecule has the strong tendency to aggregate in micelles.

These results were never reported before.

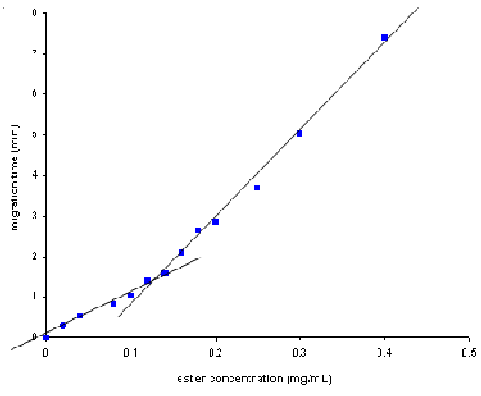

Figure 42. Linker concentration plotted as function of migration time. The change of slope corresponds to the c.m.c.

With this information, we carried out the polymer-linker coupling maintaining the concentration of the linker always below the c.m.c. and exhaustively dialysing the reaction mixture. In this way it was possible to obtain the modified polymer, as demonstrated by NMR analyses.

^{1}H and ^{13}C NMR assignment of ChitLac functionalized with the linker is shown in Figure 43, together with atom numbering of the molecule. The figure shows the 2D-^{1}H,^{1}H-TOCSY-^{1}H,^{13}C HSQC spectrum where the negative peaks (in red) indicate ^{1}H-^{1}H scalar coupling therefore aiding in the assignment. The short mixing time used results in having basically only COSY-like cross peaks. The spectrum does not show any signal from the chitosan backbone likely due to transversal relaxation loss caused by slower motions.

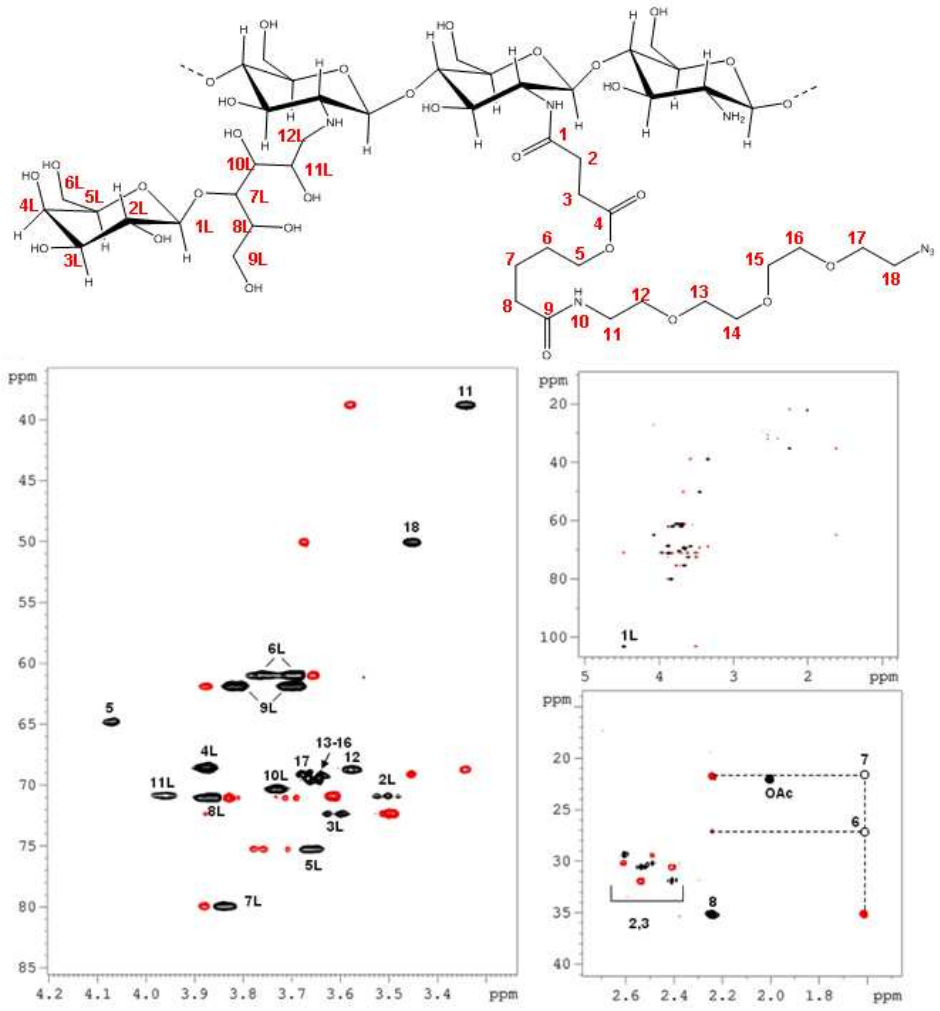

Figure 43. ^{1}H and ^{13}C NMR assignment visualized onto 2D-^{1}H,^{1}H-TOCSY-^{1}H,^{13}C HSQC spectrum. Short mixing time ensures COSY-like peaks (in red) aiding the assignment. Atom numbering is shown on the molecular structure.

The chemical shift observed for protons in positions 2 and 3 demonstrates the formation of the amidic bond between the acidic groups of the esters and the amine moieties of the backbone. These protons are in fact expected to resonate at 2.83 and 2.73 respectively when adjacent to an acidic group and 2.46 and 2.49 when adjacent to an amidic group.

The linkage was further demonstrated by diffusion measurements. As shown in Figure 44, DOSY experiment indicates that signals belonging to the ester tail (protons in positions 6, 7 and 8 for example) do diffuse with the ChitLac polymer and the acetyl moiety of the backbone. Given the huge difference in molecular weight of the two molecules a much larger diffusion coefficient would be expected for the free ester molecule in case the derivatization did not take place.

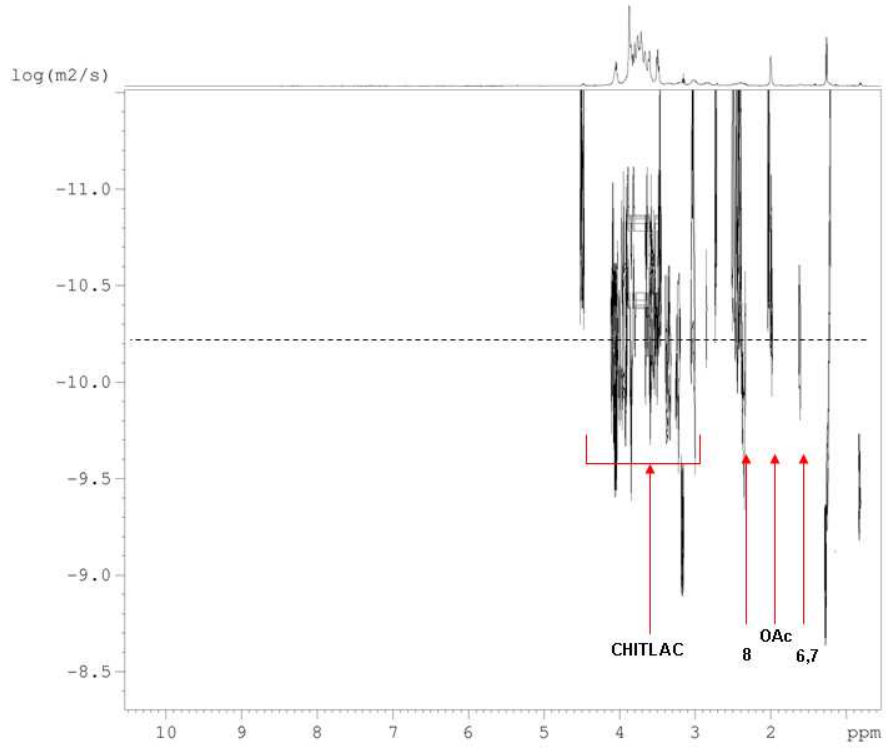

Figure 44. DOSY spectrum of chitlac derivatized with a long chain ester. Peaks from both fragments diffuse with the same diffusion coefficient indicating their mutual binding.

From NMR integrations, the total degree of substitution resulted to be equal to 1% with respect to the average repeating unit.

Enzymatic kinetic profile

Since the main focus of this synthesis was the introduction of a bond sensitive to enzymatic action, the susceptibility to the enzymatic hydrolysis of the linker, after conjugation to the polymer, was tested (see Scheme 14). The reaction was monitored following the peak corresponding to the released compound (2) in the Scheme 12, with a value of 319 m/z.

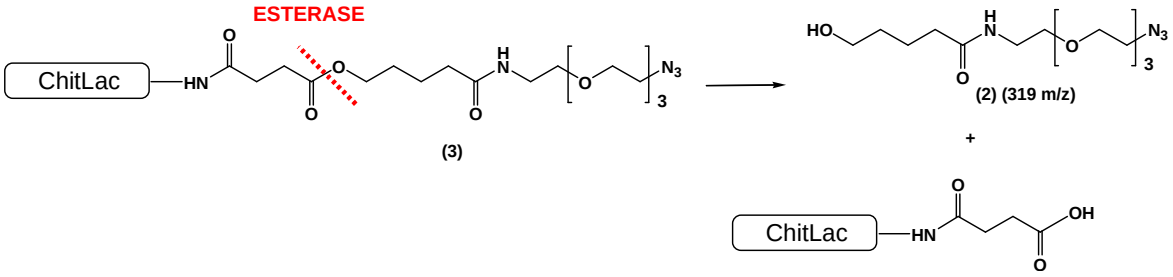

Scheme 14. Esterase action.

The esterase activity was followed both by CE-UV (MECK) (Figure 45) and ESI-MS. It was possible to demonstrate the release of the compound, meaning that no interference of the polysaccharide presence on the enzyme activity occurred.

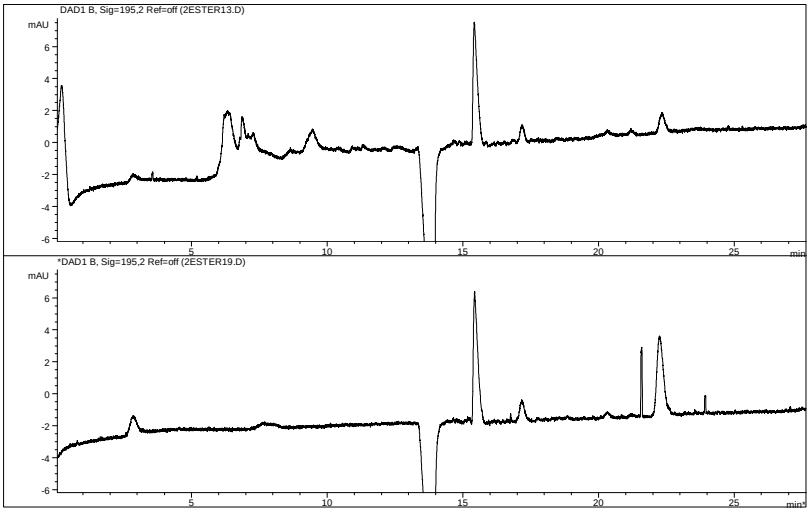

Figure 45. Electropherogram of the fraction collected after 56 hours of the reaction with esterase, diluted 1:2 (first panel) and the same with a co-injection of the compound 319 m/z standard (second panel). 319 m/z migration time 22.5 min. (Capillary electrophoretic conditions: running buffer 25 mM borax solution, 50 mM dihydrogenophosphate, 71 mM SDS; silica fused coated capillary, length 54 cm, inner diameter 50 µm; applied voltage of 20 kV; UV detection at 270 and 195 nm).

The profile of the obtained curve is reported in Figure 46. It can be observed that the reaction has a maximum at 40 hours, which is followed by a second reaction which consumes completely the linker. Probably this reaction is the hydrolysis of the amidic bond, which has been previously observed to be a secondary activity of some esterases.

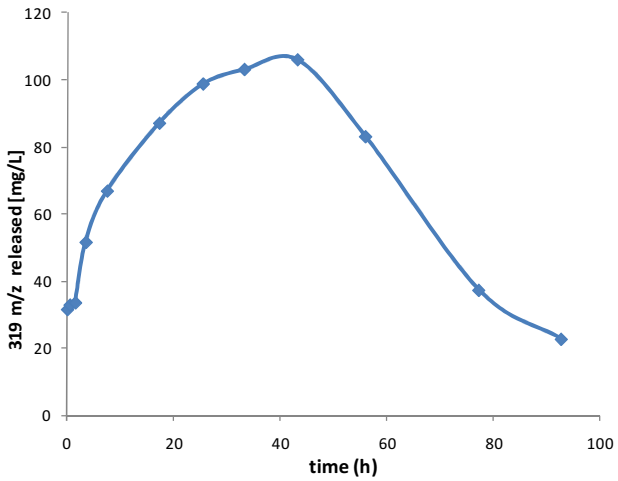

Figure 46. Kinetic profile of ChitLac-azido hydrolysis by esterase

This was also confirmed by ESI-MS analysis, where the disappearance *of peak 319 m/z* (presents in the first fractions) with the appearance of a peak with 219 m/z at 50 hours were visible (Figure 47).

However, the experiment demonstrates that ChitLac-azido is still a substrate for the esterase: the high positive charge on ChitLac and its size do not interfere with the enzymatic activity. An aliquot was incubated in the reaction buffer without the enzyme, and after 100 hours it did not show any peak related to the hydrolysis, demonstrating that slightly basic condition *per se* is not sufficient to hydrolyzed the ester in the absence of the enzyme.

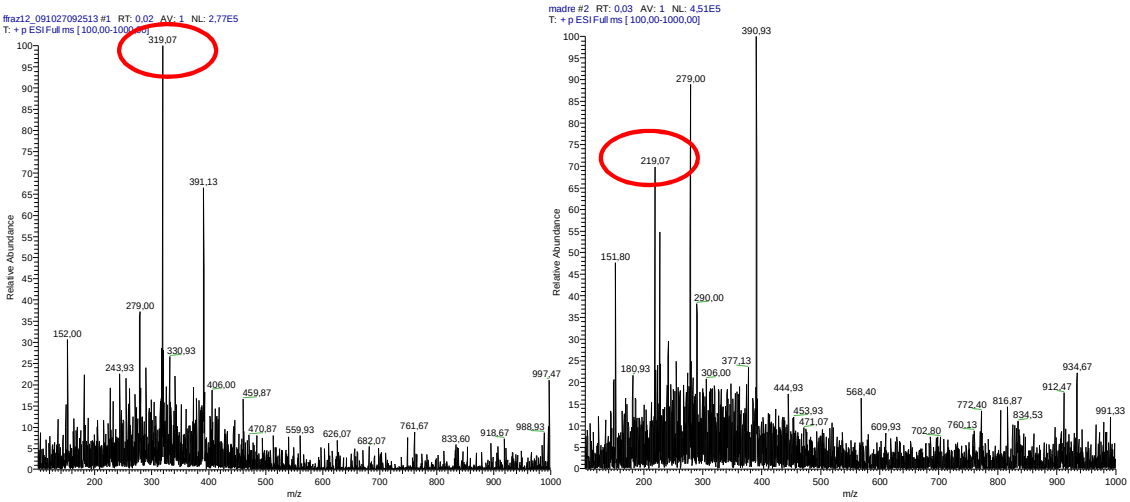

Figure 47. ESI-MS of fractions collected during esterase action. The first spectra represents the injection of a sample of one of the first fractions, while the second represents a fraction collected after 50 hours of esterase/ ChitLac-azido incubation.

BMP-fragment synthesis

The rate of the 1,3-dipolar cycloaddition of azides and alkynes is drastically increased in the presence of an appropriate catalyst such as transition-metal ions. This reaction is commonly performed in the presence of copper ions, however the cytotoxicity of copper, prompts to investigate the use of different types of catalysts: different ligands, and diverse transition metals have been examined. Azides do not react easily with alkynes in the absence of a metal catalyst since they are generally poor 1,3-dipolar acceptors. In the last years, there has been an important development of click reactions that do not require metal catalyst. In particular, in 2004, Ju and co-workers, reported a simple synthetic protocol for the 1,3 dipolar cycloaddition of azide with electron-deficient alkynes (Li et al., 2004) (Scheme 15). In this strategy the introduction of a triple bond that is activated by conjugation, permits to avoid the use of copper, making this reaction quite convenient for biological systems.

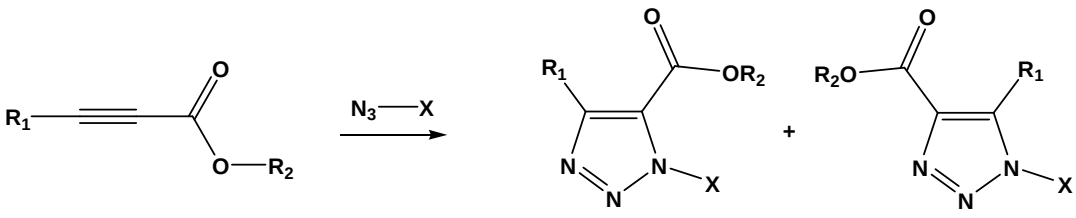

Scheme 15. Click reaction between azides and electron-deficient alkynes (where R_1= H, CH_3 or COOEt; R_2= Me or Et)

In order to test the efficacy of this intriguing chemical strategy, a first explorative experiment was performed. The reactivity of propiolic acid and 4-pentynoic acid in click chemistry reactions, was compared. Propiolic acid is a compound classified as electron-deficient alkyne: are so named those alkynes that present an electron-withdrawing functional group. The reactivity of these two species towards a compound containing an azide group (O-(2-Azidoethyl)-O-[2-(diglycolyl-amino)ethyl] heptaethylene glycol), without any catalyst, was monitored. The formation of the product was followed by capillary electrophoresis and ESI-MS. With this experiment, it was possible to verify the effective formation of the click-compound using the preactivated alkyne and not by using the other reagent. In fact, the capillary electrophoretic analysis (Figure 48) revealed the formation of the product whose identity was confirmed by ESI-MS, but also the consumption of the azide in the propiolic acid reaction, unlike for mixture containing pentynoic acid.

Figure 48. Electropherogram of click chemistry reaction copper free.

With these assumptions, the synthesis of BMP fragments with two different functional groups was performed.

A first synthesis regarded the BMP fragment functionalized at the N-terminal with the electron-deficient alkyne using propiolic acid as reagent. Unfortunately, it was not possible to obtain the functionalized product, in fact the synthesis of the peptides modified with these kinds of alkynes is particularly tricky, because of the precipitation of the propiolic acid with a

compound used in the coupling mixture reported by Neukamm and co-workers. (Neukamm et al., 2008).

Because of the lack of the functionalised BMP fragment for the strategy employing electron-deficient alkynes, the attention was focussed on the other strategy. The functionalization of the peptide with pentynoic acid (BMP-pentynoic) was performed without any problem. Besides, a preliminary control of the not cytotoxicity of a polycation treated with the copper mixture, was performed. To simulate a copper (I)-catalyzed azide-alkyne cycloaddition (CuAAC), unfunctionlized ChitLac was treated with the catalytic mixture of $CuSO_4$ and ascorbic acid, and LDH (lactate dehydrogenase) assay on alginate/hydroxyapatite beads layered with this one, was achieved (data not shown), demonstrating the biocompatibility of the beads so obtained.

Click reaction and characterization of ChitLac-(click)-BMP

The click chemistry between ChitLac-azido and BMP-pentynoic acid exploited Cu^+ as catalyst. Reaction was performed in water with $CuSO_4$ and ascorbic acid (Scheme 16). This latter constantly reduces copper (II) to copper (I) maintaining significantly high levels of the catalytic species.

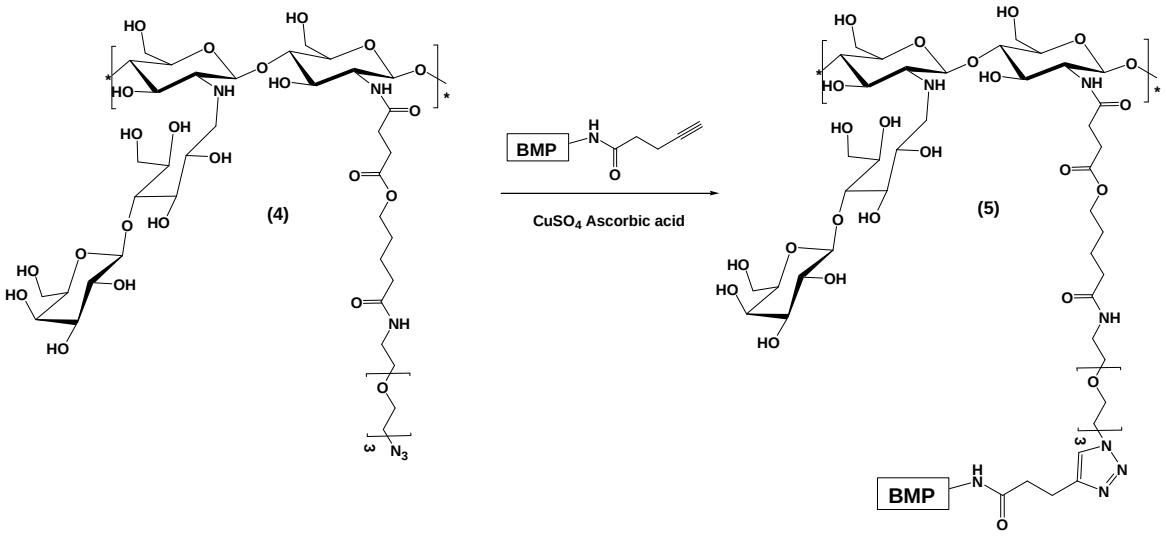

Scheme 16. Click reaction between ChitLac-azido and BMP-alkyne, catalyzed by copper.

The linkage of modified ChitLac to BMP fragment is demonstrated by the appearance in the ^{1}H-NMR spectrum (Figure 49) of a singlet at 7.32 ppm (expected at 7.30 ppm) whose intensity is approximately half of each couple of aromatic protons of tyrosine belonging to

BMP peptide. An extra smaller peak at 7.48 ppm (expected at 7.59 ppm) is probably due to a different kind of linkage indicated as B in Figure 49, showing that with this approach a mixture of the two isomers is obtained.

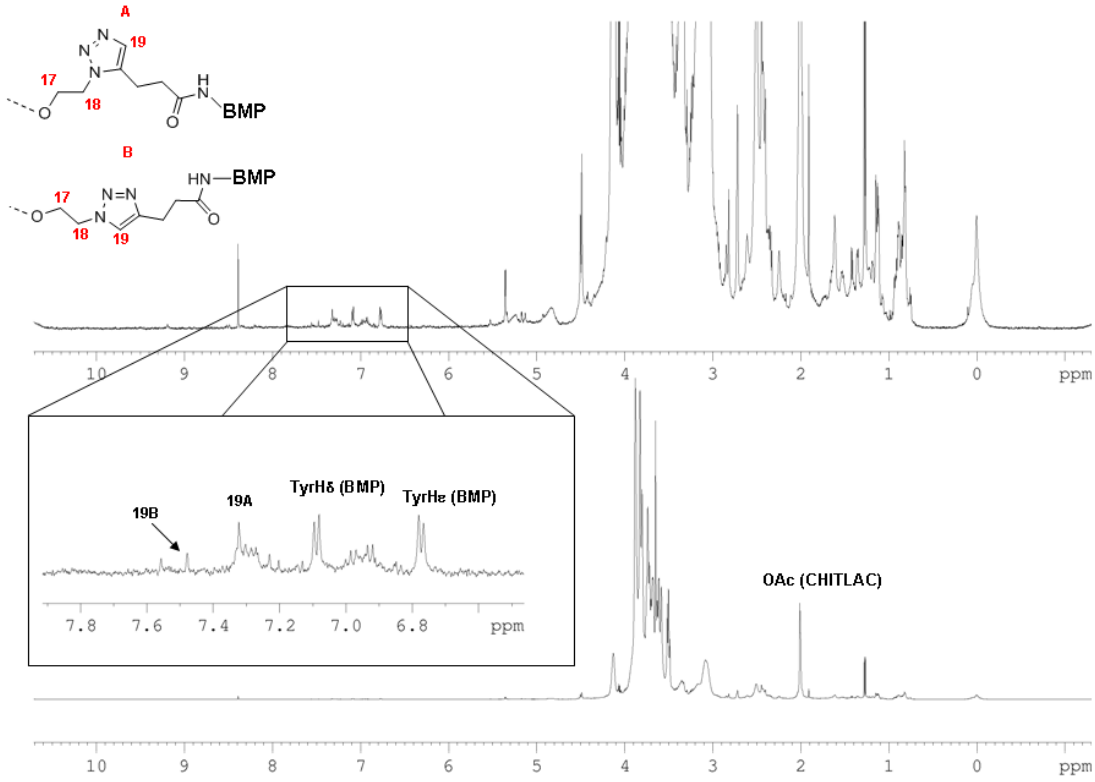

Figure 49. ^{1}H-NMR spectrum of chitlac derivatized with BMP peptide. Appearance of an aromatic peak at 7.32 ppm (in the zoomed panel) indicates the formation of a chemical bond linking the BMP to the polymer.

Esterase action on the final product

The final product was characterized again in terms of its capability to release the peptide. The sample incubated with the esterase was analyzed by means of capillary electrophoresis. After incubation the presence of two new peaks was observed (Figure 50), that were attributed to hydrolyzed linker and hydrolyzed linker-BMP (this latter more visible at 214 nm).

To evaluate the amount of linker conjugated to BMP, a quantification of compound (2) was performed, which, being an intermediate of the synthesis of the linker, was available as standard. The degree of substitution was calculated as difference between the total

substitution with the linker (measured by NMR) and the amount of the free linker released during the hydrolysis. It corresponds to 0.53% with respect to the average repeating unit.

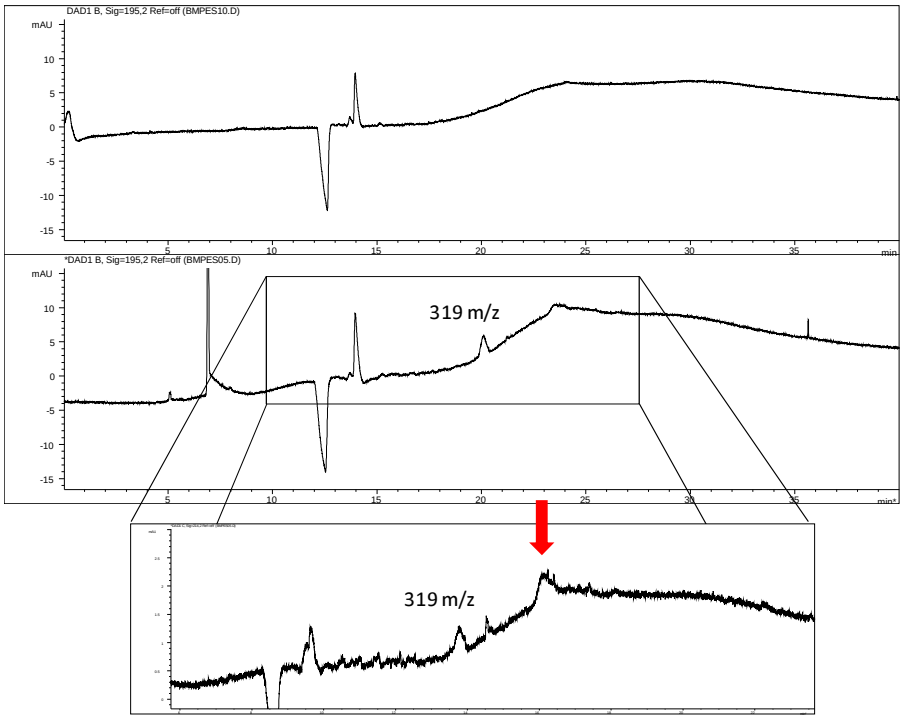

Figure 50. The esterase action on ChitLac-(click)-BMP: first panel, time 0; second panel: time 50 hours, with a zoom at 214 nm where the BMP-fragment released is indicated.

4.3.3 Partial conclusions

In this work two kind of release of the BMP fragment peptide have been explored. The first one occurs by simple diffusion form alginate/hydroxyapatite beads, and allows for a rapid peptide release that was considered useful in the first phase of fracture repair.

The second type of release is a slow and constant peptide discharge useful during the long period of the fracture repair. With this aim, a drug-delivery system sensitive to enzymatic action was desinged. A ChitLac with an enzymatic cleavable linker was functionalized with a BMP fragment. The contact with enzymes involved in fracture healing, will cause the release of the active peptide. The accessibility of the final product to enzyme was verified.

The used chemical strategy was intriguing: in the building of this peculiarly functionalized polysaccharide (named ChitLac-(click)-BMP), the attention was focalized on the use of a

simple chemistry and on performing very selective linkages obtained by click reactions. This strategy can be potentially applied to a large variety of bioactive molecules and supporting polymers, introducing simple variations in the used chemistry. Moreover, in this work, it has been demonstrated that glycolic structure, normally used as reagents for click chemistry, can give rise to micelles formations, and products have to be carefully purified and characterized before use.

The ChitLac-(click)-BMP was planned to be employed in alginate/hydroxyapatite beads associated with beads loaded with un-functionalized BMP fragment. In this manner a sum of the two kinetics release is achievable. Tests *in vitro* on mesenchymal stem cells to verify the differentiation activity of the polymer ChitLac-(click)-BMP have already been planned.

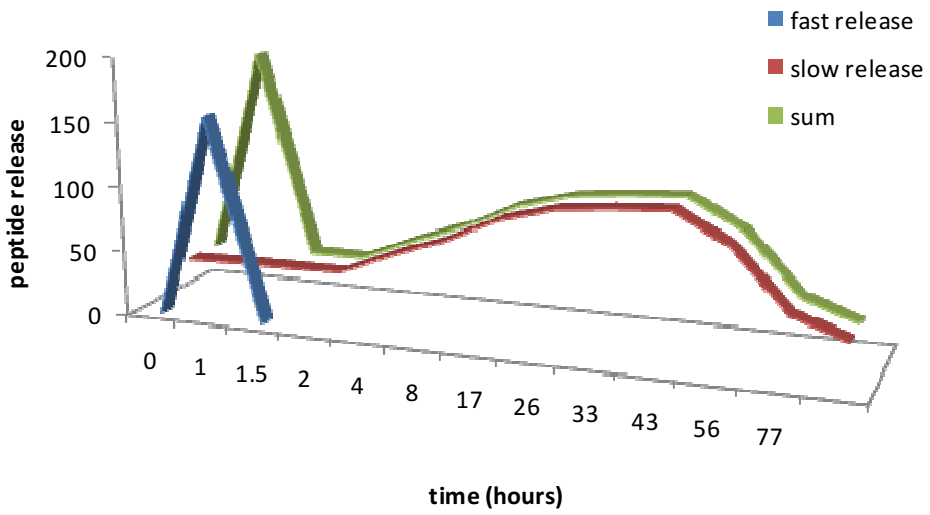

Figure 51. Theoretical sum release that it is possible to obtain associating the two BMP release types (green curve): the release from beads for diffusion (blue curve) and the controlled enzymatic release (red curve).

4.4 ANTIBACTERIAL AGENTS IN FILLER: THE LL-37 PEPTIDE

4.4.1 Introduction

The need of new antimicrobial agents

In March 1942, a 33-year-old woman lay dying of streptococcal sepsis in New Haven, Connecticut, hospital, and despite the best efforts of contemporary medical science, her doctors could not eradicate her bloodstream infection. Then they managed to obtain a small amount of a newly discovered substance called penicillin, which they cautiously injected into her. After repeated doses, her bloodstream was cleared of streptococci, she made a full recovery, and she went on to live to the age of 90 (Lax, 2004). Sixty-six years after her startling recovery, a report (Schwartz et al., 2008) described a 70-year-old man in San Francisco with endocarditis caused by vancomycin-resistant Enterococcus faecium (VRE). Despite the administration, for many days, of the best antibiotics available for combating VRE, physicians were unable to sterilize the patient's blood, and he died still bacteremic. We have come almost full circle and arrived at a point as frightening as the preantibiotic era: for patients infected with multidrug- resistant bacteria, there is no magic bullet (Arias and Murray, 2009).

Antibiotics are probably the most important class of therapeutic agents developed so far: they have revolutionised medicine, allowing treatment of infections that only 80 years ago were widely fatal and that today are considered a problem readily resolvable by taking a couple of pills. The availability of this class of medicament has created an assurance of health unknown to previous generations. It is difficult to imagine undertaking today's surgical procedures, transplantations, cancer chemotherapy, or care of the critically ill or HIV-infected without effective antimicrobial agents (Arias and Murray, 2009). This assurance, now taken for granted, could be dissipated by the phenomenon known as "antibiotic resistance", which has become a real emergency in the past decade (Livermore, 2004).

This phenomenon, which represents the other side of the wide spreading of antibiotics, has been correlated with the indiscriminate use of antibiotics also in breeding and agriculture, though bacteria are known to be "the most numerous, diverse, and adaptable organisms that have ever lived on the planet" (Spellberg et al., 2008), and their exceptional adaptability would allow the development of resistance strategies also in the absence of misuse from patients and industry. However, it has been demonstrated that the abolishment of the use of

antibiotics for the growth of food-animals has slowed down the increase of clinical isolates resistant to the antibiotics in use, as reported in Figure 52, where penicillin non-susceptibility is reported for invasive *Staphylococcus pneumoniae*. Data are based (a) on reports to the Health Protection Agency for most laboratories in England and Wales and (b) on sentinel surveillance of 23 UK hospitals under the European Antimicrobial Resistance Surveillance System (http//:http://www.earss.rivm.nl).

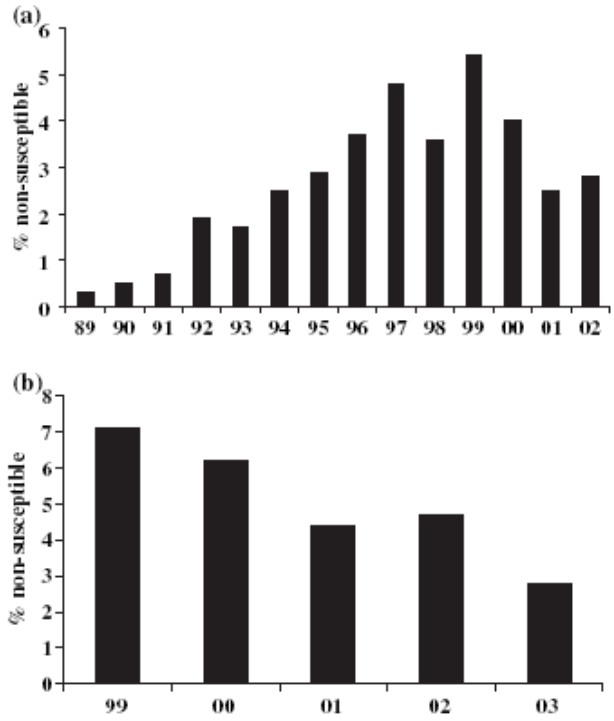

Figure 52. number of clinical isolated of *S. pneumoniae* resistant to penicillin in use from 1989 to 2002 in two different statistics (see text).

Notwithstanding these good news, the necessity to develop new antimicrobial agents with novel mechanisms of action (Payne, 2008), (Vicente et al., 2006), (Spellberg et al., 2008), (Theuretzbacher, 2009) is still an emergency (Livermore, 2004). The need for new agents is most pressing in hospital infections, where small but growing numbers of isolates, mostly Gram-negative non-fermenters of the genera *Acinetobacter* and *Pseudomonas*, have been found to be resistant to all "good" antibiotics and where growing numbers of *Enterobacteriaceae* are resistant to all except carbapenems. Whilst there is a lesser shortage of agents active against staphylococci, the prevalence of infections with methicillin-resistant

Staphylococcus aureus (MRSA) remains extremely high in many countries. *Pseudomonas aeruginosa* is also important as a pulmonary pathogen in cystic fibrosis. Gram-negative infections are becoming effectively untreatable and against these opportunists apart from tigecycline, there are few new agents in advanced development. And, whilst new treatments are becoming available for infections caused by multiresistant Gram-positive pathogens, the goal of finding a drug that is as effective, against MRSA, as penicillin was against staphylococci in the 1940s remains elusive (Livermore, 2004).

There are also strategic choices, behind this emergency, since many large pharmaceutical firms have abandoned their programs for antimicrobial development over the past decade, largely because of concerns that development costs exceed predicted profitability of injectable antimicrobial agents (Spellberg et al., 2004), (Rice, 2006). The proportion of infections that cannot be treated with present agents is small, restricting demand, and the infections are widely scattered, complicating clinical trials. Many of the largest pharmaceutical companies have concluded that drugs directed against chronic diseases offer a better revenue stream than antibacterial agents, where the courses are short and restriction is likely. Several major houses have abandoned antibacterial development and others have merged, leaving one developer where there previously were two or more. Perhaps not surprisingly, therefore, the number of antibiotics with activity against resistant Gram-negative species under development is so low. However, if the antibiotics resistance phenomenon will continue, as it is predictable, the need of new drugs will be soon a matter of fact.

In this case, it is evident that the development of new antimicrobial agents with new modes of action will be a crucial point in the pharmaceutical science of the next years. In this scenario a promising class of molecules is that of AntiMicrobial Peptides (AMPs) (Brogden, 2005).

Bone infections and post-surgical complications

Infections occurring to bone tissue are known as osteomyelitis. The bacteria or other microorganisms that cause osteomyelitis can enter the bone through an injury, or can be carried through the bloodstream to the bones from another infection occurred in a different part of the body. Bacteria can enter the bone through an open fracture, can penetrate by a sharp, by a contaminated object or during orthopedic surgery. A big problem of osteomyelitis is that the diagnosis of bone infection in the context of post-surgical inflammation is

problematic since many of the early signs of infection are similar to normal post-surgical changes (Jones-Jackson et al., 2005).

Over the last 15 years, with the advent of modern standards in the control of sterility within the operating room environment and adequate protocols of peri-operative antibiotic prophylaxis, the incidence of infections associated to orthopaedic implants has become very low. Nevertheless, the event of infection still represents one of the most serious and devastating complications which may involve prosthetic devices. It leads to complex revision procedures and, often, to the failure of the implant and the need for its complete removal. In orthopaedics, for the enormous number of surgical procedures involving invasive implant materials, even if nowadays rare, infections have a huge impact in terms of morbidity, mortality, and medical costs (Campoccia et al., 2006).

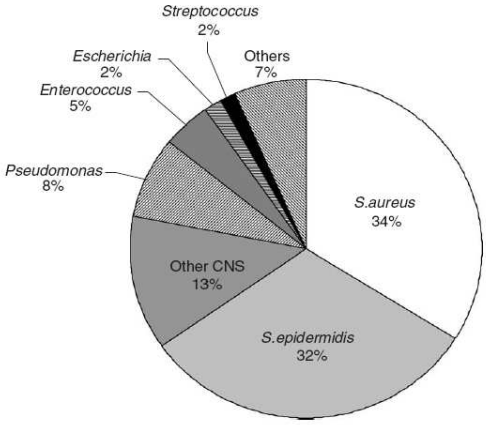

Figure 53. Frequency of main pathogenic species among orthopaedic clinical isolates of implant-associated infections.

A very large proportion of all implant-related infections are caused by staphylococci (roughly four out of five), and two single staphylococcal species, respectively *Staphylococcus aureus* and *S. epidermidis*, account together for two out of three infection isolates. They represent, in absolute, the main causative agents in orthopaedics, while CoNS (Coagulase Negative Staphylococci) species other than *S. epidermidis*, and, especially among them, *S. hominis* and *S. haemolyticus*, contribute to an additional 13% of the infections. In order of relevance in terms of prevalence then there follow *Pseudomonas aeruginosa* and *Enterococcus faecalis* (Campoccia et al., 2006).

Apart from post-surgical complications, the infection can also be carried to the bones in the bloodstream from another part of the body where an infection is present. This type of

infection is the most common form of the disease in children. In this case, though *S. aureus* remains the primary cause of osteomyelitis, other bacteria can be involved, including Group A and B *Streptococcus*, *Hemophilus influenzae*, *Enterobacteriaceae*, *Escherichia coli*, and *Salmonellae*. Beside, in some cases, more than one type of bacteria is found during the laboratory culture of blood or tissue samples.

Antimicrobial Peptides

Survival of a multicellular organism in a non-sterile environment requires a network of host defense mechanisms. The initial contact of pathogenic microorganisms with the host usually takes place at internal or external body surfaces. Animals of various phyla have developed first line defense mechanisms to inhibit the growth and invasion of microorganisms. The first line of defense against pathogenic insult is called the innate immune system, which in mammals is followed by acquired immune responses associated with activation of T and B cells aimed against specific antigens.

One principle of innate immunity is the production of endogenous antibiotic peptides (Bals and Wilson, 2003). These are ancient components of the innate immune system and represent a first line of defense against bacterial infections of plants, invertebrates and vertebrates, including humans (Nicolas and Mor, 1995), (Boman, 1995), (Bowdish et al., 2005), (Giangaspero et al., 2001). They were discovered by analyzing the antimicrobial properties demonstrated by secretions fluids, blood, leukocytes, and lymphatic tissues that had been observed at the end of the nineteenth century. Between 1920 and 1950 many antimicrobial compounds that were isolated from these secretions were shown to be selective for Gram-positive and Gram-negative bacteria. Despite the early stages of this new science, the descriptions of their characteristics, activities and modes of action were already accurate: *"…antimicrobial basic proteins and polypeptides combine with cell nucleoproteins or other negatively charged surface constituents of bacteria or viruses, thus disrupting important cell function. The union of the basic substances with negatively charged cell surfaces is believed to occur through electrostatic bonding"* (Skarnes and Watson, 1957). They were described as being inducible on exposure to infecting microorganisms, to kill or slow the growth of invading microorganisms and to aid allied mechanisms of natural and adaptive immunity. Thus these observations gave rise to the birth of the field of antimicrobial peptide (AMPs) research.

This class of compounds comprises antimicrobial peptides that are produced in many tissues and cell types of a variety of invertebrate, plant and animal species, certain cytokines and chemokines, selected neuropeptides and peptide hormones, and fragments of larger proteins. Nowadays a great interest is directed towards these molecules, since antimicrobial peptides are recognized as a possible source of pharmaceuticals for the treatment of antibiotic-resistant bacterial infections or septic shock (Ciornei et al., 2005), (Brogden, 2005). Recent studies have highlighted their importance as endogenous antibiotics, acting as effectors molecules of the innate immunity. They are mainly produced by phagocytes and epithelial cells. Whereas most antimicrobial peptides were identified based on their antimicrobial activity, they have recently been shown to display a variety of additional and partly unexpected activities. These findings have suggested a role for antimicrobial peptides in infection, immunity and wound repair (Tjabringa et al., 2005).

In humans, AMPs are present in tissues exposed to the risk of infective agents. In fact, they are found on the epithelial surface of skin, trachea, bone marrow, testes, eyes, tongue, lung and intestine.

The majority of these peptides acts at the level of the integrity of bacterial wall, thanks to two fundamental characteristics: the first is that they have a positive net charge, the second one is that they tend to have an amphipatic structure, which allows the interaction with the negatively charged bacterial wall. Moreover, AMPs activity depends on several other parameters, including sequence, size, structuring degree, cationicity, hydrophobicity and amphipathicity (Giangaspero et al., 2001). Unlike most of the classical antibiotics, which are built in a stepwise manner through a complex enzymatic synthesis, antimicrobial peptides are made from gene-encoded precursors (prepropeptides), from which the mature peptides are derived by the sequential removal of the signal peptide and of a variably extended prosequence. In general the pro-piece precedes the mature peptide, is anionic and, at least in some cases, has been suggested to play a role in targeting and/or in assisting the correct folding of the antimicrobial peptide. The preproregion is often highly conserved within families of antimicrobial peptides, as deduced from sequence analysis of the precursors at the cDNA level, thus suggesting that members of each family evolved from ancestor genes through duplication and modification (Zanetti et al., 1995).

Classification of AMPs

From a structural point of view, antimicrobial peptides isolated from vertebrates have three characteristic properties: they are relatively small (20-46 amino acid residues), basic (lysine- or arginine-rich), and amphipathic. Although these peptides differ widely in length and amino acid sequences, they may be grouped into subgroups on the basis of their amino acid composition and structure (Figure 54). A classification based on the charge on the peptide also exists and the Box reported in the next pages (Box 1) shows the complexity of this classification.

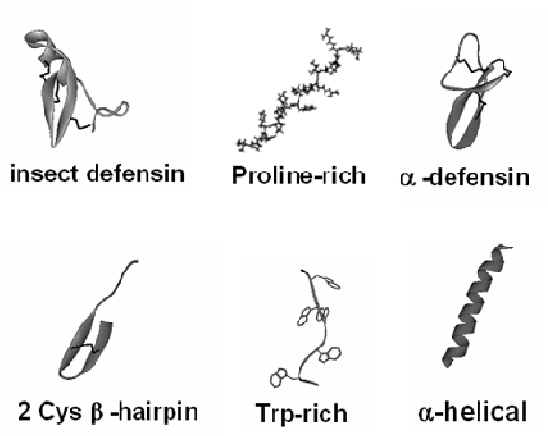

Figure 54. The structure of some of the most common classes of AMPs.

Box 1. Classification based on the charge on the peptide

Anionic peptides
Maximin H5 from amphibians
Small anionic peptides rich in glutamic and aspartic acids from sheep, cattle and humans
Dermcidin from humans
Linear cationic α-helical peptides
Cecropins (A), andropin, moricin, ceratotoxin and melittin from insects
Cecropin P1 from *Ascaris* nematodes
Magainin (2), dermaseptin, bombinin, brevinin-1, esculentins and buforin II from amphibians
Pleurocidin from skin mucous secretions of the winter flounder
Seminalplasmin, BMAP, SMAP (SMAP29, ovispirin), PMAP from cattle, sheep, and pigs
CAP18 from rabbits
LL-37 from humans

Cationic peptides enriched for specific amino acids
Proline-containing peptides include abaecin from honeybees
Proline-and arginine-containing peptides include apidaecins from honeybees; drosocin from *Drosophila*, pyrrhocoricin from the European sap-sucking bug; bactenecins from cattle (Bac7), sheep, and goats; and PR-39 from pigs.
Proline- and phenylalanine-containing peptides include prophenin from pigs
Glycine- containing peptides include hymenoptaecin from honeybees
Glycine- and proline-containing peptides include coleoptericin and holotricin from beetles
Tryptophan-containing peptides include indolicidin from cattle
Small hisitidine-rich salivary polypeptides, including the histatins from man and some higher primates
Anionic and cationic peptides that contain cysteine and form disulphide bonds
Peptides with 1 disulphide bond include brevinins
Peptides with 2 disulphide bonds include protegrin from pigs and tachyplesins from horseshoe crabs
Peptides with 3 disulphide bonds include α-defensins from humans (HNP-1, HNP-2, cryptidins), rabbits (NP-1) and rats; β-defensins from humans (HBD1, DEFB118), cattle, mice, rats, pigs, goats and poultry; and rhesus θ-defensin (RTD-1) from the rhesus monkey
Insect defensins (defensin A)
SPAG11/isoform HE2C, an typical anionic β-defensin
Peptides with >3 disulphide bonds include drosomycin in fruit flies and plant antifungal defensins defensins
Anionic and cationic peptide fragments of larger proteins
Lactoferricin from lactoferrin
Casocidin I from human casein
Antimicrobial domains from α-lactalbumin, human haemoglobin, lysozyme and ovalbumin

A common way to classify antimicrobial peptides divides them into four classes (Nicolas and Mor, 1995):

- **Defensins and β-defensins.** Mammalian defensins and β-defensins are two multimember families of cationic (Arg-rich) trisulfide-containing peptides of 29-42 residues that are stored in the azurophil granules circulating neutrophils and macrophages. These endogenous peptides play a decisive role in the non-oxidative

microbicidal mechanisms of their producing cells through delivery to phagocytic vacuoles containing ingested microorganisms. Peptides of both classes exhibit broad range microbicidal spectra encompassing gram-positive and gram-negative bacteria, mycobacteria, and spirochetes as well as some fungi and enveloped viruses. Evidence suggests that defensins and β-defensins exert their antimicrobial effect by permeating the cytoplasmic membrane target cells via a mechanism involving the formation of voltage-regulated ion channels.

- **Proline and arginine rich-peptides.** Mammalian neutrophils produce a family of Pro- and Arg-rich antibacterial peptides in addition to the defensins. So far, this family includes Bac-5 and Bac-7, which were isolated from bovine neutrophils, and PR-39, a 39-residue peptide that was first isolated from pig intestines and later found in pig bone marrow cells. These three peptides have a peculiar amino acid composition where proline (47, 47, and 49%, respectively) and arginine (21, 29, and 26%, respectively) represent more than 60% of the constitutive residues. The other amino acids, with leucine and isoleucine as the major constituents, are mainly apolar. The sequences of these peptides are highly repetitive, as characterized by several Pro-Arg-Pro and/or Arg-Pro-Pro repeating sequences. Although no obvious sequence homology can be delineated among the three peptides, their amino acid composition and their spectra of activity are very similar. Although the three peptides are mainly active against gram-negative bacteria, Bac-5 and Bac-7 decrease the ATP content and the transport of amino acids and nucleotides, while PR-39 does not lyses bacteria but may top both DNA and protein synthesis in *Escherichia coli*.
- **Amphipathic helical peptides.** The peptide secretions from amphibian dermal glands are the main source of several potent antibiotic peptides originating from the non-myeloid cells of vertebrates. The multinucleated granular glands of frog skin contain, aside from numerous mammalian-like bioactive hormones and neuropeptides, several families of broad-spectrum microbicidal peptides, large amounts of which are stored in secretory granules. These peptides are thought to be involved in the defense of the naked skin of frogs against microbial invasion. The main families of skin peptides that exhibit antimicrobial properties belong to a large group of linear amphipathic helical peptides, residues long, whose overall structure is very similar. Although differing widely in length and amino acid sequence, all

these peptides are cationic, containing a variable number of lysine residues in alternated hydrophobic and hydrophilic segments. Their unique primary structures are thought to endow these membrane-active peptides with the ability to form amphipathic α-helices in an anisotropic environment, such as a membrane interface.

- **Brevinins, esculentins, and ranalexin.** The forth family of antimicrobial peptides has been detected in the skin of *Rana brevipoda* and *Rana esculenta*, frogs of the family Ranidae. Different from all of the frog skin peptides mentioned above, the brevinins and the esculentins are characterized by the presence two cysteine residues in positions 1 and 7 as counted from the carboxyl terminus. These residues are linked in a disulfide bridge. On the basis of size and additional sequence characteristics, four subfamilies can be discerned, the brevinins-I and -2 and the esculentins-I and -2. The I-brevinins are cationic molecules of 24 residues in which six positions are occupied by the same residue in all the peptides. Typical conserved features are a Pro in position 3, an alanine doublet in positions 9-10, and a pair of basic residues at the carboxyi-terminal end. Identities between different members of the brevinins-I subfamily range from 20 to 96%.

Mode of action of antimicrobial peptides

Unlike current antibiotics, which interact strongly with specific target molecules, usually proteins, most antimicrobial peptides act by a nonspecific mechanism and often induce cell death by disrupting the plasma membrane (Henzler Wildman et al., 2003), (Zasloff, 2002). Selective antimicrobial peptides distinguish between eukaryotic cells and bacterial cells based on variations in the composition of the cell membrane (Zasloff, 2002). As outlined above, amphipathicity and positive net charge are characteristics understandably conserved among many antimicrobial peptides, and the prevailing theory is that selectivity results from electrostatic attraction of the cationic peptide to the anionic bacterial membranes (Wieprecht et al., 2000). While some highly selective peptides such as magainins and cecropins fit this model, electrostatics cannot be the only source of selectivity because other highly amphipathic cationic peptides, including melittin and mastoparan, are nonselective toxins (Dathe and Wieprecht, 1999). Thus, other aspects of membrane composition and additional peptide properties must also be important in determining selectivity.

It has been demonstrated that although electrostatic attraction increases the concentration of peptide at the membrane surface, disruption of the membrane depends on hydrophobic interactions of the peptide and membrane regardless of whether the membrane is neutral or anionic (Dathe and Wieprecht, 1999), (Dathe et al., 2001). Slight differences in charge, hydrophobicity, and relative size of hydrophobic and hydrophilic domains lead to very different behaviour in membranes in a manner that is not well understood. Apparently similar peptides exhibit a wide range of orientations, regularity and size of holes in the bilayer, and peptide effect on lipid flip-flop, headgroup tilt, curvature strain, and acyl chain disordering. Notwithstanding this large structural variety, they share a limited number of mechanisms of actions: three primary mechanisms have been proposed to explain this variation in behaviour. To interact and insert into the target membrane, antimicrobial peptides must undergo substantial conformational changes. In water, their overall structure needs to be hydrophilic. However, upon interaction with membranes they must expose a hydrophobic region to the lipidic constituent of the membrane. This can be achieved in two general ways:

1. A monomeric peptide that adopts a random structure in solution gains an amphipathic structure upon reaching the membrane
2. The peptide forms oligomers in solution such that the hydrophobic regions are buried in the lumen of the oligomer and the hydrophilic regions are exposed to the solution.

Upon reaching the membrane the organization is reversed, *i.e.*, the hydrophobic regions are exposed to the lipidic constituents of the membrane and the hydrophilic regions are segregated in the lumen of the oligomer. Some peptides, such as alamethicin, form well-defined barrel-stave pores with the peptide inserted into the bilayer and its hydrophilic face lining the water-filled pore. Other peptides have only been observed to lie on the surface of the membrane, or insert very transiently, and are considered to operate by toroidal pore or carpet mechanisms. The toroidal pore mechanism was developed based on the behaviour of magainins and involves the induction of curvature strain in the bilayer by the peptide, leading to the formation of transient, toroidal lipid-peptide pores when there is a high local concentration of peptide. An alternative mechanism for surface-oriented peptides is the carpet model, which is characterized by general disruption of the bilayer in a detergent-like manner, eventually leading to the formation of micelles at high peptide concentrations (Henzler Wildman et al., 2003). These modes of action are summarized in Figure 55.

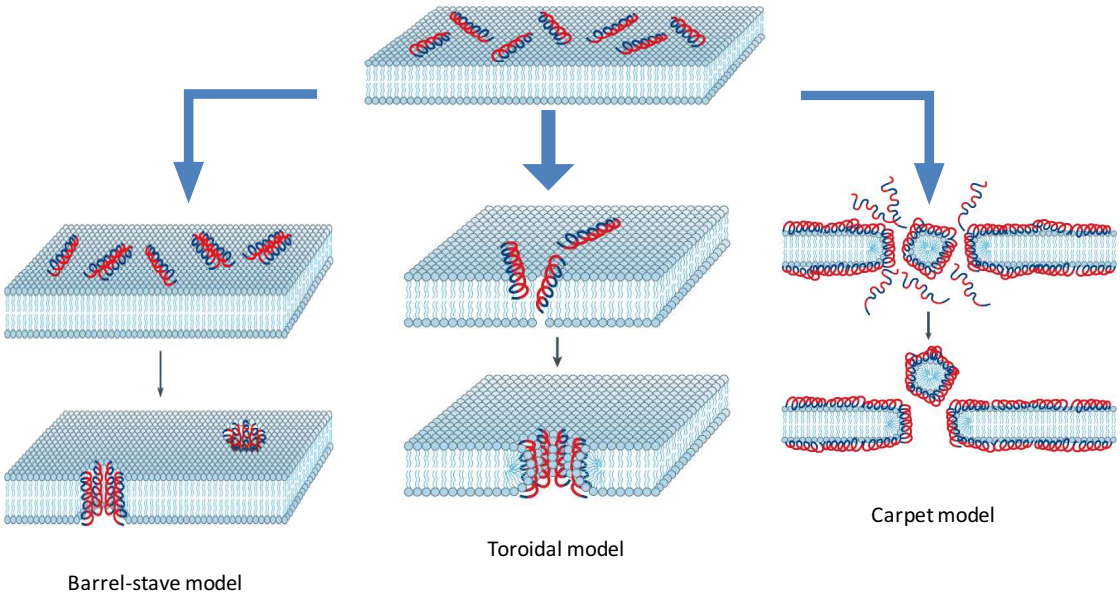

Figure 55. Proposed mechanisms involved in antimicrobial peptide-killing: In the barrel-stave model, the attached peptides aggregate and insert into the membrane bilayer so that the hydrophobic peptide regions align with the lipid core region and the hydrophilic peptide regions form the interior region of the pore. In the case of the toroidal model, the attached peptides aggregate and induce the lipid monolayers to bend continuously through the pore so that the water core is lined by both the inserted peptides and the lipid head groups. In the carpet model, the peptides disrupt the membrane by orienting parallel to the surface of the lipid bilayer and forming an extensive layer or carpet. In all three cases hydrophilic regions of the peptide are shown coloured red, while hydrophobic regions of the peptide are shown coloured blue.

Cathelicidins

The two main families of small, cationic antimicrobial peptides that have been identified in humans are the defensins and the cathelicidins.

Various human defensins have been identified, but it appears that human cationic antimicrobial protein (hCAP-18) is the only member of the cathelicidin family that is expressed in humans (Tjabringa et al., 2005).

The cathelicidin family has been individuated for the first time in 1993 (Zanetti, 2004) and rapidly members of this family have been found in countless mammalian. The type and number of peptides belonging to cathelicides depend on the species: in fact, for example, in the horse three different peptides of this family have been identified.

Peptide antibiotics of the cathelicidin family are characterized by a highly conserved signal sequence and pro-regions but show substantial heterogeneity in the C-terminal domain that encodes the mature peptide (Bals and Wilson, 2003).

The pro-sequence is termed '*cathe*lin' because this domain has been found to inhibit the activity of *cathe*psin L (cathepsin L inhibitor) and is between 99 and 114 amino acids long. The 'cathelin' protein was initially identified from pig leukocytes. Molecules with a cathelin-like pro-peptide sequence have been isolated from multiple species including cow, pig, rabbit, sheep, human, mouse, monkey and horse. The function of the cathelin pro-sequence is speculative; however, one model is that it assists in the biogenesis of the mature peptide.

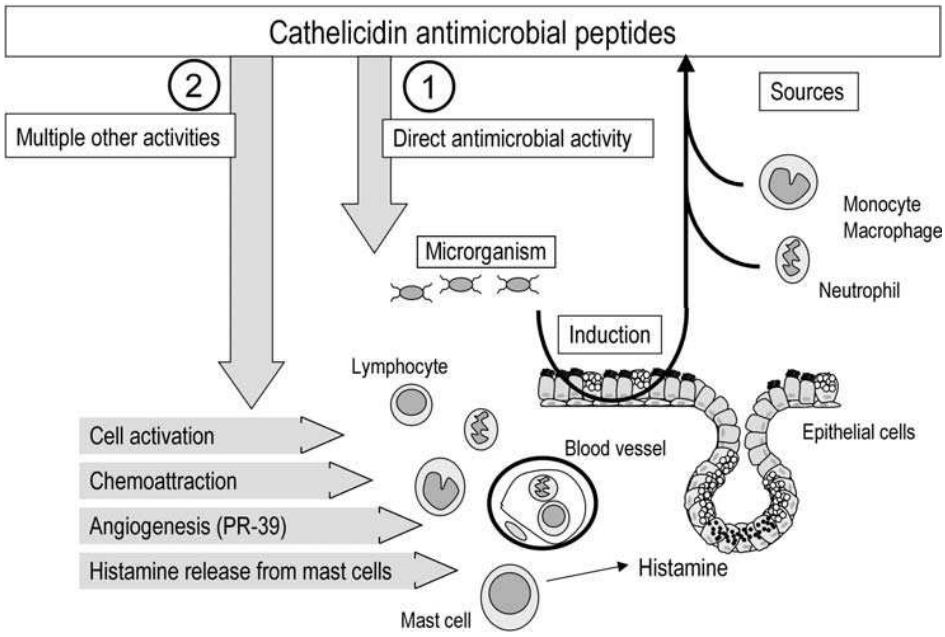

Figure 56. Biological functions of cathelicidin antimicrobial peptides. Cathelicidins are secreted by several cell types during infection and inflammation. For example, LL-37/hCAP-18 is found in airway surface fluid and originates from epithelial cells as well as professional inflammatory cells, such as macrophages, neutrophils and lymphocytes. The cathelicidin peptides have direct antimicrobial activity. Additionally, they regulate cellular responses including cell proliferation, cell migration of inflammatory cells, release of cytokines and angiogenesis. Cathelicidins are multifunctional peptides that link host defense with inflammation and angiogenesis and activate the adaptive immune system (Bals and Wilson, 2003).

The carboxy-terminal domain represents the antimicrobially active peptide that varies considerably between individual molecules in sequence, length (12–100 residues), and

function. Based on amino acid sequences, mature cathelicidin peptides can be organized into three groups:

- group I) linear, α-helical peptides without cysteines, such as LL-37/hCAP-18 from human;
- group II) peptides with an even number of cysteines linked by disulphide bridges, for example protegrins (porcine cathelicidin peptides)
- group III) peptides with an unusually high proportion of one or two amino acids, for instance PR-39 from porcine leukocytes.

The secondary and tertiary structures of the mature antimicrobial peptide have been examined for several molecules. Studies using circular dichroism and nuclear magnetic resonance (NMR) spectroscopy revealed the transition of CRAMP, PAMP-36, PAMP-37, BMAP-27, BMAP-28 and LL-37 from a random coil to an ordered, mainly α-helical form. A poly(L)-proline type II structure has been proposed for PR-39, and the bactenecins Bac-5 and Bac-7. Several structural features have been identified as relevant for the microbicidal function of antimicrobial peptides: size, sequence, charge, degree of structuring (helicity), overall hydrophobicity, amphipathicity and the angles subtended by hydrophobic and hydrophilic surfaces of the helical molecule. High mean hydrophobicity has been correlated with increased cytotoxic activity against eukaryotic membranes. There is no simple correlation between activity and charge. When the net charge becomes more positive, binding to negatively charged surfaces of microorganisms is increased; however, the formation of trans-membrane pores is inhibited. Since all these structural features are strongly interrelated, predicting the antimicrobial or cytotoxic activity from a given amino acid sequence is difficult.

Cathelin is a putative cysteine-proteinase inhibitor, first isolated from pig leucocytes, which has now also been found to constitute a proregion for many different peptide antibiotics.

The cathelicidin-protein family, now counting more than 20 members, constitutes a significant part of mammalian peptide antibiotics in a variety of species including cow, pig, sheep, rabbit, mouse and, recently, humans. Most of the cathelicidin precursors are stored in cytoplasmic granules of neutrophil leucocytes and release the antimicrobial peptides upon leucocyte activation. Members of the cathelicidin family have various structures and different killing mechanisms.

For example, PMAP-36, PMAP-37, CRAMP, BMAP-27 and BMAP-28 adopt a predominantly α-helical structure, and rapidly permeabilize the bacterial membrane. Others, which do not adopt an α-helical structure, like Bac5 and Bac7, inhibit incorporation of precursor molecules into protein and RNA, while PR-39 stops protein and DNA synthesis in Gram-negative bacteria (Oren et al., 1999).

LL-37

The antimicrobial peptide LL-37 (named also hCAP) belongs to the cathelicidin family and is the first amphipathic α-helical peptide isolated from human (Zanetti et al., 1995). LL-37 is considered to play an important role in the first line of defense against local infection and systemic invasion of pathogens at sites of inflammation and wounds. LL-37 was isolated for the first time from human granulocytes and sequence analysis indicated that it corresponded to residues 3÷39 of FALL-39, and thus has the following sequence:

LLGDFFRKSKEKIGKEFKRIVQRIKDFLRNLVPRTES

Table 6. Presence of hCAP-18/LL-37 in various cell types and body fluids

Cell type/tissue/secretion	
Leukocytes	Neutrophils
	Monocytes
	B-cells
	gd T-cells
	NK cells
	Mast cells
Epithelial cells	Lung
	Inflamed skin
	Colon
	Epididymis
	Various squamous epithelia
Body fluids	Bronchoalveolar lavage fluid
	Nasal lavage fluid
	Seminal plasma
	Saliva
	Plasma

Further studies showed that LL-37 can be detected in human wounds and blister fluids, and more recently the gene coding for LL-37 was found to be induced in human keratinocytes during inflammatory disorders. These findings suggest an important role for LL-37 in the first line of defense against local infection and systemic invasion of pathogens at sites of inflammation and wound.

Regarding the antimicrobial activity of LL-37, it was first identified as a broad-spectrum antimicrobial peptide with LPS-neutralizing activity. LL-37 kills both Gram-positive and Gram-negative bacteria and fungi, and studies using negatively charged model membranes (mimicking bacterial outer membranes) suggest disintegration of the bacterial membrane and subsequent death by LL-37 via formation of a carpet-like layer over the membrane (Tjabringa et al., 2005).

Increasing evidence suggests that a primary role of various cationic host defence peptides *in vivo* may be to modulate or prime the immune response. Although there is no doubt that under some circumstances, such peptides have antimicrobial activity in vivo; *e.g.*, at the mg/mL concentrations at which α-defensins are found in the lysosomes of neutrophils, this may not be the case for other cationic peptides in other body locations. The human cationic cathelicidin peptide LL-37, for example, has no direct antimicrobial activity *in vitro* under physiologically relevant salt and peptide concentrations but, under the same conditions, has immunomodulatory effects in model systems of mucosal surfaces. LL-37 is produced at mucosal surfaces by epithelial cells, up-regulated in response to infection and inflammation, and can be released by degranulation of neutrophils. Thus, in the process of combating infection, incoming effector cells of the innate-immune response, such as monocytes and pre-dendritic cells (DC), would be expected to be exposed to gradients of LL-37, which has been demonstrated to have a wide range of immunomodulatory properties on various cell types, including epithelial cells, peripheral blood monocytes, and monocyte-derived DC (Mo-DC), at peptide concentrations and cation levels that are found at sites of infection or inflammation. In addition, certain cytokines that are present at mucosal surfaces appear to synergise with LL-37 to alter or enhance its immomodulatory activity. It has been demonstrated that LL-37 promote angiogenesis, an essential process for host defense, for wound healing and reparation of tissue damages (Bowdish et al., 2005).

A promising characteristic of LL-37 for its clinical use is its potential as anti-septic shock drug. Indeed, this peptide is able to neutralize lipopolysaccharides (LPS) of gram-negatives both *in vitro* (by inverting LPS-induced TNF-α production in macrophages) and *in vivo*,

protecting tested animals against sepsis, (Nagaoka et al., 2002). In fact antimicrobial peptides interact with cells inhibiting the interaction between LPS and their receptor (CD14).

Moreover, LL-37 is chemotactic for human peripheral blood neutrophils, monocytes, and T lymphocytes. The chemotactic activities of human β-defensins and cathelicidin/LL-37 are mediated by human CC chemokine receptor 6 and formyl peptide receptor-like 1, respectively (Yang et al., 2001). Finally, LL-37, like other defense peptides, is able to stimulate chemotaxis indirectly, by promoting chemokines productions in different cell types. In particular, LL-37 modulates the expression of genes deputed to the synthesis of chemokines and receptors for chemokines in macrophages. LL-37 induces the production *in vitro* of interleuchine-8 (IL-8) and MCP-1 (Monocyte chemotactic protein-1) in epithelial and monocyte cells (Bowdish et al., 2005). Moreover, it directly activates endothelial cells by means of formyl peptide receptor-like 1 (FPRL-1), a G protein-coupled, seven-transmembrane cell receptor found on macrophages, neutrophils, and subsets of lymphocytes, increasing in this way *in vitro* proliferation and formation of new vessels in endothelial cells. The formation of new blood vessels is a prerequisite of tissue repair and wound healing.

Although highly charged (16 charged residues, net +6 at neutral pH), it is not as selective as some α-helical, amphipathic, antimicrobial peptides, with MICs ranging from 1 to 10 μM for a variety of gram positive and gram negative bacteria.

Some bacterial strains that colonize the lungs have developed resistance to LL-37 by adding choline headgroups to lipopolysaccharide (LPS) or other nonphospholipids in their outer membrane. This suggests that although choline headgroups do not prevent membrane disruption by LL-37, since it lyses eukaryotic cells with choline-rich membranes, the headgroups may modulate LL-37- membrane interactions either directly or through their effect on other properties of the lipid bilayer to which LL-37 is sensitive. LL-37 aggregation is also sensitive to bilayer composition, with a higher aggregation state in zwitterionic phosphatidylcholine bilayers than in negatively charged phosphatidylcholine / phosphatidylserine bilayers.

Data demonstrate that LL-37 forms a stable α-helix that lies at the polar/nonpolar interface on the surface of the bilayer. This surface orientation, which does not change with temperature, lipid headgroup charge, LL-37 concentration, or presence of aqueous ions, excludes a barrel-stave mechanism of membrane disruption. LL-37 must function by initially carpeting the surface of the membrane and inducing leakage either through the formation of toroidal pores, as supported by the induction of positive curvature strain, or less well-defined

membrane defects. Previous studies in the literature have shown that LL-37 forms a more stable helix than the usual amphipathic, α-helical, antimicrobial peptide, and does not require a membrane surface in order to fold. The third model is formation of toroidal peptide-lipid pores due to curvature strain induced by the presence of peptide. This model is consistent with the ^{31}P NMR and DSC (differential scanning calorimetry) results, which show that LL-37 induces positive curvature strain. It is also possible that locally high concentrations of LL-37 disrupt the packing of lipids in the bilayer to such an extent that transient defects form in the membrane hydrophobic barrier, allowing leakage of ions and molecules down the concentration gradient (Henzler Wildman et al., 2003).

Cytotoxicity

Whereas most known antimicrobial peptides (e.g. cecropin, magainin, dermaseptin) are cytotoxic to several microorganisms, but not to normal eukaryotic cells, high levels of LL-37 exhibits cytotoxic activity also to eukaryotic cells, causing hemolysis. Probably this effect is due to the hydrophobic interaction between the peptide and the cell membrane of eukaryotic cells (Oren et al., 1999). Other data show an apoptotic effect on smooth muscle cells (Ciornei et al., 2005). The cytotoxic effect of LL-37 is modulated by its ability to bind to plasmatic proteins, like apolipoprotein A-I (apo A-I), albumin and fibronectin, thus preserving host cells in vivo. However, also its antimicrobial activity is hampered by the same interaction.

The wide spectrum of antibacterial activity and the LPS-neutralizing effect of LL-37 would make it a molecule of choice for treatment of bacterial infections and, particularly so, in the presence of antibiotic-resistant strains (Hiemstra, 2007), (Nizet, 2006). Unfortunately, the significant toxicity of LL-37 to mammalian cells has so far hampered its use in clinical contexts. In fact, LL-37, at variance with many other antimicrobial peptides, displays a significant haemolytic activity and is toxic for human leukocytic cells and for T lymphocytes (Ciornei et al., 2005).

Conformation in water

In common with many other AMPs, LL-37 can assume an amphipathic α-helical conformation, with a moderate hydrophilicity (0.56) according to the Hopp & Woods scale (Hopp and Woods, 1981), and the presence of both positively and negatively charged residues placed in such a way as to favour salt bridge formation, which confers to the peptide a

tendency to assume a helical structure already at low salt concentration (Johansson et al., 1998). In fact LL-37, like many other α-helical peptides is disordered, but in the presence of trifluoroethanol, sodium dodecyl sulphate (SDS) micelles, phospholipid vesicles and liposomes, or Lipid A, all or part of the molecule is converted to an α-helix (Chan et al., 2005). In water LL37 exhibits a circular dichroism (CD) spectrum that is consistent with a disordered structure (Foschiatti et al., 2009).

However, in 15 mM HCO_3^-, SO_4^{2-} or $CF_3CO_2^-$, the peptide adopts a helical structure. As has been observed for buforin II, its congeners and LL-37, the extent of α-helicity correlates with the antibacterial activity against both Gram-positive and Gram-negative bacteria, increased α-helical content correlates with stronger antimicrobial activities (Yeaman and Yount, 2003). In such an ordered conformation, hydrophobic and hydrophilic residues are localized on opposite sides of the helix surface. The net positive charge (+6 at physiological pH) allows the interaction of the peptide with the negatively charged surfaces of bacteria and fungi.

The helical conformation of LL-37 is stable over a wide range of buffer conditions, including high salt, and is also the same in the presence of lipids. Sequence analysis reveals that LL-37 can form an amphipathic α-helix from residues 11-32, which matches the percent helicity determined from CD data. The formation of helical structure also correlates with LL-37 aggregation and activity, which occurs at micromolar peptide concentrations in the presence of anions.

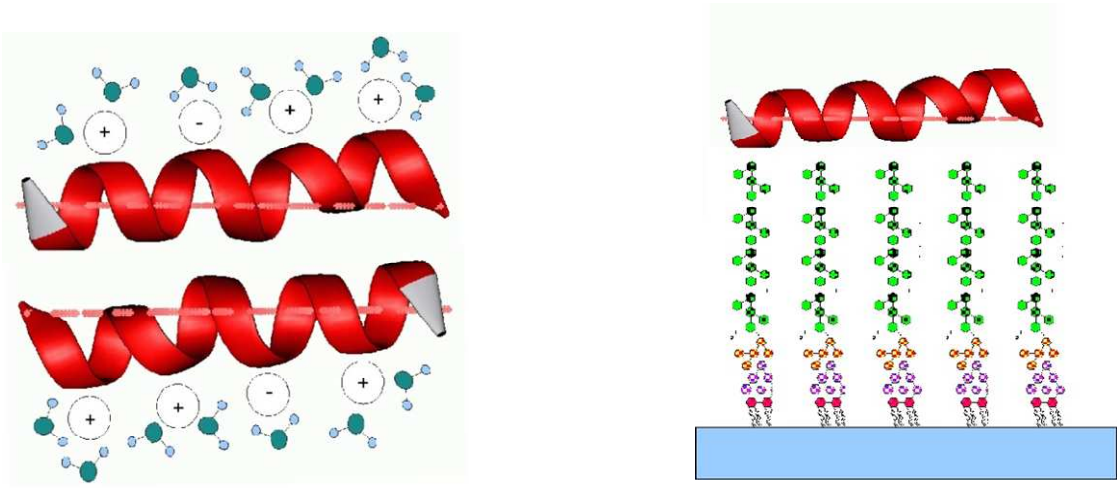

Figure 57. Oligomers formation and interaction between peptide and lipopolysaccharides of the bacterial wall.

This helical, aggregated form of LL-37 in solution is very different from other amphipathic, α-helical, antimicrobial peptides that are monomeric and unstructured in aqueous solution and only become R-helical upon association with a membrane. Calorimetric studies of magainin derivatives have shown that this conformational change from random coil to α-helix provides a large portion of the thermodynamic driving force for membrane binding and insertion. In contrast, LL-37-membrane interactions must have a different energetic basis since it is helical in both physiological buffer conditions and upon association with the membrane and does not undergo a conformational change (Henzler Wildman et al., 2003).

Interactions with polyelectrolytes

A common mechanism shared by bacteria to try to limit the effect of cationic AMPs consists in the release of polyanions, namely exopolysaccharides, of which the principal one is alginate, which act as an "auxiliary bacterial membrane" (Chan et al., 2005), limiting the accessibility of the peptides to the bacterial surface and thus decreasing their antibiotic efficacy (Llobet et al., 2008).

Studies on the transport of solutes in *P. aeruginosa* biofilms have suggested that alginate may act as a molecular sieve to reduce the diffusion of antibiotics, such as aminoglycosides, macrolides, quinolones and fluoroquinolones (Hoyle et al., 1992), (Kumon et al., 1994), (Shigeta et al., 1997), (Suci et al., 1994), although whether reduced rates of diffusion can sufficiently account for increased antibiotic resistance remains controversial. In the case of positively charged antibiotics, and AMPs, electrostatic interactions with alginate are thought to limit their transport in biofilms (Nicols et al., 1988) and treatment of the alginate with an alginate-degrading enzyme results in significantly higher antibiotic penetration rates (Hatch and Schiller, 1998). Alginate is also synthesized by other Gram-negative bacteria including *Azotobacter vinelandii* and *Pseudomonas fluorescens* (Clementi, 1997), (Govan et al., 1981) and by brown algae including *Laminaria hyperborea*, *Ascophyllum nodosum* and *Macrocystis pyrifera* (Draget et al., 2005).

The mechanism behind the interaction between AMPs like LL-37 and alginate is not so straightforward as a simple electrostatic interaction between oppositely charged molecules, and has been studied in depth (Kuo et al., 2007).

Hydrophobic sequences such as α-CAPs fold from a disordered conformation in an aqueous environment, into α-helices in a membrane, driven largely by the replacement of water-solvated peptide bonds by intramolecular H-bonding in the non-polar environment

(Kuo et al., 2007). Similar structural transition have been associated with alginate (Chan et al., 2004), suggesting that alginate is capable of mediating hydrophobic interactions with α-CAPs despite the lack of an obvious membrane-like hydrophobic core in such a water-soluble polysaccharide.

In fact, polysaccharides, can exhibit a hydrophobic character by adopting certain confromations (Neal and Goring, 1970), (Morris, 1977): a hydrophobic index based on surface area of pyranosyl C-H groups for monosaccharides has been proposed, which listed mannose (the neutral equivalent of mannuronate in alginate) as the most hydrophobic of hexoses (Masanobu and Yuki, 1985).

It has been postulated that the interaction of α-CAPs with alginate would occur in a similar manner, where D-mannuronate would interact with non-polar side chains through its hydrophobic surface which in this mannose analogue is comprised of four aligned C-H groups. However, while the L-guluronate rings lack a comparable hydrophobic face in the sense that the C-H bonds (C1, C3 and C4) are equatorial rather than axial, we observed here that Trp blue shifts were of similar magnitude in AlgM-M and AlgG-G blocks, indicating that the AlgG-G sequence must also contain significant non polar surfaces.

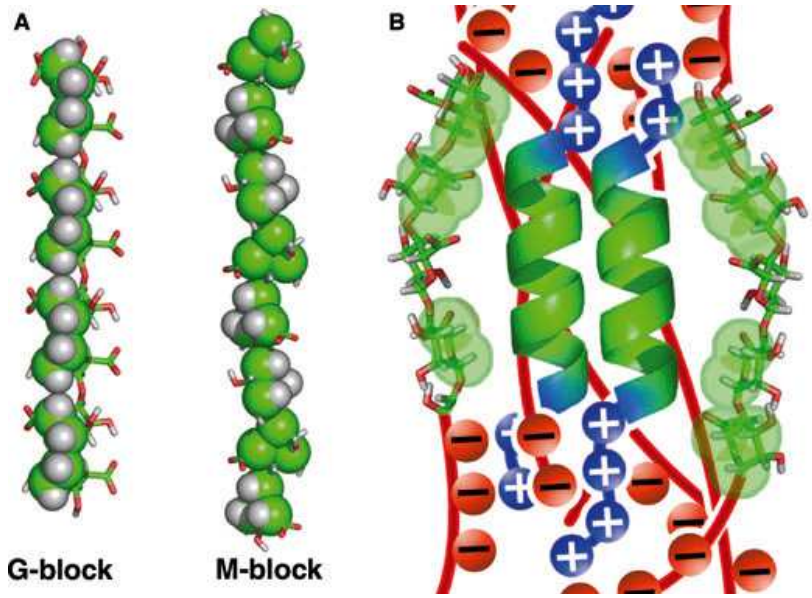

Figure 58. Hydrophobic components of M-block and G-block of alginate. (A) Model of β-(1 → 4)-D-mannuronate (M-block) and α-(1 → 4)-L-guluronate (G-block) tetrasaccharides. Hydrophobic surface as represented by clusters of pyranosyl C-H groups is shown as a space-filling overlay. (B) Schematic representation of the a-CAP–alginate complex formed by the interaction of C-H clusters with the hydrophobic peptide surface.

This finding is likely attributable to the conformation of G-blocks, which are distinct from M-blocks in their linkage modes.

Thus, M-blocks are di-equatorially linked flat and extended structures, whereby the axial C-H groups are exposed. In contrast, G-blocks are comparatively compact structures that are diaxially linked, such that the L-guluronate rings are “stacked” and hydrophobic surfaces are likely formed by the equatorial C-H groups instead (Figure 58 A).

A study using the neutral fluorophore pyrene with alginate suggested the presence of hydrophobic regions within alginate, but only at concentrations approaching the solubility limit of alginate (Neumann et al., 2003). Thus, while both M-blocks and G-blocks of alginate contain “hydrophobic regions”, their intrinsic hydrophobicity at typical concentrations is relatively weak as they would be comprised of primarily C-H groups of the pyranosyl rings and the occasional O-acetyl groups. Consistent with this scenario, alginate itself did not appear to bind strongly to the hydrophobic probe ANS, which suggests that the presence of negatively charged carboxylate groups likely masks hydrophobic contributions from C-H groups. Thus, the hydrophobic surfaces inherent in alginate become accessible under the conditions where polysaccharide carboxylate groups are locally neutralized and continuous clusters of C-H groups become exposed along the glycan chain, forming hydrophobic microdomains in the process of binding the positively charged α-CAPs (Figure 58 B).

The global mechanism of interaction between alginate and helical peptides can also be summarized in this way: the neutralization of the positive charge by the anionic polysaccharide causes a more dominant role of the peptide hydrophobicity (Chan et al., 2005), (Chan et al., 2004). Moreover, it has been demonstrated that the interaction of LL-37 with alginate induces conformational changes in the peptide structure by promoting α-helix formation and self-association (Yeaman and Yount, 2003), (Chan et al., 2004).

As a consequence, peptide structuring exposes the hydrophobic sector in the helix surface that may cause self-association of peptide molecules via hydrophobic interactions. Therefore the interaction can be considered a consequence of both a hydrophilic and a hydrophobic effect. At variance with moderately hydrophilic peptides, such as LL-37, for highly hydrophobic peptides such as the model peptide KKAAAAAAAAAAAAWAAAAAAKKKK-NH_2, helix induction is essentially caused by hydrophobic interactions with hydrophobic microdomains of alginate (Chan et al., 2004). Binding to glycosaminoglycans like heparin and dermatan sulphate also has an effect similar to that of alginate (Andersson et al., 2004). The interaction with bacterial exopolysaccharides

causes, as a general consequence, a decrease of the antimicrobial efficacy of the AMPs, and it is supposed to be the cause of failure of their antimicrobial activity in contexts such as biofilms, of which exopolysaccharides are major components.

The study of the mechanism of interaction of AMPs with bacterial capsules (Llobet et al., 2008), (Domenico et al., 1994), (Campos et al., 2004) and exopolysaccharides (Herasimenka et al., 2005), (Benincasa et al., 2009), (Foschiatti et al., 2009), is a key point for the modulation of their activity.

LL-37 containing biomaterials

A promising application of AMPs is not only that of new oral antibiotics, but, given their structural complexity and delicate stability, their use for the preparation of biomaterials enriched with antimicrobial properties, to contrast infections associated with implant surgery (Statz et al., 2008), (Shukla et al., 2010). Some attempts have been made to exploit specifically LL-37 in the preparation of antimicrobial surfaces, either by covalently linking it to the material (Gabriel et al., 2006) or by entrapping it during the scaffold preparation, thus allowing its release after implantation (Izquierdo-Barba et al., 2009), (Steinstraesser et al., 2006).

Another use of immobilized LL-37 is as enhancer of angiogenesis. It has been demonstred, in fact, that it accelerates the onset of neovascularisation in biopolymers *in vivo*. This finding suggests that LL37 might be a useful adjunct to promote angiogenesis and prevent infection for tissue engineering.

Results reported in these works are preliminary but encouraging.

4.4.2 Design of an antimicrobial composite

Interaction between Microcomposite and Specific bioactive agents:

electrostatic, between

3. **Polyanion: alginate**

   and

4. **Polycation**

   Polycation is :directly the LL-37-peptide as such

   or
   ChitLac carrying covalently bound
   BMP-fragment
   and/or
   RGD-containing peptides

Starting from the above considerations, we investigated the possibility to take advantage of the complex interaction between LL-37 and differently charged polysaccharides, with the aim of modulating the peptide availability, thus reducing its cytotoxicity by masking possible interactions with eukaryotic membranes, while maintaining its antimicrobial properties. In particular, we focussed our attention onto three polysaccharides (PS), namely alginate, hyaluronic acid and ChitLac, a derivative of chitosan prepared by reductive *N*-alkylation with lactose (Yalpani and Hall, 1984), (Donati et al., 2005) . All of these have excellent biocompatibility properties, and would be suitable for further biomedical applications.

Alginate and hyaluronic acid are polyanions, while ChitLac is a low charge density polycation. At neutral pH, the average distance between the projection of charges on the polymer axis *b*, is 4.66 Å for alginate, 9.5 Å for hyaluronic acid and 5.85 Å for chitosan, which correspond to a (dimensionless) linear charge density (ξ) of 1.53, 0.75 and 1.22, respectively. The introduction of the lactitol group on chitosan to give ChitLac causes a decrease of the charge density, which becomes approximately 0.32 at neutral pH. As LL-37 is a cation with a net charge of +6 at neutral pH, an attraction is expected to establish with alginate and hyaluronic acid, and a repulsion with ChitLac. The variation of cytotoxicity of LL-37 was tested when alginate, hyaluronic acid or ChitLac were added to the peptide solution. The most promising system would have been evaluated in terms of its antimicrobial effect on two different bacterial species. The encouraging results obtained with alginate are

the starting point for the design of new polysaccharide-based biomaterials with antimicrobial properties.

Circular Dichroism studies

As briefly reported in the introduction of this chapter, interactions occurring between LL-37 and charged polysaccharides are a complex phenomenon which cannot be reasonably explained by means of a single and simple mechanism. However, undoubtedly electrostatic forces are one of the main driving forces of this interaction. Therefore, the first variable to exploit to assess the role of electrostatics is ionic strength. It is well known that ionic interactions modulate biomolecule conformations. This is known to be the case also for LL-37.

For this reason, Circular Dichroism spectra of polysaccharide/peptide mixtures were recorded in phosphate buffer, pH 7.4, at two different values of ionic strength, a parameter which is known to strongly modulate charge attraction, to assess such conformational changes on the peptide and/or, possibly, on the polysaccharide.

The first set of analyses was carried out in 5 mM phosphate buffer, pH 7.4, ionic strength 20 mM, to reproduce the experimental conditions reported in the literature for previous analyses of PS/AMP mixtures (Herasimenka et al., 2005), while PBS, pH 7.4, ionic strength 150 mM, was used to mimic the physiological conditions. As reported in the introduction, it has been shown that the α-helical conformation of LL-37 is anion-, pH- and concentration-dependent (Chan et al., 2005). It is generally assumed that the structuring in an α-helical conformation is a phenomenon principally led by the hydrophobic effect, and the promotion of helix formation by some anions (HCO_3^-, SO_4^{2-}, CF_3COO^-, and to a significantly lesser extent Cl^-) follows the Hofmeister series (Johansson et al., 1998), (Baldwin, 1996).

In our studies, we found that the main effect is due to phosphate ions, which are particularly effective in promoting the α-helical conformation and indeed they are responsible for the *in vivo* LL-37 helical transition. The UV-CD spectra obtained for the three PS/peptide mixtures recorded in the two considered buffers are reported in Figure 59.

The concentration of LL-37 was kept constant at 10 µM during all the experiments, while the PS concentration was stepwise increased as reported in the **Materials and Methods** section (paragraph 3.2.22). For clarity, results are reported as spectra from which the CD of each PS alone at the same concentration and in the same buffer was subtracted from that of the mixture, so that the contribution of the peptide is highlighted.

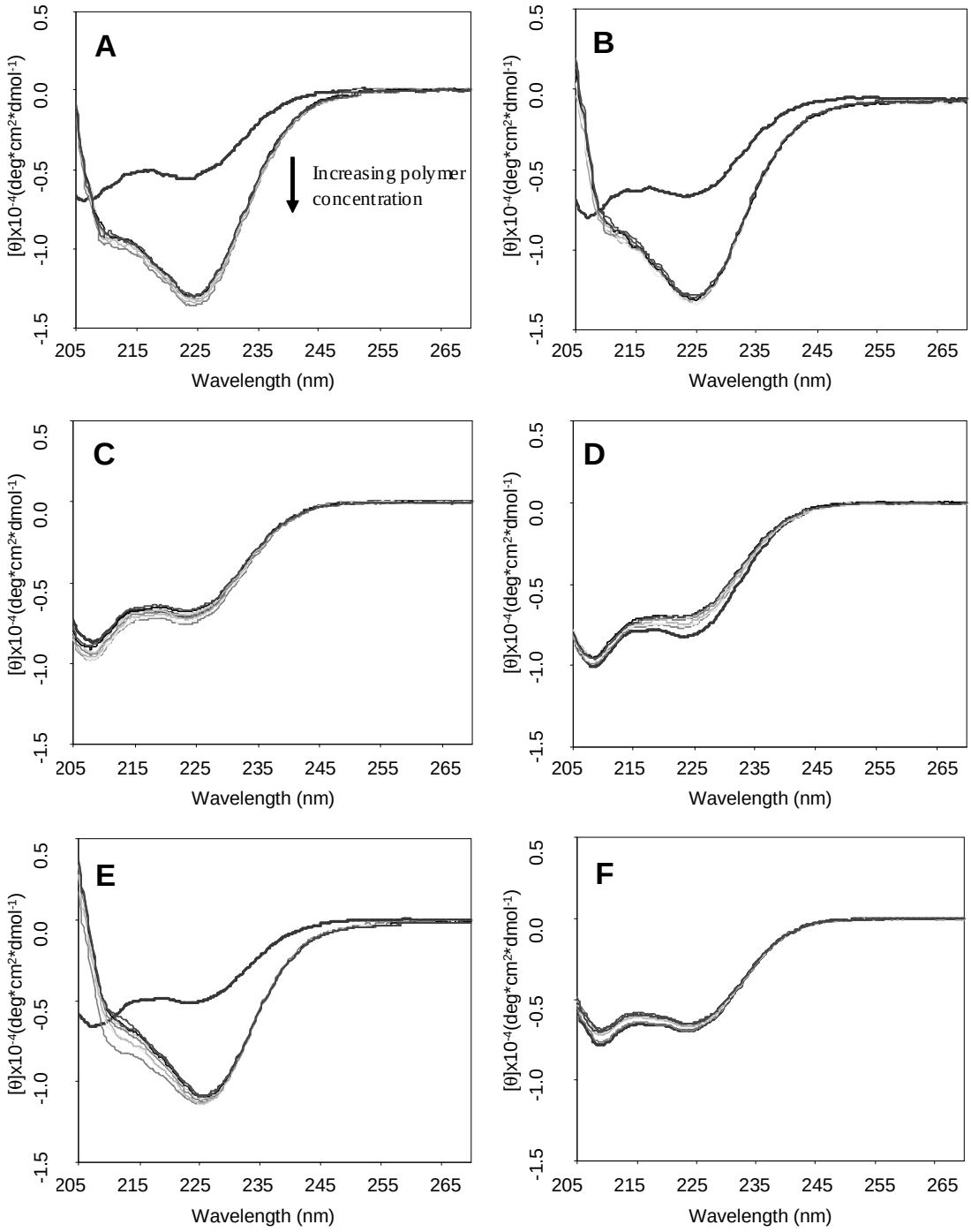

Figure 59. Spectra of LL-37/alginate, LL-37/ChitLac and LL-37/hyaluronan mixture in PI-20 buffer (A, C, E) and in PI-150 buffer (B, D, F). The spectrum of each PS alone, measured under the same conditions, was subtracted to that of the respective mixture.

Figure 59-A and Figure 59-B show that even the lowest concentration of alginate tested (50.4 μM) induces LL-37 to assume a α-helical conformation, as indicated by the appearance of a negative minimum at 222 nm (Chen et al., 1974). These results are qualitatively and quantitatively in agreement with those previously reported for alginate/AMP (Chan et al.,

2004), (Andersson et al., 2004), (Kuo et al., 2007) and, in particular, for alginate/LL-37 mixtures (Herasimenka et al., 2005), (Benincasa et al., 2009), (Foschiatti et al., 2009). As for the role of ionic strength, there is no apparent difference between the spectra recorded at low and high salt concentrations.

Figure 59-C and Figure 59-D show the spectra obtained with ChitLac/LL-37 mixtures. It is evident that the presence of the polysaccharide does not have any influence on the peptide conformation. However, a possible interaction between the two species devoid of conformational effects cannot be completely ruled out, although unlikely due to the repulsion between the two positively charged macromolecules. Also in this case there is no significant difference between the spectra recorded at the two values of ionic strength.

In contrast, the behaviour of the peptide in the presence of hyaluronic acid is peculiar. In the high ionic strength buffer, hyaluronic acid at all the concentrations tested does not have any influence on the conformation of LL-37 (Figure 59-F), while, at low ionic strength, a transition to a more helical (and probably aggregated) form takes place (Figure 59-E), although less evident than that observed for alginate (Figure 59-A).

The α-helix percentage was determined as the ratio $[\theta]/[\theta]_{\alpha}$, where $[\theta]$ is the observed molar ellipticity at 222 nm and $[\theta]_{\alpha}$ the molar ellipticity of a fully structured peptide calculated using the equation $[\theta]_{\alpha} = -40{,}000(1-2.5/n)$, where n is the number of amino acid residues in the peptide (Juban et al., 1997). Figure 60 summarizes all the CD analyses by reporting the percentage of α-helix on LL-37, in the presence of each of the three polysaccharides, as a function of the [PS]/[LL-37] ratio, in the two considered buffers.

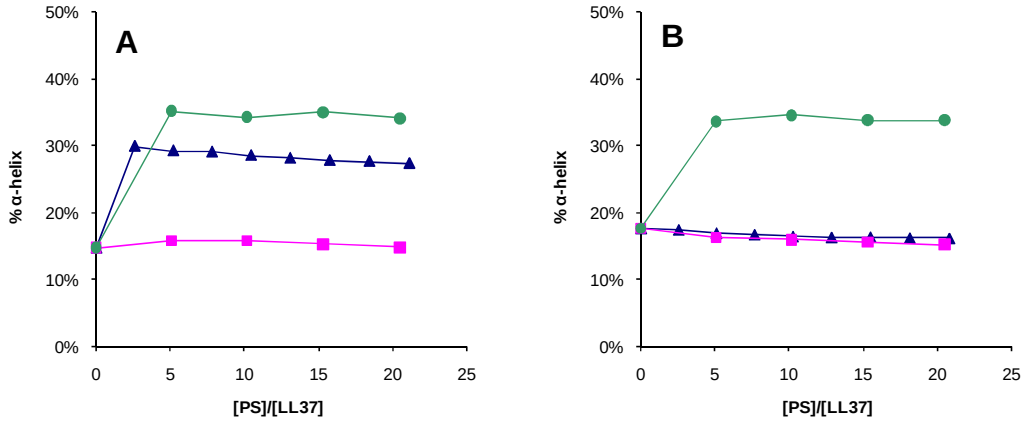

Figure 60. Percentage of α-helical content in LL-37 in the presence of alginate (circles), hyaluronic acid (triangles) and ChitLac (squares). Panel A: PI-20, Panel B: PI-150. Each value was corrected for the dilution factor.

As mentioned above, the buffer itself plays a role in inducing the conformational transition of the peptide chain independent of the PS used, as shown by the LL-37 spectra in the absence of PS. By increasing the ionic strength from 20 mM to 150 mM, the α-helix percentage in LL-37 alone rises from about 14% to 19%, which corresponds to a mean of approximately 5 and 7 residues per chain taking part into the helix, respectively.

The transition to an α-helical conformation is driven essentially by electrostatic interactions, since at high ionic strength charges of the same sign are allowed to get closer, giving rise to the helix, while at a lower salt concentration the electrostatic repulsions are predominant and destabilize the helix.

The highest percentage of α-helix is found for the LL-37/alginate mixture both in low (PI-20, Figure 60 A) and high (PI-150, Figure 60 B) ionic strength buffers. Under these conditions, a helical content of about 35% can be calculated, corresponding to a mean number of 13 residues per molecule of peptide taking part into the helix. This result is in agreement with similar studies reported in the literature (Kuo et al., 2007), and it suggests that the electrostatic interaction between LL-37 and alginate is very strong: possibly, 35% is the upper limit of helix percentage attainable in this environment (for comparison, this limit is higher than 60% in trifluoroethanol).

In the case of ChitLac, this weakly charged polycation does not have any effect on the peptide conformation. This is likely due to the fact that the two molecules are both positively charged and thus repel each other. As a consequence, the presence of the PS does not bring in any additional effect on the helical conformation in addition to that induced by the ionic strength of the medium.

Hyaluronic acid has a negative charge density which is approximately half as that of alginate. As expected, in this case the number of electrostatic interactions is lower and thus the peptide/PS interaction is more susceptible to the surrounding environment. At low ionic strength (buffer PI-20, Figure 60 A), the charge density on the polymer, albeit low, is sufficient to cause the interaction of the peptide molecules with the sugar chain. This allows the transition to the α-helical conformation, although to a lower extent compared to alginate. When the ionic strength is increased (PI-150), the interaction between opposite charges is shielded and the structuring of LL-37 cannot take place, at variance with what showed in the presence of alginate. Under these conditions, hyaluronic acid behaves similarly to ChitLac. The strong, negative dependence of the PS/peptide interaction from ionic strength suggests

that the hydrophobic interactions between LL-37 and the "*hydrophobic patch*" in hyaluronan (Scott, 1989) are comparatively small, if present.

In conclusion, alginate has a strongly helicogenic effect over one order of magnitude of ionic strength variation, while hyaluronic acid has the same effect only at low ionic strength.

Binary alginate-ChitLac system

Since alginate, as a delivery system for LL-37, could be in contact with cationic macromolecules competing for its interaction with the AMP (Etrych et al., 2005), the influence on the amount of α-helix in LL-37 in the presence of alginate was investigated after the addition of ChitLac as a model competing polycation.

In particular, the reversibility of the interaction between LL-37 and alginate was tested by gradually adding the positively charged ChitLac to the mixture, under conditions corresponding to those used to obtain the first curve of Figure 59 B (alginate 50.4 µM, LL-37 10 µM, buffer PI-150). For each addition, the ratio of the sum of the positive charges on LL-37 and ChitLac, calculated taking into account their effective charge at the given pH, over the negative ones of alginate was calculated. The investigated ratio range varied from 1.15 (initial value) to 13.15, thus reaching conditions of a large excess of potentially competing positive charges. CD spectra recorded in that ratio range can be totally superimposed (data not shown), indicating that the percentage of α-helix remains constant and that the ordered conformation stabilized by the interaction of LL-37 with alginate is very strong and cannot harassed by ChitLac.

Cytotoxicity of LL-37/polysaccharide mixtures

The aim of these experiments was to verify if the relevant cytotoxicity of LL-37 towards mammalian cells could be mitigated upon binding by charged macromolecules, accompanied by alteration of the peptide conformation in solution.

With this in mind, we carried out a series of experiments aimed at evaluating the toxic effect of LL-37 on eukaryotic cells as a function of the presence/absence of PS. The CD data reported above showed that only polyanions effectively bind LL-37 and influence its conformation. The cytotoxicity tests were therefore carried out in the presence of alginate and hyaluronic acid at the concentration of 500 µg/mL. For this purpose, the MTT assay was used on two osteoblasts-like cell lines: MG63 and Saos-2. The choice of these cell lines was based on a potential future application of the peptide/PS mixture in the field of biomaterials, and in particular for orthopaedic implants. Osteoblasts were plated at a concentration of 5000 cells

per well. The ionic strength of DMEM medium is 166 mM, very close to the PI-150 buffer used in the CD experiments.

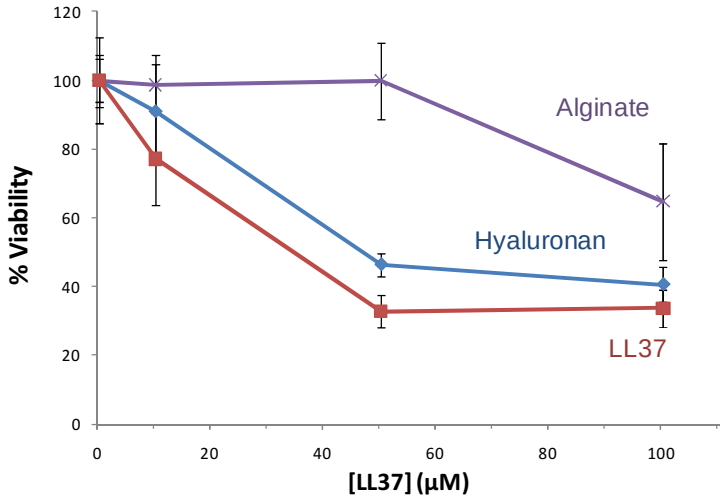

Figure 61. Cytotoxic effect on MG63 cells of increasing concentrations of LL-37 alone (triangles) or in the presence of 500 μg/mL alginate (squares) or hyaluronan (circles).

The results obtained with the MG63 cells are reported in Figure 61 and show that alginate is able to abolish the cytotoxic effect of LL-37 up to a peptide concentration of 50 μM and to significantly reduce it at higher concentration. In contrast, hyaluronan was unable to protect the cells at all the peptide concentrations tested.

The results with alginate are in good agreement with what predicted from CD data: the higher the fraction of LL-37 bound and aggregated onto alginate the lower its cytotoxic effect. Highly comparable results were also obtained with the Saos-2 cell line (data not shown).

The *in vitro* experiments with osteoblasts showed that the mixture alginate/LL-37 is the only system here tested that effectively reduces the cytotoxic activity of LL-37 and it was therefore selected for the evaluation of its antimicrobial activity on both Gram-negative and -positive bacterial species.

Antimicrobial activity of alginate/LL-37 mixtures

The antimicrobial activity of the alginate/LL-37 system was tested on *E. coli* and *S. aureus.*

The concentration of alginate was 500 μg/mL in all the experiments. Under these conditions, the kinetics of bacterial growth was followed for 4 h in the presence of two

different peptide concentrations (2 and 10 µM). As reported in Figure 62, *E. coli* cells in 20% MH grow rapidly as indicated by the fast increase of absorbance at 620 nm. The presence of alginate alone causes only a slight retardation in the growth kinetics (18% inhibition with respect to untreated cells). LL-37, at both concentrations tested, effectively blocks the growth of *E. coli* cells and this effect is preserved in the presence of 500 µg/mL alginate (Figure 62). These results indicate that under the selected conditions there is enough peptide available to affect bacterial cells, either free in solution or/and released from the complexes with alginate.

The results reported in Figure 63 show that the bacterial growth of *S. aureus* is also modestly inhibited by the presence of alginate in the medium.

On this species, LL-37 is active only at the concentration of 10 µM, and its antimicrobial activity is virtually abolished by the presence of the polysaccharide. In fact, the curve of growth kinetics can be superimposed to that of alginate alone.

To confirm these data, the experiment was replicated on two other bacterial strains, i.e. *P. aeruginosa* and *S. epidermidis* that showed the same behaviour (data not shown) depending on the Gram-type.

This result suggests that the charge density at the surface of the Gram-positive species tested is not high enough to compete with alginate for the peptide.

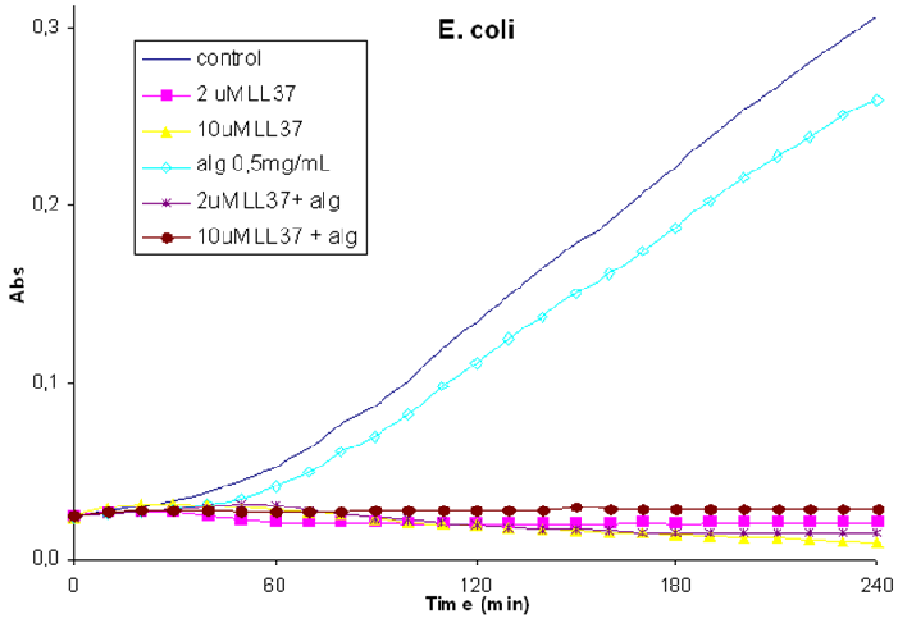

Figure 62. Growth kinetics of *E. coli* in 20% MH broth in the presence of alginate (500 µg/mL), LL-37 (2 or 10 µ M) or a mixture of both.

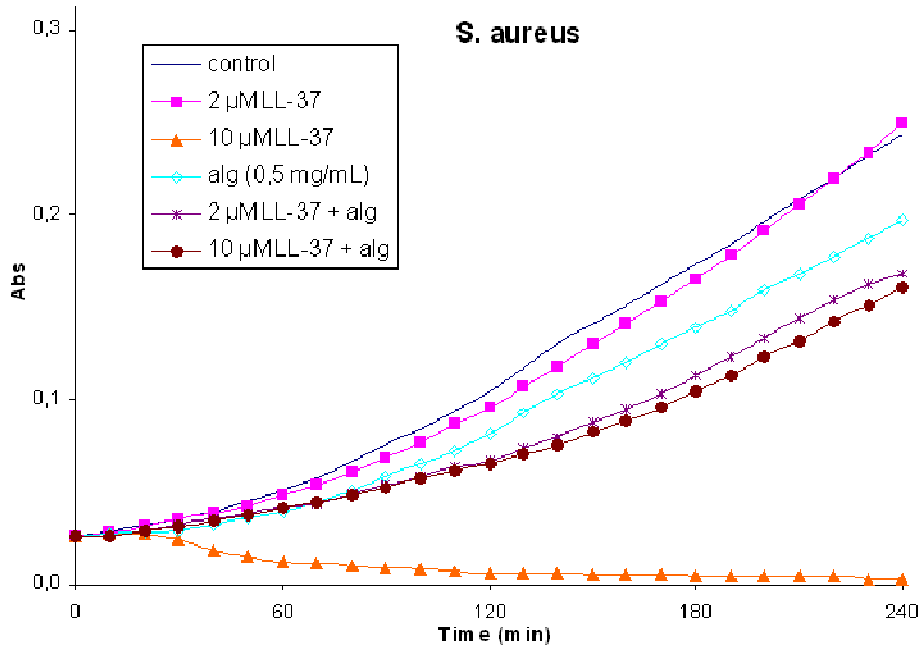

Figure 63. Growth kinetics of *S. aureus* in 20% MH broth in the presence of alginate (500 µg/mL), LL-37 (2 or 10 µ M) or a mixture of both.

Application of LL-37 to solid supports: Release from alginate/hydroxyapatite beads

INJECTABLE: Dispersion medium (provides flowability) +
Bioactive filler (provide bioactivity and elasticity at rest)

1 Dispersion medium: hyaluronan
Hyaluronan: highly biocompatible, bioactive, viscoelastic

2 Bioactive filler: Microcomposite + Specific bioactive agents

A Microcomposite (dried microbeads): alginate + HAp

Alginate: biocompatible + hydrophilic

HAp: bioactive ("inorganic" bioactivity)

B Specific bioactive agents in filler:

RGD-containing peptides: pro-adhesive
BMP-fragment peptides: pro-proliferative

LL37-peptide: antibacterial

A simple method to deliver a peptide is its entrapment in alginate beads. As already considered for BMP (p. 154), the peptide charge assumes an important role in encapsulation

efficiency; in the case of BMP the problem of the value of the charge near neutrality, which reduced encapsulation efficiency and promoted a fast release of the peptide by diffusion mechanism. In this case, as expected, the opposite situation occurred, LL-37 presents a high positive charge and the encapsulation process was highly efficient.

The encapsulation of LL-37 was performed by blending alginate and hydroxyapatite with a peptide aqueous solution, and then the mixture was dripped into a gelling solution containing calcium ions. The gel formation is supposed to be instantaneous and both the peptide and hydroxyapatite remain entrapped in the alginate gel bead. Unlike the BMP, LL-37 demonstrated an almost complete encapsulation without loss of peptide during gelation process. The amount of the peptide encapsulated was calculated after acidic hydrolysis of loaded beads and electrophoretic quantification of arginine in the hydrolysed liquid (p. 104).

The percentage of LL-37 released from loaded alginate beads was calculated in the same manner. Equal amount of wet beads were dispensed and incubated in PBS and agitated on a rotary stirrer for a certain number of days and then beads were hydrolysed. In this procedure the supernatant was never replaced. Data of collected fractions are reported in Figure 64; it can been seen that the release was very slow: after one month only 30% of the peptide was discharged from beads.

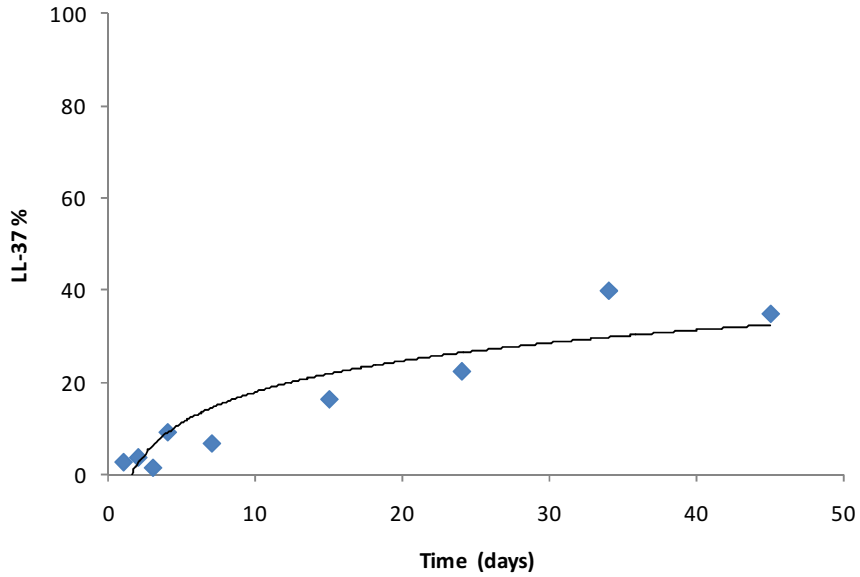

Figure 64. Release from alginate beads loaded with LL-37 peptide.

This behaviour indicates a different release process with respect to BMP loaded beads. In fact, peptides encapsulated in alginate beads can be released by two mechanisms: the diffusion of the protein through the pores of the polymer network, and the degradation of the latter (George and Abraham, 2006). In this case it is evident from the amount released and the time scale that LL-37 is liberated by means of the latter mechanism.

To confirm this release mechanism, a second type of release experiments was proposed and results are presented in Figure 65: in this case the release percentage is reported as a function of number of incubating buffer replacements that have been performed at the frequency of once a day. In this case, the release was more substantial and proceeded in parallel with the observed bead degradation: this phenomenon hindered further measurements.

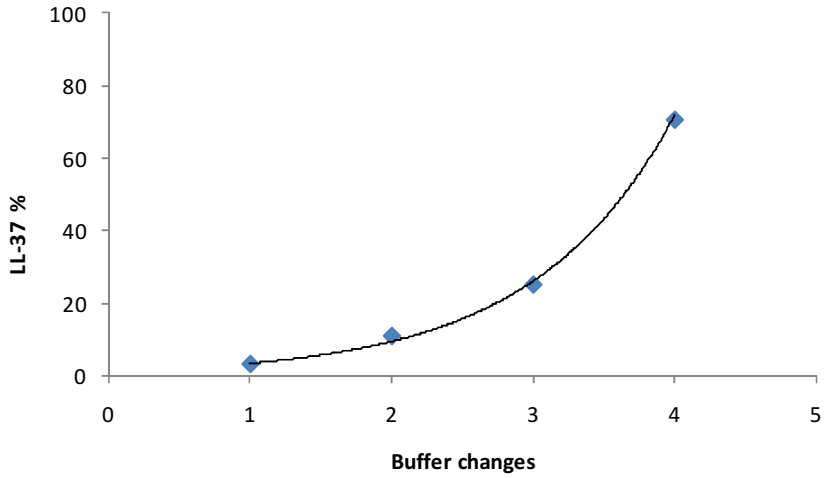

Figure 65. Release from alginate beads loaded with LL-37 by replacing the supernatant.

From this analysis it become evident that the release of LL-37 from alginate beads parallels the bead structure degradation, while the phenomenon of diffusion through gel pores seems to be almost asbent. This behaviour has an important advantage over conventional diffusion, since in this way the cytotoxic effect of LL-37 associated to a “burst” release of this molecule can be avoided and the peptide is always present as an alginate complex. From previous paragraph it can be said that in this association the toxicity of LL-37 is very low (Figure 61) and the global microbial effect of alginate beads can be described by the graphs obtained for bacterial growth in solutions containing alginate and LL-37 (Figure 62 and Figure 63). This line of research ended here having demonstrated that effective release of LL-37 from alginate matrices can be achieved only upon Ca-alginate/LL-37 bead erosion. Unfortunately, at

variance with the RGD and BMP cases in which the outer contact with environment and cells is required and the bead degradation may follow on longer times, with or without liberation of additional bioactive peptides from the inner core, the case of LL-37 is different inasmuch its efficacy depends on bead degradation from the beginning.

Application of LL-37 to solid supports: Adsorption on alginate/hydroxyapatite scaffolds

Another common way to incorporate proteins and peptides into a natural polymer-based porous carrier is, as anticipated, by physical adsorption. After having evaluated the activity of LL-37/alginate mixture in solution and assessed the practical inertia of loaded alginate beads against peptide release, we tested the effect of LL-37 adsorbed on a surface, eventually degradable, but certainly more stable to degradation than alginate beads in the used conditions and on comparable time scale.

Normally, by using this methodology, the release occurs upon desorption and this phenomenon is highly sensitive to the environmental conditions (Luginbuehl et al., 2004). In this specific case it is assumed that, as in the case of alginate beads, the release should only negligibly occur in the time of experiment and then the only available effect would be given by the contact of cells with LL-37 loaded and bound onto the surface.

To obtain an alginate construct with a similar resistance over time, a scaffold of alginate/hydroxyapatite was exploited. Alginate/hydroxyapatite scaffolds were prepared as indicated in literature (Turco et al., 2009) and they were used as a porous material for the adsorption of LL-37. This one was performed by immersion of the constructs in buffered peptide solution under mild agitation for 5 hours.

Quantification of adsorbed LL-37 on scaffolds

A precise evaluation of the peptide adsorbed on scaffolds was achieved before testing its activity on cells and bacteria. A first estimation was performed using the µBCA test, a colorimetric test that is frequently used to determine peptide and proteins release. The second one exploits the potentiality of capillary electrophoresis in the application of the analytical method presented at p. 104.

During the incubation time, the µBCA assay was performed to obtain an on-line control. The bicinchoninic acid (BCA) assay depends on the conversion of Cu^{2+} to Cu^{+} under alkaline conditions. The Cu^{+} is then detected by reaction with BCA. The reaction results in the

development of an intense purple colour with an absorbance maximum at 562 nm. The production of Cu^{+} in this assay is a function of peptide concentration and the peptide content of samples may be determined spectrophotometrically. The problem of this test is the inference with reducing sugars like alginate. For this reason, this test did not consent a precise evaluation of the adsorbed peptide but it was useful to control if the adsorption occurs during the incubation times (Smith et al., 1985).

The analysis of supernatants revealed that the adsorption on scaffolds was complete already after the first hour and remains constant during 20 hours. In fact, electrostatic interaction occurred rapidly.

A more accurate quantification was performed by hydrolysis of some scaffolds, supernatants and washing solutions and quantification of recorded arginine in hydrolysed by capillary electrophoresis. The analysis revealed the exact peptide amount adsorption on scaffolds with proof of recovering 99% of the theoretical amount used (Table 7).

Table 7. LL-37 amount quantification on scaffolds

Sample	*nmol LL-37*
Theoretical total amount	53.4
Supernatant	39.6
Scaffold	12.1
Washing solution	1.3
Sum	*52.9*

Cytotoxicity of LL-37 loaded scaffolds

Biological tests have been performed on LL-37 loaded scaffolds to evaluate the cellular viability and the activity on bacteria. The aim is to understand whether the capacity of alginate to reduce the cytotoxicity of LL-37 is maintained also when used in the solid state. For this purpose, the Alamar Blue™ assay was used on the osteoblasts-like cell line MG63 and the viability was evaluated.

The results obtained with the MG63 cells are reported in Figure 66 where the viability of non loaded scaffolds is reported as control. Data demonstrate that alginate also in this case is able to reduce the cytotoxic effect of LL-37 at start, and to abolish it after three days.

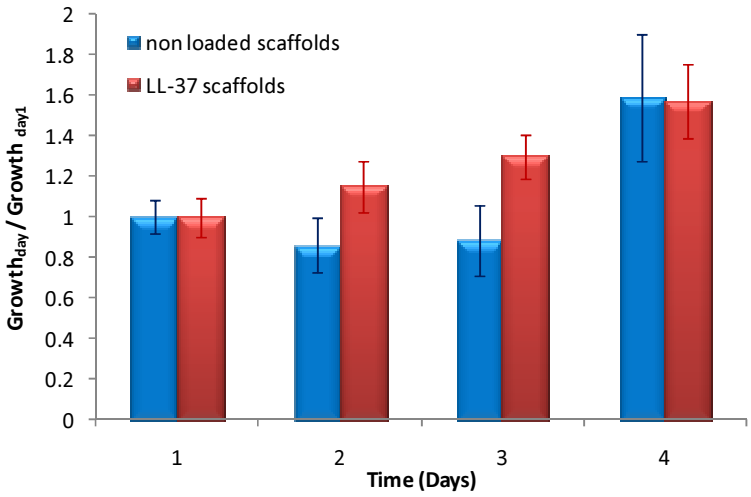

Figure 66 Alamar Blue™ assay on MG63 osteoblast-like cells on non loaded scaffolds of alginate and hydroxyapatite, and scaffolds with LL-37 adsorbed on the surface. Data were normalized at the first day.

Antimicrobial activity of LL-37 adsorbed on alginate scaffolds

Given the encouraging results obtained in *in vitro* experiments on the viability of osteoblasts, the alginate/hydroxyapatite scaffolds loaded with LL-37 were employed for the evaluation of their antimicrobial activity on *E. coli* and *S. aureus* bacteria.

The aim was to control whether the maintenance of the LL-37/alginate mixture activity on *E. coli* occurred also in the case of the peptide adsorbed on alginate constructs. The growth of the two bacteria strains incubated with loaded and non loaded scaffolds was followed at 30, 180, and 300 minutes by colony counts method. At these time intervals, the scaffold structure remains intact and no peptide release occurs due to degradation.

Unfortunately, the obtained data for both bacterial strains indicate that LL-37 was unable to inhibit the growth of bacterial cells in these conditions (data not shown). Although the inactivity on *S. aureus* just confirmed the former experiments on plates, the inefficacy on *E. coli* was unexpected. In fact in the previous experiments the LL-37/alginate mixture was able to block the growth of *E. coli* cells at a LL-37 concentration as low as 2 μM.

The results of these experiments clearly show that the only possible action mechanism of an LL-37/alginate construct is the degradation of the interchain polymer structure to release the peptide/polymer complexes in solution.

4.4.3 Partial conclusions

The Alginate/LL-37 mixture analyzed in this work appears to be a potential antimicrobial system capable of reducing the toxic effect of the peptide towards mammalian cells in defined ratios of peptide/polysaccharide, while maintaining the ability to arrests the growth of Gram-negative bacteria. In contrast, the peptide/PS mixture is poorly or not at all effective on Gram-positive bacteria.

The reason for this dissimilar behaviour is likely to be searched in the different composition of the bacterial wall of Gram-negative and Gram-positive bacteria. In fact, the surface of former group of microorganisms is rich in LPS, which confers a high density of negative charge. This density is likely high enough to shift the peptide/PS equilibrium so that at least part of the peptide is transferred to the bacterial wall, where it performs its antimicrobial activity. Under these conditions the bacterial growth is inhibited at 10 µM peptide, a concentration that results to be completely safe in terms of cytotoxicity (Figure 61).

In the case of Gram-positive bacteria, the charge on the bacterial wall likely is not sufficient to displace LL-37 from the alginate/peptide complex and the presence of the peptide causes only a slight decrease of the growth kinetics with respect to alginate alone. It can be supposed that in this case the mixture behaves as a “peptide trap” inasmuch as the presence of the peptide is not “experienced” by the microorganism.

Driven by the possibility of effectively modulate the action of LL-37 by means of its interaction with a suitable, negatively charged polyelectrolyte, we tested the use of the peptide/PS complexes in localized (semi)solid systems, such as in coating of biomaterials for orthopaedic applications.

With this aim in the second part of this chapter the conjugation of the peptide on alginate solid supports was investigated. Peptide was electrostatically immobilized either by entrapment in alginate beads or adsorbed on (alginate-based) scaffold surfaces.

In the first case a release caused by the degradation of the polymer network was shown. Whereas, an effect caused by the simple contact between cells or bacteria and alginate surface loaded with the peptide (like a loaded scaffold) was excluded by i*n vitro* experiments.

The only possible efficient release mechanism that an LL-37/alginate construct is able to perform is the degradation of the construct itself, relating to *in vitro* experiments performed in the solution state. However, this mechanism may not be compatible on the time scale with the mode of action of the RGD and BMP complexes, hampering the possibility of preparing an “universal” alginate based carrier of specific bioactive agents.

4.5 INJECTABLE FILLER

4.5.1 Introduction

Over the last few years, a lot of work has been performed in the development of injectable bone substitutes (IBS) materials and bone cements addressed to bone substitution and repair in minimally invasive surgery. In this field, the use of polymer composites is attractive since they can be used to exactly fill irregular bone defects and they respond to requisites of similarity with the replaced tissue. In fact, hard tissues in the human body are natural composite materials and they serve as templates in the development of tissue replacement constructs.

Once satisfied the requirement of biocompatibility, the last goal is the development of bioactive composites for tissue replacement and tissue regeneration purposes, obtaining composites with peculiar characteristics that may be used in specific clinical situations.

Developing a bioactive composite

Bone can be considered as a template for planning new materials for hard tissue replacement. This tissue is a natural composite material, having a complex structure in which different levels of organization, from macro to micro scale, can be distinguished. Two levels of composite structure are considered when bone substitutes are projected: first, the bone hydroxyapatite reinforced collagen forming individual lamella at the nm to µm scale, and second osteon reinforced interstitial bone at the µm to mm scale. It is the first level, the apatite-collagen composite which provides the template to plan bioactive ceramic-polymer composites as analogue biomaterials for bone replacement. As bone is an apatite-collagen composite material at the ultra-structural level, a polymer matrix composite containing a bioactive particulate component appears a natural choice for substituting cortical bone. The bioactivity of the composite, provided by the bioactive component in the composite, will promote the tissue growth at the site of the implant and the formation of a strong bond between the tissue and the implant.

Polymer composites are a well-established class of materials in which a particulate, used as reinforcing element, is dispersed in the polymer matrix. In any composite, there are, at least, two constituent materials: a matrix (or a continuous phase) and a dispersed phase (reinforcement). The association of bioactive ceramics with polymers presents the purposes of

improving at the same time mechanical and osteoconductive properties of the final construct with respect to the single materials. The continuous phase is responsible for filling the volume, as well as it surrounds, and supports the dispersed material by maintaining their relative positions. The dispersed phase is, usually, responsible for enhancing one or more properties of the matrix. Two types of reinforcements are normally used for biomedical composites: fibres and particulates. With few exceptions, reinforcements are harder and stronger than the matrix and hence reinforce the final construct.

Most of the composites target an enhancement of mechanical properties; however other properties such as erosion stability, radiopacity, density or biocompatibility can be required on the basis of the final application. For instance, the presence of a ceramic phase in a polymer is able to enhance the mechanical properties, and the strengthening mechanisms of the composites depend primarily on the amount, arrangement, geometry and type of reinforcement. On the other hand, using bioactive ceramics, such as calcium phosphates, osteoconductive properties are also improved and a major biocompatibility is assured. Generally, on designing a biomedical composite, it should be remembered that even if an excellent mechanical performance is desirable, and often targeted for improvement, the biocompatibility of the material is of dominant concern: the biological compatibility is more important than the mechanical compatibility. Beyond biocompatibility, the bioactivity is a crucial factor of biomedical composites becoming a parameter to discriminate composites. We can classify a composite as bioinert, bioactive, and bioresorbable on the basis of its bioactivity. It is evident that different requirements are necessary if the final goal is to develop an inert cement or a bioactive composite: in fact for this latter the biological functionality appears to be more important than any other type of compatibility (Wang, 2003).

The properties of the final construct are the result of the synergism of the two (or more) phases, which are unavailable from the individual constituent materials. These properties are strongly affected by a number of factors:

- Reinforcement shape, size, and size distribution
- Reinforcement properties and volume fraction (percentage)
- Bioactivity of the reinforcement (or of the matrix)
- Matrix properties (for instance molecular weight and hydrophilicity)
- Distribution of the reinforcement in the matrix
- Reinforcement-matrix state

Among these factors, properties of constituent materials are the most influent parameters. However, factors such as the composite architecture and reinforcement-matrix bonding condition also play important roles. In general, three interdependent factors must be considered in design a new composite (Dorozhkin, 2009):

- selection of the suitable matrix and dispersed materials
- choice of appropriate fabrication and processing methods
- internal and external designs of the device itself

In the study of a composite, it is important initially to consider and to test phases separately and only after to characterize the final composite.

Particulate properties

The physical characteristics of the reinforcement, such as the size distribution, shape, and concentration, are very important in determining mechanical properties of a composite. In the idealized situation, the reinforcement is normally assumed to possess a spherical shape. Actually, bioactive particulate used as reinforcement presents an irregular shape.

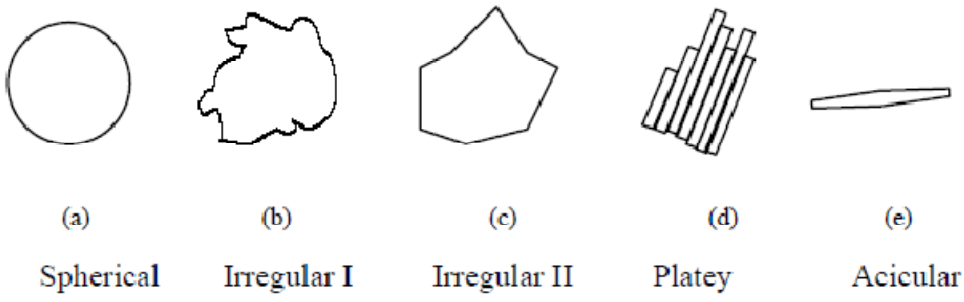

Figure 67. Shapes of bioceramic particles for biomedical composites (Wang, 2003)

In Figure 67 are reported the principal shapes of particulate that it is possible to find in a composite. Shape (b) corresponds to the example of the hydroxyapatite particles commercially available, namely spray-dried powders that can have an irregular shape. This type of shape is preferred by cells with respect to spherical shapes, therefore under a certain shear stress particles can break up into smaller particles fragments. This must be considered also during particular processing procedures. Another shape is that one presented in the Figure 67 (c) which presents sharp edges. Particles of this type cause stress concentration in the composite around the sharp edge and so are not preferred, usually sharpness is in fact

removed by an additionally processing them. The plate shape (Figure 67 d) is not usual for particles in bioactive composites. When particles of calcium phosphate produced by precipitation are used in composite without processing, the nanometer size particles generally have the acicular shape (Figure 67 e). In this situation the aspect ratio (such as the length) and the orientation assumed in the final composite are important parameters to be considered.

Another important parameter is the volume fraction used to fill the polymer matrix. This factor is important not only for the strength and mechanical properties of the final composite, but also for the bioactivity. In fact, below a certain volume even if the bioactive particulate is incorporated in the polymer, the composite may not possess the desired bioactivity. For instance, it was demonstrated that for hydroxyapatite reinforcing a polyethylene composite, the critical volume percentage was around 20% (Bonfield, 1988). Bioactive composites containing 20% or more of bioceramics are considered highly filled polymer systems, and this kind of material presents a difficult high quality production. When a highly filled system is involved, an important factor is the packing behaviour of bioceramic particles in the polymer matrix.

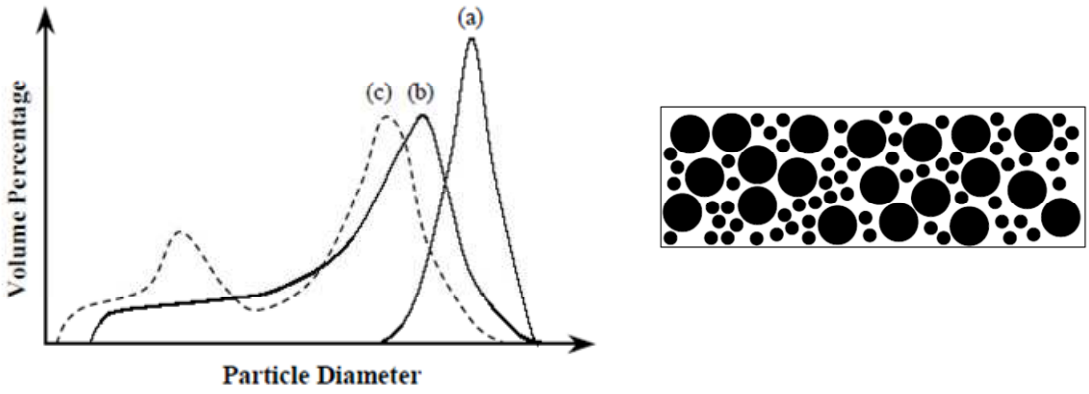

Figure 68. Schematic diagram showing particle size distributions of particulate reinforcements: (a) mono-modal size distribution, (b) mono-modal size distribution with a long tail end, (c) bi-modal size distribution. Second figure: Schematic diagram showing the distribution in a polymer matrix of bioceramic particles of a bi-modal size distribution (Wang, 2003)

The packing behaviour depends largely by size, shape, size distribution, and surface characteristics. It is normally assumed that particles have a mono-modal distribution with a sharp peak (curve a in Figure 68) and possess an uniform size, which makes it difficult to achieve high packing density. In reality, most produced ceramics have broad size

distributions, sometimes with a long tail end towards the smaller particles (as in the curve b in Figure 68). Other ceramics can exhibit bi-modal size distributions (curve c), their packing is more efficient (as indicated in the second scheme of Figure 68) because the small particles occupy the spaces between the large particles, leading a high bioceramic content per unit volume in the composite.

The control of the interface between the reinforcement and the matrix is of great interest because the mechanical behaviour and the properties of the composite are significantly affected by the interfacial state. A strong interfacial bonding can effectively transfer the load from the matrix to the reinforcement, while a weak bonding at the interface can provide a failure of the composite. For this reason chemical bonding are performed between polymer and particulate; but in most bioactive composites, chemical bonding does not exist and the interfacial bond strength totally depends on the mechanical network between the two phases (Wang, 2003).

Rheological characterization of polymer matrix

Rheology is the scientific field which studies the behaviour of a material in response to deformation, allowing the characterization of the flow and elastic properties of the material.

In order to understand the changes provided by reinforcement on the rheological behaviour of the polymer matrix, the rheological properties of the unfilled polymer may be considered before analysing the composite.

A solid or a liquid can respond in three different ways to an applied deformation: it can exhibit elastic properties, viscous properties or both of them at the same time (viscoelastic properties). A material that stores and releases all mechanical energy when deformed is defined as purely **elastic**, in this case the material will return back to its original shape and position instantaneously. A material that loses all mechanical energy, as heat, when deformed is defined as pure **viscous**. A viscous material does not return back to its original shape. As typical example of a material which exhibits only viscous behaviour would be a Newtonian fluid as for example, water, if the deformation is applied not too rapidly.

Polymers exhibit **viscoelastic** behaviour when deformed. They will simultaneously store and lose mechanical energy. A polymeric material has time dependant properties: this means that the mechanical properties depend on the frequency or rate of deformation. For what concerns polymer solutions, the concentration is the most important factor. When the concentration of the polymer exceeds the critical overlap concentration (c*), we enter in the

regions called the semi-dilute and concentrated solutions. Another critical point of concentration can be identify and is the c** or double critical overlap concentration. If c* characterizes the situation where there is a continuous contact between the polymer coils, c** represents the concentration where the polymer coils are so entangled that there is a uniform distribution of the segments in the polymer. With these premises, we can define a **solution** as **dilute** ($c < c^*$) if there is not a continuous contact between the polymer molecules, as **semi-dilute** ($c^* < c < c^{**}$) if the polymer molecules are in continuous contact with each other and as **concentrated** ($c > c^{**}$) if the concentration of the polymer is so high that there is an uniform distribution of polymer segments among the solvent molecules. In these two latter concentration regions, where $c > c^*$, the polymer chains may be linked together into a continuous network forming a gel.

True polymer solutions are defined by the conjugation of two characteristics:

1. They are thermodynamically stable systems
2. Only physical interactions exist between the coils

Rheology of polymers has been extensively studied and theoretical treatments are available at least for linear neutral chains.

It is useful to understand the rheology of polysaccharide solutions, however because of polydispersity, polymolecularity, and molecular interactions, deviation from theoretical polymer laws predicted for polymer are often observed; in particular, it is not so easy to obtain ideal polysaccharide solutions because of their propensity to extensively form hydrogen bonds. The case of polyelectrolytes is even more complicated. A polyelectrolyte is a flexible polymer electrically charged because its structure includes monomers bearing ionizable groups with charges of the same sign. The distinctive feature of polyelectrolytes is that the conformation of the macromolecule depends sharply on the ionic strength of the solvent, because the range of the electrostatic interaction decreases as the ionic concentration increases. Thus the conformation depends on both polymer and salt concentration, driving to a higher complexity with respect to neutral polysaccharides and even more to polymer solutions (Lefebvre and Doublier, 1998).

Static rheological measurements: flow behaviour of polymer solutions

One kind of rheological measurements are those performed in conditions of steady state flow. They correspond to a state under which a constant stress or shear rate is maintained for a

sufficient time to allow dynamic equilibrium. An equilibrium flow curve can be used to characterize the time-independent properties of a material.

Viscosity is the most important flow property. It represents the resistance to flow and can be defined as the ratio of the imposed shear stress, and the shear rate:

$$\boldsymbol{\eta} = \frac{\boldsymbol{shear\ stress}}{\boldsymbol{shear\ rate}} = \frac{\boldsymbol{\tau}}{\boldsymbol{\dot{\gamma}}} \qquad \textbf{(4.2)}$$

In the dilute regime, Newtonian flow behaviour and absence of viscoelasticity are generally observable in practical conditions, at least for non-charged polymers, because, statically, macromolecules are spatially non correlated; while, non-Newtonian flow behaviour and viscoelasticity of polymer solutions develop usually only for c > c*. A Newtonian liquid is definite when the shear stress (σ) is proportional to the rate of shear ($\dot{\gamma}$) with a constant viscosity of the solution (η).

$$\boldsymbol{\sigma = \eta\dot{\gamma}} \qquad \textbf{(4.3)}$$

If the viscosity is not constant, but dependent on the rate of shear and/or time, we have a non-Newtonian liquid. In this case the viscosity is no longer constant, but is a function of shear rate and/or time:

$$\boldsymbol{\sigma = \eta(\dot{\gamma}, t) \cdot \dot{\gamma}} \qquad \textbf{(4.4)}$$

There are different types of non-Newtonian behaviour, depending on how the viscosity varies with rate of shear or time. Equation (4.2) often used also for non-Newtonian liquids, when an "apparent viscosity" η_{app} is defined. This is the value of viscosity evaluated at some nominal average value of the shear rate, so, the apparent viscosity is a precise measure only when the rate of shear and/or the response to time has been given:

$$\boldsymbol{\eta_{app} = \sigma/\dot{\gamma}} \qquad \textbf{(4.5)}$$

Polysaccharide solutions at concentration higher than c* display the non-Newtonian shear behaviour typical of polymers melts and of semi-dilute or concentrated polymer solutions. In non-Newtonian fluids, the viscosity is generally found to decrease with the increase of the

shear rate, giving rise to a phenomenon known as “shear-thinning” (or “pseudoplastic”) behaviour. For these materials the curve of viscosity against shear rate indicates that only in the limit of very low shear rates the viscosity is constant, while in the limit of very high shear rates the viscosity is again constant, but at a lower level. In the intermediate shear regime, viscosity decreases with increasing shear rate. This type of behaviour is illustrated in the Figure 69 where the steady-state flow curve of a 0.4% aqueous solution of polyacrylamide is plotted against the shear rate $\dot{\gamma}$ on bilogarithmic scales.

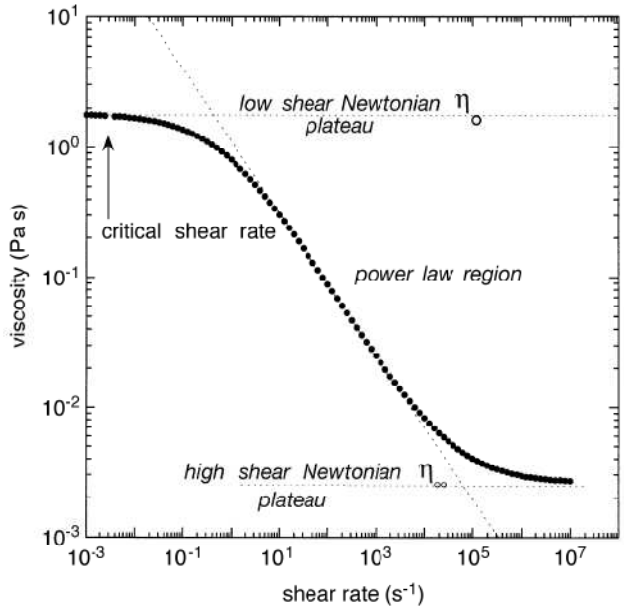

Figure 69. Flow curve of an aqueous solution of polyacrylamide (c= 0.4%) illustrating the three typical regions of polymer solutions shear thinning behaviour (Lefebvre and Doublier, 1998).

Below a critical shear rate value ($\dot{\gamma}_c$), the flow curve shows an initial region, the low-shear Newtonian plateau, where the viscosity keeps a constant value η_0 called “zero-shear viscosity”. η_0 is the magnitude of the viscosity at the lower Newtonian plateau. It is a critical material property and can prove valuable in making assessments of suspension and emulsion stability, estimates of comparative polymer molecular weight and tracking changes due to process or formulation variables.

A region ($\dot{\gamma} > \dot{\gamma}_c$), where the viscosity decreases as the shear rate increases (named shear-thinning region) follows. At higher shear rates, the viscosity tends toward a second plateau η_∞ that is seldom experimentally observed, because of instrumental limitations, but in theory

exists. η_∞ is named “infinite shear viscosity” and tells how the product is likely to behave in very high shear processing situations.

In the central part of the shear-thinning region, a power law relation $\eta \propto \dot{\gamma}^{-n}$ is accurately followed. Polymers are expected to show Newtonian behaviour as long as the rate of shear is low enough to allow the molecules to respond and the transient network of hydrated polymer chains to “reorganize”; when the velocity gradient is too large, the molecules are unable to keep up, and non-Newtonian behaviour results. A number of mathematical models have been developed for describing non-Newtonian behaviour. A useful rheological model that describes the relationship between viscosity or shear stress and shear rate over the range of shear rates where shear thinning occurs in a non-Newtonian fluid is the “power law” model. It quantifies viscosity range and degree of deviation from Newtonian behaviour. The Power Law model (sometimes known as the Ostwald model) is an easy-to-use model that is ideal for shear-thinning, relatively mobile fluids such as weak gels and low-viscosity dispersions. The model is nothing more than the Newtonian model, with an added exponent on the shear rate term. It s modelled by the formula:

$$\boldsymbol{\sigma = K\dot{\gamma}^{n}} \qquad \textbf{(4.6)}$$

$$\boldsymbol{\eta = \sigma/\dot{\gamma} = K\dot{\gamma}^{n-1}} \qquad \textbf{(4.7)}$$

Where *K* is an arbitrary constant often known as the “consistency coefficient” and it describes the overall range of viscosities across the part of the flow curve that is being modelled. The exponent *n* is known as the “power law index” (or sometimes the “rate index”). The range of *n* values is comprised between 0 and 1 ($0 < n < 1$) for a shear thinning fluid: the more shear-thinning the product, the closer *n* is to zero. The determination of intrinsic viscosity of shear thinning solutions has to be based on measurements in the primary Newtonian region. Only in this region in fact, there are the theoretical relations between intrinsic viscosity and the size and conformation of the macromolecules valid.

Dynamic rheological measurements: mechanical spectroscopy

The second rheological method used to obtain information on the molecular structure in gels and in polymers networks, is mechanical spectroscopy. Dynamic rheometric analysis is a

test in which both stress and strain vary harmonically with time and is used to study the viscoelasticity of the polymers.

In a typical sinusoidal oscillation experiment (Figure 70), the applied stress and resulting strain wave forms can be described as follows:

$$\boldsymbol{\sigma = \sigma_0 \cos \omega t} \qquad \textbf{(4.8)}$$

$$\boldsymbol{\gamma = \gamma_0 \cos(\omega t - \delta)} \qquad \textbf{(4.9)}$$

Where σ_0 and γ_0 are the stress and the strain amplitude respectively, ω is the angular frequency, t is the time and δ is the phase lag or the loss angle. The phase lag and the amplitude ratio (σ_0 / γ_0) will generally vary with frequency, but are considered material properties under linear viscoelastic conditions.

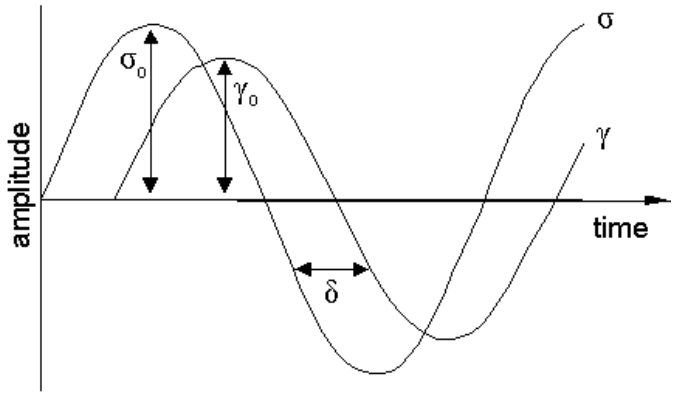

Figure 70. Sinusoidal wave forms for stress and strain functions.

For an ideal solid $\delta = 0°$ and the response is purely elastic, whereas for a Newtonian fluid yielding a purely viscous response $\delta = 90°$. The material functions can be described in terms of complex variables having both real and imaginary part. So it can speak of complex stress amplitude and complex strain amplitude.

The two primary outputs of a dynamic mechanical measurement are the shear moduli and the phase lag $\delta(\omega)$.

We can distinguish the **shear storage modulus** (G'(ω)) (or storage modulus or elastic modulus) and the **shear loss modulus** (G"(ω)) (also named loss modulus or viscous modulus):

$$\boldsymbol{G'(\omega) = \frac{\sigma_0}{\gamma_0}\cos\delta} \qquad \textbf{(4.10)}$$

$$\boldsymbol{G^{"}(\omega) = \frac{\sigma_0}{\gamma_0}\sin\delta} \qquad \textbf{(4.11)}$$

G'(ω) gives information about the elasticity or the energy stored in the material during deformation, while G"(ω) describes the viscous character of the energy dissipated as heat. For concentrated solutions and weak networks, both G' and G" are dependent on ω. The two moduli are summarized in the complex shear modulus (G*) provided by the ratio of shear and strain amplitudes, and it is defined in this manner:

$$\boldsymbol{G^* = \frac{complex\ shear\ amplitude}{complex\ strain\ amplitude} = \frac{\sigma_0}{\gamma_0}\cos\delta + i\,\frac{\sigma_0}{\gamma_0}\sin\delta} \qquad \textbf{(4.12)}$$

$$\boldsymbol{G^* = G' + iG^{"}} \qquad \textbf{(4.13)}$$

Finally, an absolute shear modulus is defined as the ratio of the amplitude of the stress to the amplitude of the strain in forced oscillation:

$$\boldsymbol{|G^*| = \sqrt{G'^2 + G^{"2}} = \frac{\sigma_0}{\gamma_0}} \qquad \textbf{(4.14)}$$

The plot of G'(ω) and G"(ω) on bilogarithmic scales over a wide range of frequencies is known as "mechanical spectrum". This consents to distinguish different kinds of behaviours and different structural conditions in the system class.

The phase lag δ is a measure of the ratio between elastic and viscous contributions in the material at a given frequency. This means that for $\delta > 45°$ (G" > G'), the response is mainly viscous, and for $\delta < 45°$ (G' > G"), it is mainly an elastic response.

Graphically this ratio is reported as loss tangent:

$$\tan \delta = \frac{G''}{G'} \qquad (4.15)$$

Table 8. Relation between G', G", δ and viscoelastic behaviour

ωτ	G', G"	δ	Behaviour
< 1	G' < G"	> 45°	Viscoleastic liquid
= 1	G' = G"	= 45°	Transition
> 1	G' > G"	< 45°	Viscoelastic solid

δ depends strongly on ω. When δ > 45° (and then tan δ < 1) the elastic component is the prevalent modulus while for δ > 45° (and then tan δ > 1) the viscous component is prevalent at that frequency of the measurement. (Smidsrød and Moe, 2008).

Additionally we can define the **complex viscosity** η* as the frequency-dependant viscosity function determined during forced harmonic oscillation of shear stress. η* can be expressed as the ratio between the complex stress amplitude and the complex strain rate amplitude obtaining in this manner:

$$\eta^* = \frac{G^*}{i\omega} = \eta' - i\eta'' \qquad (4.16)$$

Where η' is named dynamic viscosity and is the ratio of G" on the angular frequency. While the term η" that is the ratio between G' and ω, is referred to as the out-of-phase viscosity. Also in this case, the complex viscosity represents and contains both real and imaginary parts, in particular, η" represents the imaginary part, while η' the real part of the complex viscosity.

Linear viscoelastic models.

Viscoelastic materials, such as amorphous polymers, semi-crystalline polymers, and biopolymers, can be modelled in order to determine their stress or strain interactions as well as their temporal dependencies. The simple models of elastic and viscous behaviour are

defined by the laws of Hooke and Newton, respectively. Their validity, however, is restricted to small deformations and, for many fluids, to law values of shear rate. Different combinations of Newton and Hooke elements led to the formulation of linear viscoelastic models.

A formulation of the linear viscoelastic model was proposed by Maxwell. The Maxwell model, like the others linear models, is used to predict the response material under different loading conditions. In all these models, viscoelastic behaviour as elastic and viscous components are visualized as linear combinations of springs and dashpots, respectively (Figure 71). Each model differs in the arrangement of these elements.

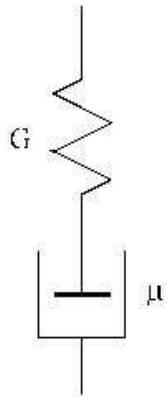

Figure 71. The Maxwell model

When the stress τ_{yx} is applied to the Maxwell element, the total strain results from the sum of both viscous (v) and elastic (e) parts:

$$\boldsymbol{\gamma_{yx}} = (\boldsymbol{\gamma_{yx}})_v + (\boldsymbol{\gamma_{yx}})_e \qquad \textbf{(4.17)}$$

Thus, also the total rate of strain $\dot{\gamma}_{yx}$ can be calculated from the viscous and elastic contributions:

$$\dot{\boldsymbol{\gamma}}_{yx} = (\dot{\boldsymbol{\gamma}}_{yx})_v + (\dot{\boldsymbol{\gamma}}_{yx})_e = \frac{\tau_{yx}}{\mu} + \frac{1}{G}\frac{d\tau_{yx}}{dt} \qquad \textbf{(4.18)}$$

This is the constitutive equation of the Maxwell fluid, which can be written also in this manner:

$$\boldsymbol{\tau_{yx} + \lambda \frac{d\tau_{yx}}{dt} = \mu \dot{\gamma}_{yx}} \quad \textbf{(4.19)}$$

where λ is the relaxation time, defined by the ratio μ/G that reflects the importance of the stress changing rate. The Newtonian fluid represents the limit case of a Maxwell fluid for $\lambda \to 0$.

Equation (4.19) can be referred to an arbitrary component of the stress tensor τ_{ij} and reported in a general form as follows:

$$\boldsymbol{\tau_{ij} + \lambda_0 \frac{d\tau_{ij}}{dt} = \eta_0 \dot{\gamma}_{ij}} \quad \textbf{(4.20)}$$

where λ_0 and η_0 replace the previous time and viscosity constants λ and μ.

The Maxwell model predicts a simple exponential stress response, when a constant shear rate $\dot{\gamma}_0$ is applied or the fluid is maintained at constant strain after its application. From the parallel combination of N Maxwell elements, it is possible to obtain the "generalized Maxwell model", where stress is the sum of the contribution of each N element (Figure 72).

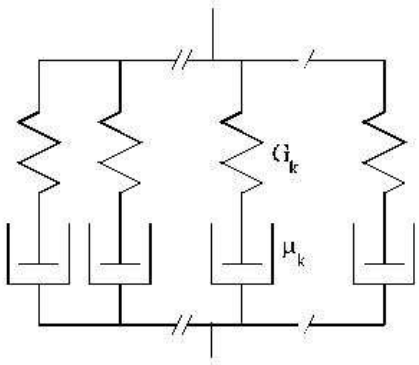

Figure 72. The generalized Maxwell model.

$$\boldsymbol{\tau_{ij} = \sum_{k=1}^{N} \tau_{ij}^{(k)}} \quad \textbf{(4.21)}$$

And each contribution $\tau_{ij}^{(k)}$ is given by the constitutive equation of the Maxwell (4.19) element:

$$\boldsymbol{\tau_{ij}^{(k)} + \lambda_k \frac{d\tau_{ij}^{(k)}}{dt} = \eta_k \dot{\gamma}_{ij}} \quad \textbf{(4.22)}$$

The constitutive equation is defined by N viscosity constants, η_k, and the discrete spectrum of N relaxation times λ_k.

When the model is applied to steady shearing flow conditions, all time derivatives of $\tau_{ij}^{(k)}$ are zero, so that:

$$\boldsymbol{\eta_0 = \sum_{k=1}^{N} \eta^{(k)}} \qquad \textbf{(4.23)}$$

The generalized Maxwell model is useful to predict stress relaxation and growth processes of monotonic type which is symmetrical to each other, as for Maxwell model, and results from the sum of the simple exponential contributions of each single Maxwell element. The following expressions are derived for the stress relaxation and growth, respectively:

$$\boldsymbol{\tau_{yx} = \eta^{-}\dot{\gamma}_0 = \dot{\gamma}_0 \sum_k \eta_k \exp\left(-t/\lambda_k\right)} \qquad \textbf{(4.24)}$$

$$\boldsymbol{\tau_{yx} = \eta^{+}\dot{\gamma}_0 = \dot{\gamma}_0 \sum_k \eta_k \left(1 - \exp(-t/\lambda_k)\right)} \qquad \textbf{(4.25)}$$

The initial stress (Eq. 4.24) and the steady state stress (Eq.4.25) for $t \to \infty$, correspond to the same viscosity η_0, independently of the applied shear rate. In fact, the generalized Maxwell model still predicts only Newtonian behaviour (Lapasin and Pricl, 1995).

These are the expressions derived for elastic and viscous moduli:

$$\boldsymbol{G' = \sum_k \frac{\eta_k \lambda_k \omega^2}{1+(\lambda_k \omega)^2}} \qquad \textbf{(4.26)}$$

$$\boldsymbol{G'' = \sum_k \frac{\eta_k \omega}{1+(\lambda_k \omega)^2}} \qquad \textbf{(4.27)}$$

Study of composites

When reinforcement is added to a polymer, a composite with particular mechanical and rheological properties is generated. Generally, the dispersion phase is used to improve the mechanical properties of polymer matrix resins such as stiffness, strength, and hardness. These properties usually increase for higher amounts of reinforcement. On the other hand, the addition of the matrix permits a better ductility of the particulate. In any case, the

incorporation of particulate into polymers alters their flow behaviour and the final properties of the composite. Micromechanical behaviour of a composite is governed by the properties of both polymer matrix and dispersed phase and by other factors such as the volume fraction of reinforcements, the presence of agglomerates and the quality of the adhesion at the interface between polymer and particulates (Alberaola et al., 1997).

The study of a composite should follow a precise way: it should study and characterize the singular parts of composite separately, after that the study of composite can be performed.

Information about composites structure and morphology can be obtained by means of optical analysis and rheological tests. As already mentioned, rheological methods can be divided into two types, according to the different cases of force exerted during tests: one is the static rheological measurements, namely the steady shear flow method under certain stress or strain, and the other one is the dynamic rheological measurements, namely the oscillatory shear flow method under periodic stress or strain. For multiphase/multicomponent polymer systems, the information provided by the first method, is limited because of the continuous effect of stress exerted during static rheological testing usually leads to the change, even to breakage, of both structure and morphology of the tested polymer, and this occurs especially for multiphase polymers. Dynamic rheology testing is believed to be a preferential method for studying these kinds of constructs, because they are performed under small-strain amplitude, which can be employed effectively to probe the structure and the morphology of the multicomponent system (Min and Qiang, 2008).

Dynamic rheological measurements provide information about the two components of a material: the elastic and the viscous modulus. Generally, it was observed that compared with the rheological behaviour of the pure polymer matrix, polymer composites exhibit pronounced elastic properties and long relaxation times (Graebling et al., 1993).

The rheological property changes of a polymer matrix induced by filler incorporation are hypothesized to be caused by two factors. One is the mechanical coupling between filler and polymer matrix, and the other is the interfacial morphological structure depending on the adhesion at the interface or on the adsorption between different phases. In this view, the physical state of reinforcements presents a significant influence on the rheological behaviour of the composite (Du et al., 2003), so the physical characteristics (shape, size and size distribution) of the reinforcement are very important in determining mechanical properties of the composite and need to be verified.

4.5.2 Design of a composite for orthopaedic applications

INJECTABLE: Dispersion medium (provides flowability) +
Bioactive filler (provide bioactivity and elasticity at rest)

1 Dispersion medium: hyaluronan
Hyaluronan: highly biocompatible, bioactive, viscoelastic

2 <u>Bioactive filler</u>: Microcomposite + Specific bioactive agents

A <u>Microcomposite</u> (dried microbeads): alginate + HAp
Alginate: biocompatible + hydrophilic
HAp: bioactive ("inorganic" bioactivity)

B Specific bioactive agents in filler:
RGD-containing peptides: pro-adhesive
BMP-fragment peptides: pro-proliferative
LL37-peptide: antibacterial

Rheological properties of hyaluronic acid

Hyaluronic acid, as the other high molecular weight polysaccharides isolated from connective tissues, has demonstrated to possess peculiar rheological properties that are function of molecular weight and concentration.

This polymer has been evaluated for medical applications because of their superior biocompatibility and rapid bioresorption. Because of its presence in vitreous humor, cartilage, and synovial fluid, it has been employed in eye surgery and in the treatment of osteoarthritis by injection in knees patients as supplement of synovial fluid (Barbucci et al., 2002). In these biomedical applications the usefulness of hyaluronic acid is provided by its mechanical cushioning and lubrificating properties.

Several studies have been performed to characterize the structure of hyaluronic acid in solution. Experimental data, reported that hyaluronic acid is a viscoelastic polymer with a cross-over point frequency dependant on pH (Scott and Heatley, 2002). Other studies compared crosslinked and non-crosslinked hyaluronic acid and measured dynamic parameters concluding that non-crosslinked hyaluronate formed entangled networks and for hyaluronic acid with a molecular weight of 1.6×10^6 the critical entanglement concentration resulted to be 2.4 mg/mL (Milas et al., 2001), (Krause et al., 2001).

The zero shear viscosity of this polysaccharide is strongly dependant on both concentration and molecular weight as demonstrated by Falcone and co-workers (Falcone et al., 2006). According to the equation:

$$\boldsymbol{\eta_0 \cong K \times MW^{3.4}} \qquad \textbf{(4.28)}$$

Generally, when a material flows rapidly through a small orifice as in the case of an injectable, it experiences very high shear forces, and at these high shear conditions, the η_0 does not adequately characterize the rheological behaviour of the material. In this case, it is necessary to study the rheology of the material in dynamic oscillatory conditions.

In the figure below, the complex viscosity plotted against frequency of several hyaluronic acid solutions characterized by different molecular weights is reported.

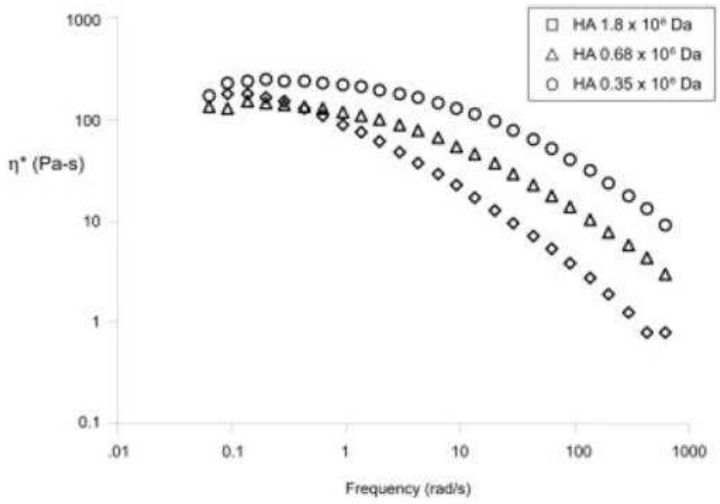

Figure 73 The complex viscosity, η*, plotted against frequency for three hyaluronate solutions of different molecular weights (0.35 x 10^6; 0.68 x 10^6 and 1.8 x 10^6 Da) (Falcone et al., 2006).

It is possible to note that the complex viscosity at low frequencies is similar for the three solutions, while at higher frequencies it decreases with increasing molecular weight. The same experiments include the measurements of G'(ω) and G"(ω) (Figure 74).

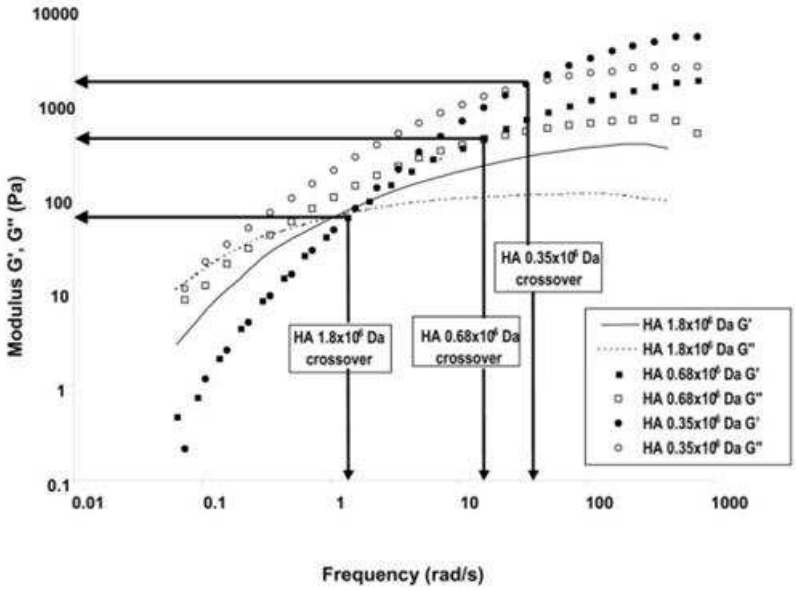

Figure 74. The frequency response of the elastic and viscous moduli for hyaluronic acid solutions of three molecular weights (0.35 x 10^6; 0.68 x 10^6 and 1.8 x 10^6 Da); the crossover points are marked for each solution. Cross-over frequency and modulus decrease as the molecular weight increases. (Falcone et al., 2006).

The cross-over points decrease with the increase of the molecular weight. For higher molecular weights, the transition from a predominantly viscous behaviour to elastic occurs at longer relaxation times. As the molecular weight of the polymer increases, it takes more time for a larger entangled polymer to disentangle and display a viscous predominant response.

From a point of view of a practical biomedical application, when hyaluronic acid is applied to injectable conditions, low molecular weight hyaluronic acid is more effective as lubricant with respect to high molecular weight, and then it should be suitable to supply synovial fluid. On the other hand, higher molecular weight hyaluronate in dynamic oscillatory conditions presents less viscosity, stiffness, and elastic response at short deformation times and these rheological properties produce a more cohesive entangled structure that rapidly and easily flows through a small orifice, rendering this polymer suitable for injectable materials (Falcone et al., 2006).

Measure of cell accessibility

A biological test to evaluate the compatibility between the dispersed phase (the µbeads) and the polymer matrix, was performed. The part of the composite filler involved in the adhesion promotion is represented by the µbeads. To prepare a composite with bioadhesive properties, beads are coated with RGD peptides. Since it is necessary that RGD peptides results available to cells to exploit their adhesive properties, we tested the biological accessibility of cells to beads when immersed in a hyaluronate solution. Hyaluronan, in fact, is a polyanion, and its possible deposition as an external layer on the bead surface, would create the risk to "cover" the peptides, making them less available to receptors and hence reducing the adhesion properties of beads. With this aim, large thiolated beads (AH-ThL) were immersed in a hyaluronate solution and their cellular adhesion was compared with the growth on the same beads immersed in simple medium and in a ChitLac polycation solution. As it is possible to note in Figure 75, the initial adhesion was the same for beads previously immersed in hyaluronic acid ("beads HA" in the graph) and in ChitLac ("beads KTL") solutions, and it was even larger with respect to beads immersed in DMEM medium ("beads DMEM"). Since no negative interference of matrix polymer was noticed, hyaluronic acid was selected to constitute the dispersive phase of the final composite filler.

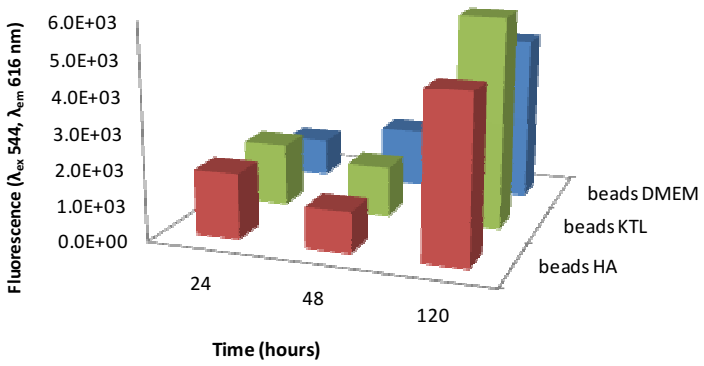

Figure 75. MG63 cells adhesion test on different types of large beads treated with different solutions: beads HA (beads treated with hyaluronic acid solution); beadsKTL (beads treated with ChitLac solution); beadsDMEM (beads treated with DMEM medium).

Particle distribution

Some physical characteristics of the particulate dried µbeads were evaluated. Below, a picture of some of them is reported.

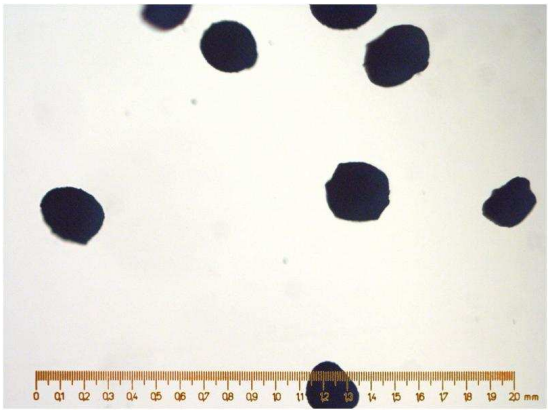

Figure 76. Picture of dried µbeads (Stereoscope LEICA DMR objective 5x/0.12 N PLAN BD). (The total ruler length is of 2 mm.

For what concerns shape, irregularity can possess both advantages and drawbacks. The irregularity is preferred to the spherical by form cells, and then it presents a better bioactivity; but under sufficient shear stress, irregular or porous particles can break into smaller particle fragments. The particulate used possess an irregular shape but does not present evident sharp corners, so no further process to remove them was necessary.

Besides, the distribution of particulate sizes was estimated. Measurements were performed by quantifying two-dimensional diameters (circular equivalent) of dried µbeads by microscope. Particles demonstrate a sharp size distribution (Figure 77), with a little fraction of small particles. Generally a uniform distribution of the dispersed phase is desirable, as it imparts consistent properties to the composite.

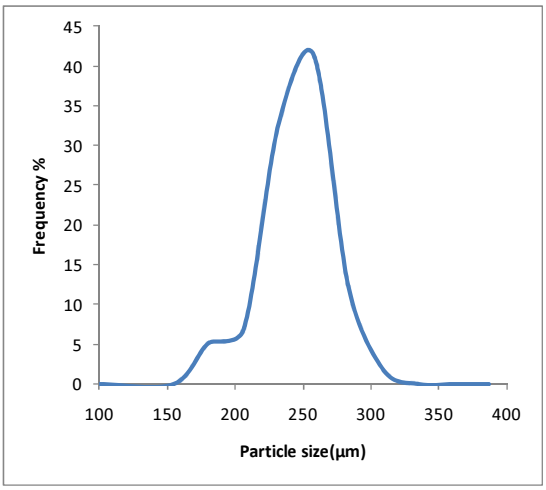

Figure 77. Particle size distribution of the dried ubeads. Measurements performed on a population of 60 µbeads. Average diameter 232 ± 26 µm; median 235 µm, asymmetry –0.38 (the distribution is approximately symmetrical).

The tight distribution is a consequence of the method used to produce µbeads: as compared to other methods of preparing ceramic µspheres described in the literature, this process presents the advantage of simplicity and it was reported that µbeads obtained by means of electrostatic beads generator present the better µsphere size distribution (Prüsse et al., 2008). Moreover, since our aim is to use the microspheres in an injectable form, their flow properties during injection will be more predictable if their shape and size are more regular.

Another characteristic surveyed was the re-swelling in water and in saline solution at the same ratio used to fill hyaluronic acid. The re-swelling was very limited at these ratios, and calculated to have an average value as low as 2%, that can be detected only at the microscopic level.

Filler construction

After having characterized the singular composite parts, the final product was prepared by mixing dried µbeads in a hyaluronic acid solution 4% w/v in the ratio of 200 µL of beads (that correspond to 146 mg of dried µbeads) in 300 µL of hyaluronic acid.

The ratio between hyaluronate solution and dried µbeads was selected to obtain composite filler similar to a paste with injectability properties, since higher volume fractions of reinforcement phase tend to improve the mechanical properties of the composites. The composite revealed good injectability and the product was not sticky. In the picture below the product composite after injection by a syringe is reported. Besides, no sedimentation effect during the time was observed.

Figure 78. Final construct of dried µbeads in a hyaluronate matrix solution

Rheological tests on the final composite

Rheological characterizations on the final product were performed to obtain information about the structure of the composite. Tests were performed both on the hyaluronic acid solution itself and on the polysaccharide filled with dried alginate-hydroxyapatite µbeads.

Performing dynamic rheology it was possible to investigate the viscoelastic response of the material under forced oscillation unveiling the internal structure. Dynamic rheological tests, such as sweep stress and frequency sweep were performed on the hyaluronic acid and the final composite.

- With the initial **stress sweep** tests it was determined the limit of the linear viscoelasticity by increasing the angle of rotation and maintaining temperature and frequency constant.
- In addition the **frequency sweep** was used to determine various characteristics of a sample across a range of frequencies obtaining viscoelasticity properties of the product.
- At the end, the **viscosity at the steady state** test was performed on the composite obtaining in this manner, an evaluation of the phase separation of the final construct.

Stress sweep test

A series of measures was performed both on hyaluronic acid solutions and on the composite. Generally, these kinds of measurements are performed to obtain a first characterization of the system. In these experiments, the material is subjected to a sinusoidally variable stress at a constant frequency which is systematically increased and the sinusoidal strain response is measured. The stress-sweep curves generally indicate that the storage modulus and the loss modulus are linear at low stresses, while at higher stresses the response is expected to be non-linear.

The measurement range of the dynamic oscillatory tests was usually chosen within the linear viscoelastic range and this range is determined by stress sweep curves. In this range the system is able to support stresses and deformations, maintaining the viscoelastic linearity. The end of linear range is conventionally chosen as that point where it is observed a deviation from linearity larger than 5%. Besides, the extent of the linear response region gives information on both the microstructure and performance characteristics.

In Figure 79, the comparison between the stress sweep curves of hyaluronic acid and the composite (indicated as filled polymer) plotted against the shear rate is reported. The curves of hyaluronate (purple and green) describe the typical trend observed for polysaccharide solutions (Falcone et al., 2006).

The trend observed for G' and G" is as expected: the elastic modulus is usually the first component that decreases because it is affected by stresses on the structure, then, G' decreases at lower stresses. If data are observed as G' and G" moduli as a function of shear rate, it is possible to note the high deformations, achievable that is a typical property of polymeric solutions that are able to deform themselves even more than 60%. For what concerns the analysis of the composite, their interpretation is more difficult because the linearity is reached already in the first part of the curve. Moduli values are larger for the composite, and the γ_c (critical) is about 3000 times lower that of hyaluronic acid alone.

Another observation regards the trend of moduli decrease. With respect to hyaluronate, the decrease is not definite, but it is composed by two intervals: a first phase ending at a deformation of 1-2% and a second interval up to 10%. This takes reference to disperse systems, and it is a clear trend at the border between dispersions and polymeric solutions. Probably, until 1% some little deformations persist that are related to weak rearrangements of the µbeads side-by-side with others beads, until a different assessment is reached. Further stresses may force beads to move in search of a new position and at this point the material collapses, it loses cohesion and the deformation is more evident.

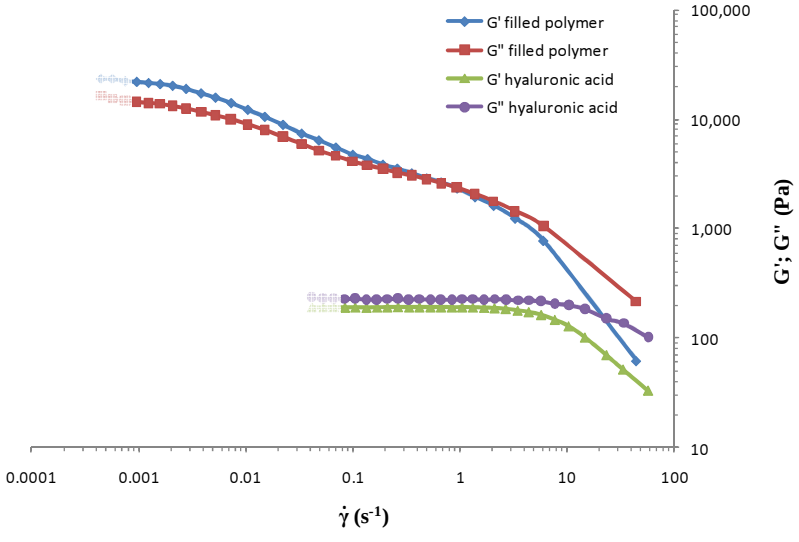

Figure 79. Stress sweep curves. Measures were performed on hyaluronic acid solutions and on µbeads dispersed on hyaluronate solution (filled polymer).

Data can be processed reporting the tan δ values that represent the weight of the component G" with respect to the component G' (Figure 80). The difference is evident: if for hyaluronate the tan delta is major then 1 because of the low elastic component, for the composite it is noticeable the contribution of the two moduli to the viscoelastic behaviour of the sample. This is in line with data reported in literature where polymer composites exhibit pronounced elastic properties with respect to the polymer matrix alone (Graebling et al., 1993).

Finally, another data elaboration of stress sweep curves is the plotting of shear stress as a function of shear rate (Figure 81). The linearity between the two functions is observed only for hyaluronic acid solution while it occupies only a range in the composite curve.

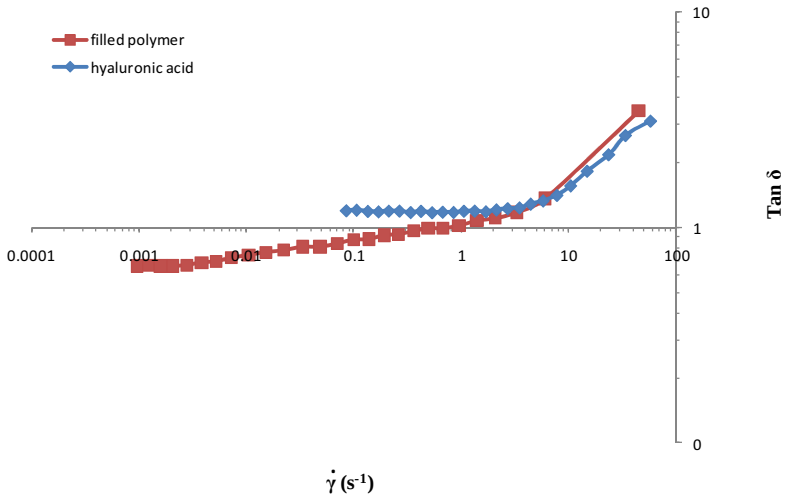

Figure 80. Tan delta of hyaluronic acid solution and composite.

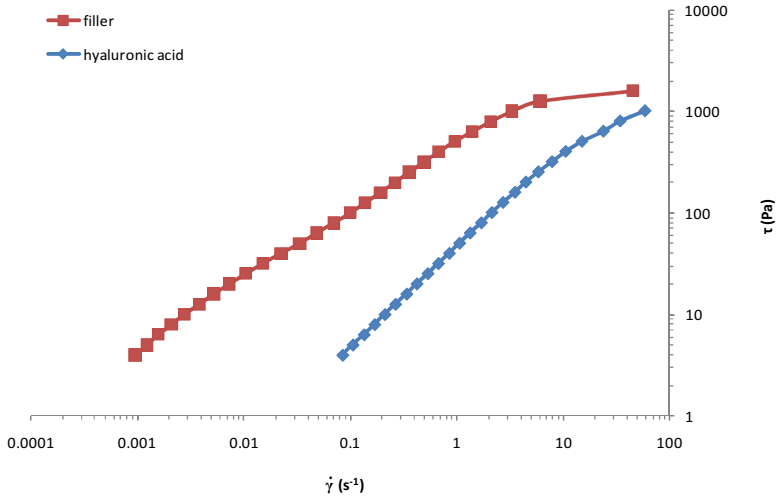

Figure 81. Shear stress as a function of shear rate.

Frequency sweep

After having tested the linear range, a frequency sweep test was performed. These measurements evaluate the viscoelastic properties of a sample as a function of the frequency applied. Several parameters can be obtained, such as G', G", and η*. The experimental curves demonstrate the evolution with frequency of the two moduli obtained in the dynamic mode. The type of modulus dominant at a particular frequency will indicate whether the fully structured material is predominantly elastic or viscous, in a process investgated on a similar time scale. The Figures below report the mechanical spectra represented by the plots of G'(ω) and G"(ω) on bi-logarithmic scales, referred to hyaluronic acid solution (Figure 82) and its composite (Figure 83).

The point where curves intersect is indicated as the "cross-over point" and represents the critical frequency (ω_c) at which the two moduli responses are equal. ω_c is a well defined point and conveniently this "cross-over" frequency and modulus were shown to be depend on the molecular weight and molecular weight distribution of some linear polymers. The cross-over point is correlated with the relaxation time:

$$\boldsymbol{\omega_c = \frac{1}{\lambda}} \qquad \textbf{(4.29)}$$

Where λ is the relaxation time and is represented by the ratio between η and G.

For what concerns the hyaluronic acid (Figure 82), the crossover of G' and G", determines two domains: at low frequency, G" > G' is a typical polymer solution behaviour while over ω_c, the elastic character of the temporary network becomes significant and as a result G' > G". A typical response for a polymer melt is to exhibit an elastic dominating behaviour at high frequencies and viscous dominated behaviour at low frequencies. In this case ω_c is about 62 sec^{-1}, indicating a very short relaxation time.

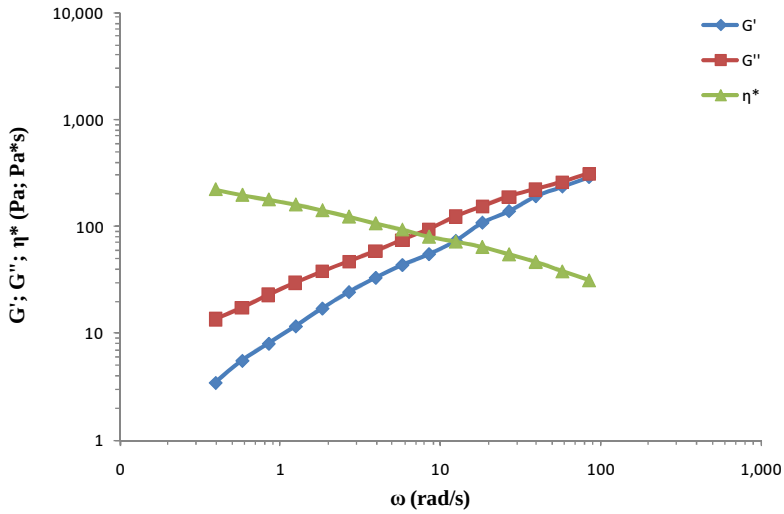

Figure 82. Frequency sweep curves of hyaluronic acid solution.

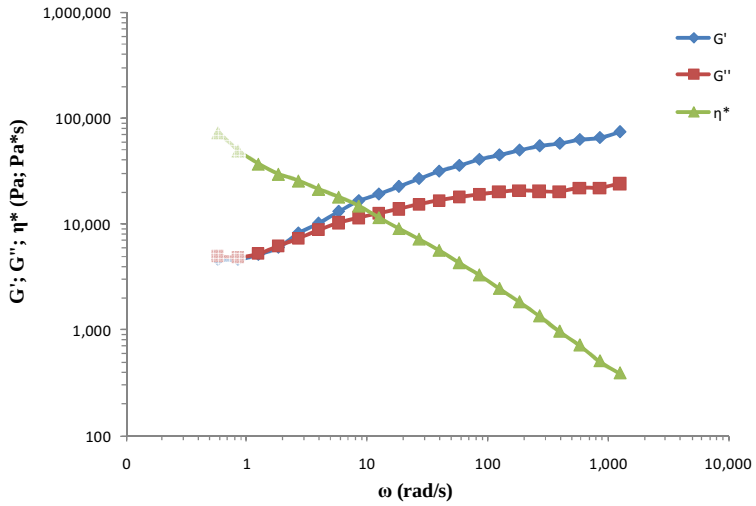

Figure 83. Frequency sweep curves of composite

In the case of composite filler (Figure 83), it is not so easy to give an interpretation of the cross-over point because of the presence, at lower frequencies, of an anomalous trend. To better identify the cross over point, the generalized Maxwell model was applied. By the application of this model it was possible to perform a comparison between cross-over points that are located with a difference of two decades, indicating a hunderfold larger response. In Figure 84 it is possible to note the shifting of the cross-over point for the composite system with respect to hyaluronic acid solution: as a whole, the cross-over increase and shifts to

lower frequency values, and moduli rise. The composite is much more elstic than hyaluronan itself.

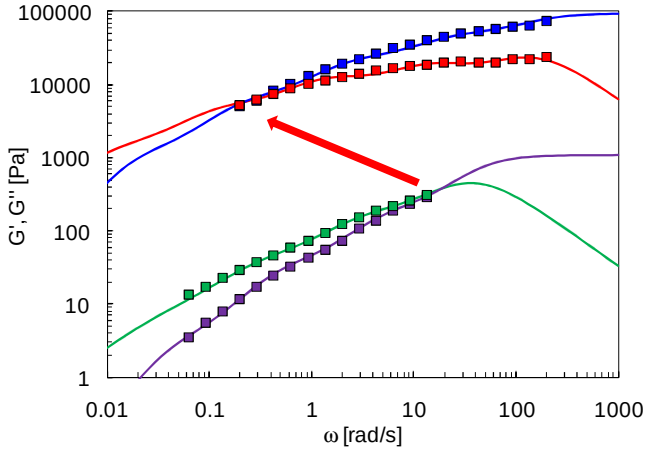

Figure 84. comparison of cross-over points of two different systems: filled polymer (blue (G') and red (G") lines) and hyaluronic acid (green and purple curves).

In addition, from the spectra of $\lambda_i(g_i)$ a comparison between relaxing times was obtained (Figure 85). The different relaxation behaviour for the two systems is clearly visible. For hyaluronic acid, there is a rapid modulus relaxation but this is 1000 times slower than filled system. At the same time, the filled system is shown to possess g_i terms 100 time larger than matrix alone. The longer relaxation times for the filled matrix reveals a higher complexity of the system as documented by the literature data (Graebling et al., 1993).

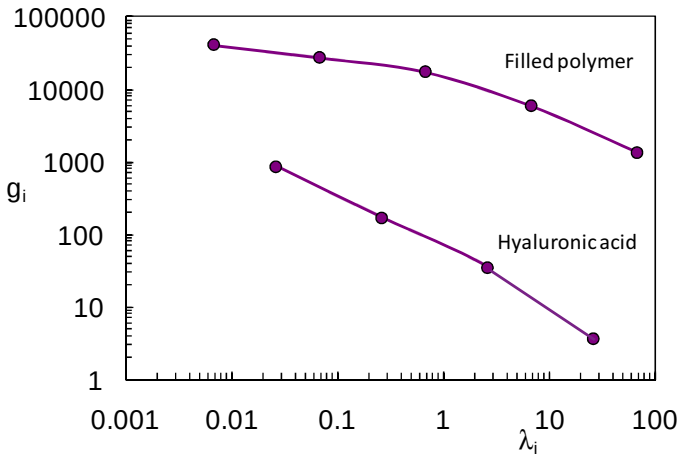

Figure 85. Relaxation times of hyaluronic acid solution and composite (filled polymer).

The increase and broadening of the relaxation time spectrum are associated with changes in the surface-layer structure and adsorption interaction, which restricts mobility, as well as their effect on the molecular packing. It can be expected that a systematic reduction in molecular mobility and an increase of the relaxation time derive as the surface area and/or the μbeads concentration increase, with an equivalent increase in the fraction of polymer in the boundary layer and a reduction in the thickness of the polymer interlayer between the particles (Lipatov et al., 1975).

Steady state

Polysaccharide solutions at high concentrations, display the non-Newtonian shear behaviour typical of polymer melts and polymer concentrated solutions. Even if these kinds of measurements are not optimal to study a composite, still it is possible to obtain from these ones information about the structure of the composite. The trend for a polymer solution at the steady state flow was reported in Figure 69. In general, they present a initial linear η_0, a decreasing curve and a non detectable η_∞. As expected, spectra reported for the final composite revealed a different trend. The plot of viscosity data against the shear rate ($\dot{\gamma}$), (Figure 86), shows that the first portion of the curve is characterized by a slow increment, as for a system with a high viscosity, and after that a negative slope is noticeable.

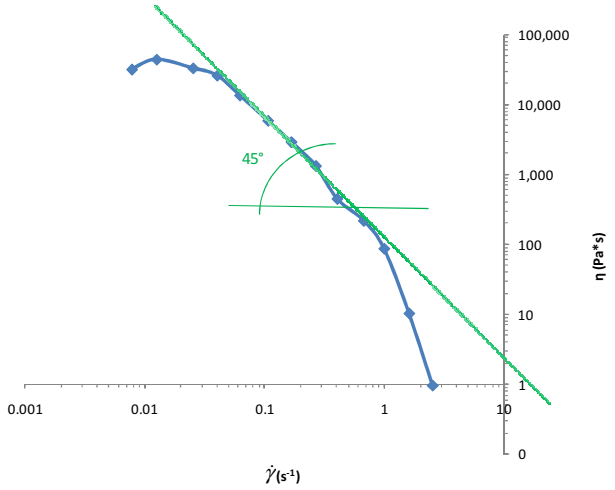

Figure 86. Flow curve of the composite

Although the negative slope is typical for polymeric solutions (see Figure 69), this is not the case for the negative slope below a conventional angle of 45°, indicating that G' > G" and then that the tested substrate behaves as an elastic solid and no longer as a viscous fluid: the granular component prevail on the viscous properties.

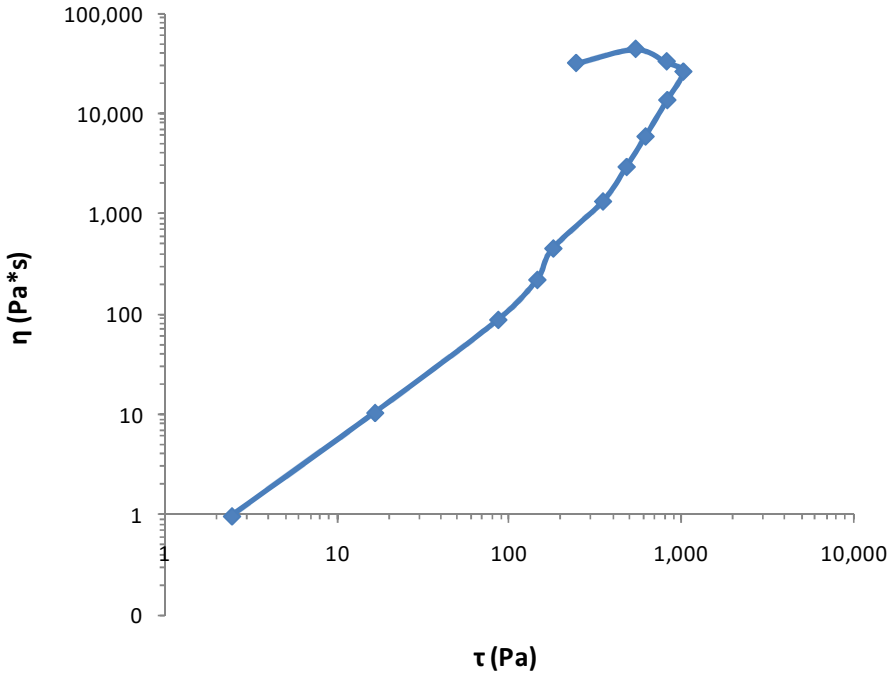

Figure 87. Flow curve of composite, data are reported as function of the shear stress.

This fact can be more evident by reporting viscosity data in function of the shear stress (Figure 87), after the fourth point a retrocession is observed, when normally, a vertical slope should be evidenced. This indicates that, in these conditions, at the fourth point the stress is sufficient to cause the coherence loss and it remains only the local friction: the composite becomes to break down after the fourth point. However it may be remembered that flow curves are not optimal tests for composite constructs. In fact, the breaking down is a predictable effect performing this kind of measurements. Attention must be focused on the linearity range and on the fact that the composite was demonstrated to be able to keep it.

4.5.3 Partial conclusions

In the design of an injectable bone filler the bioactive dried µbeads were incorporated into a polymer matrix made by a high concentration of hyaluronic acid. The properties of the two phases employed in the final construct were examined, both independently and as the entire construct. The capacity of injection and the reswelling properties of an injectable are influenced also by the granulometry of the suspended component. The size distribution of the used dried µbeads was shown to be very symmetrical, a feature that can positively influence the final performance. In addition, growth tests performed on hyaluronan-coated beads demonstrated that the polysaccharide is unable to "mask" the adhesion peptides of the beads.

A series of different rheological measurements was performed, to gain information about the viscoelastic properties and the dynamic response of the structure of the composite under stress. For a good injectable it is desirable that it flows during the injection, but that it can rapidly regain its elasticity when it occupies the site of action. This behaviour seems to be almost ideally a feature of the prepared composite. With respect to the (reference) hyaluronate solution, it its viscoelastic behaviour is greatly enhanced, with a very strong elastic component, in particular. Further work could optimize such already good performance, for instance, by varying the hyaluronic acid / µbeads ratio, or the hyaluronic acid concentration, or using a bi-modal µbeads size distribution and comparing the obtained composites with the present one by rheological tests. Finally, a study of the release of the active peptides from the dried µbeads within the composite formulation should be accompanied by the investigation of the effect of the real system on cultured cells.

CHAPTER 5. **CONCLUSIONS**

The overall objective of this study was the development and the construction of an injectable filler for application as bone graft substitute, able to promote the healing of small bone defects.

The research was focussed on the creation of a composite that associates the resorbability provided by the use of polysaccharides and some typical requirements of bone regenerative medicine as osteoconduction, osteoinduction, antimicrobial activity, and bioadhesivity. These properties are guaranteed by the employment of hydroxyapatite as a bioactive ceramic, and by the enrichment of the biomaterial with several bioactive peptides (such as the BMP fragment, LL-37, and RGD-type peptides).

With this aim, the composite design was studied stepwise, initially focussing both on the granulate and gel matrix vehicle, followed by passing to consider them as an entire construct. The particulate, composed by a core-structure of dried μbeads of alginate and hydroxyapatite, was used as a template that was properly decorated with peptides, so as to improve its bioactivity.

An important purpose of this work was to investigate the choice and the application of the optimal conjugation strategy for each peptide on the basis of the corresponding biochemical mechanisms. In this way, in some cases it resulted more advantageous to chemically immobilize the peptide, while for other peptides the electrostatic incorporation into the final construct was chosen. In some instances, modification of the polysaccharide or the peptide functionalities was necessary before proceed with the covalent coupling. The obtained materials were characterized in terms of their chemical and physical properties, and finally evaluated for their biological response *in vitro*.

The first target was the development of the granulate phase with bioadhesive properties. This was achieved by decorating μbeads with peptides containing the RGD sequence. This sequence, which belongs to fibronectin protein is able to interact with integrins localised on the cell surface of osteoblasts, mimicking the ECM, and promoting cellular adhesion. Because of its role, RGD peptides need to be bound through a covalent stable bond on the beads surface. Three chemical strategies were designed and applied, obtaining three different modified derivatives of ChitLac. The first functionalization procedure allowed to obtain the polymer called “ChitLac-(CONH)-RGD” by the conjugation of RGD peptide on a previously succinylated ChitLac, in order to introduce carboxylic groups on the polysaccharidic chain.

Unfortunately, the formation of an insoluble product inhibited its successive use for this kind of application. The conjugation of the peptide with unmodified ChitLac was performed next, obtaining the so-called “ChitLac-(NHCO)-RGD”. In this case the product was obtained with a not surprising low conjugation yield. This polysaccharide, nevertheless, revealed a higher biological pro-adhesivity, with respect to unmodified ChitLac, tested by *in vitro* experiments. The last strategy, more selective, involved the functionalization of ChitLac with thiol groups: the obtained product, ChitLac-SH, demonstrated a high capacity to form disulfide bonds with a RGD peptide containing a cysteine, and following this strategy, two kinds of beads were produced and compared. In fact, alginate/HAp beads were prepared, with the polycation either dispersed in it or coating the bead surface. The successive conjugation with peptide, led to beads with different distribution and localization of RGD.

Tests carried out on osteoblasts cultures revealed that all microbead types were devoid of any detectable cytotoxicity. Experiments on the same type of cells indicated that beads layered with ChitLac-SH and treated with RGD peptide (ChitLac-(SS)-CRGDS) (AH-ThL) showed excellent bioadhesive properties.

The second goal was the insertion of BMP-2 fragment peptides into the granulate, generating a delivery system of the peptide. BMP-2 is implicated in bone morphogenesis and promotes the differentiation of MSCs to osteoblasts. The entire recombinant protein is already approved by FDA for clinical specific uses, but the question of the design of a correct delivery system remains open. In this work, two release mechanisms have been explored to respond to biomolecular requirements of the body. In fact, literature reports a temporal activity of the BMP-2 that ranges from the first day to the third week of fracture repair. It is therefore necessary to assure a first burst release of the peptide, followed by a slower but constant one.

The first release was obtained by peptide encapsulation and occurred by simple diffusion from alginate/hydroxyapatite beads. The release profile showed a rapid burst peptide discharge that was considered useful during the first phase of fracture repair. To obtain a second type of release (*i.e.* allowing to discharge the peptide slowly and constantly during the long period of the fracture repair) a system sensitive to enzymatic action was prepared. In particular a ChitLac derivative was prepared, containing an enzymatically cleavable linker. The latter was then functionalized with a BMP fragment by means of a very selective chemical strategy known as “click-chemistry”.

The synthesis of the enzymatic cleavable spacer started from a hydrolyzed γ-valerolactone, to obtain in three steps a molecule that presents an ester group and a final functional group for

click chemistry (azido group). The spacer was used to conjugate it to ChitLac to obtain the so-called "ChitLac-azido". During this reaction the bidimensional analyses ^{1}H NMR revealed the ability of linker molecules to give rise to micelles in water; this problem was never reported before in click chemistry reactions. A wide characterization by capillary electrophoresis and ^{1}HNMR was conducted and it permitted the coupling of the spacer on ChitLac chains. The release of the linker after treatment with an esterase was verified and the possible inhibiting effect of the polymer was excluded. On the other hand the synthesis of a BMP fragment functionalized with an alkyne group to perform the click reaction was achieved and the click reaction was performed. The final product named "ChitLac-(click)-BMP" was characterized by ^{1}H NMR and capillary electrophoresis.

The achievement of an antimicrobial granulate was the third aim of this work. The use of a peptide like LL-37 that is a human antimicrobial peptide belonging to the cathelicidin family, was explored. Since it is a human endogenous peptide, LL-37 could be useful for biomedical applications, but its significant toxicity on mammalian cells, has limited so far its possible application in biomaterial field. Data of literature report the ability of charged polysaccharides, especially alginate, to induce α-helical conformation in this peptide; the same conformation that is involved in the antimicrobial effect. A circular dichroism study was performed to examine the conformations induced in the peptide structure by three different polysaccharides by means of these interactions. In detail, the study regarded the interaction induced by two polyanions, alginate and hyaluronic acid, and a polycation, ChitLac. Alginate confirmed its role of helicogenic molecule, while in contrast, ChitLac had not effect, and was not able to compete with the helicogenic effect of alginate in a mixture alginate/LL-37. Hyaluronic acid presented an intermediate behaviour, being helicogenic only at low ionic strengths, and this was reflected in an inability to modulate cytotoxicity on mammalian cells, differently by alginate that was able to abolish the cytotoxic effect of LL-37 up to a peptide concentration of 50 µM. So, the Alginate/LL-37 mixture appeared to be a potential antimicrobial system capable of reducing the toxic effect of the peptide towards mammalian cells in defined ratios of peptide/polysaccharide. The capacity to arrest the growth of Gram-negative bacteria was verified at 2-10 µM, a concentration that resulted to be completely safe in terms of cytotoxicity; in contrast, the peptide/polyanion mixture was poorly or not at all effective on Gram-positive bacteria. This different behaviour is related to the different bacterial wall composition and to the presence of negatively charged LPS, which are able to shift the peptide/alginate equilibrium, while in the case of Gram-positive bacteria, the charge

on the bacterial wall likely is not sufficient to displace LL-37. Driven by the exciting possibility to effectively modulate the action of LL-37 by means of its interaction with alginate, we tested the use of the peptide/PS complexes in localized (semi)solid systems, for orthopaedic applications. With this aim, the electrostatic interaction between LL-37 and alginate was exploited either to entrap the peptide in alginate beads or to adsorb it on the surface of alginate scaffolds. In both cases, albeit with different mechanism and time courses, the bacterial growth was not inhibited for the common cause that the electrostatic interaction binding the cationic peptide to the polyanions is so strong as to annihilate the concentration of "free" peptide necessary to kill bacteria.

The latter point of this work regarded the incorporation of dried μbeads into a polymer matrix constituted by hyaluronic acid at high concentration. The properties of the two phases employed in the final construct were examined, both independently and mixed to give the final construct. First, the granulometry of the particulate was examined in terms of size and size distribution; this one resulted to be very symmetrical: such quality is thought to be able to positively influence the final performance of injectability. In addition, biological growth tests performed on hyaluronan-coated beads demonstrated that the polysaccharide is unable to "mask" the adhesion peptides of the beads. After having assembled the composite, the rheological properties of matrix polymer and composite were evaluated. In particular, tests were performed to obtain information about the viscoelastic properties and dynamic response of the structure composite under stress. It may be desirable that during a hypothetic injection the material flows, but it should rapidly regain its elasticity when occupies the site of action.

This behaviour seemed to be a feature of the prepared composite. In fact, with respect to the polymer hyaluronan matrix, the viscoelastic behaviour denoted a very strong elastic component.

In summary, many types of peptide-polysaccharide conjugations were considered in this Thesis work: stable covalent bond and exposition of the peptide at the surface, electrostatic interactions for a release by diffusion or degradation of the gel network and enzymatically cleavable covalent bond. Even if the development of these systems was based on the functionality and bioactivity mechanisms of specific peptides, the used strategies can be potentially exported to a large variety of bioactive molecules and supporting polymers, introducing simple variations in the used chemistry.

The initial aim of this work was to prepare an injectable filler endowed with desired biological properties: the results obtained, even though very preliminary, showed that we are on the right way to achieve it.

Ongoing experiments concern the study of the pro-differentiative action of ChitLac-(click)-BMP, the preparation of beads with BMP BOTH entrapped AND linked to ChitLac, to verify the hypothesis on the release model we have so far set forth. Finally, as to LL-37, a further evaluation of the correct conformation and the maintenance of activity of the peptide during the bead degradation is under consideration. Finally, future challenges will regard *in vivo* tests.

As final goal one can imagine the preparation of a construct with a proper mixture of beads, each of them enriched with one the three different peptides dispersed in the hyaluronate matrix, so to provide the biomaterial the property to stimulate both adhesion and osteogenesis, and to protect the site of implantation from bacterial infections.

CHAPTER 6. **ACKNOWLEDGEMENTS**

First, I would like to thank my supervisor Prof. Sergio Paoletti for admitting me into his program and for providing the necessary support to conduct the research presented in this thesis work.

I would like to thank Prof. Gudmund Skjåk-Bræk for accepting the role of external supervisor.

I would like to thank my tutor Dr. Anna Coslovi for her precious guidance, support and perseverance through the course of my research. She is a strategist of the chemical synthesis.

Rheological measurements were achieved in the laboratory of Prof. Romano Lapasin and I desire to thank him for the analyses and the meticulous elucidations.

NMR analyses were achieved in the CBM laboratory and I desire to thank Dr. Nicola D'Amelio for helping me by means of his experience in NMR spectroscopy.

I would like to thank Prof. Alessandro Tossi for letting me use his laboratory equipment for the synthesis of peptides, and Dr. Nikolinka Antcheva for her support.

I would like to thank Dr. Monica Benincasa and Dr. Chiara Pelillo for helping me in performing bacteria tests.

I would like to thank Dr. Micaela Grandolfo of SISSA for confocal measurements.

A special thank to Dr. Eleonora Marsich for assisting me in performing biological tests and to Dr. Ivan Donati and the other staff members of the Paoletti's group.

My most sincere thanks go to Bracco Imaging group for giving me the possibility to take advantage of the laboratories in AREA Science Park in Basovizza, especially of the instruments for characterization and chemical synthesis; it was my pleasure to work together with good scientists like Dr. Cristiana Campa, Dr. Marco Rossi, Dr. Anna Flamigni, Dr. Valentina Sartorelli, Dr. Adele Pasqua, Dr. Andreina Toraldo and Dr. Sara Varricchio.

CHAPTER 7. **REFERENCES**

Agrawal, C.M. and Ray, C.B., 2001. Biodegradable polymeric scaffolds for musculoskeletal tissue engineering. *J. Biomed. Mater. Res.*, 55, p.141–150.

Aimin, C., Chunlin, H., Juliang, B., Tinyin, Z. and Zhichao, D., 1999. Antibiotic loaded chitosan ar. An in vitro, in vivo study of a possible treatment for osteomyelitis. *Clin. Orthop. Relat Res.*, 366, pp.239-47.

Akiyama, S., Katagiri, T., Namiki, M., Yamaji, N., Yamamoto, N., Miyama, K., Shibuya, H., Ueno, N., Wozney, J.M. and Suda, T., 1997. Constitutively active BMP type I receptors transduce BMP-2 signals without the ligand in C2C12 myoblasts. *Experimental Cell. Res.*, 235, pp.362-69.

Alberaola, N.D., Fernagut, F. and Mele, P., 1997. Binary and ternary particulate composites. I. Viscoelastic behaviour. *J. Appl. Polym. Sci.*, 63, pp.1029-40.

Alsani, P. and Kennedy, R.A., 1996. Studies on diffusion in alginate gels. I. Effect of cross-linking with calcium or zinc ions on diffusion of acetaminophen. *J. Control. Release*, 42, pp.75-82.

Alsberg, E., Anderson, K.W., Albeiru, A., Rowley, J.A. and Mooney, D.J., 2002. Engineering growing tissues. *Proc. Natl. Acad. Sci. USA*, 99, pp.12025-.

Altankov, G., Grinnell, F. and Groth, T., 1996. Studies on the biocompatibility of materials: Fibroblast reorganization of substratum-bound fibronectin on surfaces varying in wettability. *J Biomed Mater Res*, 30, pp.385-91.

Anderson, J.M., 2001. Biological responses to materials. *Annu. Rev. Mater. Res.*, 31, pp.81-110.

Andersson, E., Rydengård, V., Sonesson, A., Mörgelin, M., Björck, L. and Schmidtchen, A., 2004. Antimicrobial activities of heparin-binding peptides. *Eur. J. Biochem.*, 271, pp.1219-26.

Anon., 2007. Tissue Engineering and Regeneration. In *Principles of Regenerative Biology*. Academic Press. Inc. pp.259-70.

Anselme, K., 2000. Osteoblast adhesion on biomaterials. *Biomaterials*, pp.667-81.

Arias, C.A. and Murray, B.E., 2009. Antibiotic-resistant bugs in the 21st century - A clinical super-challenge. *N. Engl. J. Med.*, 306(5), pp.439-43.

Athanasiou, K.A., Shah, A.R., Hernandez, R.J. and LeBaron, R.G., 2001. Basic science of articular cartilage repair. *Clin. Sports Med.*, 20, pp.223-47.

Axelrad, T.W. and Einhorn, T.A., 2009. Bone morphogenetic proteins in orthopaedic surgery. *Cytokine Growth Factor Rev.*, 20, pp.481-88.

Axelrad, T.W., Steen, B., Lowenberg, D.W., Creevy, W.R. and Einhorn, T.A., 2008. Heterotropic ossification after use of commercially avaialble recombinant human bone morphogenetic proteins in four patients. *J. Bone Joint Surg. Br.* , 90, pp.1617-22.

Bais, M.V., Wigner, N., Young, M., Toholka, R., Graves, D.T., Morgan, E.F., Gerstenfeld, L.C. and Einhorn, T.A., 2009. BMP2 is essential for post natal osteogenesis but not for recruitment of osteogenic stem cells. *Bone*, 45, pp.254-66.

Baldwin, R.L., 1996. How Hofmeister ion interactions affect protein stability. *Biophysical Journal*, 71, pp.2056-63.

Bals, R. and Wilson, J.M., 2003. Cathelicidins - a family of multifunctionla antimicrobial peptides. *Cell. Mol.Life Sci.*, 60, pp.711-20.

Barbucci, R., Lamponi, S., Borzacchiello, A., Ambrosio, L., Fini, M., Torricelli, P. and Giardino, R., 2002. Hyaluronic acid hydrogel in the treatment of osteoarthritis. *Biomaterilas*, 23, pp.4503-13.

Bax, B.E., Wozney, J.M. and Ashhurst, D.E., 1999. Bone morphogenetic protein-2 increases the rate of callus formation after fracture of the rabbit tibia. *Calcif. Tissue Int.*, 65, pp.83-89.

Becer, C.R., Hoogenboom, R. and Schubert, U.S., 2009. Click chemistry beyond metal-catalyzed cycloaddition. *Angew. Chem. Int. Ed.*, 48, pp.2-11.

Becker, D., Geißler, U., Bierbaum, S., Scharnweber, D., Worch, H. and Wenzel, K.W., 2002. Proliferation and differentation of rat calvarial osteoblasts on type I collagen-coated titanium alloy. *J Biomed Mater Res*, 59, pp.516-27.

Beer, J.H., Springer, K.T. and Coller, B.S., 1992. Immobilized Arg-Gly-Asp (RGD) peptides of varying lenghts as structural probes of the platelet glycoprotein IIb/IIIa receptor. *Blood*, 79, pp.117-28.

Benincasa, M., Mattiuzzo, M., Herasimenka, Y., Cescutti, P. and Rizzo, R., 2009. Activity of anyimicrobial peptides in the presence of polysaccharides produced by pulmonary pathogens. *J. Pept. Sci.*, 15, pp.595-600.

Bennett, J.H., Carter, D.H., Alavi, A.L., Beresford, J.N. and Walsh, S., 2001. Patterns of integrin expression in a human mandibular explant model of osteoblast differentation. *Archives of Oral Biology*, 46, pp.229-38.

Bernkop-Schnürch, A., Hornof, M. and Zoidl, T., 2003. Thiolated polymers-thiomers: synthesis and in vitro evaluation of chitosan-2-iminothiolane conjugates. *Int. J. Pharm.*, 260, pp.229-37.

Bessa, P.C., Casal, M. and Reis, R.L., 2008. Bone morphogenetic proteins in tissue engineering: the road from laboratory to clinic, part II (BMP delivery). *J. Tissue Eng. Regen. Med.* , 2, pp.81-96.

Bessa, P.C., Casal, M. and Reis, R.L., 2008. Bone morphogenetic proteins in tissue engineering: the road from the laboratory to the clinic, part I (basic concepts). *J. Tissue Eng. Regen. Med.*, 2, pp.1-13.

Blanquaert, F., Barritault, D. and Caruelle, J.P., 1999. Effects of heparan-like polymers associated with growth factors on osteoblast proliferation and phenotype expression. *J. Biomed. Mater. Res.*, 44, pp.63-72.

Boman, H.G., 1995. Peptide antibiotics and their role in innate immunity. *Annu. Rev. Immunol.*, 13, pp.61-61.

Bonfield, W., 1988. Hydroxyapatite-reinforced polyethylene as an analogous materila for bone replacement. *Ann. NY Acad. Sci.* , 523, pp.173-77.

Bowdish, D.M., Davidson, D.J. and Hancock, R.E., 2005. The human cationic peptide LL-37 induces activation of the extracellular signal-regulated kinase and p38 kinase pathways in primary human monocytes. *Curr. Protein Pept. Sci.*, 268, pp.35-51.

Boyle, W.J., Simonet, W.S. and Lacey, D.L., 2003. Osteoclast differentiation and activation. *Nature*, 423, pp.337-42.

Brekke, J.S., 1996. A rationale for delivery of osteoinductive proteins. *Tissue Eng.* , 2(2), pp.97-114.

Brogden, K.A., 2005. Antimicrobial peptides: pore formers or metabolic inhibitors in bacteria? *Nat. Rev. Microbiol.*, 3, pp.238-50.

Brown, M.B. and Jones, S.A., 2005. Hyaluronic acid: a unique topical vehicle for the localized delivery of drugs to the skin. *J. Eur. Acad. Dermatol. Venereol.*, 19(3), pp.308-18.

Bulpitt, P. and Aeschlimann, D., 1999. New strategy for chemical modification of hyaluronic acid: preparation of functionalized derivatives abd their use in the formation of novel biocompatible hydrogels.. *J.Biomed. Mater. res.* , 47, pp.152-.

Buranapanitkit, B., Srinilta, V., Ingviga, N., Oungbho, K., Geater, A. and Ovatlarnporn, C., 2004. The efficacy of a hydroxyapatite composite as a biodegradable antibiotic delivery system. *Clin. Orthop. Relat. Res.*, 424, pp.244-52.

Burg, K.J., Porter, S. and Kellam, F., 2000. Biomaterial developments for bone tissue engineering. *Biomaterials*, 21, pp.2347-59.

Burr, D.B., Robling, A.G. and Turner, C.H., 2002. Effects of biomechnical stress on bones animals. *Bone*, 30, pp.781-86.

Cai, K., Hu, Y., Jandt, K.D. and Wang, Y., 2007. Surface modification of titanium thin film with chitosan via electrostatic self-assembly technique and its influence on osteoblast growth behavior. *J Mater Sci: Mater Med*.

Campoccia, D., Montanaro, L. and Arciola, C.R., 2006. The significance of infection related to orthopedic devisces and issues of antibiotic resistence. *Biomaterials*, 27, pp.2331-39.

Campos, M.A., Vargas, M.A., Regueiro, V., Llompart, V., Alberti, S. and Bengoechea, J.A., 2004. Capsule polysaccharide mediates bacterial resistance to antimicrobial peptides. *Infect. Immun.*, 72, pp.7107-14.

Celil, A.B., Hollinger, J.O. and Campbell, P.G., 2005. Osx transcriptional regulation is mediated by additonal pathways to BMP2/Smad signaling. *J. Cell. Biochem.*, 95, pp.518-28.

Chan, C., Borrows, L.L. and Deber, C.M., 2004. Helix induction in antimicrobial peptides by alginate in biofilms. *J. Biol. Chem.*, 279(37), pp.38749-54.

Chan, C., Burrows, L.L. and Deber, C.M., 2005. Alginate as an auxiliary bacterial membrane: binding of membrane-active peptides by polysaccharides. *J. Peptide Res.*, 65, p.343–351.

Chen, C., Grzegorzewski, K.J., Barash, S., Zhao, Q., Schneider, H., Wang, Q., Singh, M., Pukac, L., Bell, A.C., Duan, R., Coleman, T. and al., e., 2003. An integrated functional genomics screening program reveals a role for BMP-9 in glucose homeostasis. *Nat. Biotechnol.*, 21, pp.294-301.

Chen, Y., Hata, A., Lo, R.S., Wotton, D., Shi, Y., Pavletich, N. and Massagué, J., 1998. Determinants of specificity in TGF-β signal transduction. *Genes Dev.*, 12, pp.2144-52.

Chenite, A., Chaput, C., Wang, D., Combes, C., Buschmann, M.D., Hoemann, C.D., Leroux, J.C., Atkinson, B.L., Binette, F. and Selmani, A., 2000. Novel injectable neutral solutions of chitosan form biodegradable gels in situ. *Biomaterials*, 21, pp.2155-61.

Chen, F., Wu, Z., Sun, H., Wu, H., Xin, S., Wang, Q., Dong, G., Ma, Z., Huang, S., Zhang, Y. and Jin, Y., 2006. Release of bioactive BMP from dextran-derived microspheres: a novel delivery concept. *Int. J. Pharm.*, 307, pp.23-32.

Chen, Y.H., Yang, J.T. and Chan, K.H., 1974. Determination of the helix and β-form of proteins in aqueous solution by circular dichroism. *Biochemistry*, 13, pp.3350-59.

Chen, H., Yuan, L., Song, W., Wu, Z. and Li, D., 2008. Biocompatible polymer materials: role of protein–surface interactions. *Prog. Polym. Sci.*, 33, pp.1059-87.

Cho, T., Gerstenfeld, L.C. and Einhorn, T.A., 2002. Differential temporal expression of members of the transforming growth factor β superfamily during murine fracture healing. *J. Bone Miner. Res.*, 17(3), pp.513-20.

Cho, Y., Yeo, S., Park, J., Shin, H., Bae, Y. and Suh, J., 2008. The effects of synthetic peptide derived from hBMP-2 on bone formation in rabbit calvarial defect. *Tissue Eng. Regen. Med.*, 5(3), pp.488-97.

Chua, P.H., Neoh, K.G., Kang, E.T. and Wang, W., 2008. Surface functionalization of titanium with hyaluronic acid/chitosan polyelectrolyte multilayers and RGD for promoting osteoblast functions and inhibiting bacterial adhesion. *Biomaterials*, x, p.444.

Ciornei, C.D., Sigurdardottir, T., Schmidtchen, A. and Bodelsson, M., 2005. Antimicrobial and chemoattractant activity, lipopolysaccaride neutralization, cytotoxicity, and inhibition by serum of analogs of human cathelicidin LL-37. *Antimicrob. Agents Chemother.*, 49(7), pp.2845-50.

Ciornei, C.D., Sigurdardóttir, T., Schmidtchen, A. and Bodelsson, M., 2005. Antimicrobial and chemoattractant activity, lipopolysaccharide neutralization, cytotoxicity, and inhibition by serum of analogs of human cathelicidin LL-37. *Antimicrob. Agents Ch.*, 49(7), pp.2845-50.

Clementi, F., 1997. Alginate production by Azotobacter vinelandii. *Crit. Rev. Biotechnol.*, 17, pp.327-61.

Comisar, W.A., Kazmers, N.H., Mooney, D.J. and Linderman, J.J., 2007. Engineering RGD nanopatterned hydrogels to control preosteoblast behavior: a combined computational and experimental approach. *Biomaterials*, 28, pp.409-4417.

Cook, A.D., Hrkach, J.S., Gao, N.N., Johnson, I.M. and Pajvani, U.B., 1997. Characterization and development of RGD-peptide-modified poly(lactic acid-co-lysine) as an interactive, resorbable biomaterial. *J. Biomed. Mater. Res.*, 35, pp.513-23.

Coviello, T., Matricardi, P., Marianecci, C. and Alhaique, F., 2007. Polysaccharide hydrogels for modified release formulations. *J. Control. Release*, 119, p.5–24.

Cowles, E.A., Brailey, L.L. and Gronowicz, G.A., 2000. Integrin-mediated signaling regulates AP-1 transcription factors and proliferation in osteoblasts. *J Biomed Mater Res*, 52, pp.725-37.

Crescenzi, V., Cornelio, L., Di Meo, C., Nardecchia, S. and Lamanna, R., 2007. Novel hydrogels via click chemistry: synthesis and potential biomedical applications. *Biomacromolecules*, 8, pp.1844-50.

Daar, A.S. and Greenwood, H.L., 2007. A proposed definition of regenerative medicine. *J. Tissue Eng Regen Med*, 1, pp.179-84.

Dathe, M., Nikolenko, H., Meyer, J., Beyermann, M. and Bienert, M., 2001. Optimization of the antimicrobial activity of magainin peptides by modification of charge. *FEBS Lett.*, 501(2-3), pp.146-50.

Dathe, M. and Wieprecht, T., 1999. Structural features of helical antimicrobial peptides: their potential to modulate activity on model membranes and biological cells. *Biochim. Biophys. Acta*, 1462(1-2), pp.71-87.

Dee, K.C., Puleo, D.A. and Bizios, R., 2002. Protein-surface interactions. In *An Introduction to Tissue-Biomaterial Interactions*. John Wiley & Sons, Inc. pp.37-51.

den Boer, F.C., Bramer, J.A., Blokhuis, T.J., van Soest, E.J., Jenner, J.M., Patka, P., Bakker, F.C., Burger, E.H. and Haarman, H.J., 2002. Efect of recombinant human osetogenic prtoein-1 on the healing of a freshly closed diaphyseal fracture. *Bone*, 31(1), pp.158-64.

Derynck, R. and Zhang, Y.E., 2003. Smad-dependent and Smad-independent pathways in TGF-β family signalling. *Nature*, 425, pp.577-84.

Desimoni, E., 1996. In *Chimica analitica - Equilibri ionici e fondamenti di analisi chimica quantitativa*. Bologna: CLUEB. p.147.

Dettin, M., Conconi, M.T., Gambaretto, R., Bagno, A., Di Bello, C., Menti, A.M., Grandi, C. and Parnigotto, P.P., 2005. Effect of synthetic peptides on osteoblast adhesion. *Biomaterials*, 26, pp.4507-15.

Dimitriou, R., Tsiridis, E. and Tsiridis, P.E., 2005. Current concepts of molecular aspects for bone healing. *Injury, Int. J. Care Injured*, 36, p.1392—1404.

Domenico, P., Salo, R.J., Cross, A.S. and Cunha, B.A., 1994. Polysaccharide capsule-mediated resistance to Opsonophagocytosis in Klebsiella pneumoniae. *Infect. Immun.*, 62, pp.4495-99.

Donati, I., Coslovi, A., Gamini, A., Skjåk-Bræk, G., Vetere, A., Campa, C. and Paoletti, S., 2004. Galactose-substituted alginate 2: confromational aspects. *Biomacromolecules*, 5, pp.186-96.

Donati, I., Holtan, S., Mørch, Y.A., Borgogna, M., Dentini, M. and Skjåk-Bræk, G., 2005. New hypothesis on the role of alternating sequences in calcium-alginate gels. *Biomacromolecules*, 6, pp.1031-40.

Donati, I. and Paoletti, I., 2009. Material properties of alginates. In B.A. Rehm, ed. *Alginates: biology and applications*. Berlin: Springer. pp.1-53.

Donati, I., Stredanska, S., Silvestrini, G., Vetere, A., Marcon, P., Marsich, E., Mozetic, P., Gamini, S., Paoletti, S. and Vittur, F., 2005. The aggregation of pig articular chondrocyte and synthesis of extracellular matrix by a lactose-modified chitosan. *Biomaterials*, 26, pp.987-98.

Dorozhkin, S.V., 2009. Calcium orthophosphate-based bicomposites and hybrid biomaterilas. *J. Mater. Sci.*, 44, pp.2343-87.

Draget, I.K., Smidsrød, O. and Skjak-Bræk, G., 2005. Alginates from algae. In *Polysaccharides and polyamides in the food industry. Properties, production and patents*. Steinbuchel A, Rhee S K.

Ducy, P., Schinke, T. and Karsenty, G., 2000. The Osteoblast: A Sophisticated Fibroblast under Central Surveillance. *Science*, 289, pp.1501-04.

Du, M., Zheng, Q. and Yang, H.M., 2003. Dynamic rheological behaviour for polymer composites filled with particles. *J. Soc. Rheol. Japan*, 31(5), pp.305-11.

Eid, K., Chen, E., Griffith, L. and Glowacki, J., 2001. Effect of RGD coating on osteocompatibility of PLGA-polymer disks in a rat tibial wound. *J Biomed Mater Res*, 57, pp.224-31.

Einhorn, T.A., Majeska, R.J. and Mohaideen, A., 2003. A single percutaneous injection of recombinant human bone morphogenetic protein-2 accelerates fracture repair. *J. Bone Joint Surg. Am*, 85A, pp.1425-145.

Elbert, D.L. and Hubbell, J.A., 2001. Conjugate addition reactions combined with free-radical cross-linking for the design of materials for tissue engineering. *Biomacromolecules*, 2, pp.430-41.

Elmengaard, B., Bechtold, J.E. and Søballe, K., 2005. In vivo study of the effect of RGD treatment on bone ongrowth on press-fit titanium alloy implants. *Biomaterials*, 26, pp.3521-26.

Etrych, T., Leclercq, L., Boustta, M. and Vert, M., 2005. Polyelectrolyte complex formation and stability when mixing polyanions and polycations in salted media: A model study related to the case of body fluids. *Eur. J. Pharm. Sci.*, 25, pp.281-88.

Evangelista, M.B., Hsiong, S.X., Fernandes, R., Sampaio, P., Kong, H.J., Barrias, C.C., Salema, R., Barbosa, M.A., Mooney, D.J. and Granja, P.L., 2007. Upregulation of bone cell differentiation through immobilization within a synthetic extracellular matrix. *Biomaterials*, 28, pp.3644-55.

Falcone, S.J., Palmieri, D.M. and Berg, R.A., 2006. Rheological and cohesive porperties of hyaluronic acid. *J. Biomed. Mater. Res.*, 76A, pp.721-28.

Ferris, D.M., Moodie, G.D., Dimond, P.M., Gioranni, C.W., Ehrlich, M.G. and Valentini, R.F., 1999. RGD-coated titanium implants stimulate increased bone formation in vivo. *Biomaterials*, 20, pp.2323-31.

Fields, G.B., Lauer, J.L., Dori, Y., Forns, P., Yu, Y. and Tirrell, M., 1998. Proteinlike molecular architecture: biomaterial applications for inducing cellular receptor binding and signal transduction. *Biopolymers*, 47, pp.143-51.

Foschiatti, M., Cescutti, P., Tossi, A. and Rizzo, R., 2009. Inhibition of cathelicidin activity by bacterial exopolysaccharides. *Macromolecular Microbiology*, 72, pp.1137-46.

Fu, K., Xu, Q., Czernuszka, J., McKenna, C.E., Ebetino, F.H., Graham, R., Russel, G., Triffitt, J.T. and Xia, Z., 2010. Prolonged osteogenesis from human mesenchymal stem cells implanted in immunodeficient mice by using coralline hydroxyapatite icorporating rhBMP2 microspheres. *J. Biomed. Mater. Res.* , 92A, pp.1256-64.

Gabriel, M., Nazmi, K., Veerman, E.C., Amerongen, A.V. and Zentner, A., 2006. Preparation of LL-37-grafted titanium surfaces with bactericidal activity. *Bioconjugate Chem.*, 17, pp.548-50.

García, A.J., 2005. Get a grip: integrins in cell–biomaterial interactions. *Biomaterials*, 26, pp.7525-29.

García, A.J., 2006. Interfaces to control cell-biomaterial adhesive interactions. *Adv Polym Sci*, 203, pp.171-90.

García, A.J. and Reyes, C.D., 2005. Bio-adhesive surfaces to promote Osteoblast differentation and bone formation. *J Dent Res*, 84(5), pp.407-13.

Gåserød, O., Smidsrød, O. and Skjåk-Bræk, G., 1998. Microcapsules of alginate-chitosan - I: A quantitative study of the interaction between alginate and chitosan. *Biomaterials*, 19, pp.1815-25.

Geißler, U., Hempel, U., Wolf, C., Scharnweber, D., Worch, H. and Wenzel, K.W., 2000. Collagen type I-coating of Ti6Al4V promotes adhesion of osteoblasts. *J Biomed Mater Res*, 51, pp.752-60.

George, M. and Abraham, T.E., 2006. Polyionic hydrocolloids for the intestinal delivery of protein drugs: alginate and chitosan - a review. *J. Control. Release*, 114, p.1–14.

Giangaspero, A., Sandri, L. and Tossi, A., 2001. Anphipatic α-helical antimicrobial peptides. *Eur. J. Biochem.*, 268, pp.5589-600.

Gilboa, L., Nohe, A., Geissendörfer, T., Sebald, W., Henis, Y.I. and Knaus, P., 2000. Bone morphoegentic protein receptor complexes on the surface of live cells: a new oligomerization mode for serine/threonine kinase receptors. *Mol. Biol. Cell.*, 11, pp.1023-35.

Govan, J.R., Fyfe, J.A. and Jarman, T.R., 1981. Isolation of alginate-producing mutants of Pseudomonas flurescens, Pseudomonas pputida, and Pseudomonas mendocina. *J. Gen. Microbiol.* , 125, pp.217-20.

Govender, S., Csimma, C. and Genant, H.K., 2002. Recombinant human bone morphogenetic protein-2 for treatment of open tibial fractures: a prospective, controlled, randomized stuy of four hundered and fifty patients. *J. Bone Joint Surg, Am.*, 84A, pp.2123-34.

Graebling, D., Muller, R. and Palierne, J.F., 1993. Linear viscoelastic behaviour of some incompatible polymer blends in the melt. Interpretation of data with aa model of emuslion of viscoelastic liquis. *Macromolecules*, 26, pp.320-29.

Greish, Y.E., Bender, J.D., Lakshmi, S., Brown, P.W., Allcock, H.R. and Laurencin, C.T., 2005. Low temperature formation of hydroxyapatite-poly(alkyl oxybenzoate)phosphazene composite for biomedical applications. *Biomaterials*, 1, pp.1-9.

Gu, F., Amsden, B. and Neufeld, R., 2004. Sustained delivery of vascular endothelial growth factor with alginate beads. *J. Control. Release*, 96, p.463–472.

Gu, F., Amsden, B. and Neufeld, R., 2004. Sustained delivery of vascular endothelial growth factor with alginate beads. *J. Control. Release*, 96, p.463– 472.

Gudmundson, C. and Semb, T.H., 1971 (b). Isoenzymes of lctic dehydrogenase and esterases in regenerationg bone. *Acta Orthop. Scandinav.*, 42, pp.297-304.

Gudmundson, C. and Semb, T.H., 1971. Enzyme studies of fractures with normal and delayed union. *Acta Orthop. Scandinav.*, 42, pp.18-27.

Gupta, M.C. and Khan, S.N., 2005. Application of bone morphogenetic proteins in spinal fusion. *Cytokine Growth Factor Rev.*, 16, p.347–3551.

Harada, S. and Rodan, G.A., 2003. Control of osteoblast function and regulation of bone mass. *Nature*, 423, pp.349-55.

Hardouin, P., Anselme, K., Flautre, B., Bianchi, F., Bascoulenguet, G. and Bouxin, B., 2000. Tissue engineering and skeletal diseases. *Joint Bone Spine*, 67, pp.419-24.

Hartmann, M., Dentini, M., Draget, D.I. and Skjåk-Bræk, G., 2006. Enzymatic modification of alginates with the mannuronan C-5 epimerase AlgE4 enhances their solubility at low pH. *Carbohydr. Polym.*, 63, pp.257-62.

Hartung, A., Bitton-Worms, K., Rechtman, M.M., Wenzel, V., Boergermann, J.H., Hassel, S., Henis, Y.I. and Knaus, P., 2006. Different routes of bone morphogenic protein (BMP) receptor endocytosis influence BMP signaling. *Mol. Cell. Biol.*, 26(20), pp.7791-805.

Hatch, R.A. and Schiller, N.L., 1998. Alginate lyase promotes diffusion of aminoglycosides through the extracellular polysaccharide of mucoid Pseudomonas aeruginosa. *Antimicrob. Agents Chemother.*, 42, pp.974-77.

Heldin, C., Miyazono, K. and Dijke, P., 1997. TGF-β signalling from cell membrane to nucleus through SMAD proteins. *Nature*, 390, pp.465-71.

He, X., Ma, J. and Jabbari, E., 2008. Effect of grafting RGD and BMP-2 protein-derived peptides to a hydrogel substrate on osteogenic differentiation of marrow stromal cells. *Langmuir*, 24(21), pp.12508-16.

Hench, L.L. and Polak, J.M., 2002. Third-generation biomedical materials. *Science*, 295, pp.1014-17.

Henzler Wildman, K.A., Lee, D. and Ramamoorthy, A., 2003. Mechanism of lipid bilayer disruption by the human antimicrobial Peptide LL-37. *Biochemistry*, 42, pp.6545-58.

Herasimenka, Y., Benincasa, M., Mattiuzzo, M., Cescutti, P., Gennaro, R. and Rizzo, R., 2005. Interaction of antimicrobial peptides with bacterial polysaccharides from lung pathogens. *Peptides*, 26, pp.1127-32.

Hern, D.L. and Hubbell, J.A., 1998. Incorporation of adhesion peptides into nonadhesive hydrogels useful for tissue resurfacing. *J Biomed Mater Res*, 39, pp.266-76.

Hersel, U., Dahmen, C. and Kessler, H., 2003. RGD modified polymers: biomaterials for stimulated cell adhesion and beyond. *Biomaterials*, 24, pp.4385-415.

Hiemstra, P.S., 2007. Antimicrobial peptides in the real world: implications for cystic fibrosis. *Eur. Respir. J.*, 29, pp.617-18.

Higuchi, T., Kinoshita, A., Takahashi, K., Oda, S. and Ishikawa, I., 1999. Bone regeneration by recombinant. *human bone morphogenetic protein-2in rat mandibular defects. An experimental model of defect filling*, 1026-1031(70), p.J. Periodontol.

Hill, P.A., 1998. Bone remodelling. *BJO*, 25, pp.101-07.

Hlady, V. and Buijs, J., 1996. Protein adsorption on solid surfaces. *Curr. Opin. Biotechnol.*, 7, pp.72-77.

Hoffman, A.S., 2002. Hydrogels for biomedical appliactions. *Adv. Drug Deliv. Rev.*, 43, pp.3-12.

Hopp, T.P. and Woods, K.R., 1981. Prediction of protein antigenic determinants from amino acid sequences. *Proc. Natl. Acad. Sci. USA*, 78, pp.3824-28.

Hornof, M.D., Kast, C.E. and Bernkop-Schnürch, A., 2003. In vitro evaluation of the viscoelastic properties of chitosan-thioglycolic acid conjugates. *Eur. J. Pharm. Biopharm.*, 55, pp.185-90.

Hoyle, H., Alcantara, H. and Costerton, J.W., 1992. Pseudomonas aeruginosa biofilm as a diffusion barrier to piperacillin. *Antimicrob. Agents Chemother.*, 36, pp.2054-56.

Huang, H., Zhao, Y., Liu, Z., Zhang, Y., Zhang, H., Fu, T. and Ma, X., 2003. Enhanced osteoblast functions on RGD immobilized surface. *Journal of Oral Implantology*, 29, pp.73-79.

Hubbel, J.A., 2007. Matrix effects. In R. Lanza, R. Langer and J. Vacanti, eds. *Principles of tissue engineering*. Third Edition ed. Elsevier Academic Press. pp.297-308.

Huebsch, J.B., Fields, G.B., Triebes, T.G. and Mooradian, D.L., 1996. Photoreactive analog of peptide FN-C/H-V from the carboxy-terminal heparin-bnding domains of fibronectin supports endothelial cell adhesion and spreding on biomaterilas surfaces. *J Biomed Mater Res*, 31, pp.555-67.

Ikada, Y., 2006. Challenges in tissue engineering. *J. R. Soc. Interface*, 3, pp.589-601.

Ito, Y. and Miyazono, K., 2003. RUNX trancriptionfactors as key targets of TGF-β superfamily signaling. *Curr. Opin. Genet. Dev.*, 13, pp.43-47.

Izquierdo-Barba, I., Vallet-Regì, M., Kupferschmidt, N., Terasaki, O., Schmidtchen, A. and Malmsten, M., 2009. Incorporation of antimicrobial compounds in mesoporous silica film monolith. *Biomaterials*, 30, p.5729–5736.

Jaworska, M., Szulińska, G., Wilk, M. and Tautt, J., 1999. Capillary electrophoretic separation of N-acetylcysteine and its impurities as a method for quality control of pharmaceuticals. *J. Chromatogr. A*, 853, pp.479-85.

Jell, G., Minelli, C. and Stevens, M.M., 2009. Biomaterial-related approaches: Surface Structuring. In U. Meyer, T. Meyer, J. Handschel and H.P. Wiesmann, eds. *Foundamentals of tissue engineering and regenerative medicine*. Berlin: Springer. pp.470-84.

Jen, A., Madorin, K. and Vosbeck, K., 2002. Transforming growth factor beta-3 crystals as reservoirs for slow release of active TGF-β3. *J. Control. Release*, 78, pp.25-34.

Jeschke, B., Meyer, J., Jonczyk, A., Kessler, H., Adamietz, P., Meenen, N.M., Kantlehner, M., Goepfert, C. and Nies, B., 2002. RGD-peptides for tissue engineering of articular cartilage. *Biomaterials*, 23, pp.3455-63.

Jin, Q.M., Takita, H., Kohgo, T., Atsumi, K., Itoh, H. and Kuboki, Y., 2000. Effects of geometry of hydroxyapatite as a cell substratum in BMP-induced ectopic bone formation. *J. Biomed. Mater. Res.*, 51, pp.491-99.

Johansson, J., Gudmundsson, G.H., Rottemberg, M.E., Berndt, K.D. and Agerberth, B., 1998. Conformation-dependent antibacterial activity of the naturally occurring human peptide LL-37. *J. Biol. Chem*, 273, pp.3718-24.

Jones-Jackson, L., Walker, R., Purnell, G., McLaren, S.G., Skinner, R.A., Thomas, J.R., Suva, L.J., Anaissie, E., Miceli, M., Nelson, C.L., Ferris, E.J. and Smeltzer, M.S., 2005. Early detection of bone infection and differentation from post-surgical inflammation using 2-deoxy-2-[18F]-fluoro-D-glucose positron emission tomography (FDG-PET) in an animal model. *J. Orthop. Res.*, 23(6), pp.1484-89.

Juban, M.M., Javadpour, M.M. and Barkley, M.D., 1997. Circular dichroism studies of secondary structure of peptides. In W.M. Shafer, ed. *Antimicrobial peptide protocols*. Humana Press. pp.73-84.

Kai, D., Li, D., Zhu, X., Zhang, L., Fan, H. and Zhang, X., 2009. Addition of sodium hyaluronate and the effect on performance of the injectable calcium phosphate cement. *J. Mater. Sci. Mater. Med.*, 20, p.1595–1602.

Kang, Q., Sun, M.H., Cheng, H., Peng, Y., Montag, A.G., Deyrup, A.T., Jiang, W., Luu, H.H., Luo, J., Szatkowski, J.P., Vanichakarn, P., Park, J.Y., Li, Y., Haydon, R.C. and He, T., 2004. Characterization of the distinct orthotopic bone-forming activity of 14 BMPs using recombinant adenovirus-mediated gene delivery. *Gene Ther.*, 11, pp.1312-20.

Kantlehner, M., Schaffner, P., Finsinger, d., Meyer, J., Jonczyk, A., Diefenbach, B., Nies, B., Hölzemann, G., Goodman, S.L. and Kessler, H., 2000. Surface coating with cyclic RGD peptides stimulates osteoblast adhesion and proliferation as well as bone formation. *ChemBioChem*, 1, pp.107-14.

Kay, J.F., 2007. Tissue-engineering bone products. In R. Lanza, R. Langer and J. Vacanti, eds. *Principles of tissue engineering*. Third Edition ed. Elsevier Academic Press. pp.1225-36.

Kenley, R., Marden, L., Turek, T., Jin, L., Ron, E. and Hollinger, J., 1994. Osseous regeneration in the rat calvarium using novel delivery systems for recombinant bone morphogenetic protein 2 (rhBMP-2). *J. Biomed. Mater. Res.*, 28, pp.1139-47.

Kim, K.J., Itoh, T. and Kotake, S., 1997. Effects of recombinant human bone morphogenetic protein-2 on human bone marrow cells cultured with various biomaterials. *J. Biomed. Mater. Res.*, 35, pp.279-85.

King, A., Strand, B., Rokstad, A., Kulseng, B., Andersson, A., Skjåk-Bræk, G. and Sandler, S., 2003. Improvement of the biocompatibility of alginate/poly-L-lysine/alginate microcapsules by the use of epimerized alginate as a coating. *J. Biomed. Mater. Res.*, 64A, pp.533-39.

Kirker-Head, C., Karageorgiou, V., Hofmann, S., Fajardo, R., Betz, O., Merkle, H.P., Hilbe, M., von Rechenberg, B., McCool, J., Abrahamsen, L., Nazarian, A., Cory, E., Curtis, M., Kaplan, D. and Meinel, L., 2007. BMP-silk composite matrices heal critically sized femoral defects. *Bone*, 41, p.247–255.

Kirsch, T., Nickel, J. and Sebald, W., 2000. BMP-2 antagonists emerge from alterations in the low-affinity binding epitope for recepotr BMPR-II. *EMBO J.*, 13, pp.3314-24.

Kirsch, T., Sebald, W. and Dreyer, M.K., 2000. Crystal structure of the BMP-2/BRIA ectodomain complex. *Nat. Struct. Mol. Biol.*, 7, pp.492-96.

Kishigami, S. and Mishina, Y., 2005. BMP signaling and early embryonic patterning. *Cytokine Growth Factor Rev.*, 16, pp.265-78.

Koening, B.B., Cook, J.S., Wolsing, D.H., Ting, J., Tiesman, J.P., Correa, P.E., Olson, C.A., Pecquet, A.L., Ventura, F. and Grant, R.A., 1994. Characterization and cloning of a receptor for BMP-2 and BMP-4 from NIH 3T3 cells. *Mol. Cell. Biol.*, 14(9), pp.5961-74.

Kolb, H.C., Finn, M.G. and Sharpless, K.B., 2001. Click chemistry: diverse chemical function from a few good reactions. *Angew. Chem. Int. Ed.*, 40, pp.2004-21.

Kotze, A.F., de Boer, H.L., Verhoef, J.C. and Junginger, H.E., 1999. Chitosan for enhanced intestinal permeability: prospects for derivatves soluble in neutral and basic environments. *Eur. J. Pharm. Sci.* , 7, pp.145-51.

Krause, W.E., Bellomo, E.G. and Colby, R.H., 2001. Rheology of sodium hyaluronate under physiological conditions. *Biomacromolecules*, 2, pp.65-69.

Krause, A., Cowles, E.A. and Gronowicz, G., 2000. Integrin-mediated signaling in osteoblasts on titanium implant materials. *J Biomed Mater Res*, 52, pp.738-47.

Kumon, H., Tomochika, K., Matunaga, T., Ogawa, M. and Ohmori, H., 1994. A sandwich cup method for the penetration assay of anitmicrobial agents through the Pseudomonas exopolysaccharides. *Microbiol. Immunol.*, 38, pp.615-19.

Kuo, H.H., Chan, C., Burrows, L.L. and Deber, C.M., 2007. Hydrophobic interactions in complexes of antimicrobial peptides with bacterial polysaccharides. *Chem. Biol. Drug. Des.*, 69, pp.405-12.

Lapasin, R. and Pricl, S., 1995. *Rheology of industrial polysaccharides. Theory and applications*. NY: Aspen Publisher.

Lax, E., 2004. The mold on Florey's coat: the strory of the peniccilin miracle. *New York: Henry Holt*.

Lebaron, R.G. and Athanasiou, K.A., 2000. Extracellular matrix cell adhesion peptides: functional applications in orthopedic materials. *Tissue Engineering*, 6(2), pp.85-103.

Lee, K.Y., Alsberg, E. and Mooney, D.J., 2001. Degradable and injectable poly(alheyde guluronate) hydrogels for bone tissue engineering. *J. Biomed. Mater. Res.* , 56, pp.228-.

Lee, J.E., Kim, S.E., Kwon, I.C., Ahn, H.J., Cho, H., Lee, S.H., Kim, H.J., Seong, S.C. and Lee, M.C., 2004. Effects of a chitosan scaffold containing TGF-beta1 encapsulated chitosan microspheres on in vitro chondrocyte culture. *Artif. Organs*, 28, pp.829-39.

Lee, K.Y., Peters, M.K., Anderson, K.W. and Mooney, D.J., 2000. Controlled growth factor release from synthetic extracellular matrices. *Nature*, 408, pp.998-1000.

Lefebvre, J. and Doublier, J.L., 1998. Rheological behaviour of polysaccharides aqueous systems. In S. Dumitriu, ed. *Polysaccharides. Structural diversity and functional versatility*. NY: Marcel Dekker, Inc. pp.357-96.

Lhoest, J.B., Detrait, E., van den Bosch de Aguilar, P. and Bertrand, P., 1998. Fibronectin adsorption, conformation, and orientation on polystyrene substrates studied by radiolabbeling, XPS, and ToF SIMS. *J Biomed Mater Res*, 41, pp.95-103.

Li, M., De, P., Gondi, S.R. and Sumerlin, B.S., 2008. Responsive polymer-protein bioconjugates prepared by RAFT polymerization and copper-catalyzed azide-alkyne click chemistry. *Macromol. Rapid Commun.*, 29, pp.1172-76.

Lipatov, Y.S., Rosovitskii, V.F. and Babich, V.F., 1975. Effect of filler on relaxation-time spectra of filled polymers. *Mech. Compos. Mater.*, 11(6), pp.1091-94.

Li, Z., Seo, T.S. and Ju, J., 2004. 1,3-dipolar cycloaddition of azides with electron-deficient alkynes under mild conditions in water. *Tetrahedron Letters*, 45, pp.3143-46.

Liu, L.S., Thomson, A.Y., Heidaran, M.A., Poster, J.W. and Spiron, R.C., 1999. An osteoinductive collage hyaluronate matrix for bone regeneration. *Biomaterials*, 20, pp.1097-.

Livermore, D.M., 2004. The need for new antibiotics. *Clin. Microbiol. Infec.*, 4, pp.1-9.

Li, J., Yun, H., Gong, Y., Zhao, N. and Zhang, X., 2006. Investigation of MC3T3-E1 cell behavior on the surface of GRGDS-coupled chitosan. *Biomacromolecules*, 7, pp.1112-23.

Llobet, E., Tomás, J.M. and Bengoechea, J.A., 2008. Capsule polysaccharide is a bacterial decoy for antimicrobial peptides. *Microbiology*, 154, p.3877–3886.

Long, F.A. and Friedman, L., 1950. Determination of the mechanism of γ-lactone hydrolysis by a mass spectrometric method. *JACS*, 72, pp.3692-95.

Luginbuehl, V., Meinel, L., Merkle, H.P. and Gander, B., 2004. Localized delivery of growth factors for bone repair. *Eur. J. Pharm. Biopharm.*, 58, pp.197-208.

Lutolf, M.P., Lauer-Fields, J.L., Schmoekel, H.G., Metters, A.T., Weber, F.E., Fields, G.B. and Hubbel, J.A., 2003. Synthetic matrix metalloproteinase-sensitive hydrogels for the conduction of tissue regeneration: engineering cell-invasion characteristics. *Proc. Natl. Acad. Sci. USA*, 100, pp.5413-18.

Madihally, S.V. and Matthew, H.W., 1999. Porous chitosan scaffolds for tissue engineering. *Biomaterials*, 20, pp.1133-42.

Mano, J.F., Silva, G.A., Azevedo, H.S., Malafaya, P.B., Sousa, R.A., Silva, S.S., Boesel, L.F., Oliveira, J.M., Santos, T.C., Marques, A.P., Neves, N.M. and Reis, R.L., 2007. Natural origin biodegradable systems in tissue engineering and regenerative medicine: present status and some moving trends. *J. R. Soc. Interafce*, 4, pp.999-1030.

Mao, J.S., Cui, Y.L., Wang, X.H., Sun, Y.J., Yin, Y.J., Zhao, H.M. and De, Y.K., 2004. A preliminary study on chitosan and gelatin polyelectrolyte complex cytocompatibility by cell cycle and apoptosis analysis. *Biomaterials*, 25, pp.3973-81.

Marcon, P., Marsich, E., Vetere, A., Mozetic, P., Campa, C., Donati, I., Vittur, F., Gamini, A. and Paoletti, S., 2005. The role of Galectin-1 in the interaction between chondrocytes and a lactose-modified chitosan. *Biomaterials*, 26, pp.4975-84.

Marsich, E., Borgogna, M., Donati, I., Mozetic, P., Strand, B.L., Gomez Salvador, S., Vittur, F. and Paoletti, S., 2008. Aglinate/lactose-modified chitosan hydrogels: a bioactive biomaterial for chondrocyte encapsulation. *J. Biomed. Mater. Res.*, 84A, pp.364-76.

Martinsen, A., Skjåk-Bræk, G. and Smidsrød, O., 1989. Alginate as immobilization materila: Correlation between chemical and physical properties of alginate beads. *Biotechnol.Bioeng.*, 33, pp.79-89.

Martin, C., Winet, H. and Bao, J.Y., 1996. Acidity near eroding polyalactide-polyglycolide in vitro and in vivo rabbit tibial bone chambers. *Biomaterials*, 17, pp.2373-80.

Masanobu, J. and Yuki, Y., 1985. Hydrophobic nature of sugars as evinced by their differential affinity for polystyrene in aqueous media. *Chem. Mat. Sci.*, 14, pp.891-902.

Massia, S.P. and Hubbell, J.A., 1991. An RGD spacing of 440 nm is sufficient for integrin αVβ3-mediated fibroblast spreading and 140 nm for focal contact fiber formation. *J. Cell Biol.*, 114, pp.1089-100.

Meyer, A., Auernheimer, J., Modlinger, A. and Kessler, H., 2006. -Targeting RGD recognizing integrins: drug development, biomaterial research, tumor imaging and targeting. *Current Pharmaceutical Design*, 12(22), pp.2723-47.

Meyer, U., Büchter, A., Wiesmann, H.P., Joos, U. and Jones, D.B., 2005. Basic reactions of osteoblasts on structured material surfaces. *Europ. Cells and Mat.*, 9, pp.39-49.

Milas, M., Rinaudo, M., Roure, I., Al-Assaf, S., Phillips, G.O. and Williams, P.A., 2001. Comparative rheological behaviour of hyaluronan form bacterial and animal sources with cross-linked hyaluronan (Hylan) in aqueous solution. *Bioploymers*, 59, pp.191-204.

Min, Z. and Qiang, Z., 2008. Correlation between rheological behavior and structure of multi-component polymer systems. *Sci. China Ser. B-Chem.*, 51(1), pp.1-12.

Mistry, A.S. and Mikos, A.G., 2005. Tissue engineering strategies for bone regeneration. *Adv. Biochem. Eng./Biotechnol.*, 94, pp.1-22.

Miyazono, K., Maeda, S. and Imamura, T., 2005. BMP receptor signaling: transcriptional targets,regulation of signals, and signaling cross-talk. *Cytokine Growth Factor Rev.*, 16, p.251–263.

Moe, S.T., Skjåk-Bræk, G., Elgsaeter, A. and Smidsrød, O., 1993. Swelling of covalently crosslinked alginate gels: influence of ionic solutes and nonpolare solvents. *Macromolecules*, 26, pp.3589-97.

Mont, M.M., Ragland, P.S., Biggins, B., Friedlaender, G., Patel, T., Cook, S., Etienne, G., Shimmin, A., Kildey, R., Rueger, D.C. and Einhorn, T.A., 2004. Use of bone morphogenetic proteins for musculoskeletal applications. *JBJS*, 86-A(S2), pp.41-55.

Morris, C.J., 1977. The three essential criteria. *Trends Biochem. Sci.*.

Mumper, R.J., Hoffman, A.S., Puolakkainen, P.A., Bouchard, L.S. and Gombotz, W.R., 1994. Calcium-alginate beads for the oral delivery of transforming growth factor-β 1 (TGF-β1): stabilization of TGF-β1 by the addition of polyacrylic acid within acid-treated beads. *J. Controlled Release*, 30, pp.241-51.

Muzzarelli, R.A., 1997. Human enzymatic activities related to the therapeutic administration of chitin derivatives. *Cell Mol. Life Sci.*, 53, pp.131-40.

Muzzarelli, R.A., Tanfani, F., Emanuelli, M., Pace, D.P., Chiaruzzi, E. and Piani, M., 1984. Sulfated N-(carboxymethyl)chitosans: novel blood anticoagulants. *Carbohydr. Res.*, 126, pp.225-31.

Nagaoka, I., Hirota, S., Niyonsaba, F., Hirata, M., Adachi, Y., Tamura, H., Tanaka, S. and Heumann, D., 2002. Augmentation of the lipopolysaccharide-neutralizing activities of human cathelicidin CAP18/LL-37-derived antimicrobial peptides by replacement with hydrophobic and caationic amino acid residues. *Clin. Diagn. Lab. Immunol.* , 9(5), pp.972-82.

Nakamura, H., Sano, A. and Matsuura, K., 1998. Determination of critical micellar concentration of anionic surfactants by capillary electrophoresis using 2-naphthalenemethanol as a maerker for micelle formation. *Anal. Sci.*, 14, pp.379-82.

Navarro, M., Michiardi, A., Castano, O. and Planell, J.A., 2008. Biomaterials in orthopaedics. *J. R. Soc. Interface* , 5, p.1137–1158.

Neal, J.L. and Goring, D.A., 1970. Hydrophobic folding of maltose in aqueous solution. *Can. J. Chem.*, 48, pp.3745-47.

Neukamm, M.A., Pinto, A. and Metzler-Nolte, N., 2008. Synthesis and cytotoxicity of a cobaltcarbonyl-alkyne enkephalin bioconjugate. *Chem. Commun.*, pp.232-34.

Neumann, M.G., Schmitt, C.C. and Iamazaki, E.T., 2003. A fluorescence study of the interactions between sodium alginate and surfactants. *Carbohydr. Res.*, 338, pp.1109-13.

Nicolas, P. and Mor, A., 1995. Peptides as weapons against microorganisms in the chemical defense system of vertebrates. *Annu. Rev. Microbiol.*, 49, pp.277-304.

Nicols, W.W., Dorrington, S.M. and Slack, M.P., 1988. Inhibition of tobramycin diffusion by binding to alginate. *Antimicrob. Agents Chemother.*, 32, pp.518-23.

Nimni, M.E., 1997. Polypeptide growth factors: targeted delivey systems. *Biomaterials*, 18, pp.1201-25.

Niu, X., Feng, Q., Wang, M., Guo, X. and Zheng, Q., 2009. In vitro degradation an release behavior of porous poly(lactic acid) scaffolds containing chitosan microspheres as a carrier for BMP-2-derived synthetic peptide. *Polyme. Degrad. Stab.*, 94, pp.176-82.

Nizet, V., 2006. Antimicrobial Peptide Resistance Mechanisms of human bacterial pathogens. *Curr. Issues Mol. Biol.*, 8, pp.11-26.

Nohe, A., Hassel, S., Ehrlich, M., Neubauer, F., Sebald, W., Henis, Y.I. and Knaus, P., 2002. The mode of bone morphogenetic protein (BMP) receptor oligomerization determines different BMP-2 signaling pathways. *J. Biol. Chem.*, 277(7), pp.5330-38.

Oren, Z., Lerman, J.C., Gudmundsson, H.G., Agerberth, B. and Shai, Y., 1999. Structure and organization of human antimicrobial peptide LL-37 in phospholipids membranes: relevance to the molecular basis for its non-cell-selective activity. *Biochem. J.*, 341, pp.501-13.

Park, D., Choi, B., Zhu, S., Huh, J., Kim, B. and Lee, S., 2005. Injectable bone using chitosan-alginate gel/mesenchymal stem cells/BMP-2 composites. *J. Craniomaxillofac. Surg.*, 33, pp.50-54.

Patel, Z.S., Yamamoto, M., Ueda, H., Tabata, Y. and Mikos, A.G., 2008. Biodegradable gelatin microparticles as delivery systems for the controlled release of bone morphogenetic protein-2. *Acta Biomaterialia*, 4, p.1126–1138.

Patel, W., Zhao, L. and Wong, P., 2006. Controlling bone morphogenetic protein diffusion and bonemorphogenetic protein stimulated bone growth using fibrin glue. *Spine*, 31, p.1201–1206.

Payne, D.J., 2008. Desperately seeking new antibiotics. *Science*, 321, pp.1644-45.

Petreaca, M. and Martins-Green, M., 2007. The dynamics of cell-ECM interactions. In R. Lanza, R. Langer and J. Vacanti, eds. *Principles of tissue engineering*. Third edition ed. Elsevier Academic Press. pp.81-99.

Pierschbacher, M., Hayman, E.G. and Ruoslahti, E., 1983. Synthetic peptide with cell attachment activity of fibronectin. *Proc Natl Acad Sci USA*, 80, pp.1224-27.

Prüsse, U., Bilancetti, L., Bučko, M., Bugarski, B., Bukowski, J., Gemeiner, P., Lewińska, D., Manojlovic, V., Massart, B., Nastruzzi, C., Nedovic, V., Poncelet, D., Siebenhaar, S., Tobler, L., Tosi, A., Vikartvská, A. and Vorlop, K., 2008. Comparison of different technologies for alginate beads production. *Chem. Pap.*, 62(4), pp.364-74.

Quirk, R.A., Chan, W.C., Davies, M.C., Tendler, S.J. and Shakesheff, K.M., 2001. Poly(L-lysine)-GRGDS as a biomimetic surface modfier for poly(lactic acid). *Biomaterials*, 22, pp.865-72.

Ramkumar, R. and Podder, S.K., 2000. Elucidation of the emchanism of interaction of sheep spleen galectin-1 with splenocytes and its role in cell matrix adhesion. *J. Mol. Recognit.* , 13, pp.299-309.

Reddi, A.H., 2001. Bone morphogentic proteins: from basic science to clinical applications. *JB&JS*, 83-A(S1), pp.1-6.

Reddi, A.H., 2005. BMPs: from bone morphogenic proteins to body morphogenic proteins. *Cytokine Growth Factor Rev.*, 16, pp.249-50.

Reddi, A.H., 2007. Morphogenesis and tissue engineering. In R. Lanza, R. Langer and J. Vacanti, eds. *Principles of tissue engineering*. Third Edition ed. Elsevier Academic Press. pp.117-28.

Rice, L.B., 2006. Challenges in identifying new antimicrobial agents effective for treating infections with Acinetobacter baumannii and Pseudomonas aeruginosa. *Clin. Infect. Dis.*, 43(Suppl 2), pp.S100-05.

Ripamonti, U., 2002. Tissue engineering of bone by novel substrata instructing gene expression during de nov bone formation. *Science in Africa, March, Merck Feature by Janice Limson*.

Rizzo, D., 2006. *Fondamentals of Anatomy & Physiology*. 2nd ed. Thomson Delmar Learning.

Roach, P., Eglin, D., Rohde, K. and Perry, C.C., 2007. Modern biomaterials: a review-bulk properties and implications of surface modifications. *J Mater Sci: Mater Med*, 18, pp.1263-77.

Rodan, G.A. and Martin, T.J., 2000. Therapeutic Approaches to Bone Diseases. *Science*, 289, pp.1508-14.

Rodriguez, B., Romero, A., Soto, O. and Varorna, O., 2004. Biomaterilas for orthopedics. *Applications of engineering mechanics in medicine, GED - Univeristy of Puerto Rico, Mayaguez*, pp.1-26.

Rosen, V., 2009. BMP2 signaling in bone development and repair. *Cytokine Growth Factor Rev.*, 20, pp.475-80.

Rowley, J.A., Madlambatan, G. and Mooney, D.J., 1999. Alginate hydrogels as synthetic extracellular matrix mayterials. *Biomaterials*, 20, pp.45-53.

Ruppert, R., Hoffman, E. and Sebald, W., 1996. Human bone morphogenetic protein 2 contains a heparin-binding site which modifies its biological activity. *Eur. J. Biochem.*, 237, pp.295-302.

Saito, N., Okada, T., Horiuchi, H., Murakami, N., Takahashi, J., Nawata, M., Ota, H., Miyamoto, S., Nozaki, K. and Takao, K., 2001. Biodegradable poly-D,L-lactic acid-polyethylene glycol block copolymers as a BMP delivery system for inducing bone. *J Bone Joint Surg Am.* , 83, pp.92-98.

Saito, A., Suzuki, Y., Ogata, S., Ohtsuki, C. and Tanihara, M., 2003. Activation of osteo-progenitor cells by a novel synthetic peptide derived from the bone morphogenic protein-2 knuckle epitope. *Biochim. Biophys. Acta*, 1651, pp.60-67.

Saito, A., Suzuki, Y., Ogata, S., Ohtsuki, C. and Tanihara, M., 2004. Prolonged ectopic calcification induced by BMP-2-derived synthetic peptide. *J. Biomed. Mater. Res.*, 70A, pp.115-21.

Scheufler, C., Sebald, W. and Hülsmeyer, M., 1999. Crystal structure of human bone morphogenetic protein-2 at 2.7 Å resolution. *J. Mol. Biol.*, 287, pp.103-15.

Schliephake, H., Weich, H.A., Dullin, C., Gruber, R. and Frahse, S., 2008. Mandibular bone repair by implantation of rhBMP-2 in a slow release carrier of polylactic-acid - An experimental study in rats. *Biomaterials*, 29, pp.103-10.

Schmitt-Kopplin, P., 2008. *Capillary electrophoresis -Methods and protocols-*. Humana Press.

Schneiders, W., Reinstorf, A., Pompe, W., Grass, R., Biewener, A., Holch, M., Zwipp, H. and Rammelt, S., 2007. Effect of modification of hydroxyapatite/collagen composites with sodium citrate, phosphoserine, phosphoserine/RGD-peptide and calcium carbonate on bone remodelling. *Bone*, 40, pp.1048-59.

Schwartz, B.S., Ngo, P.D. and Guglielmo, B.J., 2008. Daptomycin treatment failure for vancomycin-resistant Enterococcus faecium infective endocarditis: impact of protein binding? *Ann. Pharmacother.*, 42, pp.289-90.

Scott, J.E., 1989. Secondary structures in hyaluronan solutions: chemical and biological implications. The biology of hyaluronan. *Ciba Foundation Symposium*, 25, pp.281-88.

Scott, J.E. and Heatley, F., 2002. Biological properties of hyaluronan in aqueous solution are controlled and sequestred by reversible tertiary structures, defined by NMR spectroscopy. *Biomacromolecules*, 3, pp.547-53.

Seal, B.L., Otero, T.C. and Panitch, A., 2001. Polymeric biomaterilas for tissue and organ regeneration. *Mater. Sci. Eng.*, 34, pp.147-230.

Secchi, A.G., Grigoriou, V., Shapiro, I.M., Cavalcanti-Adam, E.A., Composto, R.J., Ducheyne, P. and Adams, C.S., 2007. RGDS peptides immobilized on titanium alloy stimulatebone cell attachment, differentiation and confer resistance to apoptosis. *J. Biomed. Mater. Res.*, 83A, pp.577-84.

Seeherman, H., 2001. The influence of delibery vehicles and their properties on the repair of segmental defects and fractures with osteogenic factors. *JBJS*, 83A(Suppl.1), pp.79-81.

Seeherman, H., Li, R. and Woozney, J., 2003. A review of preclinical program development for evaluating injectable carriers for osteogenic factors. *J. Bone Joint Surg. Am.*, 85A(Suppl.3), pp.96-108.

Seeherman, H. and Wozney, J.M., 2005. Delivery of bone morphogenetic protens for orthopedic tissue regeneration. *Cytokine Growth Factor Rev.*, 16, pp.329-45.

Seeherman, H., Wozney, J. and Li, R., 2002. Bone morphogenetic protein delivery systems. *Spine*, 27(16S), pp.S16-23.

Semb, T.H., 1970. Isozymes of bone esterases. *Calc. Tiss. Res.*, 6, pp.77-80.

Senta, H., Park, H., Bergeron, E., Drevelle, O., Fong, D., Leblanc, E., Cabana, F., Roux, S., Grenier, G. and Faucheux, N., 2009. Cell responses to bone morphogenetic protens and petpides derived from them: Biomedical applications and limitations. *Cytokine Growth Factor Rev.*, 20, pp.213-22.

Shigeta, M., Tanaka, G., Komatsuzawa, H., Sugai, M., Suginaka, H. and Usui, T., 1997. Penetration of antimicrobial agents through Pseudomonas aeruginosa biofilms: a simple method. *Chemother.*, 43, pp.340-45.

Shin, H., Jo, S. and Mikos, A.G., 2003. Biomimetic materilas for tissue engineering. *Biomaterials*, 24, pp.4353-64.

Shukla, A., Fleming, K.E., Chuang, H.F., Chau, T.M., Loose, C.R., Stephanopoulos, G.N. and Hammond, P.T., 2010. Controlling the release of peptide antimicrobial agents from surfaces. *Biomaterials*, 31(8), pp.2348-57.

Sieber, C., Kopf, J., Hiepen, C. and Knaus, P., 2009. Recent advances in BMP receptor signaling. *Cytokine Growth Factor Rev.*, 20, pp.343-55.

Siebers, M.C., Brugge, P.J., Walboomers, X.F. and Jansen, J.A., 2005. Integrins as linker proteins between osteoblasts and bone replacing materials. A critical review. *Biomaterials*, 26, pp.137-46.

Skarnes, R.C. and Watson, D.W., 1957. Antimicrobial factors of normal tissues and fluids. *Bacteriol. Rev.*, 21, pp.273-94.

Smidsrød, O. and Moe, S.T., 2008. *Biopolymer Chemistry*. Tapir academic press.

Smidsrød, O. and Skjåk-Bræk, G., 1990. Algiate as immobilization matrix for cells. *TIBTECH*, 8, pp.71-78.

Smith, P.K., Krohn, R.I., Hermanson, G., Mallia, A.K., Gartner, F.H., Fujimoto, E.K., Goeke, N.M., Olson, B.J. and Klenk, D.C., 1985. Measurement of protein using bicinchommc acid. *Anal. Biochem.*, 150, pp.76-5.

Song, B., Estrada, K.D. and Lyons, K.M., 2009. Smad signaling in skeletal development and regeneration. *Cytokine Growth Factor Rev.*, 20, p.379–388.

Soriler, P., Denuziere, A., Viton, C. and Domard, A., 2001. Relation between the degree of acetylation and the electrostatic properties of chitin and chitosan. *Biomacromolecules*, 2, pp.765-72.

Sotome, S., Uemura, T., Kikuchic, M., Chen, J., Itoh, S., Tanaka, J., Tateishi, T. and Shinomiya, K., 2004. Synthesis and in vivo evaluation of a novel hydroxyapatite/collagen–alginate as a bone filler and a drug delivery carrier of bone morphogenetic protein. *Mater. Sci. Eng.*, 24, p.341–347.

Sotome, S., Uemura, T., Kikuchi, M., Chen, J., Itoh, S., Tanaka, J., Tateishi, T. and Shinomiya, K., 2004. Synthesis and in vivo evaluation of a novel hydroxyapatite/collagen-alginate carrier as a bone filler and a drug delivery carrier of bone morphogenetic protein. *Mater. Sci. Eng.*, 24, pp.341-47.

Spellberg, B., Guidos, R., Gilbert, D., Bradley, J., Boucher, H.W., Scheld, W.M., Bartlett, J.G. and Edwards, J.J., 2008. The epidemic of antibiotic-resistant infections: a call to action for the medical community from the Infectious Diseases of Society of America. *Clin. Infect. Dis.*, 46(2), pp.155-64.

Spellberg, B., Guidos, R., Gilbert, D., Bradley, J., Boucher, H.W., Scheld, W.M., Bartlett, J.G. and Edwards, J., 2008. The epidemic of antibiotic-resistant infections: a call to action for the medical community from the infectious diseases society of America. *Clin. Infect. Dis.*, 46, pp.155-64.

Spellberg, B., Powers, J.H., Brass, E.P., Miller, L.G. and Edwards, J.E., 2004. Trends in antimicrobial drug development: implications for the future. *Clin. Infect. Dis.*, 38, pp.1279-86.

Statz, A.R., Park, J.P., Chongsiriwatana, N.P., Barron, A.E. and Messersmith, P.B., 2008. Surface-immobilized antimicrobial peptoids. *Biofouling.*, 24(6), pp.439-48.

Steinstraesser, L., Ring, A., Bals, R., Steinau, H.U. and Langer, S., 2006. The human host defense peptide LL37/hCAP accelerates angiogenesis in PEGT/PBT biopolymers. *Ann. Plast. Surg.*, 56, p.93–98.

Stile, R.A. and Healy, K.E., 2001. Thermo-responsive peptide-modified hydrogles for tissue regeneration. *Biomacromolecules*, 2, pp.185-94.

Stocum, D.L., 2006. *Regenerative Biology and Medicine*. Elsevier Inc.

Strand, B.L., Gaserod, O., Kulseng, B., Espevik, T. and Skjåk-Bræk, G., 2002. Alginate-polylysine-alginate microcapsules: effect of size reduction on capsule properties. *J. Microencapsul.*, 19(5), pp.615-30.

Strand, B.L., Mørch, Y.A. and Skjåk-Bræk, G., 2000. Aglginate as immobilization matrix for cells. *Minerva Biotec.*, 12, pp.223-33.

Suci, P., Mittelman, M.W., Yu, F.P. and Geesy, G.G., 1994. INvestigation of ciprofloxacin penetration into Pseudomonas aeruginosa biofilms. *Antimicrob. Agents Chemother.*, 38, pp.2125-33.

Suh, J.K. and Matthew, H.W., 2000. Application of chitosan-based polysaccharide biomaterials in cartilage tissue engineering: a review. *Biomaterials*, 21, pp.2589-98.

Suzuki, Y., Tanihara, M., Suzuki, K., Saitou, A., Sufan, W. and Nishimura, Y., 2000. Alginate hydrogel linked with synthetic oligopeptide derived from BMP-2 allows ectopic osteoinduction in vivo. *J. Biomed. Mater. Res.*, 50, pp.405-09.

Swiontkowski, M.F., Aro, H.T. and Donell, S., 2006. Recombinant human bone morphogenetic protein-2 in opne tibial fractures. A subgroup analysis of data combined from two prospective randomized studies. *J. Bone Joint Surg. Am.*, 88, pp.1258-65.

Tabata, Y., 2003. Tissue regeneration based on growth factor release. *Tissue Eng.*, 9(S1), pp.5-15.

Teitelbaum, S.L., 2000. Bone Resorption by Osteoclasts. *Science*, 289, pp.1504-08.

Teßmar, J., Brandl, F. and Göpferich, A., 2009. Hydrogels for tissue engineering. In U. Meyer, T. Meyer, J. Handschel and H.P. Wiesmann, eds. *Foundamentals of tissue egnineering and regenerative medicine*. Berlin: Springer. pp.495-517.

Theuretzbacher, U., 2009. Future antibiotics scenarios: is the tide starting to turn? *Int. J. Antimicrob. Agents*, 34(1), pp.15-20.

Thu, B., Bruheim, P., Espevik, T., Smidsrød, O., Soon-Shiong, P. and Skjåk-Bræk, G., 1996. Alginate polycation microcapsules. II. Some functional properties. *Biomaterials*, 17, pp.1069-79.

Tjabringa, G.S., Rabe, K.F. and Hiemstra, P.S., 2005. The human cathelicidin LL-37: a multifunctional peptide involved in infection and inflammation in the lung. *Pulm. Pharmacol. Ther.*, 18, pp.321-27.

Travan, A., Donati, I., Marsich, E., Bellomo, F., Achanta, S., Toppazzini, M., Semeraro, S., Scarpa, T., Spreafico, V. and Paoletti, S., 2010. Surface modification and polysaccharide deposition on BisGMA/TEGDMA thermoset. *Biomacromolecules*, 11(3), pp.583-92.

Tron, G.C., Pirali, T., Billington, R.A., Canonico, P.L., Sorba, G. and Genazzani, A.A., 2008. Click chemistry reactions in medicinal chemistry: applications of the 1,3-dipolar cycloaddition between azides and alkynes. *Med. Res. Rev.*, 28(2), pp.278-308.

Tsuji, K., Bandyopadhyay, A., Harfe, B.D., Cox, K., Kakar, S., Gerstenfeld, L., Einhorn, T., Tabin, C.J. and Rosen, V., 2006. BMP2 activity, although dispensable for bone formation, is required for the initiation of fracture healing. *Nature Genet.*, 38(12), pp.1424-29.

Tsumaki, N. and Yoshikawa, H., 2005. The role of bone morphogenetic proteins in endochondral bone formation. *Cytokine Growth Factor Rev.*, 16, pp.279-85.

Turco, G., Marsich, E., Bellomo, F., Semeraro, S., Donati, I., Brun, F., Grandolfo, M., Accardo, A. and Paoletti, S., 2009. Alginate/Hydroxyapatite biocomposites for bone ingrowth: a trabecular structre with high and isotropic connectivity. *Biomacromolecules*, 10, pp.1575-83.

Uebersax, L., Merkle, H.P. and Meinel, L., 2009. Biopolymer-based Growth Factor delivery for tissue repair: from natural concepts to engineered systems. *Tissue Eng. Part B*, 15(3), pp.263-89.

Uludag, H., Gao, T., Porter, T.J., Friess, W. and Wozney, J.M., 2001. Delivery systems for BMPs: factors contributing to protein retentation at an application site. *JBJS*, 83A(Suppl.1), pp.128-35.

Valentin-Opran, A., Wozney, J., Csimma, C., Lilly, L. and Riedel, G.E., 2002. Clinical evaluation of recombinant human bone morphogenetic protein-2. *Clin. Orthop. Relat. Res.*, 395, pp.110-20.

Vandevord, P.J., Matthew, H.W., DeSilva, S.P., Matyon, L., Wu, B. and Wooley, P.H., 2002. Evaluation of the biocompatibility of a chitosan scaffold in mice. *J. Biomed. Mater. Res.*, 59, pp.585-90.

Verrier, S., Pallu, S., Bareille, R., Jonczyk, A., Meyer, J., Dard, M. and Amédée, J., 2002. Function of linear and cyclic RGD-containing peptides in osteoprogenitor cells adhesion process. *Biomaterials*, 23, pp.585-96.

Vicente, M., Hodgson, J., Massidda, O., Tonjum, T., Henriques-Normark, B. and Ron, E.Z., 2006. The fallacies of hope: will we discover new antibiotic to combat pathogenic bacteria in time? *FEMS Microbiol. Rev.*, 30, pp.841-52.

von Friesen, A. and Schäfer, W., 2006. Bone replacement materials in hand surgery. *Eur. J. Trauma*, 32, p.172–178.

Wang, M., 2003. Developing bioacitve composite materilas for tissue replacement. *Biomaterials*, 24, pp.2133-51.

Wang, E.A., Rosen, V., D'Alessandro, J.S., Bauduy, M., Cordes, P., Harada, T., Israel, D.I., Hewick, R.M., Kerns, K.M., Lapan, P., Luxenberg, D.P., McQuaid, D., Moutsatsos, I.K., Nove, J. and Wozney, J.M., 1990. Recombinant human bone morphogenetic protein induces bone formation. *Proc. Natl. Acad. Sci. USA*, 87, pp.2220-24.

Wieprecht, T., Apostolov, O., Beyermann, M. and Seelig, J., 2000. Interaction of a mitochondrial presequence with lipid membranes: role of the helix formation for membrane binding and perturbation. *Biochemistry*, 39(50), pp.15297-305.

Xing, L., Dawei, C., Liping, X. and Rongqing, Z., 2003. Oral colon-specific drug delivery for bee venom peptide: development of a coated calcium algnate gel beads-entrapped liposome. *J. Control. Release*, 93, pp.293-300.

Yalpani, M. and Hall, L.D., 1984. Some Chemical and analytical aspects of polysaccharide modifications.Formation of branched-chain, soluble chitosan derivatives. *Macormolecules*, 17, pp.272-81.

Yanagita, M., 2005. BMP antagonists: their roles in development and involvement in pathophysiology. *Cytokine Growth Factor Rev.*, 16, pp.309-17.

Yang, D., Chertov, O. and Oppenheim, J.J., 2001. Participation of mammalian defensins and cathelicidins in antimicrobial immunity: receptors and activities of human defensins and cathelicidin (LL-37). *J. Leukoc. Biol.*, 69, pp.691-97.

Yang, T.C., Chou, C.C. and Li, C.F., 2005. Antibacterial activity of N-alkylated disaccharide chitosan derivatives. *Int. J. Food Microbiol.* , 97, pp.237-45.

Yang, X.B., Roach, H.I., Clarke, N.M., Howdle, S.M., Quirk, R., Shakesheff, K.M. and Oreffo, R.O., 2001. Human osteoprogenitor growth and differentiation on synthetic biodegradable structures after surface modification. *Bone*, 29(6), pp.523-31.

Yeaman, M.R. and Yount, N.Y., 2003. Mechanisms of antimicrobial peptide action and resistance. *Pharmacol. Rev.*, 2003, pp.27-55.

Yilgor, P., Tuzlakoglu, K., Reis, R.L., Hasirci, N. and Hasirci, V., 2009. Incorporation of a sequential BMP-2/BMP-7 delivery system into chitosan-based scaffolds for bone tissue engineering. *Biomaterials*, 30, p.3551–3559.

Yu, Y.Y., Lieu, S., Lu, C., Miclau, T., Marcucio, R.S. and Colnot, C., 2009. Immunolocalization of BMPs, BMP antagonists, receptors, and effectors during fracture repair. *Bone*, pp.841-51.

Zanetti, M., 2004. The Role of cathelicidins in the innate host defenses of mammals. *Curr. Issues Mol. Biol.*, 7, pp.179-96.

Zanetti, M., Gennaro, R. and Romeo, D., 1995. Cathelicidins: a novel protein family with a common proregion and a variable C-terminal anti-microbial domain. *FEBS Lett.*, 374, pp.1-5.

Zasloff, M., 2002. Antimicrobial peptides of multicellular organisms. *Nature*, 415, pp.389-95.

Zelzer, E. and Olsen, B.R., 2003. The genetic basis for skeletal diseases. *Nature*, 423, pp.343-48.

Zhang, H. and Bradley, A., 1996. Mice deficient of BMP-2 are nonviable and have defects in amnion/chorion and cardiac development. *Development*, 122, pp.2977-89.

Zhang, Y. and Zhang, M., 2004. Cell growth and function on calcium phosphate reinforced chitosan scaffolds. *J. Mater. Sci. Mater. Med.*, 15, pp.255-60.

Zoricic, S., Maric, I., Bobinac, D. and Vukicevic, S., 2003. Expression of bone morphogenetic proteins and cartilage-derived morphogenetic proteins during osteophyte formation in humans. *J. Anat.*, 202, pp.269-77.